Università degli Studi di Ferrara

RESEARCH DOCTORATE IN

BIOMEDICAL AND BIOTECHNOLOGICAL SCIENCES

CYCLE XXXIII

COORDINATOR Prof. Pinton Paolo

Altering the biological functions of microRNAs by the miRNA-masking approach as a possible therapeutic strategy for rare diseases

Scientific Disciplinary Sector BIO/10

PhD candidate

Dr. Sultan Shaiq

Tutor

Prof. Borgatti Monica

Prof. Gambari Roberto

YEARS 2017/2021

INDEX **Page No.**

ABBREVIATIONS

μM:	Micro Molar
αMEMα:	Minimal Essential Medium
ADA:	Adamantyl Acetic Acid
AGO:	ArGOnaute
aM:	Atto Molar
AMO:	Anti MiRNA Oligonucleotide
AMPS:	Ammonium PerSulfate
bp:	base pairs
BSA:	Bovine Serum Albumin
CF:	cystic fibrosis
CFTR:	cystic fibrosis transmembrane conductance regulator gene
CFBE:	Human CF bronchial epithelial cell line
cfDNA:	circulating Free DNA
cDNA:	complementary DNA
cDNA:	circulating DNA
CDS:	coding Domain Sequence
CNV:	copy number variation
CRISPR:	clustered regularly interspaced short palindromic repeats
Ct:	threshold cycle value
cffDNA:	cell Free Fetal DNA
cmiRNA:	circulating microRNA
CT:	cycle Number
CT Scan:	computed Tomography Scan

Da:	Dalton
DAPI:	4’-6-diamidino-2-phenylindole
DAZ:	deleted in azoospermia
ddNTP:	dideoxynucleoside triphosphate
DHPLC:	denaturing high performance liquid chromatography
dPCR:	digital polymeration chain reaction
dUTP:	2’-deoxyuridine 5’-triphosphate
DMSO:	di Methyl SulfOxide
DNA:	deoxy Ribonucleic Acid
DNMT:	dNA Methyl Transferase inhibitor
dNTP:	deoxynucleotide
DPBS:	dulbecco’s phosphate-buffered saline
dsDNA:	double Strand DNA
DSN:	duplex Specific Nuclease
FACS:	fluorescence-activated cell sorting
FAM^{TM}:	carboxyfluorescein
FANA:	2’-deoxy-2’fluoro-β-D-arabino nucleic acid
FDA:	food and drug administration
FBS:	fetal Bovine Serum
FISH:	fluorescence *in situ* hybridization
FRET:	fluorescence resonance energy transfer
FXS:	fragile X syndrome
GC-SPR:	grating coupled-surface plasmon resonance
GMO:	genetic modified organism

GVHD: graft versus host disease

Hb: hemoglobin

HbA: adult hemoglobin

HBA: alfa globin

HBB: beta globin

HbF: fetal haemoglobin

HD: Huntington disease gene

HDR: homology directed repair

HEX™: carboxyhexachlorofluorescein

HIV: human immunodeficiency virus

HIV: human immunodeficiency virus

HPFH: hereditary persistence of fetal haemoglobin

HPLC: high performance liquid chromatography

HRM-PCR: high resolution melt-polymerase chain reaction

HSPC: hematopoietic stem and progenitor cell

IE: ineffective erythropoiesis

IFC: integrated microfluidic cartridge

ISH: *in situ* hybridization

IVS: intervening sequence

Kb: kilobase

KLF: Krüppel like factor 1

LED: light-emitting diode

LSPR: localized surface plasmon resonance

LDL: low Density Lipoprotein

LNA: locked Nucleic Acid

lncRNA: long Non Coding RNA

LOD:	limit Of Detection
LOH:	loss Of Heterozygosity
MAA:	marketing authorisation application
MeDIP:	methylation DNA immunoprecipitation
MF:	morpholino phosphoroamidate
M-FISH:	multicolour fluorescence *in situ* hybridization
miRNA:	microRNA
MLPA:	multiplex ligation-dependent probe amplification
MNP:	multiple nucleotide polymorphism
mRNA:	messenger RNA
MgCl:	magnesium Chloride
miRISC:	miRNA-Induced Silencing Complex
miRNA/miR:	microRNA
mmu:	mus MUsculus
MSD:	matched sibling donor
MW:	molecular weight
MTH:	mithramycin
NF-κB:	nuclear Factor Kappa-light-chain-enhancer of activated B cells
ncRNA:	non Coding RNA
NF-kB:	nuclear factor kappa B
NFQ:	non-fluorescent quencher
NGS:	next generation sequencing
NHEJ:	non-homologous end joining
NP:	N3'-P5' phosphoroamidate
NRBC:	nucleated red blood cell

NTDT:	non transfusion dependent thalassemia
PAH:	phenylalanine hydroxylase gene
PAP:	pyrophosphorolysis-activated polymerization
PAPP-A:	pregnancy-associated plasma protein-A
PBS:	phosphate buffered saline
PCR:	polymerase chain reaction
PNA:	peptide nucleic acid
PPi:	pyrophosphate
PTC:	premature termination codon
Q-FISH:	quantitative fluorescence *in situ* hybridization
QF-PCR:	quantitative fluorescence polymerase chain reaction
qRT-PCR:	quantitative real time polymeration chain reaction
RT:	Room temprature
R8:	poly Arginine Peptide
RBC:	red blood cell
RFLP-PCR:	restriction fragment length polymorphisms-polymerase chain reaction
RFU:	relative fluorescence unit
RhD:	rhesus D
ROX^{TM}:	rhodamine X
RU:	resonance unit
RUfin:	final resonance units
RUin:	initial resonance units
RUres:	residual resonance units
RNApol:	RNA Polymerase

RPMI:	Roswell Park Memorial Institute
SA:	streptavidin
SNP:	single nucleotide polymorphism
snRNA:	small nuclear RNA
SPR:	surface plasmon resonance
SDS:	sodium Dodecyl Sulfate
tcDNA:	tricycle DNA
TSBs:	Target site blockers
TDT:	transfusion dependent thalassemia
TEAA:	triethylammonium acetate
TAE:	tris Acetic acid EDTA
tRNA:	transfer RNA
TF:	transcription Factor
Taq:	thermus AQuaticus
Tm:	melting temperature
UTR:	untranslated region
3'UTR:	3 prime end untranslated region
5'UTR:	5 prime end untranslated region
VIC®:	chlorophenyldichlorocarboxyfluorescein
VX-809:	Lumacaftor
VX-770:	Ivacaftor
wt:	wild type

ABSTRACT

Cystic fibrosis (CF) as a chronic illness affects secretory epithelium of the sweat and biliary glands, pancreas, the digestive and respiratory tracts, resulting in generalized malnutrition and chronic respiratory infections. It is an autosomal recessive genetic disease; therefore all individuals diagnosed clinically with CF have mutations in both Cystic Fibrosis Transmembrane conductance Regulator (CFTR) gene alleles. Regulation of CFTR by microRNAs (miRNAs) has been explored in CF for many years. In this study, we have tried to modulate miRNAs expression using peptide-nucleic acids (PNAs)-based antagomiRNAs and miRNA-masking PNAs. Peptide nucleic acids are very useful tools for gene regulation at different levels, but in particular in the last years their use for targeting microRNAs has provided impressive advancements. In particular, targeting of microRNAs involved in the repression of the expression of the *CFTR Gene*, which is defective in cystic fibrosis (CF), is a key step in the development of new types of treatment protocols.

Main Objectives were (a) studies on changes of the *CFTR Gene* expression using PNAs targeting CFTR-regulating miRNAs (the miRNA antisense approach); (b) studies on changes of the *CFTR Gene* expression by masking the miRNA-binding sites with PNAs complementary to the 3'UTR sequence of the CFTR mRNA (the miRNA masking approach); (c) combined treatments, with particular focus on using CFTR correctors and potentiators; (d) validation of the miRNA masking approach in modifying the expression of key genes involved in other genetic diseases (i.e. KLF4 in β-thalassemia).

Studies focusing on microRNAs involved in the repression of *CFTR Gene*, which is defective in cystic fibrosis, are of great importance in the development of new type of treatments of clinical impact.

In the first part of our study, the use of an anti-miR PNA targeting the microRNA miR-145-5p was considered, as this miRNA is known to suppress CFTR expression. Octaarginine-anti-miR PNA conjugates were delivered to Calu-3 cells, for sequence dependent targeting of miR-145-5p. This allowed enhancing expression of the miR-145 regulated *CFTR Gene*, analyzed at mRNA and CFTR protein level. The objective of this part of the study was to design a PNA targeting miR-145, determine its activity in inhibiting miR-145, and verify whether it was able to induce an increase of CFTR production. Moreover, our preliminary results as shown above the effectivity of anti-miR-145-5p role in interfering the target binding sites related to miR-145-5p and how does it effects the *CFTR Gene* mRNA and

protein content not only in non CF CALU-3 cells but also in CF cell lines such as CFBE e.g CFBE-41oΔF-508.

In the second part of our study, we analyzed the effects of the anti-miR-145-5p PNA on another cell line, in order to confirm the results obtained on Calu-3cells and propose this strategy for CF patients. For this purpose, we used the CFBE-41o ΔF-508 cell line in order to demonstrate the effects of this miR-145-5p interference on *CFTR Gene* at mRNA and protein level.

In the third part of our study, we tested a different approach to modify the biological activity of microRNAs, i.e. the strategy of masking the miRNA binding sites present within the 3'UTR region of the target mRNAs. The objective of this part of the study was to design a miRNA-masking PNA able to strongly interact with the binding sites of the miR-145-5p present within the 3'UTR of the CFTR mRNA and to determine its activity in inhibiting miR-145-5p function, with particular focus on the expression of both CFTR mRNA and CFTR protein in Calu-3 cells. The results obtained support the concept that the miR-145-masking PNA was able to interfere with miR-145-5p biological functions, leading to both an increase of CFTR mRNA and CFTR protein content.

Then we moved from Calu-3 cells to cystic fibrosis CFBE41o- cells having a genetic F508del/F508del background. We first employed two CFBE41o- cells lines, one carrying and overexpressing a plasmid containing WT CFTR sequences (CFBE41o-WT), the other carrying and overexpressing F508del CFTR (CFBE41o-F508del). In these cell lines, we tested various combined treatments using the miRNA-masking PNA with the Vertex compounds VX-809 (a CFTR corrector) and VX-770 (a CFTR potentiator) and observed results supporting the use of these combined treatments to develop possible therapeutic protocols for CF patients. It should be considered that these Vertex compounds which already validated and in use for experimental therapy of cystic fibrosis patients. But with the combination of these molecules with the miR-145-masking PNA we have shown in our studies significant increases level of CFTR protein by targetting the miR-145-5p function successfully. In this context, there are many other miRNAs and binding sites available which can be considered to design optimal miRNA-masking strategy to achieve target specific results. This strategy is sustained by the fact that specific targeting the CFTR in 3'UTR region for miR-145-5p sites increased CFTR expression and anion channel activity and further enhanced the effects of Ivacaftor/Lumacaftor in CFBEs.

The CFTR functional analysis was performed using CFBE41o- ΔF508del-YFP-CFTR cells, a cell line containing a plasmid over-expression ΔF508del CFTR and a reported plasmid (YFP). This cell line, was important to prove the fact that CFTR channels activity was enhanced after the different treatments employed.

In summary, we demonstrated that PNAs against miR-145-5p induce increase of CFTR in Calu-3 and CFBE41o-WT CFTR cells. In addition, we have studied specificity and efficacy of a PNA masking miR-145-5p binding sites, which was demonstrated to increase CFTR mRNA content. We have also studied these modifiers in combination with CFTR potentiators and correctors. The data obtained demonstrate that the maximum level of CFTR content is achieved in CFBE-41o-WT and CFBE-ΔF508 cells by combining miR145-maskingPNA with VX809 and VX770. In addition of that, CFTR functional analysis also proved that miR145-maskingPNA/VX809/VX770 combination was the most effective in stimulating CFTR-mediated chloride efflux in the CFBE41o- F508del CFTR YFP cell line. The major output was the identification protocols of interest in translational medicine, with the objective of modifying gene expression of cystic fibrosis cells, and, in particular, of increasing stability/expression of the CFTR protein. This therapeutic goal is very important for the treatment of cystic fibrosis.

A final part of this study was to validate the miRNA-masking strategy to other genetic disorders (β-thalassemia). For that purpose, we identified Krüppel-like factor (KLF4) as a very interesting gene to modulate; in fact, up-regulation of this gene might be associated with upregulation of gamma-globin genes and increase of fetal hemoglobin (HbF) which is a strategy to tackle β-thalassemia. As a first point, we reasoned that it was important to identify for this target gene the miRNAs possibly involved in its regulation. In this respect, miR-145-5p is known to repress KLF4. In addition, it is reported that KLF4 is a direct and functional target of miR-152.

In order to validate and describe possible effects of PNA masking in erythroid cells we identified K562 cells as a useful cellular model for our experiments. Therefore, we designed a masked PNA targeting miR-145-5p and miR-152-3p, and verified whether they were able to induce an increase of KLF-4 gene expression.

The results obtained demonstrated that treatment with these masking PNAs increases the expression of KLF-4 gene in the K562 cell line, associated with increased accumulation of γ-globin mRNA and hemoglobin production.

Despite the fact that these data should be confirmed using erythroid precursor cell from β-thalassemia patients, our approach is the proof of principle that the miRNA masking strategy might be employed to control KLF4 expression and to HbF induction.

ABSTRACT

La fibrosi cistica (CF, *cystic fibrosis*) è una malattia cronica che colpisce l'epitelio secretorio delle ghiandole sudoripare e biliari, del pancreas, dell'apparato digerente e respiratorio, con conseguente malnutrizione generalizzata e infezioni respiratorie croniche. È una patologia genetica autosomica recessiva; pertanto tutti gli individui con diagnosi clinica di CF presentano mutazioni in entrambi gli alleli del gene *cystic fibrosis transmembrane conductance regulator* (CFTR). Per molti anni è stata studiata la regolazione dell'espressione di CFTR da parte dei microRNA (miRNA) nella CF. In questo studio abbiamo cercato di modulare l'espressione dei miRNA utilizzando acidi peptido-nucleici (PNA) antagomiRNA e PNA di masking. I PNA sono degli strumenti molto utili per la regolazione genica a differenti livelli, ma, in particolare negli ultimi anni, il loro utilizzo nel bersagliare i miRNA ha permesso enormi progressi. Nello specifico, bersagliare i miRNA coinvolti nella repressione del gene CFTR, il quale è difettivo nella CF, è fondamentale nello sviluppo di nuovi tipi di protocolli terapeutici.

Gli obiettivi principali sono stati: (a) studiare la modulazione dell'espressione genica di CFTR usando PNA diretti contro miRNA implicati nella regolazione di CFTR (approccio antisenso); (b) e PNA, complementari alla sequenza 3'UTR dell'mRNA di CFTR, che mascherano i siti di legame dei miRNA (approccio di masking); (c) trattamenti combinati, con particolare attenzione all'utilizzo di correttori e potenziatori di CFTR; (d) convalidare l'approccio di masking dei miRNA nel modificare l'espressione di geni fondamentalli coinvolti in altre patologie genetiche, come ad esempio il gene KLF4 nella β-talassemia.

Nella prima parte del nostro studio, l'attenzione è stata posta sul PNA anti-miR diretto contro il microRNA miR-145-5p, il quale è ben noto essere un repressore dell'espressione di CFTR. L'octaaginine-anti-miR-145-5p PNA è stato addizionato alle cellule Calu-3 determinando un incremento dell'espressione di CFTR, regolato dal miR-145, sia a livello di mRNA che proteico. L'obiettivo di questo studio è stato di progettare un PNA diretto contro miR-145, determinarne l'attività di inibizione del miR-145, e verificare se inducesse un aumento della produzione di CFTR. Inoltre, i nostri risultati preliminari, come detto precedentemente, hanno mostrato l'efficacia di anti-miR-145-5p nell'interferire con i siti di legame del miR-145-5p al bersaglio, e come ciò influisca sull'mRNA del gene CFTR e sul contenuto proteico, non solo in cellule non fibrocistiche Calu-3, ma anche in linee cellulari di CF come CFBE (e.g. CFBE-41oΔF-508).

Infatti, nella seconda parte del nostro studio, abbiamo esteso l'analisi del PNA anti-miR-145-5p ad altre linee cellulari proprio per confermare i risultati ottenuti sulle cellule Calu-3 e proporre questa strategia per i pazienti CF. A tale scopo, abbiamo utilizzato la linea cellulare CFBE-41oΔF-508 per verificare gli effetti del anti-miR-145-5p PNA sul gene CFTR, sia a livello di mRNA che di contenuto proteico.

Nella terza parte del nostro studio, abbiamo analizzato un differente approccio per modificare l'attività biologica dei miRNA: la strategia di mascherare i siti di legame dei miRNA presenti nella regione 3'UTR dell'mRNA bersaglio. L'obiettivo di questo studio è stato quello di progettare un PNA che mascherasse il sito di legame del miR-145-5p sul 3'UTR dell'mRNA CFTR, e di determinare la sua attività nell'inibire la funzione di miR-145-5p, con particolare attenzione all'espressione sia dell'mRNA di CFTR che della relativa proteina nelle cellule Calu-3. I risultati ottenuti supportano il concetto che il PNA che maschera il sito di legame per miR-145-5p sull'mRNA CFTR è in grado di interferire con le funzioni biologiche di miR-145-5p, portando ad un aumento sia dell'mRNA CFTR che del contenuto proteico.

Successivamente abbiamo utilizzato le cellule fibrocistiche CFBE41o- (F508del/F508del). Abbiamo inizialmente impiegato due linee cellulari CFBE41o-, una che presenta un plasmide per la sovraespressione di CFTR wild type (CFBE-41o-WT), e l'altra che presenta un plasmide per la sovraespressione di CFTR F508del (CFBE-41o-F508del). In queste linee cellulari abbiamo testato vari trattamenti combinati di PNA di masking con composti Vertex (Correttore VX-809 e Potenziatore VX-770) e ottenuto risultati piuttosto favorevoli per proporre queste strategie combinate personalizzate ai pazienti.

Oltre a ciò, merita attenzione che questi composti Vertex sono già stati convalidati per l'utilizzo in pazienti fibrocistici. La combinazione di queste molecole con il miR-145-masking PNA ha mostrato un aumento significativo del livello di proteina CFTR andando a colpire con successo il miR-145-5p. Ci sono, però, ancora molti altri miRNA e siti di legame disponibili che possono essere utilizzati e colpiti per progettare una strategia di masking tale da ottenere risultati specifici per il bersaglio. Questa strategia è supportata dal fatto che l'azione specifica del PNA su CFTR nella regione 3'UTR, contenente i siti per miR-145-5p, ha aumentato l'espressione di CFTR e l'attività del canale anionico, e ha ulteriormente migliorato gli effetti con Ivacaftor/Lumacaftor in cellule CFBE41o-.

L'analisi funzionale di CFTR è stata fatta usando le cellule CFBE41o-ΔF-508-YFP-CFTR, una linea cellulare comprendente un plasmide per la sovraespressione di CFTR con

mutazione **Δ**F508 ed un altro per l'espressione di YFP. Questa linea cellulare è stata importante perché utilizzata per dimostrare il miglioramento dell'attività dei canali CFTR dopo i relativi trattamenti con diverse combinazioni terapeutiche.

In conclusione, abbiamo dimostrato che i PNA contro miR-145-5p inducono un aumento di CFTR nelle cellule Calu-3 e CFBE41o-WT. Inoltre, abbiamo studiato la specificità e l'efficacia di un PNA che maschera i siti di legame di miR-145-5p, che ha dimostrato di aumentare il contenuto di mRNA di CFTR. Abbiamo anche studiato questi modificatori in combinazione con potenziatori e correttori di CFTR. I dati ottenuti dimostrano che il livello massimo di contenuto di CFTR si ottiene in cellule CFBE-41o-WT e CFBE-ΔF508 combinando il miR145-maskingPNA con VX809 e VX770. Oltre a ciò, l'analisi funzionale di CFTR ha anche dimostrato che la combinazione miR145-maskingPNA/VX809/VX770 è stata la più efficace nello stimolare l'efflusso di ioni cloruro mediato da CFTR nella linea cellulare CFBE41o-ΔF-508-YFP-CFTR. Il risultato principale è stato l'identificazione di protocolli di interesse nella medicina traslazionale, con l'obiettivo di modificare l'espressione genica delle cellule fibrocistiche e, in particolare, di aumentare la stabilità/espressione della proteina CFTR. Questo obiettivo terapeutico è molto importante per il trattamento della CF.

La parte finale di questo studio ha previsto l'estensione di questa strategia di masking ad altre malattie genetiche (β-talassemia). A tale scopo abbiamo identificato il *Krüppel-like factor* (KLF4) come gene interessante da modulare; infatti, l'up-regolazione di questo gene potrebbe essere associata alla up-regolazione dei geni della gamma globina e all'incremento della emoglobina fetale (HbF), che è una delle strategie terapeutiche per fronteggiare la β-talassemia. In primo luogo, abbiamo ritenuto necessario identificare dei miRNA coinvolti nella regolazione di tale fattore. Il miR-145-5p è ben noto essere un repressore di KLF4. Inoltre, è riportato in letteratura che KLF4 è un bersaglio diretto del miR-152.

Allo scopo di identificare i possibili effetti del PNA masking nelle cellule eritroidi, abbiamo scelto le cellule K562 come modello cellulare per i nostri esperimenti. Pertanto, abbiamo progettato un PNA di masking contro miR-145-5p e uno contro miR-152-3p, e abbiamo verificato se fossero in grado di incrementare l'espressione KLF4.

I risultati ottenuti hanno dimostrato che il trattamento con questi PNA di masking, oltre ad incrementare l'espressione genica di KLF4 nelle cellule K562, aumentano i livelli dell'mRNA della gamma globina e la produzione di emoglobina.

Anche se questi dati necessitano di essere confermati impiegando precursori eritroidi derivanti da pazienti talassemici, l'approccio da noi proposto è la dimostrazione che la strategia di masking dei miRNA potrebbe essere impiegata per controllare l'espressione di KLF4 e l'induzione di HbF.

1. INTRODUCTION

1.1. Cystic Fibrosis

Cystic fibrosis (CF) affects secretory epithelium of the sweat and biliary glands, pancreas, the digestive and respiratory tracts, resulting in generalized malnutrition and chronic respiratory infections. It is an autosomal recessive genetic disease; therefore all individuals diagnosed clinically with CF have mutations in both *CFTR Gene* alleles. CF affects about 85,000 persons worldwide, 1 newborn out of 3,500 in the USA (WHO) and 1 per 2,000-3,000 in Europe with an average 40-year life expectancy. Life expectancy in CF has improved substantially over the last 75 years because of earlier diagnosis and better treatments aimed at end-organ complications. Survival is estimated to be 40 years for men and 37 for women, a great breakthrough considering that the median age of survival of children with CF in 1959 was six months. Obviously, being a chronic illness, is very difficult to manage and can compromise the quality of life (QOL) of the patients [Dekkers et al., 2016; Palomo et al., 2014].

CF, although being a rare disease, is the most common life-shortening genetic defect in Caucasian. Around 1 in 25 people of European descent is carrier of a CF mutation. Heterozygote advantage could be the reason why such a lethal mutation has persisted and spread in human population. Resistance to the following have all been proposed as possible sources of heterozygote advantage: cholera (because cholera toxin requires normal host CFTR to function properly), typhoid (because *Salmonella Typhi* needs normal CFTR for entry into cells), tuberculosis but there are confirmations yet [Dekkers et al., 2016; Palomo et al., 2014; Prickett et al., 2013].

This pathology is caused by mutations within the *Cystic Fibrosis Transmembrane conductance Regulator* (CFTR) gene that encodes an epithelial anion channel [Dekkers et al., 2016; Palomo et al., 2014; Prickett et al., 2013]. A wide spectrum of phenotypes (www.CFTR2.org), including CF or milder single-organ CFTR-related diseases, are correlated to approximately 2000 CFTR mutations identified (www.genet.sickkids.on.ca) [Dekkers et al., 2016].

The most common mutation, discovered by Francis Collins,Lap-Chee Tsui, and John R. Riordan [Vijftigschild et al., 2016] is a deletion of phenylalanine at position 508 (p.Phe508del, F508del), estimated to be up to 52,000 years old and it is present in about 90% of subjects with CF, of which ~65% are F508del homozygotes (www.genet.sickkids.on.ca).

Besides CF disease expression is highly variable between subjects due to the complex relations between CFTR genotype, modifier genes, epigenetic components and environmental factors, which are unique for each individual [Vijftigschild et al., 2016].

Many of the basic genetic, physiological, and clinical consequences associated with CF have been studied in great detail, making CF one of the most investigated diseases in modern medicine [Griesenbach and Alton., 2011; Cohen and Prince., 2012].

Being an autosomal recessive disorder that affects approximately one in 2500 births among most Caucasian populations, though its frequency may vary in specific groups.CF is caused by mutations in a single gene on chromosome 7 that encodes the cystic fibrosis transmembrane conductance regulator (CFTR) which functions as a chloride channel in epithelial membranes.

1.1.1. HISTORY

Until the 1930s, the entire clinical spectrum of CF was not recognized, certain aspects of CF were identified much earlier. Indeed, literature from Germany and Switzerland in the 1700s warned ‘’Wehe dem Kind, das beim Kuß auf die Stirn salzig schmekt, er ist verhext und muss bald sterbe’’ or "Woe is the child who tastes salty from a kiss on the brow, for he is cursed, and soon must die," recognizing the association between the salt loss in CF and illness [Busch .R., 1990]. In the 19th century, Carl von Rokitansky described a case of fetal death with meconium peritonitis, a complication of meconium ileus associated with cystic fibrosis. Meconium ileus was first described in 1905 by Karl Landsteiner. In 1936, Guido Fanconi published a paper describing a connection between celiac disease, cystic fibrosis of the pancreas, and bronchiectasis [Fanconi G et al., 1936].

In 1938 Dorothy Hansine Andersen published an article, "Cystic Fibrosis of the Pancreas and Its Relation to Celiac Disease: a Clinical and Pathological Study," in the American Journal of Diseases of Children. She was the first to describe the characteristic cystic fibrosis of the pancreas and to correlate it with the lung and intestinal disease prominent in CF [Andersen DH et al., 1938]. She also first hypothesized that CF was a recessive disease and first used pancreatic enzyme replacement to treat affected children. In 1952 Paul di Sant' Agnese discovered abnormalities in sweat electrolytes; a sweat test was developed and improved over the next decade [Di Sant PA et al., 1953].

In 1988 the first mutation for CF, ΔF508 was discovered by Francis Collins, Lap-Chee Tsui and John R. Riordan on the seventh chromosome. Subsequent research has found over 1,000 different mutations that cause CF. Because mutations in the *CFTR Gene* are typically small, classical genetics techniques had been unable to accurately pinpoint the mutated gene [Riordan JR et al., 1989]. Using protein markers, gene-linkage studies were able to map the mutation to chromosome 7. Chromosome-walking and -jumping techniques were then used to identify and sequence the gene [Rommens JM et al., 1989]. In 1989 Lap-Chee Tsui led a team of researchers at the Hospital for Sick Children in Toronto that discovered the gene responsible for CF in 1989. Cystic fibrosis represents the first genetic disorder elucidated strictly by the process of reverse genetics.

1.1.2. CLINICAL ASPECTS

Expression of the cystic fibrosis transmembrane conductance regulatory gene is found in areas that are lined with epithelial tissue. Some of these places include ciliated epithelium of high airways, the gastrointestinal tract, salivary and sweat glands, cervix, uterus, fallopian tubes, epididymis and the vas deferens. These tissues all show some form of pathological involvement with cystic fibrosis **[Figure1.1]**.

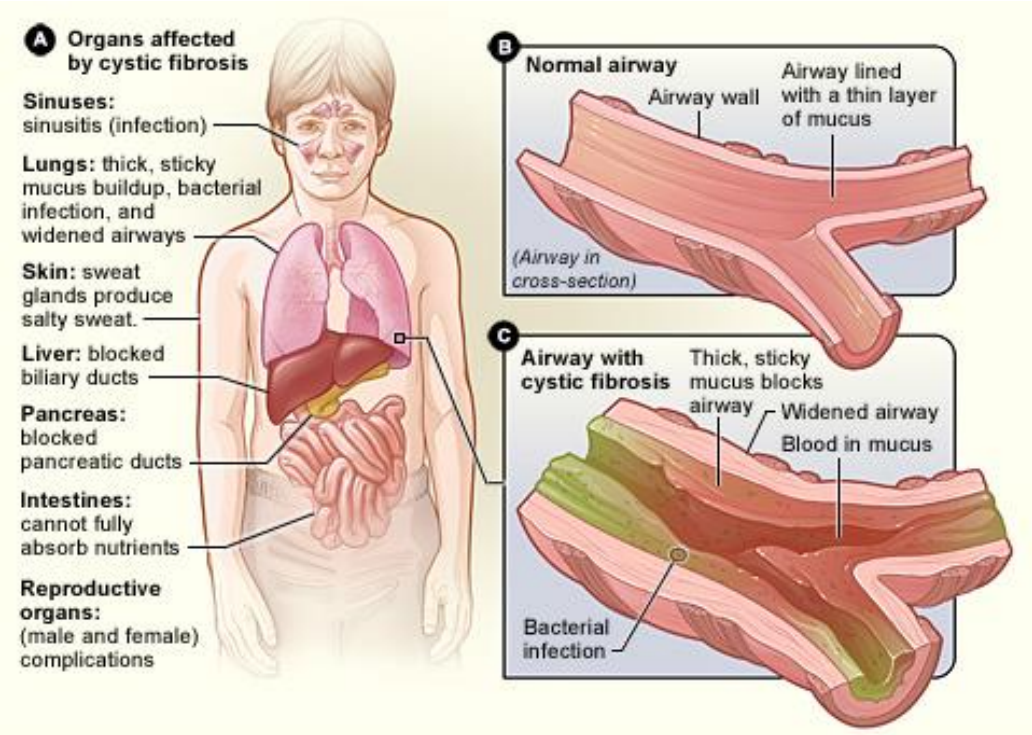

Figure 1.1: Pathological involvement in cystic fibrosis. Picture taken from https://www.physio-pedia.com/File:Cysticfibrosis.

1.1.2.1. Pulmonary effects

Lung disease is the major cause of morbidity and virtually all mortality: in patients with cystic fibrosis, progression of lung disease is insidious and patients may be relatively asymptomatic before irreversible changes and chronic bacterial colonization occur. The first detectable evidence of lung disease in patients with cystic fibrosis is infection and inflammation in Broncho alveolar lavage fluid (BLF), denoted by elevated counts of interleukin-8 and neutrophils and the presence of microorganisms [Khan TZ et al., 1995, Balough K et al., 1995]. Overall, *Pseudomonas aeruginosa* (PAO) is the most common isolate, followed by Haemophilus influenza and Staphylococcus aureus: chronic colonization with *P. aeruginosa* is associated with a more rapid decline in lung function [Govan JR et al., 1996, Schaedel C et al., 2002].

An exaggerated, sustained and axtended inflammatory response to bacterial and viral pathogens – characterized by neutrophil dominated airway inflammation – is the feature of lung disease in cystic fibrosis. Inflammation is present even in clinically stable patients with some lung disease and in young infants diagnosed by neonatal screening. Quantification of airway inflammation is necessary to monitor its evolution over time and the effect of anti-inflammatory treatment. This monitoring remains a difficult task, since reliable non invasive markers of airway inflammation are not available.

1.1.2.2. Gastrointestinal, liver and pancreatic Effects

Prior to prenatal and newborn screening, cystic fibrosis was often diagnosed when a newborn infant failed to pass feces (meconium). Meconium may completely block the intestines and cause serious illness. This condition, called meconium ileus, occurs in 10% of newborns with CF [Eggermont E et al., 1991]. In addition, protrusion of internal rectal membranes (rectal prolapse) is more common in CF because of increased fecal volume, malnutrition, and increased intra–abdominal pressure due to coughing [Kulczycki LL et al., 1958]. The thick mucus seen in the lungs has a counterpart in thickened secretions from the pancreas, an organ responsible for providing digestive juices that help break down food. These secretions block the movement of the digestive enzymes into the duodenum and result in irreversible damage to the pancreas, often with painful inflammation (pancreatitis) [Cohn JA et al., 1998]. The lack of digestive enzymes leads to difficulty absorbing nutrients with their subsequent excretion in the feces, a disorder known as malabsorption. Malabsorption leads to malnutrition and poor growth and development because of caloric loss. Individuals

with CF also have difficulties absorbing the fat-soluble vitamins A, D, E, and K. In addition to the pancreas problems, CF patients experience more heartburn, intestinal blockage by intussusception, and constipation [Malfroot A et al., 1991]. Older CF patients may also develop distal intestinal obstruction syndrome when thickened feces cause intestinal blockage [Khoshoo V et al., 1994]. Thickened secretions also may cause liver problems in patients with CF. Bile secreted by the liver to aid in digestion may block the bile ducts, leading to liver damage. Over time, this can lead to cirrhosis, in which the liver fails to rid the blood of toxins and does not produce important proteins such as those responsible for blood clotting [William SG et al., 1992, Colombo C et al., 2006].

1.1.2.3. Endocrinal effects

The pancreas contains the islets of Langerhans, which are responsible for making insulin, a hormone that helps regulate blood glucose. Damage of the pancreas can lead to loss of the islet cells, leading to a type of diabetes that is unique to those with the disease [Moran A et al., 1994]. This Cystic Fibrosis Related Diabetes (CFRD) shares characteristics that can be found in Type 1 and Type 2 diabetics and is one of the principal non-pulmonary complications of CF [Alves Cde A et al., 2007].

1.1.2.4. Osteoporosis

Vitamin D is involved in calcium and phosphorus regulation. Poor uptake of vitamin D from the diet because of malabsorption can lead to the bone disease osteoporosis in which weakened bones are more susceptible to fractures [Haworth CS et al., 1999]. In addition, CF patients often develop clubbing of their fingers and toes due to the effects of chronic illness and low oxygen in their tissues.

1.1.2.5. Infertility

Infertility affects both men and women. At least 97 percent of men with cystic fibrosis are infertile but are not sterile and can have children with assisted reproductive techniques [McCallum TJ et al., 2000]. These men make normal sperm but are missing the tube (vas deferens), which connects the testes to the ejaculatory ducts of the penis [Dodge JA et al., 1995]. Many men found to have congenital absence of the vas deferens during evaluation for infertility have a mild, previously undiagnosed form of CF [Augarten A et al., 1994]. Some women have fertility difficulties due to thickened cervical mucus or malnutrition. In severe cases, malnutrition disrupts ovulation and causes amenorrhea [Gilljam M et al., 2000].

1.2. DIAGNOSIS AND MONITORING

Cystic fibrosis may be diagnosed by many different categories of testing including those such as, newborn screening, sweat testing, or genetic testing. The newborn screen initially measures for raised blood concentration of immunoreactivity trypsinogen [Davies JC et al., 2007]. Infants with an abnormal newborn screen need a sweat test in order to confirm the CF diagnosis. Trypsinogen levels can be increased in individuals who have a single mutated copy of the *CFTR Gene* (carriers) or, in rare instances, even in individuals with two normal copies of the *CFTR Gene*. Due to these false positives, CF screening in new-borns is somewhat controversial [Ross LF et al., 2008, Assael BM et al., 2002]. Therefore, most individuals are diagnosed after symptoms prompt an evaluation for cystic fibrosis. The most commonly used form of testing is the sweat test. Sweat-testing involves application of a medication that stimulates sweating (pilocarpine) to one electrode of an apparatus and running electric current to a separate electrode on the skin. This process, called iontophoresis, causes sweating; the sweat is then collected on filter paper or in a capillary tube and analyzed for abnormal amounts of sodium and chloride. CF patients have increased amounts of sodium and chloride in their sweat **[Figure1.2]**. CF can also be diagnosed by identification of mutations in the *CFTR Gene* [Stern RC et al., 1997].

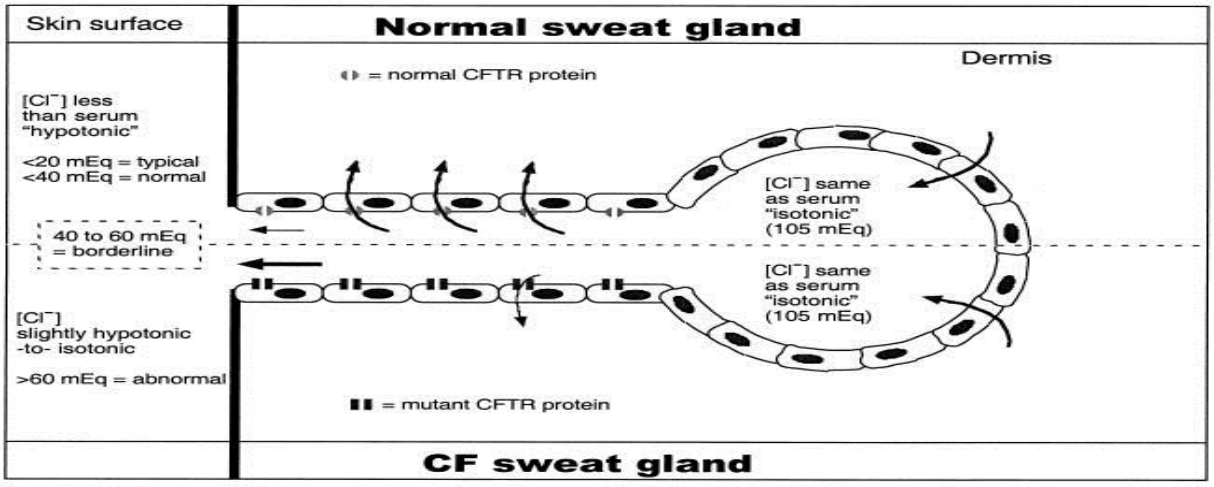

Figure 1.2: Diagram of a sweat gland, showing paths taken by chloride ions (arrows) during secretion. In both normal and CF sweat glands in the dermis, chloride is present in secretions at a concentration of 105 mEq, equaling that in serum ("isotonic"). (Top) In the normal sweat gland, chloride is absorbed out of the sweat in a CFTR-dependent manner as the sweat travels from the gland to the skin surface. As a result, the chloride concentration in normal sweat is below that in serum ("hypotonic"), with <40 mEq considered normal and <20 mEq being typical. (Bottom) In the CF sweat gland, chloride absorption is hindered by defective CFTR function. As a result, sweat which reaches the skin surface has higher than normal chloride concentrations (>60 mEq).

A multitude of tests are used to identify complications of CF and to monitor disease progression. X-rays and CAT scans are used to examine the lungs for signs of damage or infection. The examination of the sputum is required to isolate organisms which may be causing an infection or colonising the lower respiratory tract so that effective antimicrobial therapy can be provided. Culture for organisms such as Pseudomonas aeruginosa is required for candidates of lung transplantation as persistent bacterial colonisation reduces the chances of survival.

Pulmonary function tests measure how well the lungs are functioning, and are used to measure the need for and response to antibiotic therapy. Blood tests can identify liver abnormalities, vitamin deficiencies, and the onset of diabetes. DEXA scans can screen for osteoporosis and testing for faecal elastase can help diagnose insufficient digestive enzymes.

1.2.1. PARENTAL DIAGNOSIS

Couples who are pregnant or who are planning a pregnancy can themselves be tested for *CFTR Gene* mutations to determine the degree of risk that their child will be born with cystic fibrosis. Testing is typically performed first on one or both parents and, if the risk of CF is found to be high, testing on the fetus can then be performed. Because development of CF in the fetus requires each parent to pass on a mutated copy of the *CFTR Gene* and because CF testing is expensive, testing is often performed on just one parent initially. If that parent is found to be a carrier of a *CFTR Gene* mutation, the other parent is then tested to calculate the risk that their children will have CF. CF can result from more than a thousand different mutations and it is not possible to test for each one. Testing analyses the blood for the most common mutations such as ΔF508 - most commercially available tests look for 32 or fewer different mutations. If a family has a known uncommon mutation, specific screening for that mutation can be performed. Because not all known mutations are found on current tests, a negative screen does not guarantee that a child will not have CF [Elias S et al., 1991]. In addition, because the mutations tested are necessarily those most common in the highest risk groups, testing in lower risk ethnicities is less successful because the mutations commonly seen in these groups are less common in the general population. Couples who are at high risk for having a child with CF will often opt to perform further testing before or during pregnancy. In vitro fertilization with preimplantation genetic diagnosis offers the possibility to examine the embryo prior to its placement into the uterus. The test, performed three days after fertilization, looks for the presence of abnormal CF genes. If two mutated *CFTR Gene*s

are identified, the embryo is not used for embryo transfer and an embryo with at least one normal gene is implanted. During pregnancy, testing can be performed on the placenta (chorionic villus sampling) or the fluid around the foetus (amniocentesis).

1.3. CFTR: CYSTIC FIBROSIS TRANSMEMBRANE CONDUCTANCE REGULATOR

1.3.1. CFTR PROTEIN

Cystic fibrosis transmembrane conductance regulator (CFTR) is a phosphorylation-dependent epithelial Cl- channel. It is located primarily in the apical membrane, where it provides a pathway for Cl- movement across epithelia and regulates the rate of Cl- flow. Thus, CFTR is central in determining trans epithelial salt transport, fluid flow, and ion concentrations. In the intestine, pancreas, and sweat gland secretory coil, CFTR plays a key role in fluid and electrolyte secretion, and in sweat gland duct and airway epithelia, it participates in fluid and electrolyte absorption.

CFTR can also regulate other membrane proteins [Stutts MJ et al., 1997]. The most thoroughly documented regulatory role for CFTR is its negative regulation of the amiloride-sensitive epithelial Na+ channel (ENaC). CFTR decreases ENaC's open probability (Po) and reverses its usual increases to elevations of [cAMP]i [Knowles MR et al., 1983]. When CFTR function is lost, the Na+ conductance is markedly increased in CF human airways [Grubb BR et al., 1994] and CF mouse nasal epithelia [Reddy MM et al., 1997], but apparently not in human sweat ducts [Stutts MJ et al., 1995]. CFTR's channel and regulatory [Hyde SC et al., 1990] functions require that it has to be phosphorylated by various kinases, especially cAMP-dependent protein kinase (PKA).

To summarize, CFTR is an anion channel and a channel regulator that plays multiple roles in epithelial transport. Although other functions have been proposed for CFTR, most present hypotheses of CF disease emphasize CFTR's roles in ion transport. Besides chloride transport, CFTR is also a bicarbonate channel, with important implications **[Figure1.3].**

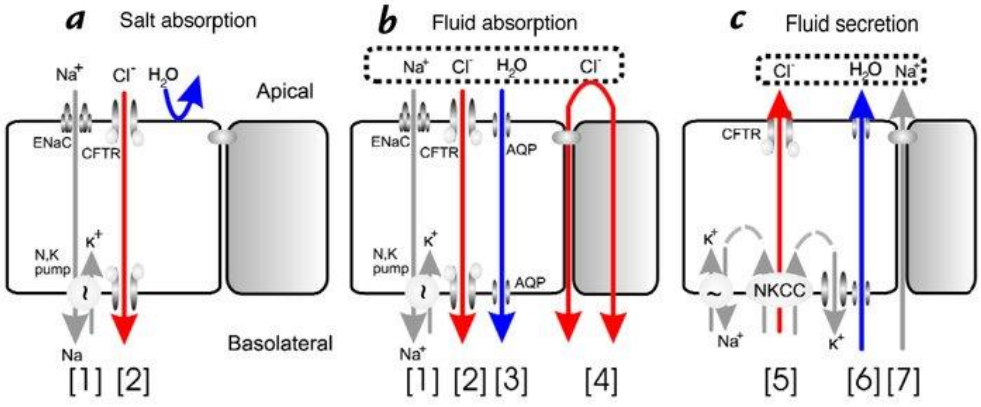

FIGURE 1.3: CFTR's multiple roles in fluid and electrolyte transport. (a) Salt absorption. In the sweat duct, high apical conductance for Na+ [1] and Cl– [2] and relatively low water conductance allows salt to be reabsorbed in excess of water (hypertonic absorption) leaving a hypotonic luminal fluid. In the sweat duct CFTR is the only available anion conductance pathway, and when it is lost in CF the lumen quickly becomes highly electronegative and transport virtually ceases, resulting in high (similar to plasma) luminal salt. **(b)** Fluid absorption. In epithelia with high water permeability [3] relative to electrolyte permeability water will absorbed osmotically with salt to decrease the volume of luminal fluid. If no other osmolytes or forces are present, the salt concentration will remain unchanged. If water-retaining forces are present, permeant electrolytes can be reduced preferentially. The consequences of eliminating CFTR depend on the magnitude of such forces, the relative magnitude of alternate pathways for transepithelial anion flow [4], and how CFTR affects other ion channels. The high salt and low volume hypotheses differ on each of these points. **(c)** Anion-mediated fluid secretion. Secreting epithelia lack a significant apical Na+ conductance. Basolateral transporters such as NKCC move Cl– uphill into the cell; it then flows passively into the lumen via CFTR [5], K+ exits basolaterally, Na+ flows paracellularly [7] and water follows transcellularly [6]. Elimination of CFTR eliminates secretion [Wine., 1999].

CFTR is a member of the ATP-binding cassette (ABC) transporter family, and it contains the features characteristic of this family: two nucleotide binding domains (NBDs) and two six-membrane-spanning domains (MSDs) **[Figure1.4]**.

Moreover, CFTR also contains the R domain (RD), a unique sequence not found in other ABC transporters or any other proteins. The R domain serves as the major physiologic regulator of the CFTR Cl- channel. When cAMP level increase, cAMP-dependent protein kinase (PKA) phosphorylates the multiple serine residues within the R domain allowing ATP to open the channel.

PKA is the primary kinase that phosphorylates CFTR, although protein kinase C, cGMP-dependent protein kinase, and tyrosine phosphorylation can also stimulate channel activity [Myles H et al., 2000].

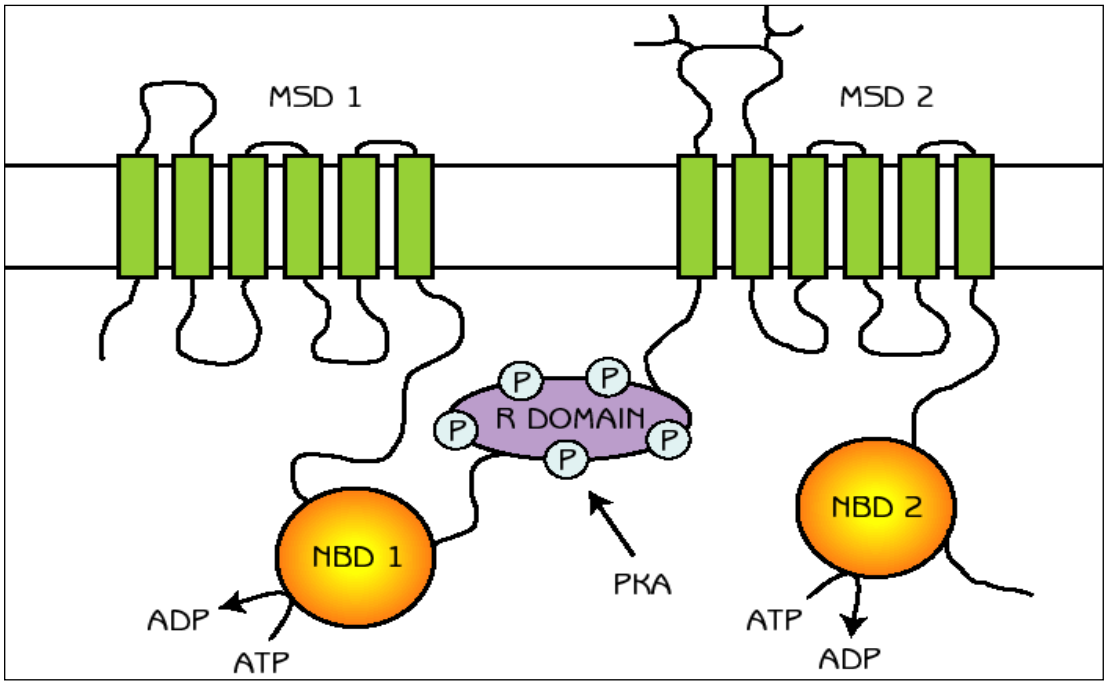

Figure 1.4: Model showing proposed domain structure of cystic fibrosis transmembrane conductance regulator (CFTR). MSD, membrane-spanning domain; NBD, nucleotide-binding domain; R, regulatory domain; PKA, cAMP-dependent protein kinase. [59]

Once the R domain is phosphorylated, channel gating is regulated by a cycle of ATP hydrolysis at the NBDs. Finally, protein phosphatases dephosphorylate the R domain and return the channel to its quiescent state. At the moment, how phosphorylation activates the channel is not well understood. Some models propose that the R domain prevents the channel from opening and that phosphorylation relieves this inhibition. Other models suggest that phosphorylation of the R domain stimulates activity.

These channels have several distinguishing characteristics:

- They have a small single-channel conductance (6–10 pS).
- The current-voltage (I-V) relationship is linear.
- They are selective for anions over cations.
- The anion permeability sequence is $Br^- \geq Cl^- > I^-$.
- They show time- and voltage-independent gating behaviour.
- Their activity is regulated by cAMP-dependent phosphorylation and by intracellular nucleotides. These features are conferred on CFTR Cl^- channels by the function of the MSDs, the NBDs, and the R domain.

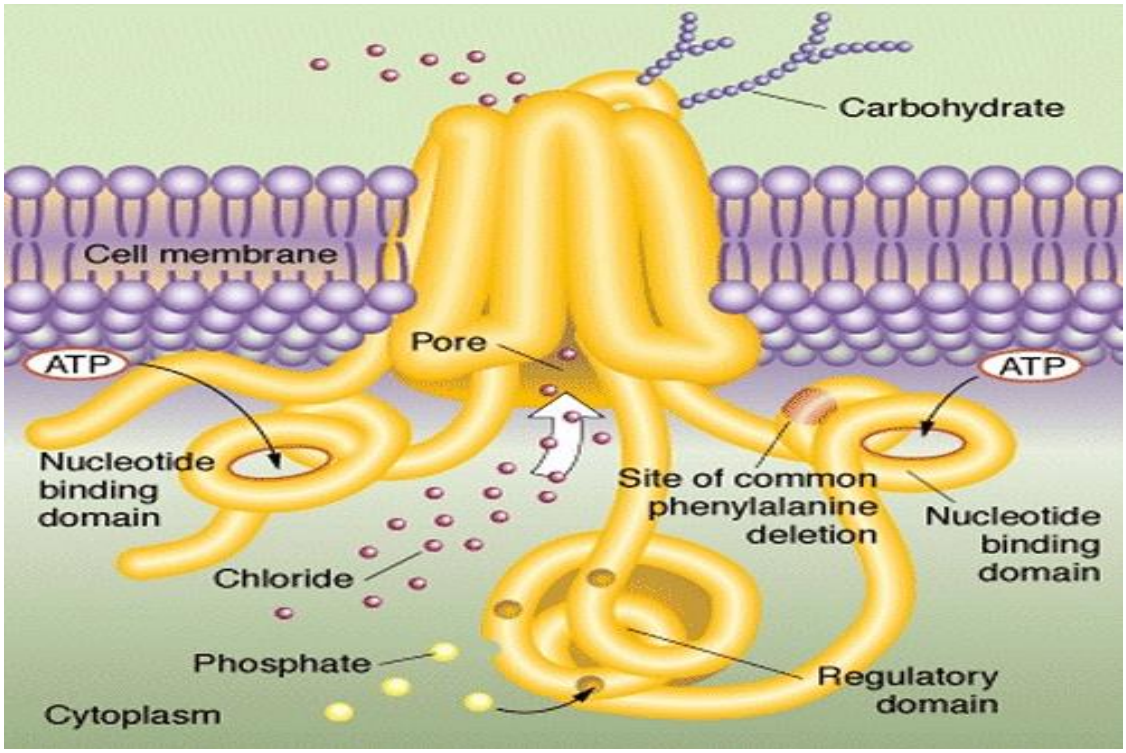

Figure 1.5: CFTR structure; Picture taken from http://www.cfgenetherapy.org.uk/.

In the proposed transmembrane topology **[Figure1.5]**, which is supported by experimental evidence [Riordan JR et al., 1989, Sheppard DN et al., 1999], 77% of the protein is in the cytoplasm, 19% in membrane spanning segments, and 4% in extracellular loops.

The minimum channel diameter was inferred to be 5.3 Å based on the size of the largest permeant anion [Linsdell P et al., 1997]. Further studies using patches with larger numbers of channels showed that anions as large as lactobionate (10–13 Å in diameter) were slightly permeable. Thus, at least transiently, the diameter of the channel must be 10–13 Å. In the presence of cytoplasmic ATP the large anions were only permeable from the cytoplasmic side [Linsdell et al., 1998]. The molecular basis for asymmetric permeation by large anions is unknown.

1.3.2. THE *CFTR GENE*

The gene responsible for CFTR was identified to reside on the long arm of chromosome 7 (7q.31.2) and subsequently isolated by positional cloning in 1989 [3-5, 75].

Availability of the gene sequence and direct mutation analysis were turning points in the history of CF and opened a new chapter of molecular and cellular studies in CF research.

The gene, named the CF transmembrane conductance regulator (CFTR), consists of a TATA-less promoter and 27 exons spanning about 215 kb of genomic sequence **[Figure 1.6-a]** [Zielenski et al., 1991]. The *CFTR Gene* encodes a 170 kDa (1480 amino acids) transmembrane protein with a symmetrical, multi-domain structure, consisting of two membrane-spanning domains (MSD1, MSD2), two nucleotide-binding domains (NBD1, NBD2) and a central, highly charged regulatory domain (RD) with multiple phosphorylation consensus sites **[Figure 1.6b-c]** [Riordan et al., 1989]. The principal function of CFTR is that of cAMP-regulated chloride transport at the apical membranes of epithelial cells but has also been implicated in many other processes such as regulation of other ion channels, membrane trafficking, pH regulation and apoptosis.

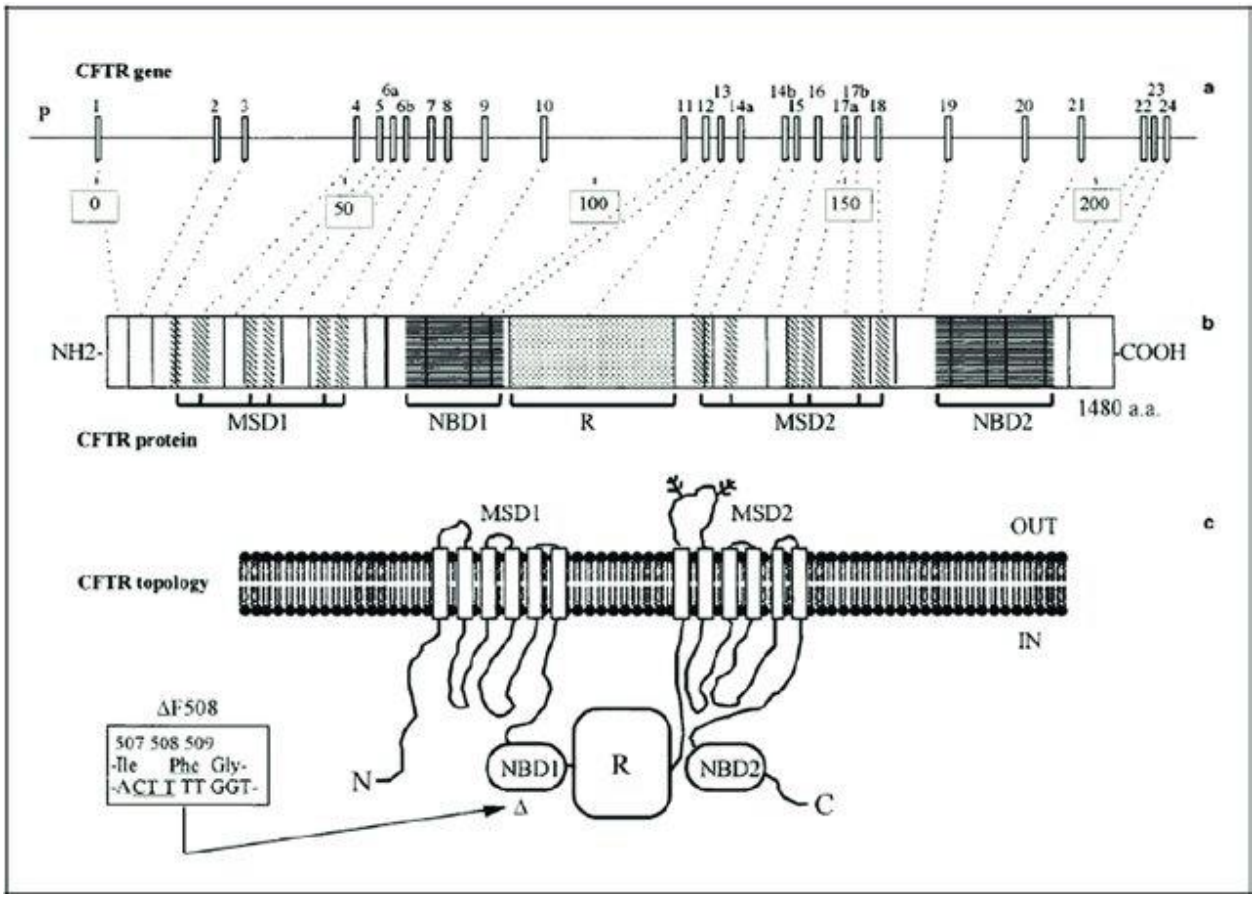

Figure 1.6: Schematic diagram of the *CFTR Gene*. (a) Structure of the *CFTR Gene* consisting of promoter region (P) and 27 exons. The size of the introns is based on the sequences of genomic BAC clones 068P20 and 133K23 (submitted to GenBank by Washington University). (b) CFTR polypeptide with predicted domains (highlighted). (c) Topology of the CFTR protein relative to the cytoplasmic membrane and position of the most common mutation, ΔF508. MSD1 and MSD2 = Membrane spanning domains 1 and 2; NBD1 and NBD2 = nucleotide-binding domains 1 and 2; R = regulatory domain. Box: Deletion of 3 nucleotides, CTT (underlined), and subsequent loss of phenylalanine (underlined) at position 508 of the CFTR protein. [Zielenski J et al., 1991]

1.3.3. CFTR MUTATIONS

The first, and as it turned out, the most common CFTR defect identified among Caucasians was the ΔF508 mutation [fig.11], a 3-bp deletion in exon 10 causing a loss of phenylalanine at the amino acid position 508 of the protein product [fig. 8c][Kerem B et al., 1989]. Presently, 10 years after the discovery of the *CFTR Gene*, more than 850 different alleles have been reported as proven or putative disease causing mutations (CFGAC website: http://www.genet.sickkids.on.ca/cftr/).

All types of mutations are represented (missense, frameshift, nonsense, splice, small and large in-frame deletions or insertions), and are distributed throughout the entire gene **[Figure1.7]**. The potential of a mutation to contribute to the severity of a CF phenotype depends on multiple factors.

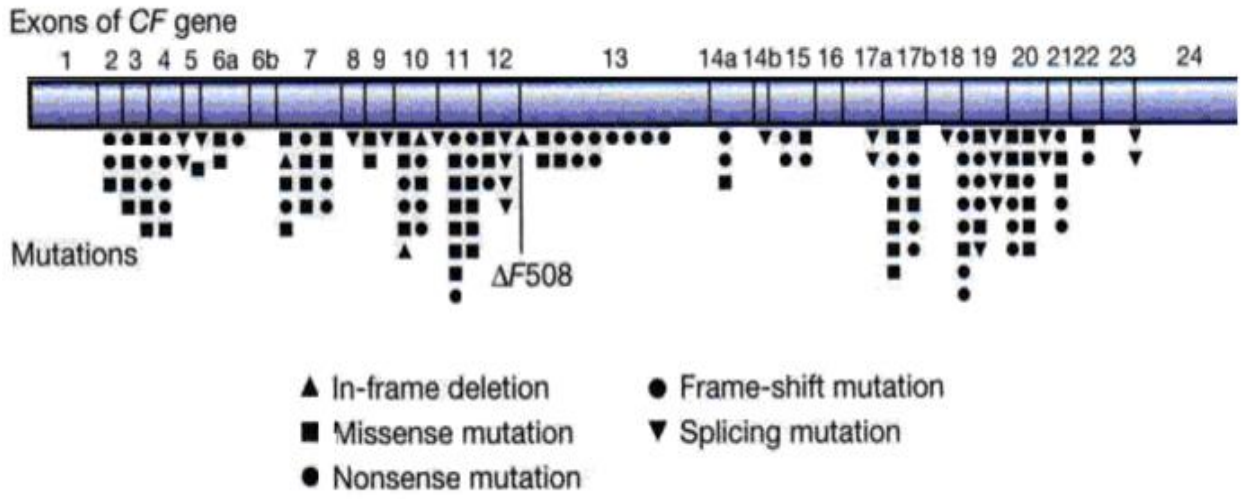

Figure 1.7: Over 550 different mutations have been characterised in the CF gene CFTR.

Firstly, it is inherent to a characteristic mutation profile on the molecular and cellular levels as determined by its type (A), class (B) and position in the gene (C). Secondly, it depends on the other intragenic factors (E) such as a presence of other changes within the gene (complex allele), influence of a second mutation in the genotype (F) and secondary genetic and environmental factors associated with a pathogenesis of the affected organ (G). Due to a large number of disease-contributing mutations affecting the function of the *CFTR Gene* to a different degree, a CFTR genotype has high potential as a primary source of phenotypic variability in CF.

1.3.3.1. MOLECULAR MECHANISMS OF CFTR MUTATIONS

Various mutations can be grouped into different classes **[Figure 1.8]** based on their known or predicted molecular mechanisms of dysfunction and functional consequences for the CFTR protein. Although schematic, such classification can often be a good indication of a mutation's severity and provides a rationale for their phenotypic consequences.

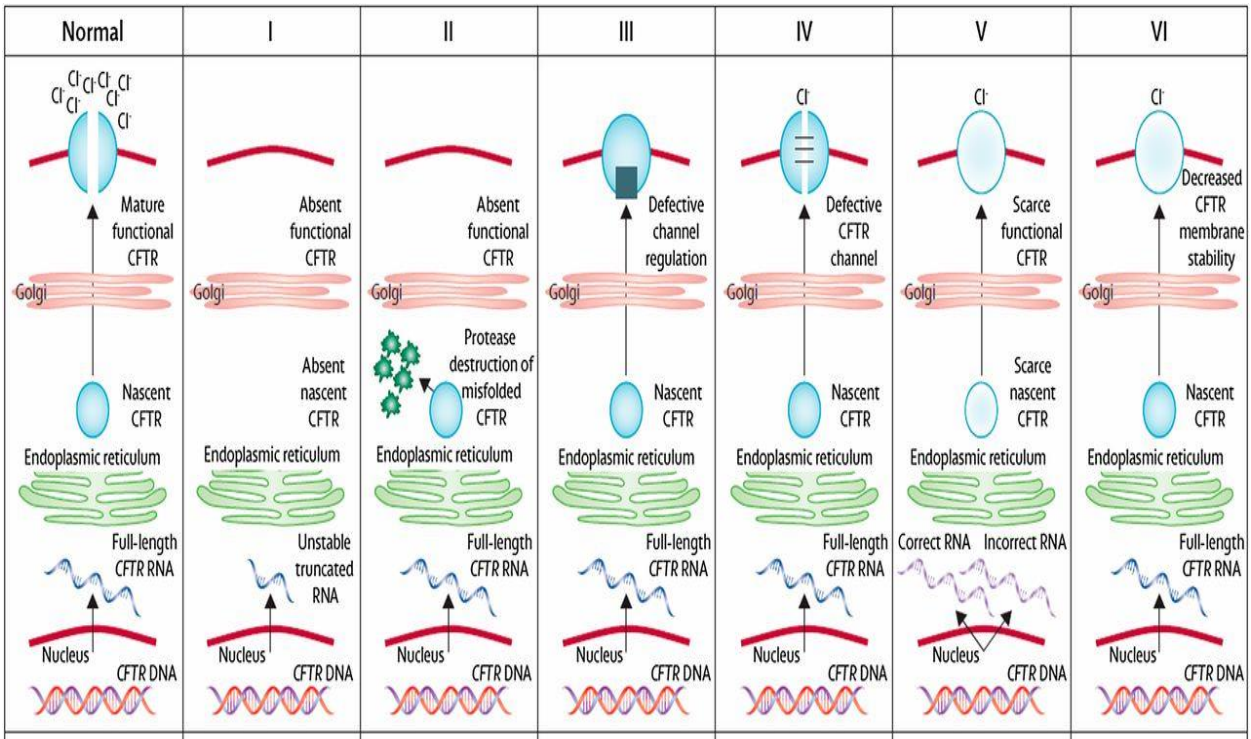

Figure 1.8: Six classes of CFTR Mutations. CFTR mutations have been grouped into 6 distinct classes based on abnormalities of CFTR synthesis, structure, and function. Reprinted from The Lancet Respiratory Medicine, Vol. 1, Issue 2, Boyle MP, DeBoeck K, "A new era in the treatment of cystic fibrosis: correction of the underlying CFTR defect," pages 158–163, (C) April 2013, with permission from Elsevier.

- CLASS I: DEFECTIVE PROTEIN SYNTHESIS

Net Effect: No CFTR Protein at the Apical Membrane. Mutations that belong to this category are associated with lack of biosynthesis or defective biosynthesis producing abnormal protein

variants (truncation, deletion, etc.). These are usually nonsense, frameshift, RNA splice-type mutations or missense mutations changing translation initiation codon (methionine at position 1). Due to their grossly altered structure, they tend to be unstable and efficiently cleared from the cell. In effect, virtually no functional CFTR is present at the apical membrane of the epithelial cells and as a consequence phenotypic effects of class I mutations tend to be severe.

- CLASS II: ABNORMAL PROCESSING AND TRAFFICKING

Net Effect: No CFTR Protein at the Apical Membrane. Many *CFTR Gene* variants expressed in various heterologous systems fail to be properly processed to a mature glycosylated form and transported to the apical membrane. Because of their absence in the membrane, these mutant CFTR variants are typically associated with severe CF phenotypes. Interestingly, some of the class II mutations – such as the most common ΔF508 mutation **[Figure1.9]** – if correctly processed, possess residual Cl channel activity and may lead to a sustained normal or only mildly affected phenotype. For this reason, mutations in this group – in particular the common ΔF508 deletion – are the targets of potential therapies, aimed at correcting the processing and delivery of a mutated CFTR protein to the apical membrane.

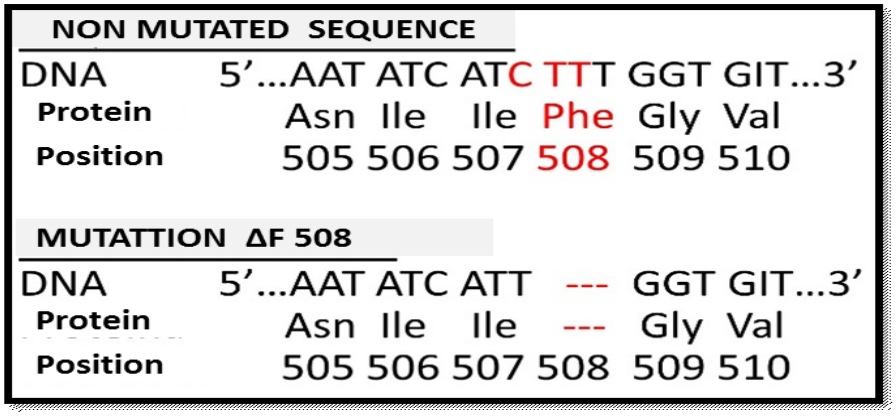

Figure 1.9: The ΔF508 deletion is the most common cause of cystic fibrosis.

Recent studies of endogenous CFTR expression in CF-relevant epithelial tissues from patients homozygous for the ΔF508 mutation demonstrated however that immunolocalized distribution of CFTR in certain tissues (respiratory and intestinal) is indistinguishable from that observed in the corresponding wild-type cells [Kalin N et al., 1999]. The ΔF508 CFTR protein was absent only in sweat gland ducts of those patients. It is still possible that the ΔF508 CFTR is compartmentalized in vesicles in close proximity to the cell membrane and

therefore gives the appearance of being embedded in the membrane. It should be noted, however, that the efficiency of processing and trafficking of the ΔF508 CFTR protein may vary conside ably between different epithelial cells. Therefore, different intracellular conditions may result in variable severity of tissue- or organ-specific pathophysiology.

- CLASS III: DEFECTIVE REGULATION

Net Effect: Normal Amount of Nonfunctional CFTR at the Apical Membrane. Mutations in this class affect the regulation of CFTR function by preventing ATP binding and hydrolysis at the nucleotide binding domains (NBD1; NBD2) required for the channel activation. Alterations within NBD1 (such as missense mutation G551D) may also affect CFTR regulation of other channels such as the outwardly rectifying chloride channel [Fulmer SB et al., 1995] or ROMK2 potassium channel [McNicholas CM et al., 1996]. This is an example of a mutation mechanism which affects some regulatory functions of CFTR in addition to its chloride transporting function.

- CLASS IV: DECREASED CONDUCTANCE

Net Effect: Normal Amount of CFTR with Some Residual Function at the Apical Membrane. Several mutations (R117H, R334W, R347P) were shown to affect the properties of CFTR single-channel conductance [Sheppard DN et al., 1993]. Interestingly, these mutations are located within MSD1 which is implicated in forming the pore of the channel [Akabas MH et al., 1994] and the corresponding CFTR variants retain residual function. Alleles in this class are typically associated with a milder pancreatic phenotype: this includes patients with pancreatic sufficiency (PS).

- CLASS V: REDUCED SYNTHESIS/TRAFFICKING

Net Effect: Reduced Amount of Functional CFTR at the Apical Membrane. Various mutations may be associated with reduced biosynthesis of fully active CFTR due to partially aberrant splicing (3849+10kbC→T) [Highsmith WE et al., 1994], promoter mutations or inefficient trafficking (A455E) [De Braekeleer M et al., 1997, Sheppard DN et al., 1995]. These mutations result in reduced expression of functional CFTR channels in the apical membrane. Class V mutations are associated with a milder CF phenotype.

- CLASS VI: DECREASED STABILITY

Net Effect: Functional but Unstable CFTR Present at the Apical Membrane. According to a new study, truncation of the C-terminus of CFTR leads to the marked instability of an otherwise fully processed and functional variant. These are usually nonsense or frameshift mutations (Q1412X, 4326delTC, 4279insA) causing a 70- to 100-bp truncation of the C terminus of the CFTR [Haardt M et al., 1999] and associated with severe CF presentation. The above classification categorizes CFTR mutations according to their molecular mechanisms and consequences for different aspects of CFTR biogenesis, metabolism and function but it does not exclude an association of a mutation with more than one mechanism (e.g. mislocalization and decreased function).

1.4. THERAPIES

Although no definite cure has been discovered for cystic fibrosis as of yet, many treatments have been developed to improve the quality of life for those who suffer from this disorder. Since CF causes a build-up of mucus in the lung tissue, the respiratory diseases which result are often the actual cause of death, not CF itself. Besides mucus accumulation, CF is also featured by bacterial and mycotic infections and inflammation with severe tissue damage.

1.4.1. Symptomatic therapies:

Therapy that eases the symptoms without addressing the basic cause of the disease. For example, symptomatic treatment of advanced lung cancer that has spread (metastasized) beyond the lung is designed to decrease the pain and other symptoms but not to eradicate the disease.

1.4.1.1. Aerosol therapy

Aerosol therapy is a medical treatment that is used to treat a variety of breathing conditions. It can be used in the treatment of asthma, chronic obstructive pulmonary disorder (COPD) or other illnesses that impact airway function. Aerosol therapy delivers small amounts of medicine into the lungs)

1.4.1.2. Antibiotics

Antibiotics are medicines that help stop infections caused by bacteria. They do this by killing the bacteria or by keeping them from copying themselves or reproducing. The word antibiotic means “against life.” Any drug that kills germs in your body is technically an antibiotic

1.4.1.3. Anti-Inflammatory

Anti-inflammatory (or anti-inflammatory) is the property of a substance or treatment that reduces inflammation or swelling. Anti-inflammatory drugs make up about half of analgesics, remedying pain by reducing inflammation as opposed to opioids, which affect the central nervous system to block pain signalling to the brain. Inflammation plays a major role in the pathophysiology of lung disease in CF. This response is probably triggered primarily as a reaction to the inability of the affected lung to resist the invasion of the most common bacterial pathogens seen in this disease.

Anti-inflammatory therapy can be provided in various forms: these include the use of oral corticosteroids which are potentially highly effective but which carry with them the risk of long-term systemic side effects.

Inhaled corticosteroids also have considerable potential because of their local action within the lung. Their potential therapeutic disadvantage is the difficulty of penetrating the viscid mucus which lines the airway in CF patients particularly as the disease progresses.

Other anti-inflammatory agents such as ibuprofen have considerable potential and have been the subject of various studies over the years.

More recently macrolides have come forward as potent anti-inflammatory agents and are beginning to have an established place in the therapeutic regimen for patients with long-term Pseudomonas aeruginosa infection. Other agents which have been used include immunoglobulins and dornase alpha (DNase) that may have an anti-inflammatory role as well as being mucolytic.

1.4.1.4. Pancreatic enzymes

Pancreatic enzymes (Pancreatic enzyme replacement therapy involves taking the digestive enzymes you need in the form of a tablet (capsule). All enzyme supplements contain Pancreatin – a mixture of pancreatic enzymes, lipase, amylase and protease. These assist the digestion of fat, carbohydrates and proteins.)

1.4.1.5. Physiotherapy

Physiotherapy is the treatment of injury, disease and disorders through physical methods — such as exercise, massage, manipulation and other treatments — over medication and

surgery. In the hospital setting, chest physiotherapy (CPT) is utilized; a respiratory therapist percusses an individual's chest with his or her hands several times a day, to loosen up secretions. Devices that recreate this percussive therapy include the Therapy Vest and the intra-pulmonary percussive ventilator (IPV). Newer methods such as biphasic cuirass ventilation (BCV), and associated clearance mode available in such devices, integrate a cough assistance phase, as well as a vibration phase for dislodging secretions. Biphasic Cuirass Ventilation is also shown to provide a bridge to transplantation. These are portable and adapted tools for home use [Van der Schans et al., 2000].

Physiotherapy is essential to help manage an individual's chest on a long term basis, and can also teach techniques for the older child and teenager to manage themselves at home. Aerobic exercise is of great benefit to people with cystic fibrosis. Not only does exercise increase sputum clearance but it also improves cardiovascular and overall health.Aerosolized medications that help loosen secretions include dornase alfa and hypertonic saline [Kuver R et al., 2006]. Dornase is a recombinant human deoxyribonuclease, which breaks down DNA in the sputum, thus decreasing its viscosity [Lieberman J et al., 1968]. N-Acetylcysteine may also decrease sputum viscosity, but research and experience have shown its benefits to be minimal. Albuterol and ipratropium bromide are inhaled to increase the size of the small airways by relaxing the surrounding muscles.

As lung disease worsens, mechanical breathing support may become necessary. Individuals with CF may need to wear special masks at night that help push air into their lungs. These machines, known as bi-level positive airway pressure (BiPAP) ventilators, help prevent low blood oxygen levels during sleep. BiPAP may also be used during physical therapy to improve sputum clearance [Moran F et al., 2003]. During severe illness, a tube may be placed in the throat (a procedure known as a tracheostomy) to enable breathing supported by a ventilator.

1.4.1.6. Pulmonary transplantation

Double lung or heart-lung transplantation is a treatment option for patients with cystic fibrosis and end-stage lung disease. Overall survival of lung-transplant patients is poorer than for other organ transplantation, with 3-year survival of about 60% in patients with cystic fibrosis [Bennet LE et al., 2000]. Generally, survival is better for adults than for children [Liou TG et al., 2001], but some centres have reported a survival benefit in children [Aurora P et al., 1999].

1.4.1.7. Chemotherapy

Many CF patients are on one or more antibiotic at all times, even when they are considered healthy, in order to prophylactically suppress infection. Antibiotics are absolutely necessary whenever pneumonia is suspected or a lung function decline has been noticeable, and are usually chosen based on the results of a sputum analysis and the patient's past response. Many bacteria common in cystic fibrosis are resistant to multiple antibiotics and require weeks of treatment with Intravenous antibiotics such as vancomycin, tobramycin, meropenem, ciprofloxacin and piperacillin. This prolonged therapy often necessitates hospitalization and insertion of a more permanent IV such as a peripherally inserted central catheter (PICC) line or Port-a-Cath. Inhaled therapy with antibiotics such as tobramycin and colistin is often given for months at a time in order to improve lung function by impeding the growth of colonized bacteria [Pai VB et al., 2001, Westerman EM et al., 2004]. Inhaled antibiotic therapy with aztreonam is also being developed and clinical trials are underway [McCoy KS et al., 2008]. Oral antibiotics such as ciprofloxacin or azithromycin are given to help prevent infection or to control ongoing infection [Hansen CR et al., 2005]. Several of the antibiotics commonly used to treat CF patients, such as tobramycin and vancomycin, can cause hearing loss, damage to the balance system in the inner ear or kidney problems with long-term use. In order to prevent these side effects, the amount of antibiotics in the blood are routinely measured and adjusted accordingly.

1.4.2 Innovative Therapies:

1.4.2.1 CFTR potentiators

CFTR potentiators are compounds that increase the open channel probability of CFTR. Ivacaftor VX-770 is one of those molecules. The effects of VX-770 on CFTR-mediated Cl^- secretion in vitro were assessed in both recombinant cell lines and primary cultures of HBE isolated from the bronchi of CF and non-CF donor lungs. There are currently no approved therapies that target CFTR. Here we describe the in vitro pharmacology of VX-770, an orally bioavailable CFTR potentiator already approved by EMA and FDA in clinical development for the treatment of CF. [Van goor et al., 2009]

1.4.2.2 CFTR correctors

CFTR correctors are molecules that improve intracellular trafficking of misfolded CFTR to the apical surface of the cells. Lumacaftor VX-809 is one of those molecules. One strategy to

treat these patients is to correct the processing of F508del-CFTR with small molecules. Here we describe the in vitro pharmacology of VX-809, a CFTR corrector already approved by EMA and FDA that was advanced into clinical development for the treatment of CF. [Van goor et al., 2009]

Tezacaftor, another CFTR corrector, when used in combination with ivacaftor in p.Phe508del homozygotes or heterozygotes with a residual function CFTR allele, can deliver similar clinical benefits. [Elborn et al., 2016; Rowe et al.,2017]

1.4.2.3 Nonsense suppression molecules inducing PTC read-through

Chemical-induced read through of premature stop codons might be exploited as a potential treatment strategy for genetic disorders caused by nonsense mutations. Despite the promise of this approach, only a few read-through compounds (RTCs) have been discovered to date. These include aminoglycosides (e.g., gentamicin and G418) and no aminoglycosides. [Du et al., 2013]

1.4.2.4 Gene editing

Cystic fibrosis should be an ideal candidate for gene therapy, for four main reasons: (1) it is a single gene defect; (2) it is a recessive condition, with heterozygotes being phenotypically normal (suggesting gene dosage effects are not critical); (3) the main pathology is in the lung, which is accessible for treatment; and (4) it is a progressive disease with a virtually normal phenotype at birth, offering a therapeutic window.

It has been suggested that only 5–10% of normal CFTR function is required to reverse the chloride channel defect [Johnson LG et al., 1995], although it is not clear whether this has to be achieved in the majority of the airway epithelial cells, or whether a minority of cells expressing much higher levels would suffice. In clinical trials to date, two main vector systems have been harnessed to deliver the CFTR cDNA with appropriate promoter into host cells [Flotte TR et al., 2001, Driskell RA et al., 2003]. First, viral vectors with the CFTR cDNA incorporated into the viral genome exploit the efficiency of viruses to enter host cells and achieve relatively high levels of gene expression. Secondly, cationic liposomes mixed with plasmid DNA encoding CFTR enhance the transport of the DNA into host cells. Although cationic liposomes seem to generate a lower immune response than current viral vector systems, the levels of CFTR expression using this delivery system have been relatively poor.

The ideal vector system would have the following characteristics: (1) an adequate carrying capacity; (2) to be undetectable by the immune system; (3) to be non-inflammatory; (4) to be safe to the patients with pre-existing lung inflammation; (5) to have an efficiency sufficient to correct the cystic fibrosis phenotype; and (6) to have long duration of expression and/or the ability to be safely re-administered.

In-vivo gene therapy trials in patients with cystic fibrosis have been done with viral vectors and cationic lipids, [Perricone MA et al., 2001, Kitson C et al., 1999] however, long-term effects were not achieved. Repeat administration of adenovirus vectors reduces efficacy of transfection because of formation of specific antibodies, whereas lipids might not specifically target CFTR-expressing cells. Therefore, although much progress has been made in gene therapy, it is presently not a treatment option for patients with cystic fibrosis.

1.4.2.5. Therapeutic miRNAs

As FDA-approved small RNA drugs start to enter clinical medicine, ongoing studies for the microRNA (miRNA) class of small RNAs expand its preclinical and clinical research applications. A growing number of reports suggest a significant utility of miRNAs as biomarkers for pathogenic conditions, modulators of drug resistance, and/or as drugs for medical intervention in almost all human health conditions. The pleiotropic nature of this class of nonprotein-coding RNAs makes them particularly attractive drug targets for diseases with a multifactorial origin and no current effective treatments. As candidate miRNAs begin to proceed toward initiation and completion of potential phase 3 and 4 trials in the future, the landscape of both diagnostic and interventional medicine will arguably continue to evolve. [Johora et al., 2019]

1.5. Non Coding RNAs

Non coding RNAs (ncRNAs) are a class of RNA molecules that are able to regulate gene expression at transcriptional or at post-transcriptional level. NcRNAs can be divided in two main groups: short or small ncRNA, that are generally, less than 30 nucleotides in length, and long ncRNAs (lncRNAs) that are characterized by a length of at least 200 nucleotides.

High-throughput sequencing and microarray analysis demonstrate that the alteration of ncRNA profile is the base for different types of diseases. Cancer is only an example of pathology in which ncRNAs dysregulation plays a key role. In particular, different works correlate ncRNA profile with neoplastic phenotype or disease progression suggesting

ncRNAs not only, as biomarkers for diagnosis or prognosis but also, as targets for novel agents in cancer therapy [Cowie et al., 2015].

1.6. Long non coding RNAs

LncRNAs are a class of protein non-coding RNAs with a length greater than 200 nucleotides, which transcripts generally, reside in the introns of protein-coding genes. Currently, only a fraction of the thousands of mammalian lncRNA have been characterized. Increasing evidences suggest that they are involved in a broad spectrum of biological processes including cell proliferation, differentiation, apoptosis and stem cell self-renewal. Owing to their ability to bind DNA and RNA they are able to modulate protein activity [Quinn et al., 2015]. These regulatory RNAs are heterogeneous as regards characteristics, localization and modes of action. The subcellular localization of lncRNA is considered a good indicator of their mode of action [Kung et al., 2013]. LncRNA localized in the nucleus are involved in gene regulatory processes, including promoter-specific repression, activation of transcription or epigenetic gene regulation. Furthermore, several nuclear lncRNA were found to regulate the maintenance of nuclear architecture, particularly, they seem to regulate the abundance of nuclear structures called paraspeckles, that are involved in mRNAs retention [Chen et al., 2009]. On the contrary, lncRNAs localized in the cytoplasm seem to be involved in the post-transcriptional gene regulation processes like regulation of mRNA stability, regulation of miRNAs accessibility or translation pathways [Yoon et al., 2013]. Increasingly strong evidences have proposed lncRNA as molecules with a key role in neoplastic disease; in fact, these RNA molecules can act as oncogenes or as tumor suppressor, depending on the signalling pathway in which they are involved. For example, HOTAIR, one of the most studied lncRNA, in colorectal cancer (CRC) seems to be related to tumor invasion and metastasis, indeed has been demonstrated that CRC patients with higher HOTAIR expression have higher recurrence rates and shorter overall survival compared with patients with lower HOTAIR expression [Wu et al., 2014].

1.7. Small non coding RNAs

In the recent years, small non coding RNAs have emerged as key regulators of gene expression in different pathways and a growing number of small regulatory RNA classes have been discovered. MicroRNAs are still, the best-characterized class; however, other

small RNA molecules have been investigated, such as piwi-associated RNAs (piRNAs) and small nucleolar RNAs (snoRNAs).

1.8. PiRNAs

PiRNAs (24-32 nucleotides in length) performed their main activity in the germline where they target and repress expression of transposable and repetitive elements to maintain genomic stability [Siomi et al., 2011]. They are processed from single-stranded RNA precursors that are transcribed from intergenic repetitive elements called piRNA clusters. Unlike miRNA, they are processed by a Dicer-independent mechanism. As the name suggest, piRNAs are associated with PIWI proteins, which are germline-specific members of AGO protein family. The association between piRNA and PIWI proteins forms the piRNA-induced silencing complex (piRISC) that recognizes and silences complementary targets RNA.

1.9. SnoRNAs

Small Nucleolar RNAs (snoRNAs) are well-conserved, abundant, short non-coding RNA molecules, 60-300 nucleotides in length. They are localized in the nucleolus into eukaryotic cells nucleus and are involved in the chemical modification of ribosomal RNA. The majority of snoRNAs are encoded in the introns of protein coding genes and aretranscribed simultaneously by RNA Polymerase II [Sana et al., 2012]. Despite, they are frequently used as reference genes in miRNA expression analysis, snoRNA are significantly modulated in several diseases, including cancer.

1.10. MicroRNA

MicroRNAs (miRNAs or miRs) are a family of small (19-25 nucleotides in length) non-coding RNAs that have a key role in the regulation of gene expression through the inhibition or the reduction of protein synthesis. They will be discussed in details following. MicroRNA are non-coding small RNA molecules, found in both prokaryotes and eukaryotes, that are able to negatively regulate gene expression at post-transcriptional level by targeting mRNA. They were firstly introduced in 1993, when Lee [Lee et al., 1993] and Wightman [Wightman et al., 1993] independently reported that a small transcript: lin-4 binds the 3' untranslated (UTR) region of the *C.Elegans* gene lin-14, negatively regulating lin-14 protein expression. By this discovery several others miRs have been found, and at moment the

known human mature miRNAs registered in miRBase are 38589 (miRBase.org, release 22.1, October 2018), and probably, will continue to increase.

1.10.1. Nomenclature of miRNA

The complete name of a miRNA can be divided into three parts: the first part, composed generally by three characters is referred to the species; hsa (Homo sapiens), mmu (Mus musculus) and cel (Caenorhabditis elegans) are only some examples. 'miR' is the second part and it is universal, followed by the third part, that is a number, specific for every miRNA sequence. At this general scheme can be added some others information for example:

- If two miRNAs with identical sequence are transcribed from different gene loci of

the genome, they get a second number, after the identification number: for example miR-92-1 and miR-92-2.

- If two miRNAs differ only in one or two nucleotides, they get a character after the

number: for example, miR-200a and miR-200b.

- If both strands of miRNA duplex maturate the less abundant is marked by a '*'

- If the miRNA precursor is cleaved close to 5' end the miRNA name is followed by -

5p, instead if the cleavage is closer to the 3' end the miRNA name is followed by -3p.

1.10.2. microRNA genes

MiRNA genes are distributed not randomly in human genome and have been found in all chromosome except in Y chromosome [Ghorai et al., 2014]. As regard miRNA genes location, it has been demonstrated that miRNA can be divided in two groups: intragenic miRNA and intergenic miRNA. Intergenic miRNAs are located between genes and their transcription is independent of coding gene, in fact they are generally transcribed by RNA polymerase III (RNApol III). Moreover, some studies reported that intergenic miRNAs are more evolutionary conserved than intragenic miRNA [Schanen et al., 2011]. Intragenic miRNAs are embedded within exon or introns of protein-coding genes, so are co-transcribed with their host genes by RNA polymerase II. Moreover, a small percentage of miRNAs have

been found to be interspersed among repetitive elements and transcribed by RNApol III. MiRNA expression is regulated by transcription factors (TFs), enhancers and silencing elements and the regulation is development- and tissue-specific. The protooncogene c-MYC is only an example of transcription factor that is able to regulate miRNA expression [O'Donnell et al., 2005]. MiRNAs are generally located in cluster or miRNA families such as miR-200 family that presents two different clusters one in human chromosome 1, which expresses miR-200a, miR-200b and miR-429, and a second cluster located in human chromosome 12 which expresses miR-141 and miR-200c [Korpal et al., 2008]. MiRNA clusters generally include miRNAs with the same target site or with the same function.

1.10.3. miRNA biogenesis

The first step of miRNA biogenesis takes place in the nucleus, where the transcription of miRNA gene locus by RNApol II or RNApol III generates a long primary RNA called pri-miRNA, that can contain more than one miRNA sequence. MiRNA precursor is several kilobases-long and presents a 7-methylguanosine cap in 5' position and a poly-adenyl tail in 3'. Pri-miRNA fold is into a hairpin, which contains a terminal loop, a stem (dsRNA) of about 33 bp and two flanking regions of single stranded RNA. This structure is processed by miRNA processor complex that is composed by Drosha and DGCR8 (DiGeorge syndrome critical Chromosome Region 8) also called Pasha (Partner of Drosha). Drosha is a member of class II ribonuclease III proteins and presents an amino-terminal proline-rich and serine-arginine- rich region responsible for the nuclear localization, a middle region that interacts with DGCR8, two RNase III domain (RIIIDs) that interact with each other to make a dimer with catalytic activity, and a double stranded RNA-binding domain (dsRBD) [Han et al., 2006]. In the first step (substrate recognition) DGCR8 recognises the ssRNA-dsRNA junction (SD) and the 33 bp stem in the pri-miRNA followed by the interaction between Drosha and DGCR8 that activates the second step (catalytic reaction).

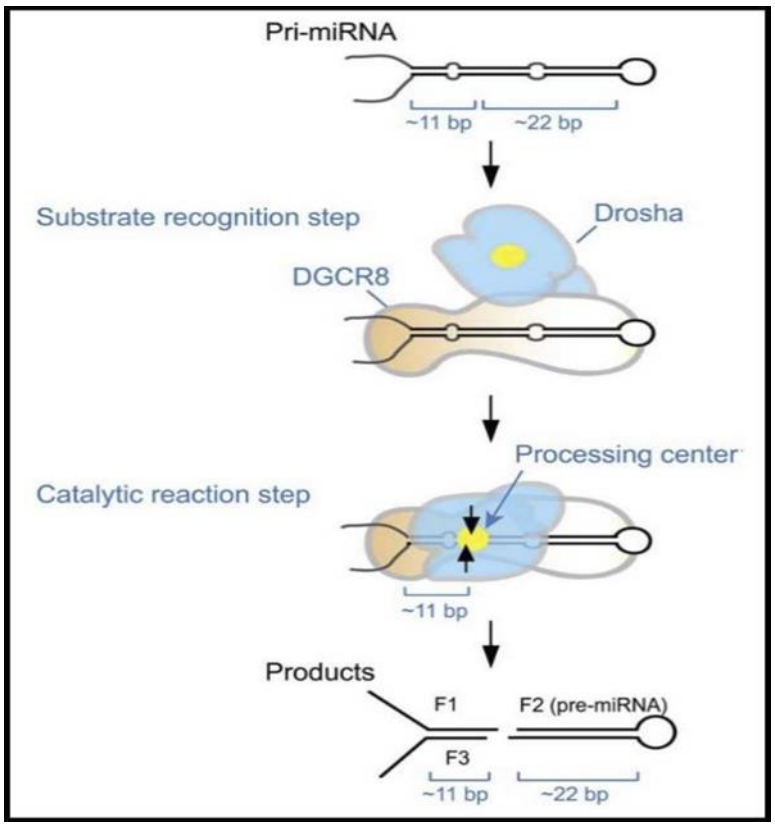

Figure 1.10: Pri-miRNA processing. DGCR8 recognises the ssRNA-dsRNA junction, then Drosha interacts with the substrate for catalysis. Picture taken from Han et al.,2006. Drosha interacts with DGCR8 anchored stem in a region that is 11 bp from SD junction and cleaves the two strands generating a smaller hairpin-like miRNA precursor called pre-miRNA.

miRNA, containing 2 nucleotides 3' overhang. Exportin-5 receptor (EXP-5) associated with RanGTP (Ran Guanosine Tri-Phosphate) recognises the 2 nt overhang of the pre-miRNA and actively transports pre-miRNA from the nucleus to the cytoplasm [Bartel, 2004]. Once in the cytoplasm, pre-miRNA undergoes to two important modifications: 1) urilydation or less frequently adenylation, at 3'UTR and 2) methylation at 5'end. These modifications are very important because affect the pre-miRNA stability and allow an accurate cleavage in the following step [Park et al., 2011]

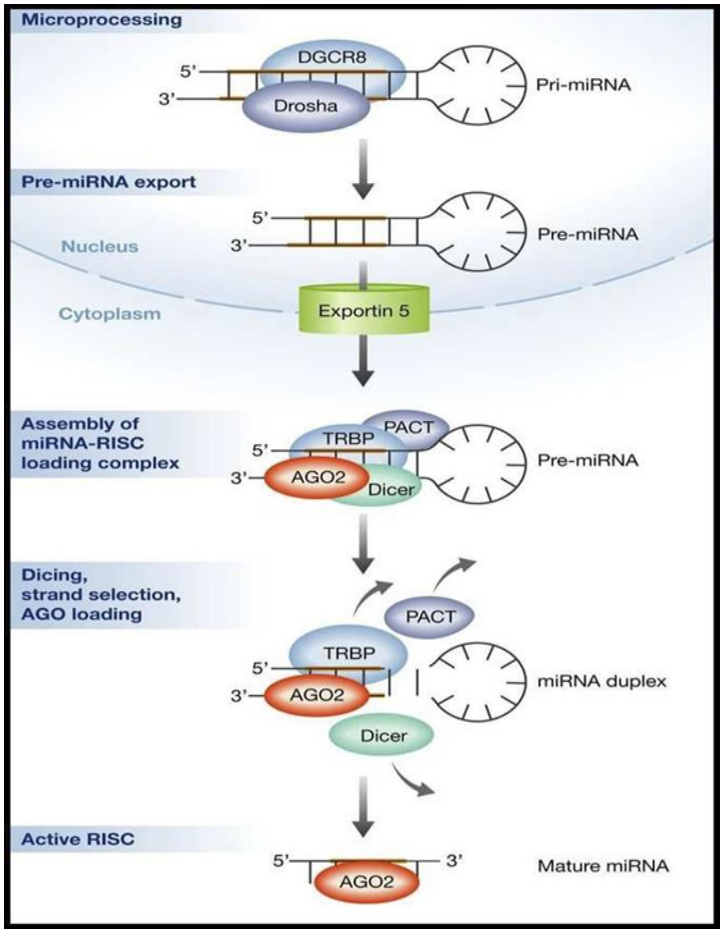

Figure 1.11: Canonical pathways for miRNA maturation. After transcription, the initial pri-miRNA transcript is processed by the Drosha/DGCR8 complex. The resultant intermediate precursor, pre-miRNA,is a 70-nt hairpin that is exported from the nucleus into the cytoplasm by Exportin 5. In the cytoplasmpre-miRNA is recognized by Dicer complex/miRNA-RISC-loading complex. Upon disassembly of the RISC-loading complex, AGO protein has a key role in strand selection. Picture taken from Emde et al., 2014.

A protein complex: RISC Loading Complex (RLC) binds to pre-miRNA to cleavage it. RLC is composed by three principal elements:

- Dicer: an endoribonuclease that takes part of RNase III-family and is essential for miRNAs maturation. Dicer presents several domains and between these, particularly important is PAZ (Piwi/Argonaute/Zwille) domain that has two pockets: the first one recognises and binds 2 nucleotides overhang at the 3' of the pre-miRNA. The second one, that is positively charged, binds the 5' terminal, negative charged phosphate group of the hairpin duplex [Macrae et al., 2006]. Moreover, essential for the premiRNA cleavage are the two catalytic RNase III domains.

- Double-Stranded RNA-Binding Proteins (dsRBPs) bind one of Dicer domain, generating a conformational rearrangement that results in Dicer activation.

Moreover, as Wilson and colleagues described, these proteins, in particular TRBP (Tar RNA-Binding Protein) have an important role in strand selection [Wilson et al., 2015].

- Argonaute-2 (AGO2) is a member of Argonaute family, which includes 8 different proteins, but between these only one, AGO-2 presents catalytic nuclease activity, while others one inhibit the translation, but the mechanism of action is at moment not clear [Hock et al., 2008].

After the cleavage by Dicer miRNA duplex is transported by Dicer to one of Argonaute proteins (AGO). The bind between miRNA duplex (5p strand-3p strand) and AGO is possible thanks to Hsp90 (Heat Shock Protein 90) that mediates a conformational change in AGO, allowing the bond [Pare et al. 2009]. AGO-2 binds at N-terminal PAZ domain the 3'end of the guide strand (5p strand) of the miRNA duplex, starting the duplex unwinding. Generally, the strand with the weaker bind at 5'end is chosen as guide strand, maybe because duplex opening is easier there. The other one (generally, 3p strand) is normally degraded, but there are several cases, in which is equally or even more important of 5p strand. The mature single strand, AGO proteins, and several others, not fully understood, proteins are part of a complex called miRISC (miRNA Induced Silencing Complex) that represents the functional unit of miRNA-mediated gene regulation.

1.10.4. miRNA target recognition

MiRNA associated with RISC in the miRISC complex is able to exert its function through the recognition of its complementary sequence in target mRNA. Nucleotides in miRNA sequence that are essential for the bond with the target mRNA, constitute the seed region. Seed region generally takes place from the 2nd and the 7th nucleotide on the 5'end of the mature miRNA and in most of cases recognises a complementary sequence in the 3'UTR of the target mRNA. However, is not uncommon that miRNAs can recognise target sequences also in 5'UTR and in highly conserved sequences of the coding domain sequence (CDS). If the role of miRNA targeting 3'UTR is well characterized, the regulatory functions of miRNAs targeting CDS or 5'UTR appear currently not completely clear [Brummer et al., 2014] and the issue is still much debated. Some authors argue that gene regulation is less effective when miRNA target sequence is located in the coding region [Marin et al., 2013] or in the 5'UTR [Grimson et al., 2007]. In fact, these authors postulate that in the CDS is possible that ribosomes displace RISC from the target site before RISC effects the

translational repression. Others, as Hausser and colleagues, demonstrate that CDS and 3'UTR target sites have, not only similar sequence and structure proprieties, but also present similar efficiency in inducing translational repression of the mRNA; with an important difference: miRNAs targeting 3'UTR are more effective in inducing mRNA degradation [Hausser et al., 2013]. MiR-148 is only an example of miRNA that is able to down-regulate its target (the protein DMNT3b) through the bond with the complementary mRNA in the coding region [Duursma et al., 2008]. The seed sequence of miRNA can pair with target mRNA in different ways. The canonical way takes place when the seed region pairs with mRNA with 7 seed region nucleotides and

- the nucleotide opposite the 1st miRNA nucleotide is adenine (7mer-A1 site)

- the 8th nucleotide pairs with the opposite nucleotide (7mer-m8 site)

-in the first place is adenine and the 8th nucleotide pairs (8mer site).

To predict miRNA possible mRNA targets several methods are available, even if, generally the first step is a bioinformatics analysis through which is possible to predict miRNA targets in silico. This kind of analysis uses bioinformatical algorithms that allow to analyse three important parameters:

- Watson-Crick complementary between seed region of the miRNA and its target
- Evolutional conservation of the sequence through the species
- Thermodynamic proprieties of the target mRNA

For this propose several software are free available such as TargetScan (www.TargetScan.com), miRWalk (www.umm.uni-heidelberg.de/apps/zmf/mirwalk). After this first step the confirmation of in silico data must be performed.

1.10.5. miRNA detection techniques

The unique characteristics of miRNA, such as small size, low abundance and sequence similarity among family members make miRNA detection very complex. Because of the small miRNAs size, the GC content in miRNA sequences is very variable, leading to a wide range of melting temperature (Tm). Also, short primers are required for Polymerase Chain Reaction (PCR) leading to low oligonucleotide annealing temperature that causes the decrease of hybridization stringency and the consequent increase of cross-hybridization risk

[Pritchard et al, 2012]. Furthermore, miRNAs represent only the 0.01% of total RNA [Dong et al., 2013], so bioanalysis devices must be able to differentiate very small amount of miRNA in the presence of total RNA. Another important characteristic to consider, is the extremely variable abundance of miRNAs, that can vary from a copy to 50.000 copies for a single cell [Bartel, 2004]. Currently a wide range of approaches have been explored for miRNA profiling. Besides traditional methods strategies as RTqPCR (Quantitative Reverse Transcription PCR), Northern Blot, microarray and RNA Seq, others strategies based, for example, on Surface Plasmon Resonance (SPR) are emerging. All of them require different sample input and present different Limit Of Detection (LOD) that is the lowest quantity of analyte that can be distinguished from the blank value. Moreover, some of these techniques present the ability to analyse multiple targets in the same run. It is important to underline that sample processing and RNA extraction have a substantial impact on the results of miRNA profiling.

1.10.5.1. Quantitative reverse transcription polymerase chain reaction

Actually is considered the gold-standard for miRNA detection, but it is used for single or small panel, miRNA detection. This technique is characterised by a wide dynamic range, high sensitivity: few nanograms of total RNA are sufficient, high accuracy; low assay cost and can easily provide absolute miRNA quantification [Baker, 2010]. The technique relies on reverse transcription of miRNA to cDNA followed by quantitative real time polymerase chain reaction, monitoring the accumulation of reaction product.

Two main strategies are used for priming the reverse transcription of miRNA to cDNA: the addition of a polyA tail at 3' of all miRNAs by E.Coli poly(A) polymerase (PAP), followed by reverse transcription using universal primers consisting on an oligo dT sequence. The PCR product formation is then quantified using a dsDNA-intercaling dye, such as SYBR Green [Pritchard et al., 2012].

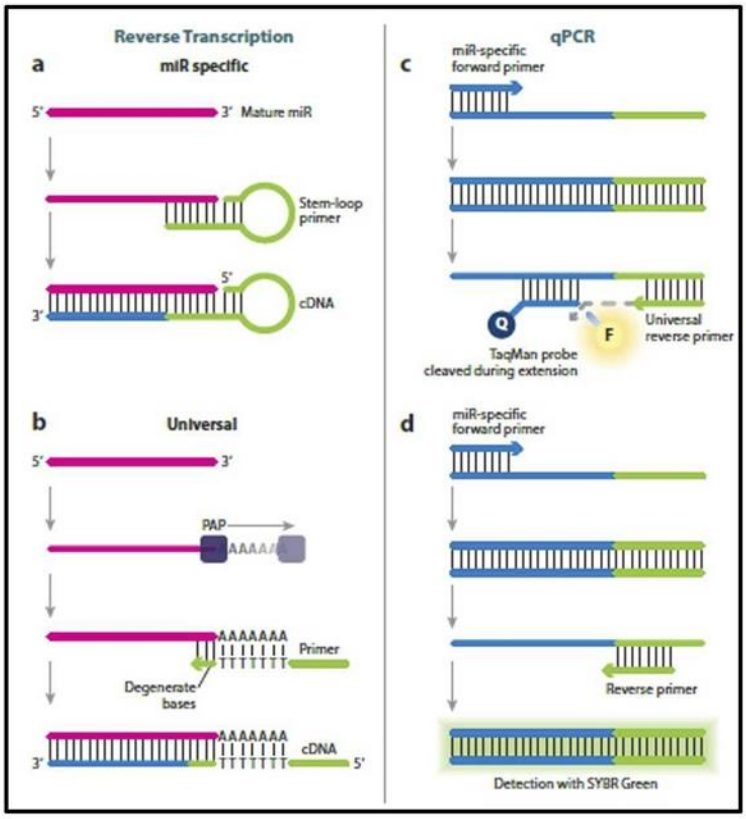

Figure 1.12: PCR-based miRNA detection. Panel a: miRNA specific reverse transcription using stem-loop primer followed by qPCR amplification using TaqMan probe (Panel c). Panel b universal miRNA reverse transcription and relative qPCR amplification using LNA primers and SYBR Green (Panel d). The Figure was taken from Hunt et al., 2004.

Some researchers consider this method more suitable to detect miRNA from small amount of starting material (for example plasma sample). Another reverse transcription method is based on the use of stem loop primer: miRNA-specific primers that reversely transcribe only a particular miRNA. Stem loop primers are designed to contain 6-8 nucleotide overhang on the 3' end that is complementary to target miRNA. After the hybridization between primer and the complementary miRNA the reverse transcription extends from miRNA 3' end. These kind of primers are able to differentiate between mature miRNA and pre- or pri-miRNA and present more specificity thanks to the optimization of Tm. Every stem loop primer can be recognized by a standard PCR primer, so the PCR amplification is performed using a universal reverse primer that binds to the conserved stem loop region of all RT products and a forward, miRNA-specific primer that recognizes the 3' and of the miRNA. To increase the specificity, the assay employs a TaqMan probe, that hybridizes in the region between the forward and reverse primer. In both SYBR Green and TaqMan detection method, the signal is measured as a function of cycle number (CT). In order to use RTqPCR approach for miRNA profiling are commercially

available plates or cards that allows to analyse a small set of miRNA involved in a pathway of interest, that partially solve the problem of multiplex analysis. The main drawback of RTqPCR remains the complex primer design and the run to run variability in PCR amplification, that makes necessary the use of internal controls, as housekeeping genes [Peltier et al., 2008] or the spike-in of non-natural miRNA before RNA extraction step [Sarkar et al., 2009].

1.11. Therapies targeting miRNAs

Recently, miRNAs and the protein machinery involved in their biogenesis and activity have become targets for new therapeutic approach in several diseases. Until now, some studies of tumor gene therapy targeting miRNA have obtained anti-tumor effects in vivo and in vitro, and laid a foundation for the safe and effective application for tumor patients. The potential of miRNAs as treatment targets in cancers has been explored by many studies. The therapeutics strategies either introducing tumor suppressor miRNAs or blocking oncogenic miRNAs have developed rapidly in recent years. The number of miRNA-based therapeutic is summarized in the following Table 1. [Weidan et al., 2017].

MicroRNA	Functions	Targets
miR-145	Tumor Suppressor	ROCK1,MMP11,Ra27a, FSCN-1, LASP-1, MTDH, SENP1, E2F3,c-MYC
miR-34a	Tumor Suppressor	CDK6,SIRT1,E2F3,c-Met,Notch,c-Myc,Fra-1, TPD52,c-SRC, Bcl-2, MYCN
miR-29b	Tumor Suppressor	DNMT3A/3B, CDK6, MCL-1,TCL-1, Bcl-2, KDM2A, MMP2,TNFAIP3/A20, BCL2L2
miR-340	Tumor Suppressor	ROCK1, MYO10, MET, CDH1,NF-x03BA/B1, JAK1, EZH2
Let-7a	Tumor	K-RAS, N-RAS , MYC, CDK6, RTKN, CDC25A

	Suppressor	E2F2, HMGA2
miR-495	Tumor Suppressor	MYB, Bim-1, MTA3,JAM-A, PRL-3
miR-155	Oncogene	SHIP-1,,C/EBP ZDHHC2 b, S0CS1, SOCS6,
miR-21	Oncogene	PDCD4 , BTG-2 , PTEN, Cdc25A , TPM1, FOXO1

Table 1.1: MiRNA-based molecules in therapy. Taken from Weidan at al., 2017.

This new therapeutic approach can have two possible goals: the inhibition or the restore of miRNA activity, depending on miRNA function.

1.11.1. Tumor suppressor miRNAs

Tumor suppressor miRNAs (miR supp) act to impede cancer cell proliferation through targeting oncogenes post-transcriptionally and they have been found to be often downregulated in tumors.[Liu G et al.,2015] demonstrated that miR-18a has a protective role in colorectal carcinoma where it binds TBP-like 1 gene and reduces proliferation, invasion and migration of the cancer cells.

MiR-148a was shown to be significantly downregulated in renal cell carcinoma (RCC) tissues and cell lines; this is associated with large tumor size and lymph node metastasis. It was seen that overexpression of miR-148a significantly inhibited RCC cell proliferation, colony formation, migration and invasion and in vivo studies revealed that high levels of miR-148a suppress RCC xenograft tumor growth; as confirm of this, is the fact that AKT2 is a direct target and it is negatively correlated with miR-148a expression (Cao H, 2010). Another example of tumor suppressor miRNA is miR-124-3p which is involved in the regulation of gastrulation and neural development in brain, and it targets some important genes, such as RAC1, the androgen receptor, SPHK1, ROCK2 and EZH2. Recently, in breast cancer it was found that miR-124-3p is constitutively downregulated and it can suppress the proliferation and invasion of breast cancer cells. Mechanistic studies revealed that miR-124-3p directly binds the CBL 3'-UTR and inhibits CBL (Cbl proto-oncogene, E3 ubiquitin protein ligase) expression; this could be a reason why the downregulation of miR-

124-3p can promote the development of breast cancer (Wang S, 2015).

The family of miR-181 is involved in the regulation of myeloid cells development and the expression of these miRNAs causes uncontrolled progression and proliferation of myeloid cells that leads to chronic lymphocytic leukemia (Sun et al., 2015).

The decreased expression of miR-101 instead has been shown to have an effect on the growing of neuroblastoma. Normally this miRNA inhibits excessive cell proliferation by hitting the proto-oncogene MYCN, but decreased expression of miR-101 causes excessive levels of MYCN causing an uncontrolled division and massive cell growth that leads to the development of neuroblastoma (Buechner J, 2011).

1.11.2. MIR-145

In molecular biology, miR-145 microRNA is a short RNA molecule that in humans is encoded by the MiR145 gene. MicroRNAs function to regulate the expression levels of other genes by several mechanisms . miR-145 is hypothesised to be a tumor suppressor.(Sachdeva et al., 2009) miR-145 has been shown to be down-regulated in breast cancer. (Gotte et al., 2010) miR-145 is also involved in colon cancer (Zhang et al., 2011) (Salby et al., 2007) (Mazza et al., 2016)) and acute myeloid leukemia (Starczynowski et al., 2011) and genetic disorders e.g Cystic fibrosis (Shaiq et al., 2020).

(Collison et al., 2011) demonstrated an induction of miR-145 in the airway wall from an animal model of allergic airways inflammation that mimics the hallmark features of allergic asthma. Inhibition of miR-145 inhibited eosinophilic inflammation, Th2 cytokine production, airway hyperresponsiveness and mucus hypersecretion. They suggested that miR-145 played a proinflammatory role for the onset of allergic airways disease, and the effects of miR-145 antagonism were comparable to steroid treatment.

(Xu et al., 2009) also reported that expression of microRNA-145 (miR-145) is low in self-renewing human embryonic stem cells (hESCs) but highly upregulated during differentiation. Further identified the pluripotency factors OCT4, SOX2, and KLF4 as direct targets of miR-145 and show that endogenous miR-145 represses the 3' untranslated regions of OCT4, SOX2, and KLF4. Increased miR-145 expression inhibits hESC self-renewal, represses expression of pluripotency genes, and induces lineage-restricted differentiation. Loss of miR-145 impairs differentiation and elevates OCT4, SOX2, and KLF4. Furthermore, founnd that the miR-145 promoter is bound and repressed by OCT4 in hESCs.

This work reveals a direct link between the core reprogramming factors and miR-145 and uncovers a double-negative feedback loop involving OCT4, SOX2, KLF4, and miR-145.

The expression of miR-145 has been reported to be down-regulated in cervical , hepatic [Varambally et al., 2008] and hepatocellular [Gramantieri et al., 2007], colorectal [Bandres et al., 2006], serous ovarian [Nam et al., 2008], ovarian [Iorio et al., 2007], colon [Schepeler et al., 2008], oral [Yu et al., 2009], prostate [Schaefer et al., 2009], gastric [Takagi et al., 2009], bladder [Ichimi et al., 2009], nasopharyngeal [Chen et al., 2009], lung [Liu et al., 2009], ACTH-secreting pituitary [Amaral et al., 2009], B-CLL (B cell chronic lymphocytic leukemia) [Wang et al., 2009] and breast [Sempre et al., 2007] cancers, dedifferentiated VSMCs and balloon-injured arteries [Zhang et al., 2009], acute and chronic vascular stress [Elia et al., 2009], myelodysplastic syndrome [Starczynowski et al., 2009]. Whereas, in pancreatic ductal adenocarcinoma [Wang et al., 2009], polycythemia vera [Bruchova et al., 2008], multiple sclerosis [Kelleret al., 2009], the expression of miR-145 was found to be up-regulated. Suggestions of miR-145 playing a role in the development of colon and rectal cancers but not in its progression [Wang et al., 2009] have been made, thus raising a question about its exact role in tumour initiation and development. It was, therefore, pertinent to understand the dual role of miR-145 in cancer, using both in vitro and cellular assays.

1.11.3. MiRNAs replacement therapy

This kind of therapeutic approach is based on the use of molecules that are able to restore physiological levels of miRNA and is particularly useful for example to increase levels of tumor suppressor miRNAs. The use of miRNA mimics presents several advantages: one of the most important is that these molecules present the same sequence of the endogenous miRNA, so they are expected to target the same mRNA, and non-specific off target effects are expected [Bader et al., 2010]. Moreover, every miRNA presents several targets, so using a single molecule is possible to influence several pathways. On the other hand, the delivery of miRNA mimic is not cell-specific and the accumulation of exogenous miRNA in not-affected cells may influence physiological cellular functions. At the moment, no significative data are available, about miRNA mimics toxicity in in vivo models. One of the most studied way to replace physiological miRNA levels is the use of expression vectors carrying miRNA sequence. For example, miR-26a levels were restored in hepatocellular carcinoma cells using an adenoviral vector [Kota et al., 2009]. In other cases, synthetic miRNA mimic are delivered into cells. As Wiggins and colleagues propose the delivery of

a synthetic miR-34a mimic is able to restore miR-34a levels and consequently inhibits lung tumor growth in mouse models [Wiggins et al., 2010]. In some disease, as in cancer, was observed a global miRNA down-regulation, in this case the use of a single miRNA mimic molecule is not sufficient, and a therapy that is able to restore the global 'miRNAome' may be required [Esteller, 2011]. At this propose a molecule called enoxacin was studied for its ability to promote miRNAs processing. Enoxacin has been tested both in cancer cell lines and in in vivo models where was shown that it is able to restore the physiological miRNAs expression pattern, with no effects in normal cells [Melo et al., 2011].

1.11.4. MiRNA inhibition strategies

MiRNA inhibition strategy involves the use of molecules with sequences complementary to the endogenous miRNA in order to inhibit miRNA function. Several types of molecules are able to perform this function and each of them presents different chemical modifications in order to enhance miRNA affinity. Some of these molecules act trapping endogenous miRNA in a configuration that cannot be processed by RISC, in other case can be use molecules that induce miRNAs degradation.

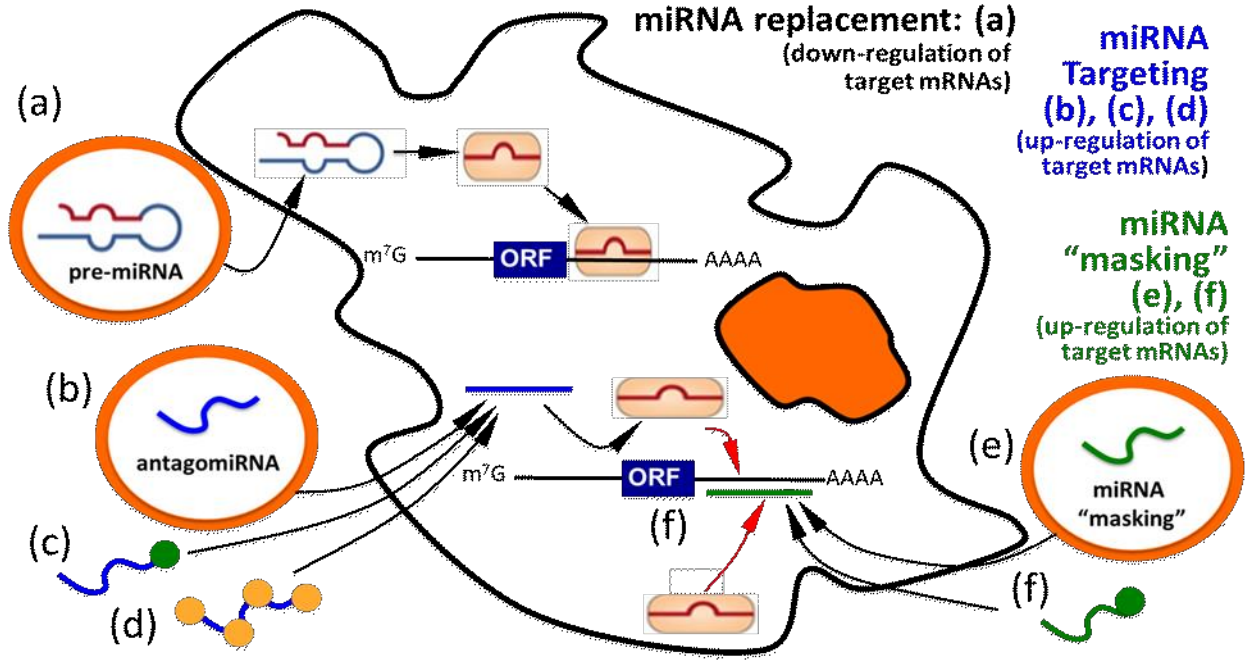

Figure 1.13: MiRNAs targeting therapeutic approach. (a) miRNA replacement approach **(b,c,d)** miRNA Targetting approach **(e,f)** miRNA Masking (Gambari et al., 2014)

These strategies include miRNA Targetting and miRNA Masking. In miRNA targetting which can also be called as Antisense PNA strategy targets the miRNA and up-regulates the

all mRNAs by miRNA reduction. While, the PNA masking is an strategy which Targets the miRNA binding sites and up-regulates the Specific (selective) effects only on a single target mRNA (e.g CFTR mRNA). In the last few years the use of PNAs for targeting microRNAs (anti-miRNA PNAs) has provided impressive advancements. In particular, targeting of microRNAs involved in the repression of the expression of the cystic fibrosis transmembrane conductance regulator (CFTR) gene. **[Figure 1.13]**

1.11.5. Anti-miRNA Oligonucleotides (AMOs)

The therapeutically inhibition of miRNAs function is based on the use of Anti-MiRNA Oligonucleotides (AMOs) a heterogeneous class of molecules that present a sequence complementary to their target, miRNA. The most important features of these kind of molecules are the specificity and the high binding affinity with RNA. The bond between miRNA and the complementary AMO results in miRNA function inactivation as miRNA is

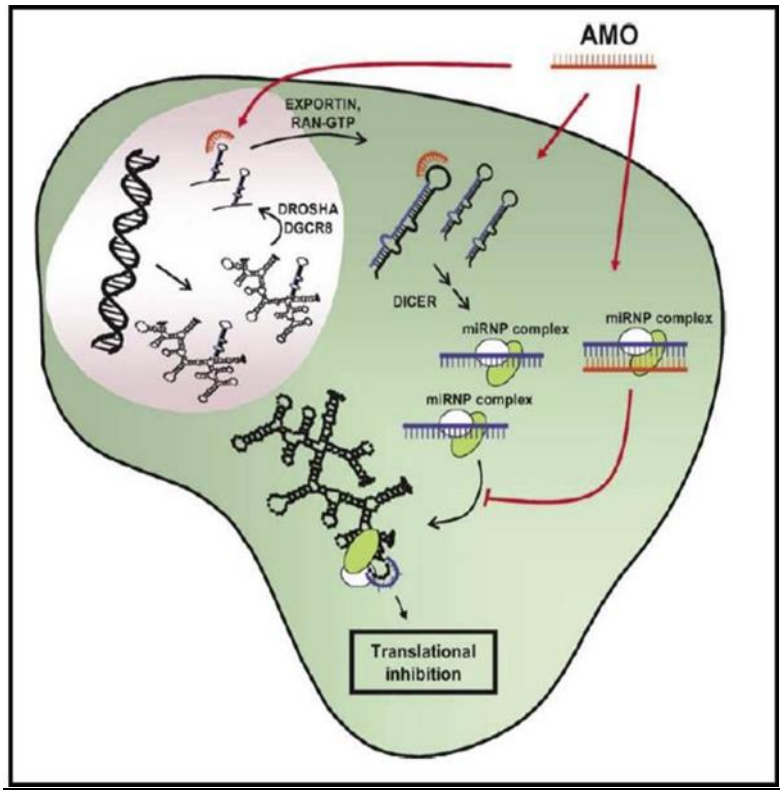

Figure 1.14: AMO strategy. Reduction in miRNA content can be obtained using anti-miRNA oligonucleotides (AMOs).

no longer able to bind its natural target. In the last years several modifications were performed in order to obtain increasing specificity for miRNA. One of the most successful modification leads to the design of Locked Nucleic Acids AMOs. Locked Nucleic Acids

(LNA) are RNA analogs in which the ribose ring is 'locked' by a methylene bridge, connecting the 2'-O atom and the 4'-C atom. They contain the common nucleobases that appear in DNA and RNA and are able to form base pairs according to Watson-Crick base pairing law. LNAs modification leads to a thermodynamically stronger duplex formation and the bound between the LNA AMOs and miRNA results in inhibition of miRNA function [Weiler et al., 2006]. Levels of miR-155 were significative decrease in mouse models of B-cell Lymphoma, using a 8mer complementary LNA [Zhang et al., 2015]. In the most of cases silencing a single miRNA is not sufficient, for this reason, recently several researchers try to produce a Multiple-Target anti-MiRNA Oligonucleotide (MTgAMO) that is able to inhibit at same time, several miRNA, using a single molecule [Lu et al., 2011]. Lu and co-workers synthesize an MTgAMO that is able to target at same time three onco-miRNAs: miR-21, miR-155 and miR-17-5p that are over-expressed in several types of tumor.

1.11.6. MiRNA sponges

MiRNA sponges are vectors containing multiple artificial miRNA binding sites, under the control of strong promoters [Esteller, 2011]. In this way, after the transfection, this vector is able to express high quantities of target multiple transcripts, which will be bind by the miRNAs, preventing the association between the miRNA and its natural target. The major advantage is that this kind of molecule is able to block a whole family of related miRNAs. For example, Ma and colleagues used this strategy to recruit miR-9, involved in the reduction of E-cadherin protein production that results in tumor metastasis [Ma et al., 2014].

1.11.7. Peptide Nucleic Acids (PNA)

Peptide Nucleic Acids (PNA) are synthetic oligonucleotide that are able to bind with high specificity and affinity for target DNA or RNA molecules. A more detailed discussion about PNA will be present in the following chapter.

1.11.8. MiRNA delivery

One of the major obstacles in the miRNAs based therapy is the delivery of miRNA or miRNA-targeting molecules. Several problems have been encountered in miRNA delivery as poor in vivo stability, inappropriate biodistribution, disruption and saturation of endogenous RNA machinery [Zhang et al., 2013]. Elaboration of miRNA delivery systems

is essential for clinical application of miRNA-based therapy, in fact delivery systems not only allow cells internalization of the molecules, but also stabilize miRNAs and prevent their degradation. Even if viral vectors are at the moment the most efficient vehicles, safety concerns limit their employment and focus the attention of researchers to non-viral approaches. Between non-viral strategies, lipid-based delivery is probably the most used and consists in a mixture of cationic lipids and helper lipids (for example polyethylene glycol: PEG or 1,2- dioleoylphosphatidylethanolamine: DOPE). Positive charges of cationic lipids interact electrostatically with negative charged nucleic acids to form lipoplexes that are internalized by cells through endosomal pathway [Piao et al., 2012]. Liposomes are routinely used in laboratory practice to perform miRNA or siRNA transfection. Lipofectamine ® (Invitrogen) or Siport ® (Ambion) are only two common examples. Despite a big optimization have been reached as regard loading capacity and delivery efficiency, the major limit is still the toxicity. Several examples of miRNA in vivo delivery using lipoplexes have been reported. Wu and colleagues employed lipoplexes to deliver miR-29a both in vitro and in vivo (murine xenografts) models of lung cancer, reaching an increase of miR-29a content of about five fold. To reduce toxicity and have a more biocompatible system, exosomes have been proposed as miRNAs vehicles. In term of composition exosomes are similar to liposomes, both in fact present bilayered phospholipids but are cells themselves to produce them. Exosomes are small membrane vesicles, in which endogenous miRNAs are physiologically encapsulated to prevent their degradation in body fluids. Generally, miRNAs are introduced into exosomes through electroporation of mature exosomes. Ohno research group isolated exosomes from HEK293 cells and introduced into them synthetic miR-let-7 that has been delivered in epidermal growth factor receptor (EGFR)-expressing breast cancer cells [Ohno et al., 2013]. More importantly Alvarez-Erviti and co-workers demonstrate that exosomes functionalization with neuron-specific RVG peptide are able to cross the blood-brain barrier in mouse models opening a new field for the miRNA-based treatment of brain diseases [Alvarez-Erviti et al., 2011]. Other kinds of vehicle are borrowed by DNA delivery as the polymer polyethylene imine (PEI) a positive charged molecule that interact with anionic polysaccharides on cell membranes. Moreover, studies demonstrate that PEI facilitates miRNAs release from endosomes thanks to their disruption due to an influx of hydrogen ions and water into endosomes [Boussif et al., 1995]. Interestingly, PEI functionalized with RVG peptide transports through the blood-brain barrier miR-124a, even if, unfortunately no functional effects were found [Hwang et al., 2011]. Likewise, PolyLactic-co-Glycolic Acids (PLGA) a family of water insoluble

polymers have been employed mostly for antagomiR molecules transfection because of their ability to protect nucleic acids from degradation and their high loading capacity. Even these carriers give good results in in vivo models in which have been transfected a PNA against miR-155 [Babar et al., 2012]. Often miRNAs can be complexed with nanoparticles. Materials it constitutes nanoparticles are very heterogeneous but all are monodispersed particle size and present optical proprieties. Two well-known examples are silica nanoparticles and gold nanoparticles [Crew et al., 2012]. As regard silica nanoparticles miRNA-based molecules are entrapped into the nanoparticles in a non-covalently way and then are released following the hydrolysis of the matrix. Nanoparticles are functionalised with receptor-targeting ligand that is essential for the interaction with cells surface and internalization. GD2 (disialoganglioside) has been employed as receptor-targeting ligand for the delivery of miR-34a into neuroblastoma cells [Tivnan et al., 2012]. For both, even if the transfection has been shown to be efficient, several doubts relative to their toxicity and clearance are still present.

1.12. Peptide Nucleic Acids (PNA)

Peptide Nucleic Acids (PNA) are synthetic oligonucleotides that are able to bind with high specificity and affinity target DNA or RNA molecules. In PNA the typical sugarphosphate back-bone of nucleic acids is replaced by a synthetic peptide backbone: 2-aminoetyl glycine and the nucleobases are linked to the backbone with a methyl carbonyl linker [Gaglione et al., 2011].

This chemical change removes completely the charge (negative charge) that is typical of nucleic acids and makes these molecules biologically and chemically stable. Despite their radical change in structure respect to nucleic acids, they are able to hybridize with DNA or RNA following Watson-Crick rules and the hybrid complex is thermodynamically stable. Not less important, PNAs present high resistance to both DNase and protease [Dean, 2000]. Thanks to their features, PNAs are employed in several application fields as potential therapeutic molecules to modulate gene expression [Nielsen et al, 2010] or as diagnostic probes, for the detection of mutations and SNPs, in biosensors such as BIAcore [Itonaga et al., 2016].

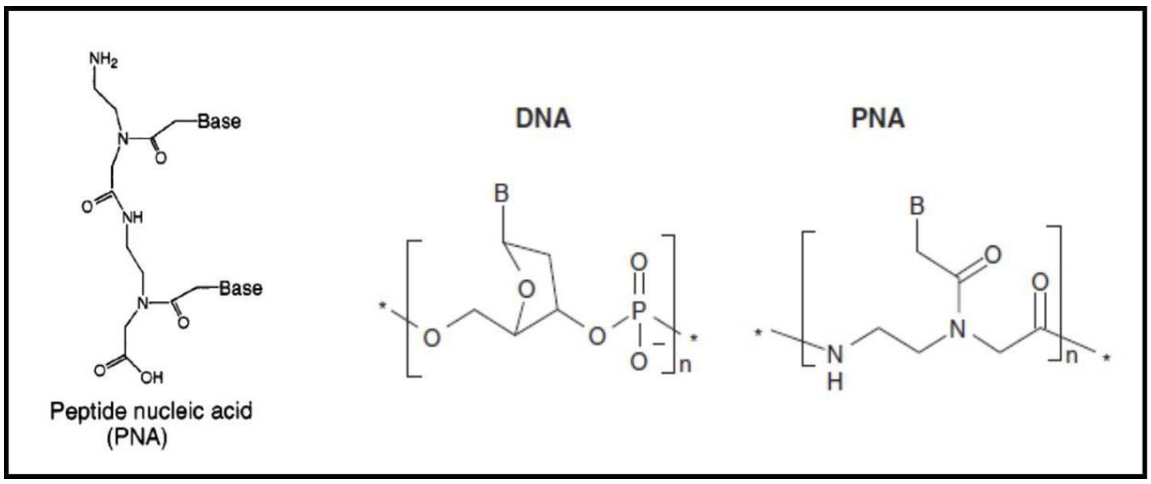

Figure 1.15: PNA structure. The sugar-phosphate back-bone typical of nucleic acids is replaced by a synthetic peptide back-bone.

1.12.2. PNA as therapeutic molecules

For their affinity for RNA, that is even higher than the affinity for DNA [Gambari et al., 2014], PNAs have been proposed as tools for miRNA levels regulation. Even if PNAs are synthesized to bind miRNAs, the end point of PNA against miRNA strategy is targeting miRNA-regulated genes. Several works demonstrate that PNAs through miRNA repression are able to restore levels of endogenous, target of the miRNA, mRNA. For example, Brognara and colleagues to increase levels of p27-kip1 protein, that is one of miR-221 targets, employed a PNA against miR-221 with good results [Brognara et al., 2012]

1.12.3. Anti-sense PNA strategy

Anti-sense PNA strategy is another strategy, which play important role to determine the gene expression. Interestingly, miRNAs can be inhibited not only at mature state, but also during their biogenesis [Figure 20]. Avitabile and colleagues, synthesize a PNA perfect complementary to the sense strand of the pre-miRNA. Starting from the evidence that bases belonging to the stem are not perfectly complementary, they hypothesized that the mismatched duplex of the pre-miRNA could be easily opened by PNA oligomers, perfectly complementary to the sense strand of the pre-miRNA [Avitabile et al., 2012] **[Figure 1.16].** Data confirmed their hypothesis, providing an additional strategy for miRNA inhibition.

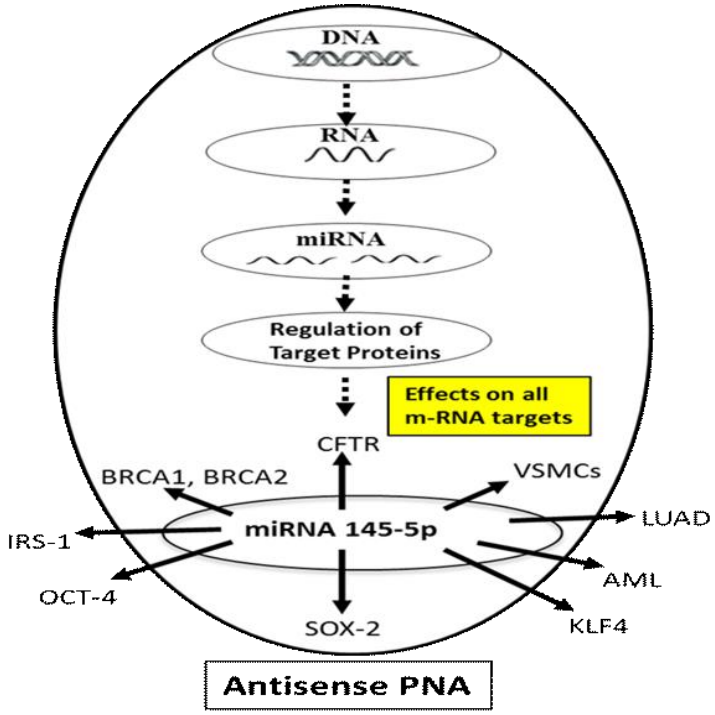

Figure 1.16: Anti sense PNA strategy: Overall mechanism of Antisense PNA strategy with targetting the various genes.

1.12.4. PNA Masking

PNA masking is also another novel approach for modulating the gene expression. As **[Figure 1.17]** explains this mechanism and how Masking is quiet efficient and effective to target the genes. MiRNAs are not the only biological molecules that can be targeted by PNAs, these kind of molecules, in fact have been also used to block mRNA transcription from DNA. In this case PNA binds gene promoter forming a triple-helix structure that inhibits transcription. An example was proposed by Tonelli and co-workers, which developed an antigene PNA that inhibits NMYC gene transcription in neuroblastoma cell lines [Tonelli et al., 2005]. Using the same mechanism of action PNAs can be used also to target Transcription Factors (TFs). Two possible effects can be achieved: PNA can bind TF, preventing the interaction between TF and gene promoter, this results in the reduction of gene expression [Vickers et al, 1996]. On the contrary, also PNAs, that are able to interact with gene promoter mimicking the function of true TFs, have been described [Møllegaard et al., 1994].

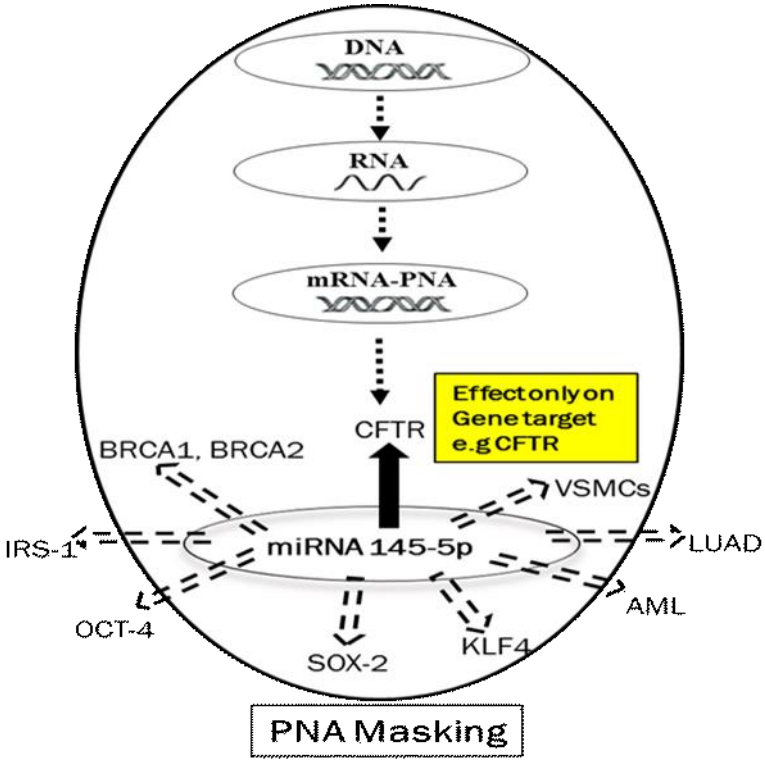

Figure 1.17: PNA Masking strategy. Overall mechanism of PNA Masking strategy with targetting the various genes and their efficacy on specific target gene as compared to all the genes.

1.12.5. PNA cellular delivery

To realize PNAs therapeutic potential, an efficient intracellular delivery method is required. Generally, these molecules present low cellular uptake and eukaryotic cells have been shown to be almost impermeable to micromolar concentration of naked PNA, for this reason several transfection protocols have been set up.

1.12.5.1. Cellular delivery of unmodified PNAs

At the beginning, a series of techniques that not require PNA sequence modification have been evaluated to internalize PNAs in cells. Between these techniques is included microinjection which was probably the first method used for PNA cellular internalization, but it is very laborious and applicable only in small scale experiment set-ups [Koppelhus et al., 2002]. After the transfection about 50% of target inhibition was achieved reaching the estimated concentration of 1 μM of PNA within cells [Hanvey et al., 1992]. A more feasible transfection method respect to microinjection is electroporation, which have been employed in several studies with good results. These methods, that can be define 'physical' methods, present the advantage to be efficient and selective, but are also harmful for cells and above all are not applicable in vivo.

Another effective strategy for PNA delivery is co-transfection.

In this case PNA is hybridized with a partially complementary DNA oligomers and the resulting PNA-DNA complex is than, conveyed into cells using cationic lipids [Hamilton et al., 1999]. Others researchers pre-treated cells with streptolisyn-O to permeabilize cells for PNA up-take but using fluorescent labelled PNA have demonstrated that a large amount of PNA was located in cytoplasm, while only a little percentage was internalized in the nucleus [Faruqi et al., 1998]. Others methods that do not require PNA modification are the internalization of PNA in cationic liposomes [Borgatti et al., 2002], microsphere [Chiarantini et al., 2006] or more recently, nanoparticles [Fang et al., 2009], but in these case is important to consider the toxicity of the vehicles, especially in primary cells.

1.12.5.2. Cellular delivery of modified PNAs

In these case cell permeability is obtained modifying directly the PNA molecule itself. At this propose, several modifications have been attempted during the years, with different results. Several research groups proposed the conjugation of PNA with lipophilic moiety such as Adamantyl Acetic Acid (Ada) [Ljungstrom et al., 1999] or triphenylphosphonium cation [Muratovska et al., 2001] but in both cases transfection efficiency is closely related to cell type and specific PNA sequence. In other cases PNAs were conjugated with short peptides named Cell Penetrating Peptide (CPP) and able to transport molecules such as oligonucleotides across cellular membrane, without involving membrane receptors. The mode of action of CPPs is still unclear. Penetratin (RQIKIYFQNRRMKWKK) a 16 residues peptide, was the first small peptide used at this propose and allow a diffuse PNA distribution both in cytoplasm and nucleus [Simmons et al., 1997]. CPPs are normally classified into two main groups, depending on the way they interact with PNA. Some CPP are covalently bounded to PNA, such as polyarginine peptide (R8) sequence. In another cases, peptides can form non-covalent complex with PNA.

Generally, are employed short amphipathic peptide carriers consisting of a hydrophilic (polar) domain and a hydrophobic (non-polar) domain, as Pep-1. The mode of action of CPPs is still unclear. All data confirm that an important role is played by positive charges in the peptide sequence, which interact with phospholipids in the cellular membrane. Some authors hypothesize that PNAs are internalised with an endocytosis-

like mechanism and transferred in the cytoplasm trapped into vesicles [Richard et al., 2003]. Another possibility is that CPPs interacts with negatively charged phospholipids, inducing the formation of an inverted micelle inside the lipid bilayer [Derossi et al., 1996]. Maybe, these mechanisms could also, occur simultaneously [Drin et al., 2003]. Often, is particularly important to vehicle PNAs only in specific cells to avoid adverse side-effects, for these reason PNAs functionalized with peptide sequence that is bounded only by specific cell surface receptors have been developed [Basu et al., 1997].

1.13. Untranslated region

In molecular genetics, an untranslated region (or UTR) refers to either of two sections, one on each side of a coding sequence on a strand of mRNA. If it is found on the 5' side, it is called the 5' UTR (or leader sequence), or if it is found on the 3' side, it is called the 3' UTR (or trailer sequence). mRNA is RNA that carries information from DNA to the ribosome, the site of protein synthesis (translation) within a cell. The mRNA is initially transcribed from the corresponding DNA sequence and then translated into protein. However, several regions of the mRNA are usually not translated into protein, including the 5' and 3' UTRs.

Although they are called untranslated regions, and do not form the protein-coding region of the gene, uORFs located within the 5' UTR can be translated into peptides.[Vilela et al., 2003] **[Figure 1.18]**

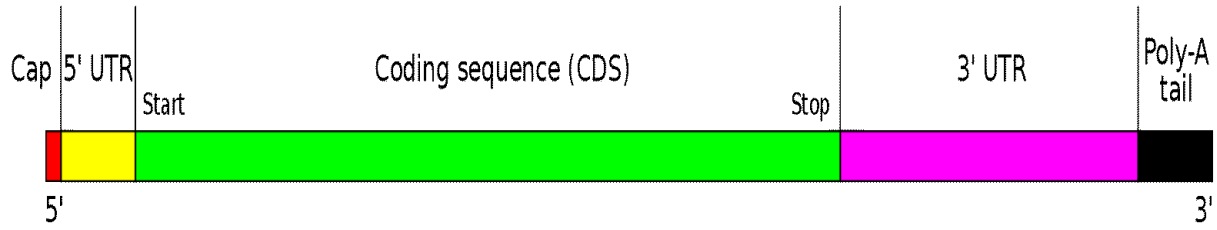

Figure 1.18: UTRs, The structure of typical human protein coding mRNA including the Untranslated Regions(UTRs). [Vilela et al., 2003]

1.13.1. Five Prime 5′ untranslated region (5′ UTR)

The 5′ untranslated region (5′ UTR) (also known as a leader sequence or leader RNA) is the region of an mRNA that is directly upstream from the initiation codon. This region is important for the regulation of translation of a transcript by differing

mechanisms in viruses, prokaryotes and eukaryotes. While called untranslated, the 5′ UTR or a portion of it is sometimes translated into a protein product. This product can then regulate the translation of the main coding sequence of the mRNA. In many organisms, however, the 5′ UTR is completely untranslated, instead forming complex secondary structure to regulate translation.

The 5′ UTR has been found to interact with proteins relating to metabolism, and proteins translate sequences within the 5′ UTR. The 5′ UTR begins at the transcription start site and ends one nucleotide (nt) before the initiation sequence (usually AUG) of the coding region. In prokaryotes, the length of the 5′ UTR tends to be 3–10 nucleotides long, while in eukaryotes it tends to be anywhere from 100 to several thousand nucleotides long.[Lodish et al., 2004]

1.13.1.1. Role in transcriptional regulation

Transcription of the msl-2 transcript is regulated by multiple binding sites for Sxl at the 5′ UTR. In particular, these poly-uracil sites are located close to a small intron that is spliced in males, but kept in females through splicing inhibition. This splicing inhibition is maintained by Sxl. When present, Sxl will repress the translation of msl2 by increasing translation of a start codon located in a uORF in the 5′ UTR (see above for more information on uORFs). Also, Sxl outcompetes TIA-1 to a poly(U) region and prevents snRNP (a step in alternative splicing) recruitment to the 5′ splice sit. [Penalva et al., 2003]

1.13.2. Three prime untranslated region (3'-UTR)

In molecular genetics, the three prime untranslated region (3'-UTR) is the section of messenger RNA (mRNA) that immediately follows the translation termination codon. The 3'-UTR often contains regulatory regions that post-transcriptionally influence gene expression.During gene expression, an mRNA molecule is transcribed from the DNA sequence and is later translated into a protein. Several regions of the mRNA molecule are not translated into a protein including the 5' cap, 5' untranslated region, 3' untranslated region and poly(A) tail. Regulatory regions within the 3'-untranslated region can influence polyadenylation, translation efficiency, localization, and stability of the mRNA. [Pichon et al., 2012] The 3'-UTR contains both binding sites for regulatory proteins as well as microRNAs (miRNAs). By binding to specific sites

within the 3'-UTR, miRNAs can decrease gene expression of various mRNAs by either inhibiting translation or directly causing degradation of the transcript. The 3'-UTR also has silencer regions which bind to repressor proteins and will inhibit the expression of the mRNA.

1.13.2.1. Role in gene expression

The 3'-untranslated region plays a crucial role in gene expression by influencing the localization, stability, export, and translation efficiency of an mRNA. It contains various sequences that are involved in gene expression, including microRNA response elements (MREs), AU-rich elements (AREs), and the poly(A) tail. In addition, the structural characteristics of the 3'-UTR as well as its use of alternative polyadenylation play a role in gene expression.

3'-UTR mutations can be very consequential because one alteration can be responsible for the altered expression of many genes. Transcriptionally, a mutation may affect only the allele and genes that are physically linked. However, since 3'-UTR binding proteins also function in the processing and nuclear export of mRNA, a mutation can also affect other unrelated genes [Chatterjee et al., 2009]**[Figure 1.20]**

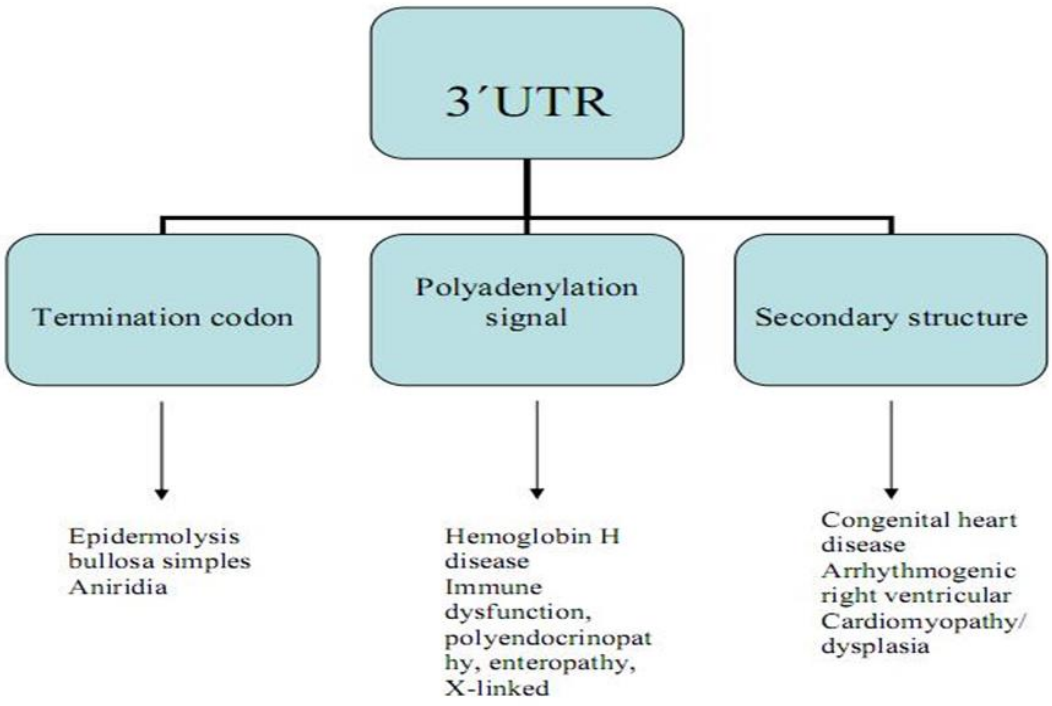

Figure 1.19: Diseases caused by different mutations within the 3'-UTR. [Chatterjee et al., 2009]

1.14. B-thalassemia

1.14.1. Definition and epidemiology

The term thalassemia derives from the Greek, thalassa (sea) and haima (blood) [Galanello and Origa 2010].B thalassemia syndromes are a group of hereditary disorders characterized by a genetic deficiency in the synthesis of fully functional β globin chains of adult hemoglobin. The effect of genetic alterations can consist in total absence of protein synthesis, imbalance in the synthesis rate of different globins, or production of unstable chains. In any case, an imbalance between α and non-α globin chains occurs, that is responsible for the pathophysiology of the disease [Silvestroni et al., 1998].

It is mainly present among Mediterranean, Middle-East, Transcaucasian, Central Asian, subcontinental Indian, and Far East populations. It is also relatively common in African populations. The highest incidences are reported in Cyprus (14%), Sardinia (12%), and South East Asia [Weatherall 1980; Galanello 2010].

In Italy Sardinia is the region at highest risk, with about 12.6% carriers of β thalassemia [Cao A 1978]. High incidence is also present in the Delta Padano area, in Sicily and in the Southern regions, mainly in coastal areas [Silvestroni et al., 1998]. This particular geographic distribution led to the hypothesis that the disease provides a benefit to lethal factors like malaria, as the condition of healthy carrier can prevent infection by Plasmodium falciparum [Harding et al. 1998; J.Weatherall et al., 2003], even though the mechanism is not known yet [Weatherall DJ. In: Williams WJ 1991].

Recently, migratory movements have brought the development of β thalassemia also in Northern Italy, Australia and USA [Silvestroni et al.,1998], making it one of the most common genetic autosomal recessive diseases worldwide [Maria-Domenica cappellini et al.,2008].

1.14.2. Molecular bases

The extensive application of DNA study methods has allowed in a few years the identification of a high number of defects in globin structural genes or regulatory regions, allowing the identification of genotype-phenotype correlation for β thalassemia.

More than 200 mutations have been identified almost everywhere in the β globin gene, resulting in a total (β0) or partial (β+) deficit of the globin chain synthesis and a subsequent quantitative reduction in β globin amount [Silvestroni et al., 1998; Thein 2005].

Pathogenetic mutations include deletions and point mutations.

Gene deletions are rare and have a variable extension. They can affect the entire β gene or its promoter and generally lead to β0 thalassemia with increased levels of HbA2 [Silvestroni et al.,1998].

Point mutations can affect different molecular mechanisms:

- Defects of transcription

In most cases they result from point mutations in the β globin gene promoter that cause reduction of transcription from 75% to 80%, typically giving rise to β+thalassemia [Lacerra, Prezioso et al. 2013].

- Alteration of post transcriptional modifications of pre-mRNA

About half of the β thalassemias is caused by splicing defects [Silvestroni et al., 1998, where several cases can occur:

1.14.3. Mutations in introns (IVS, Intervening Sequences)

a- The mutation can destroy one of the two invariant dinucleotides, GT or AG, necessary for the normal splicing, that cannot take place. Therefore a β0 thalassemia results, due to the degradation of mRNA;

b- The mutation can reduce the efficiency of the splicing site, by altering its consensus sequence: generally this kind of alterations cause β+ thalassemia;

c- The mutation can create a new splicing site, by generating a new GT or AG in a cryptic site, usually resulting in a β+ thalassemia.

1.14.4. Mutations in exons

Generally these mutations activate a cryptic site located in a coding sequence, which will be used together with the normal site. As this new site is rarely recognized, however, the resulting phenotype is that of a mild β+ thalassemia [Lacerra, Prezioso et al., 2013].

- Defects of translation

These mutations are numerous and usually give rise to β0 thalassemia. They frequently affect exons and comprise nonsense mutations, introducing a termination codon, and frameshift mutations, causing a change in the reading frame of mRNA: they both lead to β0 thalassemia. Also the start codon, the stop codon and the 3' UTR may be interested: the two last conditions lead to β+ thalassemia [Silvestroni et al., 1998].

- Production of unstable globin chains

These defects include frameshift, nonsense mutations, or deletions of few nucleotides and give origin to unstable globin chains, which rapidly precipitate in the red blood cells and are not functional [Silvestroni et al.,1998].The most frequent Italian mutations for β thalassemia are four: β039 C□T, β+IVSI-110 G□A, β+IVSI-6 T□C and β0IVSI-1 G□A [Rigoli, Meo et al. 2001]. The same mutations have been described in many Mediterranean countries [Huisman THJ et al., 1997].

1.14.5. Understanding globin regulation in β-thalassemia: it's as simple as α, β, γ, δ

Studies of the regulation of the human β-globin gene locus have provided powerful insights into human gene expression in general at the molecular level. The human globin loci are among the best characterized in the human genome at the gene and protein levels. The β–locus control region (β-LCR) — a dominant control region located upstream of the globin structural genes — is a strong enhancer of the expression of the downstream structural globin genes [Figure 1.28A]. The structural globin gene located furthest upstream is the ε-globin gene, which is active in early fetal life [Figure 1.28A]. The α-globin gene and 2 γ-globin genes, Gγ and Aγ, are the major genes expressed throughout fetal life [Figure 1.28 A and B]; the δ- and β-globin genes are activated late in fetal life, with the β-globin gene being most highly expressed in erythroid cells during adult life. Globin gene expression is controlled by the complex interactions between cis-acting sequences (the β-LCR and structural globin gene sequences) on the one hand and trans-acting factors (including transcription factors and chromatin remodeling activities) on the other. Many new details regarding these interactions have recently been described [Patrinos et al.,2004].

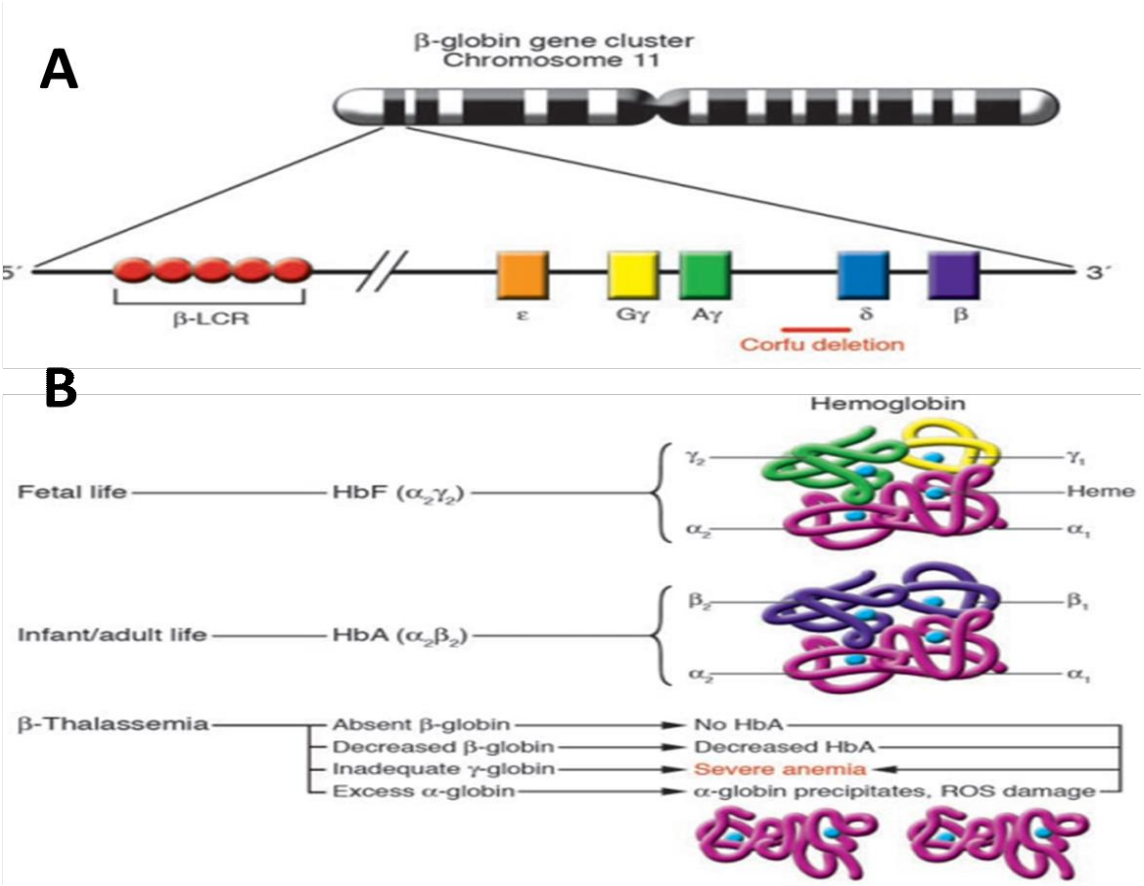

Figure 1.20: The human globin loci and their role in β-thalassemia. (A) The β-LCR and structural genes (ε, Gγ, Aγ, δ, and β) within the β-globin locus on chromosome 11 are shown. The Corfu deletion, which includes part of the structural δ-globin gene and γ–δ intergenic sequences, is also shown. **(B)** In early fetal life, the α- and γ-globin chains combine to form HbF (α2γ2), the main β-globin–like globin during the remainder of fetal life and early postnatal life. In late postnatal and adult life, normal hemoglobin (HbA, α2β2) predominates. In homozygous β-thalassemia, decreased or absent β-globin production leads to decreased or absent HbA levels, respectively. The synthesis of γ-globin does not increase enough to compensate for the reduced or absent β-globin level. As a result, excess α-globin accumulates and precipitates in erythroid cells and causes damage due to the action of ROS and apoptosis of the damaged cells. Severe anemia results [Bank A et al., 2005].

The globin genes are transcribed into mRNA precursors in the nucleus and then processed to mature mRNAs, which become associated with ribosomes and are translated into globin polypeptides in the cell cytoplasm. The most stable configuration of hemoglobin is as tetramers of globin chains associated with heme groups [Figure 1.28B]. Homozygous β-thalassemia (also known as Cooley anemia) has long been a model for the study of diseases caused by mutations and deletions at a single genetic locus, in this case, the β-globin locus. During normal fetal life, optimal γ-globin synthesis balances α-globin synthesis [Figure 1.28B], which results in the production of adequate amounts of fetal hemoglobin (HbF, α2γ2). In β-thalassemia, point mutations in the β-globin structural gene are largely responsible for decreased or absent β-globin synthesis. In β-thalassemia homozygotes, γ-globin production is inadequate to compensate for the deficit in β-globin and hemoglobin A

(HbA, α2β2), despite optimal γ-globin synthesis in these patients in fetal life. As a result, a vast excess of α-globin accumulates and usually associates with heme to form hemoglobin. Possessing no single stable molecular configuration, α-hemoglobin aggregates and precipitates in early hemoglobin-producing cells in the bone marrow, which leads to apoptosis of these cells and ineffective erythropoiesis [Figure 1.28B]. The red cells that reach the peripheral blood also contain excess α-globin; this causes the formation of inclusion bodies and an increase in reactive oxygen species levels, which leads to membrane damage and causes these cells to be preferentially hemolyzed [Figure 1.28B].

The current therapy for β-thalassemia is blood transfusions supplemented by iron chelation. Decreasing α-globin accumulation and/or reactivating γ-globin production would greatly ameliorate the anemia present in β-thalassemia. In this issue of the JCI, [Han et al., 2005], illustrate a novel mechanism for decreasing α-globin levels in a murine model of β-thalassemia. Other recent advances in understanding the fate of α-globin and the regulation of HbF synthesis have also provided new insights into the pathogenesis of human β-thalassemia and may lead to new treatments.

1.14.6. Kruppel-like factor 4 (*KLF4*)

Kruppel-like factor 4 (KLF4; gut-enriched Krüppel-like factor or GKLF) is a member of the KLF family of zinc finger transcription factors, which belongs to the relatively large family of SP1-like transcription factors. KLF4 is involved in the regulation of proliferation, differentiation, apoptosis and somatic cell reprogramming. Evidence also suggests that KLF4 is a tumor suppressor in certain cancers, including colorectal cancer. It has three C2H2-zinc fingers at its carboxyl terminus that are closely related to another KLF, KLF2. It has two nuclear localization sequences that signal it to localize to the nucleus. In embryonic stem cells (ESCs), KLF4 has been demonstrated to be a good indicator of stem-like capacity. It is suggested that the same is true in mesenchymal stem cells (MSCs).

In humans, the protein is 513 amino acids, with a predicted molecular weight of approximately 55kDa, and is encoded by the *KLF4 gene*. The *KLF4 gene* is conserved in chimpanzee, rhesus monkey, dog, cow, mouse, rat, chicken, zebrafish, and frog. Krüppel-like factor 4 (KLF4) is an evolutionarily conserved zinc finger-containing transcription factor that regulates diverse cellular processes such as cell growth, proliferation, and differentiation. Since its discovery in 1996, KLF4 has been gaining a lot of attention, after it was shown in

2006 as one of four factors required for the induction of pluripotent stem cells (iPSCs) [Ghaleb et al., 2017].

1.14.7. Role in disease regulation

KLF4 role in disease is context dependent where under certain conditions it may play one role and under different conditions it may assume a complete opposite role. KLF4 is an anti-tumorigenic factor and its expression is often lost in various human cancers.

However, in some cancer types KLF4 may act as a tumor promoter where increased KLF4 expression has been reported, such as in oral squamous cell carcinoma and in primary breast ductal carcinoma. Also, overexpression of KLF4 in skin resulted in hyperplasia and dysplasia, which lead to the development of squamous cell carcinoma. Similar finding in esophageal epithelium was observed, where overexpression of KLF4 resulted in increased inflammation that eventually lead to the development of esophageal squamous cell cancer in mice.

MicroRNAs (miRNAs) are posttranscriptional modulators of gene expression and play an important role in many developmental processes. The expression of microRNA-145 (miR-145) is low in self-renewing human embryonic stem cells (hESCs) but highly upregulated during differentiation. We identify the pluripotency factors OCT4, SOX2, and KLF4 as direct targets of miR-145 and show that endogenous miR-145 represses the 30 untranslated regions of OCT4, SOX2, and KLF4. Increased miR-145 expression inhibits hESC self-renewal, represses expression of pluripotency genes, and induces lineage-restricted differentiation. Loss of miR-145 impairs differentiation and elevates OCT4, SOX2, and KLF4 [Na xu et al., 2009]. Moreover, the in vivo study showed that miR-152 over-expression and KLF4 knockdown produced the smallest tumor volume and the longest survival in nude mice. Taken together, these results elucidated the function of miR-152 in GSCs progression and suggested a promising application of it in glioma treatment [Jun ma et al., 2014].

2. AIM OF THESIS

The aim of thesis was to develop new therapeutic approaches to correct biomedical applications in rare genetic disorders. For that purpose, we studied CFTR and *KLF4 gene*s expressions in the presence of PNAs targeting miRNAs able to interact with the 3'-UTR region of the CFTR and KLF4 by masking strategy.

In preliminary studies, we started with Antisense strategies based on the use of PNA-antimiR and determined optimal Concentration of different PNAs. Further, identification of various miRs and binding sites related to them, which could be further used to study the CFTR and *KLF4 gene* expression and related activities.

In addition to these preliminary studies, we also determined the optimal Concentration of PNA-145 5p in Calu-3 cells. Real Time qPCR analysis of PNA-145-5p related to different miRNAs was also performed. It was also further quantified through RT q-PCR of the transcription *CFTR Gene* and quantification of CFTR protein levels by western blot assay.

The principal purpose of the first part of the research proposed in this thesis, was the development of the effectivity of anti-miR-145-5p role in interfering the target binding sites related to miR-145-5p and how does it effects the *CFTR Gene* mRNA and protein content not only in non CF CALU-3 cells but also in CF cell lines such as CFBE e.g CFBE-41oΔF-508. Further, we expanded anti-miR-145-5p role, on CF cell lines just to verify our results and demonstrate the results for further analysis and propose this strategy for CF patients. For this purpose, we used the CFBE-41o ΔF-508 cell line to demonstrate the effects of this interference in *CFTR Gene* with anti-miR-145-5p and verified them both on mRNA and protein content level.

In addition to the anti-miRNA therapeutic strategy, inhibition of miRNA functions can be reached by masking the miRNA binding sites present within the 3'UTR region of the target mRNAs. Therefore, we designed a PNA, masked the binding sites of the miR-145-5p present within the 3'UTR of the CFTR mRNA and to determine its activity in inhibiting miR-145-5p function, with particular focus on the expression of both CFTR mRNA and CFTR protein in Calu-3 cells. The results obtained support the concept that the PNA masking the miR-145-5p binding site of the CFTR mRNA is able to interfere with miR-145-5p biological functions, leading to both an increase of CFTR mRNA and CFTR protein content. The objective of this part of study was to design a PNA masking the miR-145-5p binding site present within the

3'UTR of the CFTR mRNA and to determine its activity in inhibiting miR-145-5p function, with particular focus on the expression of both CFTR mRNA and CFTR protein in Calu-3 cells. As the experimental model system, the Calu-3, CFBE and K562 cell lines were selected for their respective roles in defining the respective gene expression. These cells are a well-differentiated and characterized cell line derived from human bronchial submucosal glands and extensively used to study CFTR expression, immunological behavior, *KLF4 gene* expression and their effects.

Further, focus was to check miR145-maskingPNA also on CF cell lines such as CFBE, including cell lines carrying mutated and wild type plasmid CFTR (CFBE-410, CFBE-ΔF508). In addition to that, Co-administration of PNA-Masking with Vertex compounds Correctors (VX-809), Potentiators (VX-770) and read through molecules e.g Tobramycin was also done to enhance the CFTR level expression and effectivity.

In last part of this study, aim was to not only restrict masking only in cystic fibrosis like genetic disorder but also tried to propagate this masking strategy to other genetic disorder like β-thalassemia. For that purpose, firstly we identified the target gene in respective genetic disorder e.g Krüppel-like factor (KLF4); it can also be seen from the literature that *KLF4 gene* expression is quiet viable in B-thalassemia. Further, we identified various miRs and binding sites related to them, which could be further used to study the *KLF4 gene* expression. Lastly, effects of different treatments in increase of hemoglobin containing positive cells were done by Benzidine Assay, Effects of Masked LNAs on the Gamma globin (γ) and Alpha Globin (α) in K562 Cells and *KLF4 gene* expression was calculated by real RT q-PCR.

3. MATERIALS AND METHODS

3.1. Cellular models for cystic Fibrosis

3.1.1. IB3-1 Cell line

IB3-1 is an immortalized cell line created in 1992 from a primary culture of bronchial epithelia cells isolated from a patient with cystic fibrosis. The culture was transformed with a hybrid virus, adeno-12-SV40 [Zietlin et al., 1991]. The IB3-1 are deficient in cyclic AMP-medicated protein kinase A activation of chloride conductance, which is diagnostic of Cystic Fibrosis [Flotte et al., 1993]. Genotypically, the cell line is a compound heterozygote containing the delta F508 mutation and a nonsense mutation, W1282X, with a premature termination signal [Schneider et al., 1999]. The cells stain positively for SV40 T antigen [Zietlin et al., 1991]. They can be used for studies of the mutant cystic fibrosis transmembrane regulatory protein and its interaction with the chloride channel. The S9 cell line (ATCC CRL-2778) and the C38 cell line (ATCC CRL-2779) were derived from the IB3-1 cell line. The CF phenotype present in the IB3-1 cells was corrected in the S9 and C38 cell line by transfection with wild-type adeno-associated viral cystic fibrosis transmembrane conductance regulator (AAVCFTR). This cell line aattaches with the surface for growing, briefly rinse the cell layer with 0.25% (w/v) Trypsin- 0.53 mM EDTA solution to remove all traces of serum that contains trypsin inhibitor. Add 2.0 to 3.0 ml of Trypsin-EDTA solution to flask and observe cells under an inverted microscope until cell layer is dispersed. Cells that are difficult to detach may be placed at 37°C to facilitate dispersal Add 6.0 to 8.0 ml of complete growth medium and aspirate cells by gently pipetting. Incubate cultures at 37°C.

3.1.2. Calu-3 cell line

Calu-3 is a human lung cancer cell line commonly used in cancer research and drug development. Calu-3 cells are epithelial and can act as respiratory models in preclinical applications [Zhu et al., 2010]. Briefly rinse the cell layer with 0.25% (w/v) Trypsin- 0.53 mM EDTA solution to remove all traces of serum that contains trypsin inhibitor. Add 2.0 to 3.0 mL of Trypsin-EDTA solution to flask and observe cells under an inverted microscope until cell layer is dispersed (usually within 5 to 15 minutes). To avoid clumping do not agitate the cells by hitting or shaking the flask while waiting for the cells to detach. Cells that are difficult to detach may be placed at 37°C to facilitate dispersal. Add 6.0 to 8.0 mL of complete growth medium and aspirate cells by gently pipetting. Incubate cultures at 37°C.

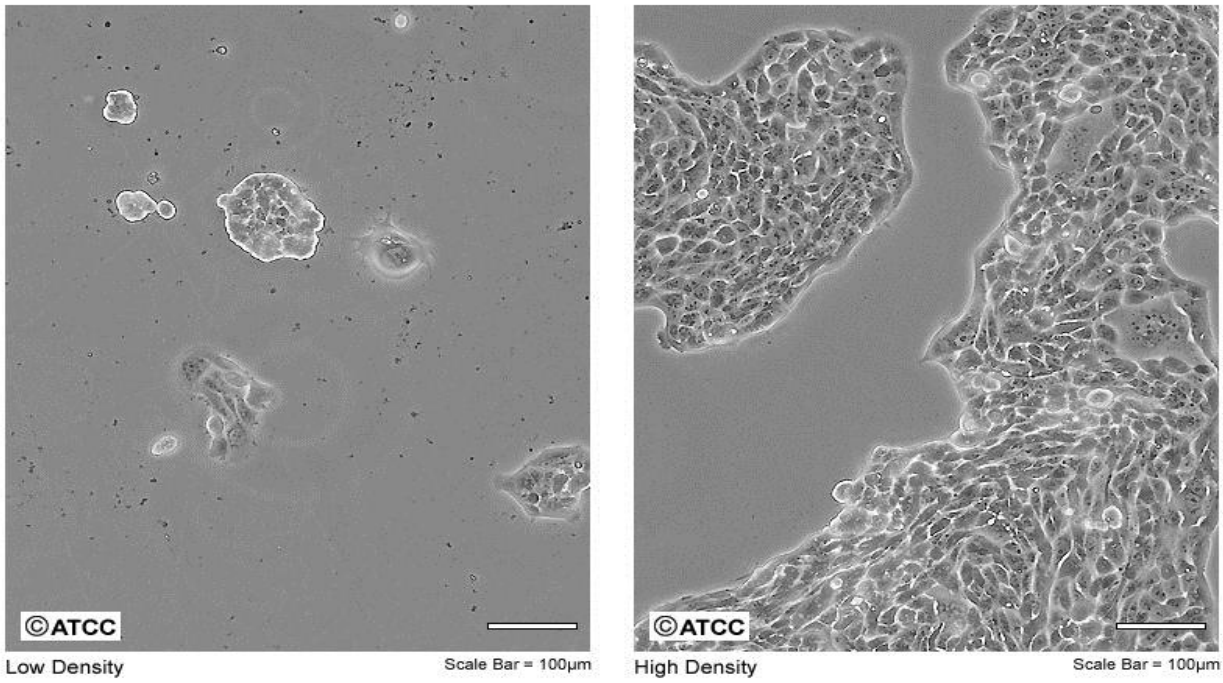

Figure 3.1 Calu-3 cell line with low and high density images. ATCC website

3.1.3. CFBE cell line

Cystic Fibrosis (CF) is a lethal autosomal recessive disease caused by mutations in the CF transmembrane conductance regulator (CFTR) gene which functions as a cAMP-activated and phosphorylated-regulated Cl channel. The predominant mutation in the *CFTR Gene* is a trinucleotide deletion that results in loss of a phenylalanine at amino acids 508 (ΔF508) in the CFTR protein. This mutation accounts for ~66% of all CF alleles. Presently, There are different types of CFBE cell lines with respect to its additional plasmid. Which are following.,

3.1.3.1. CFBE-41o: (F508del/F508del)

CFBE41o- is a CF human bronchial epithelial cell line, derived from a CF patient homozygous for the ΔF508 CFTR mutation and immortalized with the origin-of-replication defective SV40 plasmid (pSVori-) (1,2). CFBE41o- displays all ion transport properties characteristic of cystic fibrosis such as defective cAMP-dependent chloride transport and intact calcium-dependent chloride transport. Under appropriate culture conditions, CFBE41o- forms tight junctions to give a polarized epithelium [Illek et al., 2008]. It has

F508del/F508del mutation but it also contains the over-expressed wild type CFTR plasmid. While antibiotic puromycin is used regarding growing these cells, other process remains the same for all the cell types. Human bronchial epithelial cells CFBE41o− stably overexpressing WT-CFTR (WT-CFBE) and F508del/F508del-CFTR (F508del-CFBE) were grown in Eagle's-minimum essential-medium E-MEM, supplemented with 10% of FBS, 2 mM glutamine, and 2 μg/mL puromicyn for F508del-CFBE and 0.5 μg/mL for WT-CFBE.

3.1.3.2. CFBE-ΔF508: (F508del/F508del)

CFBE- ΔF508 has F508del/F508del mutation and it does contain the over-expression F508del CFTR plasmid. While antibiotic puromycin is used regarding growing these cells Human bronchial epithelial cells CFBE41o− stably overexpressing WT-CFTR (WT-CFBE) and F508del/F508del-CFTR (F508del-CFBE) were grown in Eagle's-minimum essential-medium E-MEM, supplemented with 10% of FBS, 2 mM glutamine, and 2 μg/mL puromicyn for F508del-CFBE and 0.5 μg/mL for WT-CFBE.

3.1.3.3. CFBE- ΔF508 YFP: (F508del/F508del)

CFBE- ΔF508 YFP also has F508del/F508del mutation and it does contain the over-expression F508del CFTR plasmid and YFP plasmid. Further in this case, antibiotic puromycin and gentamycin is used regarding growing these cells and to growing these cells CF human bronchial epithelial cell line CFBE41o- stably coexpressing human F508del-CFTR (CFBE-F508del) and the high-sensitivity halide-sensing green fluorescent analog yellow fluorescent protein (HS-YFP) YFP-H148Q/ I152L were grown on substrates coated with an extracellular matrix containing fibronectin/bovine collagen type I/BSA in MEM supplemented with 10% fetal calf serum, 2 mM L-glutamine, Nonessential Aminoacid 100x (Euroclone) and 2 μg/mL of Puromycin and 750 μg/mL of Geneticin (G418) as positive selection of expression of F508del CFTR and YFP, respectively. [Sondo et al., 2011]

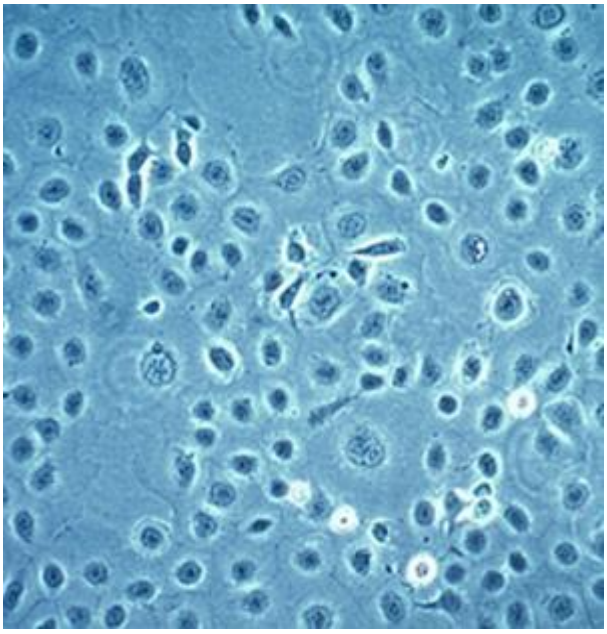

Figure 3.2 CFBE cell line image from ATCC website.

3.2. Cellular treatments

For our experiments the different cell lines were seeded when they reached about 80% of confluence in the culture flask; for the24-hour 48-hour and 72-hour treatments they were plated onto a 6-well plate, 12-well plate and2 4 well plate at a different densities regarding different cell lines with final volume also varies from 1 to 3 ml.

The treatments were performed the day after seeding. After having removed the medium, rinsed the cells with DPBS (Lonza, Verviers, Belgium) to remove any trace of debris and replace the medium with a fresh one, cells were treated with the compounds in analysis.

3.2.1. Coating solution

Prepare under bio-safety cabinetFor 100 ml:

- Human fibronectin (Prodotti Sacco. Code: L003868 Ref. Cat. 354008) (1 mg vial): Resuspend well with10 ml of LCH-BASAL Medium and collect all in the container with filter membrane of 150 ml.

- Bovine Collagen Type I 30 mg: 1 ml (Prodotti Sacco Code: L004228 ref. Cat. 354231)

- BSA (1mg/ml; aliquots in -20 °C): 100ul

- LCH-BASAL MEDIUM: make up to 100 ml.

Filter in the container with filter membrane 0.2 μM of 150 ml and store at + 4 °C. This solution can be used 3 times by always filtering it before use.

3.2.2. Culture medium

Prepare under Bio-safety cabinet

-450 ml MEM WITH Earle's SALTS (Euroclone Cod. ECB2071L)

-50 ml of FBS (10% of the final medium)

-5 ml of glutamine 100X

-5 ml Non-Essential Aminoacids 100x (Euroclone COD. ECB3054D)

-100 ul of Puromycin (Stock Solution 10mg/ml in the medium is diluted to 2 ug/ml)

When preparing the medium take a bottle of MEM remove 50 ml and Add FBS, Glutamine, amino acids and Puromycin and gentamycin depending upon cell line. Filter in the container with filter membrane 0.2 μM of 500 ml and store at + 4 °C. Replace itin the cells flasks in alternate days evaluating cell growth.

Use 5ml x T25, 12-15ml x T75, 25-30ml x T150 of medium.

3.2.3. Detachment Solution

Trypsin 0.05% EDTA 0.02 WITH PHENOL RED, 100ml (Euroclone Code ECM0920D). Filter Under Bio-safety cabinet in the container with filter membrane 0.2 □m of 150 ml and store at + 4 °C. PBS w/o Calcium and Magnesium (Lonza company Cod. 17-516 F) Store at room temperature.

3.3. RNA samples preparation

3.3.1. RNA Total Extraction

Extracting total RNA is an important process that has the aim to evaluate gene or miRNA expression after cell specific treatments. Total RNA was isolated with Trizol Reagent (Sigma Aldrich), a mixture of guanidine thiocyanate and phenol in a monophasic solution, which has the ability to separate effectively RNA to DNA and proteins, preserving intact the nucleic acid. Cells were separated from supernatant after a 4000 rpm centrifugation for 4 minutes at room temperature.

From manufacturers instruction it was used 1 ml of Trizol Reagent to lyse 5-10 x 106 cells by repeated pipetting, then to ensure complete dissociation of nucleoprotein complexes, the samples incubated for 3 minutes at room temperature. Thus, 200 µl of Chloroform per ml of Trizol Reagent, were added, shaked vigorously for 15 seconds. After waiting 3 minutes, the resulting mixture was centrifuged at 12000 rpm for 10 minutes at 4°C, to separate protein, the red organic phase, DNA in interphase, and RNA, the colorless upper aqueous phase. Then, 500 µl of 2-propanol were added to the aqueous phase.

Samples were mixed, by inverting the tube at least seven time. The samples were left for 10 minutes at room temperature, and then they were centrifuged at 12000 rpm for 10 minutes at 4°C to precipitate RNA. The pellet of RNA was washed with 500 µl of 75% EtOH, was centrifuged at 12000 rpm for 15 minutes at 4°C, dried and dissolved in nuclease-free water. Samples were stored at -80°C until the execution of qualitative and quantitative assays.

Also the extraction of microRNAs was performed following this protocol of total RNA extraction.

3.3.1.1. RNA extraction using silica columns

[Qiagen, Hilden, Germany] according to the manufacturer's protocol with some minor changes. 150 µ L of cell culture were lysed with 5 volumes (750 µ L) of Qiazol Lysis Reagent, which contains a solution of phenol and cyanoguanidine. The mixture plasma-QIAzol was vigorously shaken and incubated at room temperature for 5 minutes. At the end of the incubation 400 amoles of synthetic mature Cel-miR-39-3p [miRVana, Thermo Fisher Scientific, Waltham, Massachussetts, USA] were spiked into the mixture as exogenous control to evaluate extraction efficiency. 150 µL of nuclease free chloroform [Sigma-Aldrich, Saint Louis, Missouri, USA] was added to each sample, the mixture was shaken vigorously for 15 seconds and then incubated at room temperature for 3 minutes. Samples were centrifuged at 4°C for 15 minutes at 12000g in order to separate three phases: the lower organic phase, a white interphase and an upper aqueous phase, which contains RNA. The upper phase was collected avoid touching interphase or organic phases, and transferred to a new clean tube. The collected aqueous phase was measured and 1,5 volumes of 100% nuclease free ethanol [Carlo Erba, Milano, Italy] was added. 700 µ L of solution were added for each time to miRNeasy MinElute Spin Column, columns were centrifuged at 8000g for 30 seconds at room temperature and the flow-through was discarded. This step was repeated until all the volume of the mixture was added to the Columns were washed with two

solutions, purchased from the kit: RWT Buffer and RPE Buffer. Firstly, 700 µ L of RWT Buffer were added to the columns, which was centrifuged at 8000g for 30 seconds at RT and the flow-through was discarded. In the second step, 500 µL of RPE buffer were added to the column, the columns were centrifuged at 8000g for 30 seconds at RT and the flow-through was discarded. Columns were washed with 80% ethanol, centrifuged at 8000g for 2 minutes at RT. Flow-through was discarded, and collection tube was replaced with a new collection tube. Columns with open lid, were centrifuged at 12000 rpm for 5 minutes to dry completely the filter. Collection tube was discarded and column was placed in a new collection tube. 18 µ L of nuclease free water were placed in the centre of the column, without touching walls. After an incubation of 10 minutes at room temperature, columns were centrifuged at 14000g for 1 minute at room temperature. Collected RNA was stored at -80°C for further applications.

3.3.1.2. RNA extraction from cell-culture supernatants

RNA extraction from cell-culture supernatants was performed as indicated in Turchinovich et al., 2011 with some minor variations. A combination of phenol-chloroform and columns based extraction was employed. 400 µ L of supernatants, isolated from 72 hours cell-culture were lysed with 1,2 mL of TRIzol LS Reagent [Invitrogen, Thermo Fisher Scientific, Waltham, Massachussetts, USA], and incubated for 5 minutes at room temperature. At the end of the incubation respectively a) 400 amoles of synthetic, mature Cel-miR-39-3p [miRVana, Thermo Fisher Scientific, Waltham, Massachussetts, USA] and b) 12 µg of nuclease free glycogen [Ambion, Thermo Fisher Scientific, Waltham, Massachussetts, USA], were added. 320 µ L of nuclease free chloroform [Sigma-Aldrich, Saint Louis, Missouri, USA] were added, the mixture was vigorously shaken, incubated for 5 min at room temperature and then centrifuged at 14000g for 20 min at 4°C. After phase separation, the aqueous phase, containing RNA, was collected and transferred in a new tube. RNA was purified from the collected aqueous phase using miRNeasy Serum Plasma columns [Qiagen, Hilden, Germany] as explained in detail in 'RNA extraction from plasma using silica columns' chapter. RNA was eluted using 18 µ L of nuclease-free water [SigmaAldrich, Saint Louis, Missouri, USA] and stored at -80°C.

3.3.2. RNA extraction from cells

In order to isolate total RNA cells were isolated by centrifugation at 1200 rpm for 10 minutes at 4°C, washed twice in 1 mL of DPBS 1X [Gibco, Thermo Fischer Scientific, Waltham,

Massachussetts, USA] and lysed with Tri-Reagent [Sigma-Aldrich, Saint Louis, Missouri, USA], using the ratio 1 mL of Tri-Reagent for 1x106 cells. After 5 minutes incubation with Tri-Reagent, 200 µ L of nuclease free chloroform [Sigma-Aldrich, Saint Louis, Missouri, USA] for each mL of Tri-Reagent were added, the mixture was shaken vigorously and incubated at RT for 3 minutes. Samples were centrifuged at 12000 rpm for 10 minutes in order to obtain phase separation. The aqueous, upper phase was collected and transferred to a new collection tube, and 500 µL of nuclease free isopropanol [SigmaAldrich, Saint Louis, Missouri, USA] were added for 1 mL of starting Tri-Reagent. The mixture was incubated at room temperature for 10 minutes and then centrifuged at 12000 rpm for 15 minutes to precipitate RNA. Supernatant was removed and RNA was washed with 1 mL of cold 75% ethanol. After 5 minutes centrifugation at 12000 rpm at 4°C, ethanol was aspirated and RNA pellet was air-dried and resuspended in a suitable nuclease free water volume. Obtained RNA was stored at -80°C for further applications.

3.3.3. RNA electrophoresis on agarose gel

Qualitative analysis of RNA confirms the effective extraction and the integrity of RNA itself, providing a visual check of the extracted RNA quality as the absence of DNA or protein contaminations. Electrophoresis is a methodology through which molecules having an electric charge move with different speeds, depending on their charge and size, in an electrical field separating from each other.

The gel used in this technique was a 1% agarose gel able to separate nucleic acid fragments from 500 bp to 20000 bp through its ability to retain between the meshes of the gel the larger fragments, impeding the race, and instead leaving migrate the smaller fragments, which then will be observed in the lower part of the gel.

The 1% agarose gel was prepared by dissolving 1 g of agarose powder in 100 ml of TAE 1X. TAE 1X is a buffer solution, obtained by dilution from 50X TAE = 2 M Tris-HCl, 0.05 M EDTA pH=8 and 5.71% acid acetic 99.8%, and allows to maintain stable pH and concentration of ions in the gel, facilitating electrical conduction and uniform movement of the nucleic acids fragments during electrophoresis. EtBr 10 g/ml was added to the solution; intercalating to the nitrogenous bases of acid nucleic makes visible migration of fragments in the UV light. RNA is negatively charged so when the electric field of 80-90 V is applied, samples migrate toward the positive pole. When the run ended the gel was observed and photographed in UV light using UV trans illuminator, Gel Doc 2000 (Biorad, Hercules, CA,

USA).

3.3.4. RNA quantification

The concentration of RNA should be determined by measuring the absorbance at 260 nm (A260) in spectrophotometer. The concentration is obtained by the equation:

$$g/ml = OD \times 40 \times DIL$$

where OD is the value read from the instrument, 40 is the correction coefficient for reading the RNA at the spectrophotometer (according to the Lambert-Beer law) and DIL is the dilution factor. An absorbance of 1 unit at 260 nm corresponds to 40 µg of RNA per ml (A260 = 1 = 40 µg/ml). This relation is valid only for measurements in water.

3.3.5. RNA quality control

The most common way to verify RNA quality and integrity is to perform an agarose gel, RNA check. Generally, for RNA analysis an agarose gel at 0,8 % is prepared dissolving agarose powder [Sigma-Aldrich, Saint Louis, Missouri, USA] in an appropriate volume of TAE 1X buffer (40 mM Tris-Acetate, 1 mM EDTA, pH 8) and boiling until agarose is completely dissolved. Solution is cooled and 0,5 µg/mL ethidium bromide [Sigma-Aldrich, Saint Louis, Missouri, USA] was added. Gel was done solidify for about 30 minutes in a base plate with 0,75 mm combs and then immersed into 1X TAE buffer. A solution containing 500 ng of RNA sample and 1 µL of loading buffer, composed by 0.25% Orange G [NEB, New England BioLabs, Ipswich, Massachusetts, USA], 50% glycerol in TE buffer, was prepared, reaching the final volume of 10 µL with nuclease free water. Samples were loaded and migration was performed for 30 minutes at 80 Volts. RNA, which is negative charged, migrates toward the anode in the presence of electric current. RNA was visualised using ChemiDoc MP System [Bio-Rad, Hercules, California, USA] and images were elaborated using Image Lab software [Bio-Rad, Hercules, California, USA]. Mammalian total RNA presents two intensive band, which correspond to 28s and 18s ribosomal RNA.

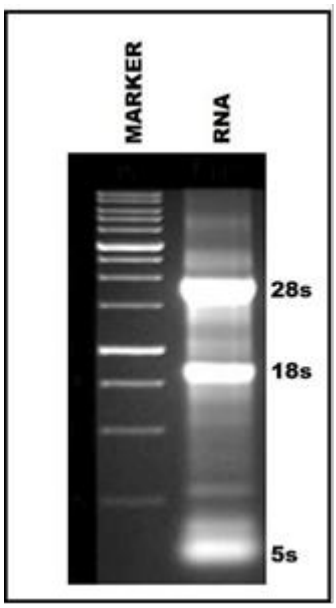

Figure 3.3 Example of RNA sample in agarose gel. Three bands can be distinguished, an upper band, which is most intense and corresponds to 28s ribosomal subunit of RNA, a middle band which correspond to 18s subunit and a lower weak band that relative to 5s ribosomal subunit.

and a weaker band which corresponds to 5s ribosomal RNA. Generally, 28s and 18s bands are present with the ratio 2:1. Furthermore, electrophoretic analysis of RNA can give information about the presence of possible DNA contamination in the sample; in this case, a further band at high molecular weight can be detected at UV analysis.

3.3.6. ΔΔCt normalization model

ΔΔCt normalization model is a relative quantification method in which the normalization is performed using a reference gene. This model involves the comparison of Ct (threshold cycle) values between treated and non-treated samples. Ct values obtained, both the treated samples and the control (untreated), are normalized to an adequate endogenous miRNA housekeeping. In practical terms, the Delta Delta Ct is given from mathematical operation in which the housekeeping gene Ct are subtracted from the target gene Ct value. Each Ct obtained is compared to the ΔCt of the control sample.

$$\Delta Ct = Ct \text{ target gene} - Ct \text{ housekeeping gene}$$

$$\Delta\Delta Ct = \Delta Ct \text{ treated sample} - \Delta Ct \text{ control sample}$$

$$\text{Fold difference} = 2^{-\Delta\Delta Ct}$$

The fold difference allowed to determine the relative expression of the target gene in the treated sample with respect to the control sample.

3.3.7. Benzidine staining assay

Haemoglobin containing cells were detected by specific reaction with a benzidine/hydrogen peroxide solution containing 0,2% benzidine dihydrochloride [Sigma-Aldrich, Saint Louis, Missouri, USA] in 5 M glacial acetic acid [Sigma-Aldrich, Saint Louis, Missouri, USA], activated, immediately before the use with 10% (v/v) of a solution 30% H2O2 [Sigma-Aldrich, Saint Louis, Missouri, USA]. 5µL of culture medium containing cells were added to 5 µL of benzidine-H2O2 solution, cells were observed at microscope and

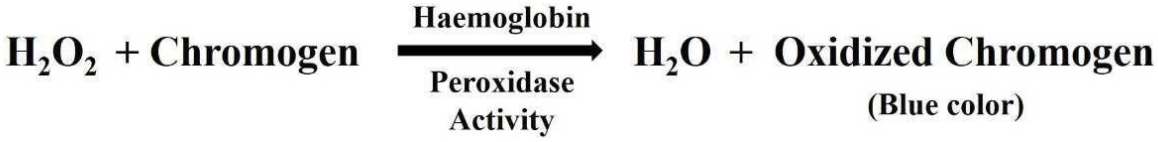

benzidine reactive cells, which were blue coloured, were counted. Data are expressed as benzidine positive cells (blue cells) respect to total number of cells (blue and colourless cells). Test is based on the peroxidase activity of heme group contained in haemoglobin. In fact the peroxidase activity of heme group caused H2O2 reduction and at same time the chromogen (benzidine) oxidation resulting in blue colour as indicated here.

3.4. MiRNA detection methods

Several techniques have been developed in the recent years to detect and quantify miRNAs. In this thesis we employed two methods: PCR-based methods and microarray method, both methods present advantages and disadvantages. The choice depends on several factors, including number of analysed miRNAs, samples type and type of final output.

3.4.1. PCR-based techniques

PCR-based techniques are considered the gold standard for miRNAs detection, the low quantity of starting material required, the dynamic range and the relative low costs make this technique the first choice for miRNA analysis. The major limit is the low number of miRNAs, which can be analysed starting from single sample, despite in the recent years several microfluidic platforms able to profile small or medium panels of miRNAs and based on PCR, have been developed.

3.4.1.1. Reverse transcription

All PCR based techniques before the amplification require an additional step, in which

extracted target miRNAs are reverse transcribed to a cDNA, which is then amplified by PCR. This step is called reverse transcription and at the moment two different reverse transcription methods are available. The first one, is able to generate a universal cDNA, in which all miRNAs contained in the starting sample are reverse transcribed. The enzyme poly(A) polymerase (PAP) catalyses the addition of a poly A tail at the 3' of all miRNAs and then a universal primer containing an oligo dT sequence is employed as starter for reverse transcriptase enzyme. This reverse transcription method is considered very useful when small amount of starting RNA are available, in fact starting from the same reverse transcription reaction, several miRNAs can be analysed. The major disadvantage is associated to the specificity; in fact, this method is considered less specific than method based on the use of miRNA specific primers. In this case, each reverse transcription reaction is performed using a stem loop primer, containing 6-8 nucleotide overhang on the 3' end, which is complementary to target miRNA. In this case only a miRNA can be reverse transcribed for each reaction mix, but this method is considered more specific and also, able to discriminate between mature miRNA and miRNA precursors, such as pre-miRNAs and pri-miRNAs.

3.4.1.1.1. MiRNA reverse transcription using universal primer

RNA extracted from plasma and isolated from control group and athletes which underwent to ABT was reverse transcribed using miRCURY LNA Universal RT microRNA PCR [Exiqon, Qiagen, Vedbaek, Denmark], which is probably the most used reverse transcription kit based on the use of universal primers. 3 µ L of extracted RNA were reverse transcribed in a final volume of 10 µ L.

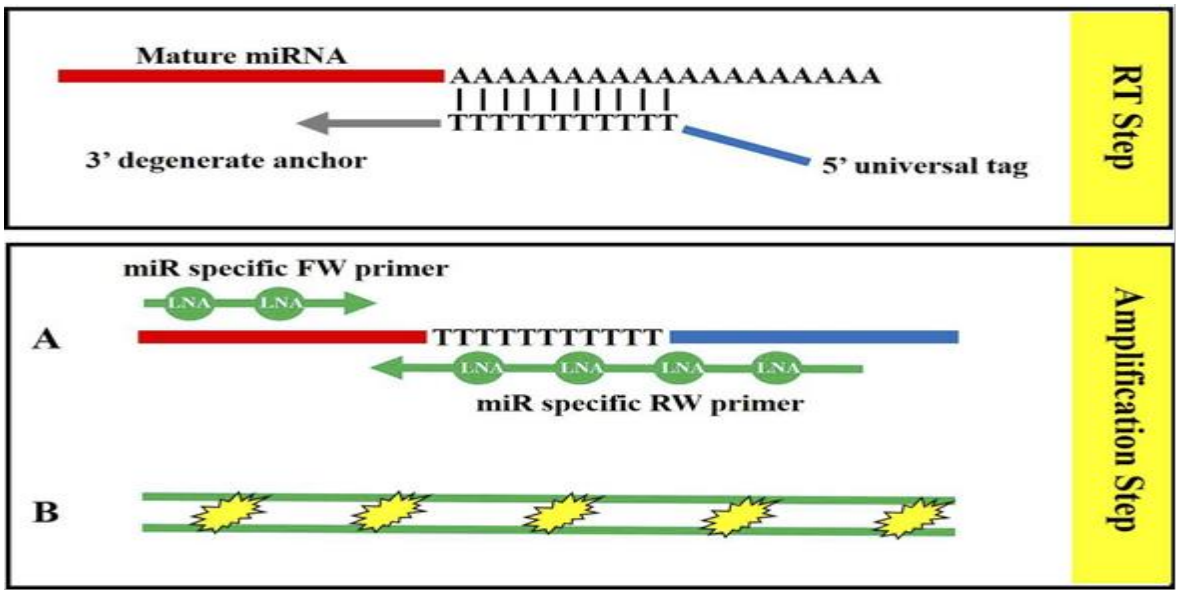

Figure 3.4 Reverse transcription and amplification using universal primer. A poly (A) was added at the 3' end of mature miRNA. A universal primer containing a oligo dT sequence is employed as starter for reverse transcriptase enzyme. Amplification reaction is performed using a couple of miRNA-specific RNA primers and a DNA binding dye.

The reaction mix contains 3 µ L of RNA, 2 µ L of 5X Reaction Buffer, 1µ L of enzyme mix (10X) and the final volume of 10 µ L was reached using nuclease free water purchased from the kit. The reverse transcription reaction was incubated at 42°C for 60 minutes and then at 95° C for 5 minutes to inactivate the enzyme activity. Obtained cDNA was stored at -80°C until the moment of use

3.4.1.1.2. MiRNA reverse transcription using a specific primer

MiRNAs isolated from plasma of CRC patients and healthy donors, miRNAs analysed in CRC cells or culture medium, miRNAs analysed in plasma or tissues isolated from xenografted mouse, miRNAs analysed in ErPCs after the MTH treatment and miRNAs quantified after the transfection with ML122 or commercial agents were reverse transcribed using TaqMan MicroRNA Reverse Transcription Kit [Applied Biosystems, Thermo Fisher Scientific, Waltham, Massachussetts, USA].

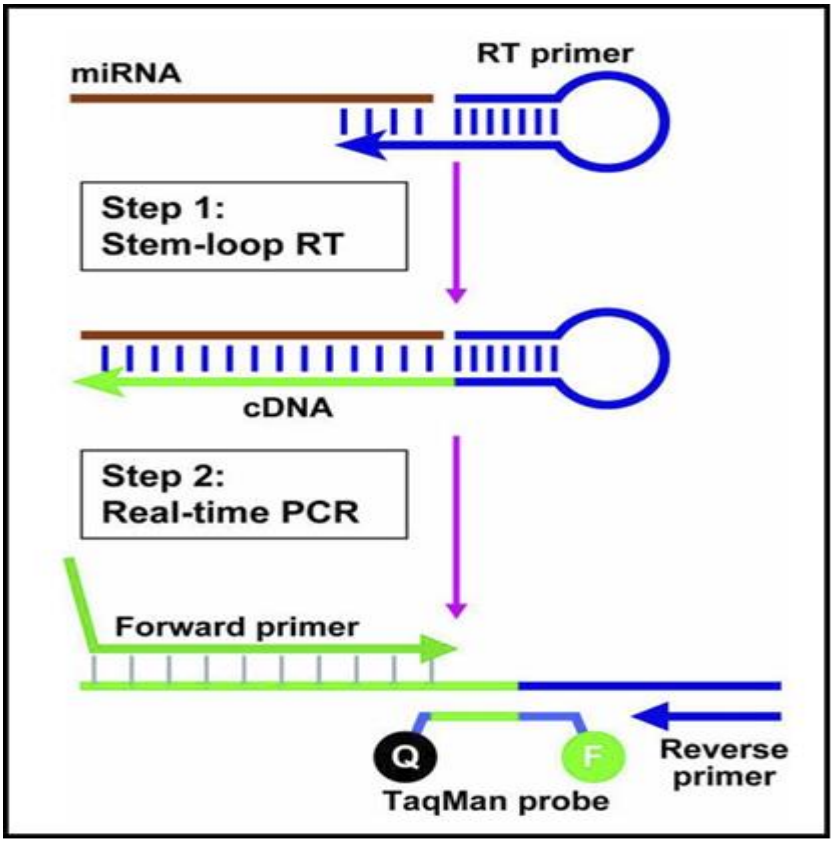

Figure 3.5 MiRNA reverse transcription using specific primer. A specific stem loop primer, containing 6-8 nucleotide overhang on the 3' end, is employed to perform reverse transcription. A

couple of primers is employed to performed RTqPCR. While forward primer is specific for each miRNA, reverse primer is universal for reverse transcription products.

Reverse transcription was performed starting from a) 3 µ L of eluted RNA, when RNA isolated from plasma samples was employed or b) 300 ng of total RNA when RNA isolated from cultured cells or tissue was employed. In order to reverse transcribe more than one miRNA for single reverse transcription reaction. we optimized a reverse transcription protocol in which in a single reverse transcription reaction we reverse transcribed three miRNAs. Is important to underline that before to reverse transcribe more than one miRNA for each reaction, miRNA sequence was analysed, in order to avoid the contemporary reverse transcription of miRNAs with similar sequence,Especially at the 3' end. For RNA samples obtained from plasma a) the reverse transcription reaction was performed in a final volume of 20 µL, while for samples obtained for cells or tissues the final volume of 30 µL was reached. In both cases a) and b) a mix of three primers at final concentration of 25 nM was prepared and RNA was added. The mixture was incubated at 16°C for 30 minutes in order to allow primers annealing. Then a reverse transcription mix, composed by dNTP's (with dTTP) final concentration of 1 mM, 5 U/µ L of MultiScribe Reverse transcriptase, 1X Reverse Transcription Buffer, 0,25 U/µ L of RNase Inhibitor, was prepared and added to samples. The reverse transcription reaction was incubated at 42°C for 30 minutes, followed by a step at 98°C for 5 minutes to inactivate the enzyme. The obtained cDNA was stored at -80°C until the moment of the use.

3.4.1.2. RTqPCR using miRNA TaqMan probes

MiRNA assays based on TaqMan probes are composed by a couple of primers: the forward primer is specific for every miRNA and binds the 3'end of the miRNA sequence, while reverse primer is the same for each assay and binds a sequence present in the stem loop region of the reverse transcription primer. Moreover, the specificity of the assay is further increased by the employment of a TaqMan probe which binds the region between the forward and reverse primer. RTqPCR reaction was performed starting from 3 µL of obtained cDNA, which were mixed with RTqPCR reaction mix composed by TaqMan Universal PCR Master Mix, no AmpErase UNG 2X [Applied Biosystems, Thermo Fischer Scientific, Waltham, Massachussetts, USA] and 20X miRNA assay (assay name and code are indicated in the Table 13), in a final volume of 25 µ L.

miRNA	Assay ID
Hsa-miR-433	000463
Hsa-miR-221-3p	000524
Hsa-miR-145-5p	002278
Hsa-let-7c	000379
Hsa-snRNAU6	001973

Table 3.1 MiRNA assays employed in the thesis.

Each amplification reaction was performed in duplicate. The following amplification programme was employed: 95°C for 10 minutes to activate Taq polymerase enzyme, 95°C for 15 seconds to denature cDNA double-strand structure followed by a step at 60°C for 1 minute to allow primers and probe annealing. The last two steps were repeated for 50 cycles, and at the end of each cycle fluorescence was measured. All RTqPCR analysis were performed using CFX96 instrument [Bio-Rad, Hercules, California, USA], while for data elaboration and analysis Bio-Rad CFX Manager Software [Bio-Rad, Hercules, California, USA] was employed. For relative expression analysis, fold change analysis was performed using Livak method [Livak et al., 2011] (2^-ΔΔCT). All data were normalised using as references miR-let-7c and snRNAU6. While for miRNA absolute quantification in cells, supernatants, tumour tissue and plasma, a standard curve was employed. For each miRNA (miR-141-3p, miR-221-3p and miR-222-3p) a standard curve was created using a synthetic mature miRNA [IDT, Integrated DNA Technology, Coralville, Iowa, USA] at different concentrations from 60 amoles to 0,018 amoles. Absolute concentration of samples has been extrapolated from standard curve using Microsoft Excel.

3.5. Extraction of genomic DNA and Plasmid DNA

QIAprep 2.0 Spin Columns contain a unique silica membrane that binds up to 20 μg DNA in the presence of a high concentration of chaotropic salt, and allows elution in a small volume of low-salt buffer. QIAprep membrane technology eliminates time consuming phenol–

chloroform extraction and alcohol precipitation, as well as the problems and inconvenience associated with loose resins and slurries.

Plasmid purification using QIAprep Kits follows a simple bind-wash-elute procedure (see flowchart "The QIAprep procedure"). First, bacterial cultures are lysed and the lysates are cleared by centrifugation. The cleared lysates are then applied to the QIAprep 2.0 module where plasmid DNA adsorbs to the silica membrane. Impurities are washed away and pure DNA is eluted in a small volume of elution buffer or water. In addition to that plasmid DNA was also extracted from the same kit in this thesis.

3.6. Employed compound and biological molecules

3.6.1. PremiRNA and antimiRNA and mature miRNA molecules

PremiRNA and antimiRNA molecules were purchased from Ambion [Ambion, ThermoFischer Scientific, Waltham, Massachusetts, USA], while mature miRNAs were synthesized by IDT [Integrated DNA Technology, Coralville, Iowa, USA]. PremiRNA and antimiRNA molecules were resuspended at stock concentration of 100 µM in nuclease free water (provided with premiRNA or antimiRNA) and conserved at -80°C until the use. While, mature miRNAs were resuspended with nuclease free water [Sigma-Aldrich, Saint Louis, Missouri, USA] at stock concentration of 1 mM and maintained at -80°C until the moment of use.

MiRNA name	Sequence	Base Pair
miR-145-5p	GTCCAGTTTTCCCAGGAA	18

Table 3.2 Employed mature miRNAs**.**

3.6.2. Peptide Nucleic Acids (PNA):

Peptide nucleic acids (PNA) employed for data presented in the thesis are synthetized from Universita of PARMA, Department of chemical science and life and environmental sustainability.

3.6.2.1. PNA against miR-145-5p binding sequence in 3UTR CFTR region

In our study, we have specifically designed the miR-145-5p keeping in mind the efficacy and uptake ability of this miR and when the treatment is given within the cellular model. PNA against miR-145-5p binding sequence, employed to reduce CFTR transcription factor levels were kindly provided by Professor Roberto corradini research group in above mentioned institute. PNAs were resuspended in sterile water at final concentration of 602 µM and stored at -20°C until the moment of use. According to our previously experience with PNAs, for preliminary tests, we employed PNAs final concentration of 0.5 , 1 and 2, 3,4 µM concentrations. For a treatment (48-72 hours) different cellular models (K562, CALU-3, CFBE cell lines) were used at starting concentration of 1x104 cells/mL, immediately after the treatment with PNAs cells were collected for further investigation. Both PNAs present a polyarginine peptide (R8) sequence that allows PNA cells internalization.

PNA	**Sequence**
PNA miR-145-5p	NH2-Gly-AAGGACCCTTTTGACCTG-RRRRRRRR
PNAmiR-145-5p MUT	NH2-Gly-AGAGATGCCTTGGAGAAC-RRRRRRRR

Table 3.3 Employed PNA targeting 3'UTR CFTR sequence.

3.6.2.2. PNA Masked against miR-145-5p

Another strategy used in this study is PNA masking for miR-145 and this Masked PNA is also being synthesized by Professor Roberto corradini research group in above mentioned institute. PNAs were resuspended in sterile water at final concentration of 257 µM and stored at -20°C until the moment of use. According to our previously experience with PNAs, for preliminary tests, we employed PNAs final concentration of 0.5 , 1 and 2 µM concentrations. For a treatment (48-72 hours) different cellular models (CALU-3, CFBE cell lines) were used at starting concentration of 1x104 cells/mL, immediately after the treatment with PNAs cells were collected for further investigation. Masked PNAs present a polyarginine peptide (R8) sequence that allows PNA cells internalization.

Masked PNA	Sequence
Masked miR-145-5p	NH2-Gly-AATTCATTACTATTGACC-RRRRRRRR
Masked miR-152-3p	+T+C+T +G+A+A +A+C+C +A+C+A +G+T+G +C+A+T
Masked mir-32-5p	+T+G+T +A+C+A +A+A+T +T+A+T +T+G+C +A+C+A
Masked miR-145-5p	+A+A+T +G+A+T +A+G+A +A+G+A +T+C+C +A+G+T

Table 3.4 Employed Masked-PNA targeting 3'UTR CFTR sequence.

3.6.3. Vertex compounds:

Vertex advanced the first of these potential medicines into clinical development in 2006. Since then, four breakthrough medicines have become available to people with CF and in this study we have used certain compounds like Lumacaftor and Ivacaftor individually and with combination of Masked PNA to target the *CFTR Gene* and protein.

3.6.3.1. Lumacaftor (VX-809) and Ivacaftor (VX-770):

Lumacaftor/ivacaftor, available under the brand name Orkambi among others, is a combination of lumacaftor and ivacaftor used to treat people with cystic fibrosis who have two copies of the ΔF508 mutation.

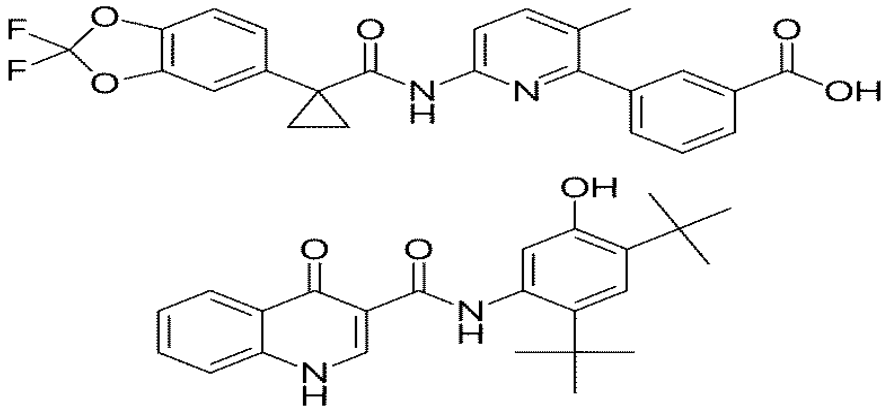

Figure 3.6 Skeletal Formula of Lumacaftor/Ivacaftor

3.7. mRNA expression analysis

mRNA expression was analysed using Reverse Transcription quantitative Polymerase Chain Reaction (RTqPCR). Briefly, RNA obtained after RNA extraction was reverse transcribed to a complementary DNA (cDNA) using a MMLV (Moloney Murine Leukemia Virus) reverse transcriptase enzyme and oligonucleotides with random sequences (random examers) as reverse transcription primers. The obtained cDNA was then used as template for RTqPCR.

3.7.1. mRNA Reverse transcription reaction

Reverse transcription reaction was performed using TaqMan Reverse Transcription Reagents [Applied Biosystems, ThermoFischer Scientific, Waltham, Massachusetts, USA]. A mixture containing 300 ng of total RNA and nuclease free water [Sigma-Aldrich, Saint Louis, Missouri, USA] was heated at 60°C for 5 minutes to disrupt RNA secondary structure.

After the incubation, sample was put immediately on ice and RNAse inhibitor enzyme was added at final concentration of 0,4 U/µL. Moreover, reverse transcriptase enzyme to synthesize cDNA requires the presence of primers able to bind mRNA template. At this purpose, we have chosen short sequences composed by six nucleotides called random examers, which can potentially anneal to all RNA sequences present in the sample and can also recognise sequence in degraded RNA. Random examers were added to the reverse transcription reaction mix at final concentration of 2,5 µM, and the mixture was incubated 10 minutes at 20°C to allow primers annealing. At the end of primer annealing step, others reagents necessary for reverse transcription reaction were added, including: dNTPs at final concentration of 2 mM, MgCl (magnesium chloride) 5,5 mM, RT Buffer 1X and MultiScribe Reverse Transcriptase 1,25 U/µ L. The mixture was incubated at 42°C for 30 minutes to allow mRNA reverse transcription, followed by a step at 98°C for 5 minutes to inactivate reverse transcriptase enzyme. Obtained cDNA was stored at -80°C until RTqPCR was performed.

3.7.2. mRNA quantification using RTqPCR

Quantification of mRNA using RTqPCR can be obtained using different fluorescent labelling techniques. To quantify our transcripts, we employed the two most common techniques: TaqMan probes and Sybr Green.

3.7.2.1. RTqPCR using TaqMan probes

Each TaqMan probe-based assay is composed by a couple of primers specific for the target of interest, a primer forward (FW), a primer reverse (RW) and a probe, which is a oligonucleotide containing at the 5' end a fluorescent reporter at the 5' end, and a quencher in 3' end. Probe binds a sequence in the region between primer FW and primer RW. When the probe sequence is intact, the fluorescence of the reporter is quenched due to its proximity to the quencher. During the annealing and extension step of the amplification reaction, the probe hybridizes to the target, but the exonuclease activity of DNA polymerase enzyme cleaves the reporter. In this way, reporter is separated by the quencher and its fluorescence is no more quenched. This result in an emission of fluorescence that is directly proportional to the amount of amplified product in reaction well. In real time PCR, emission of fluorescence is measured at the end of each cycle and values are collected in a graphical representation called amplification curve. All RT-PCR assay employed in this thesis are reported in **Table 21**. Briefly a PCR reaction mix composed by 1µ L of cDNA, 1,25µ L of 20X TaqMan assay for the transcript of the interest, 12,5 µL of TaqMan Universal PCR Master Mix 2X [Applied Biosystems, ThermoFischer Scientific, Waltham, Massachusetts, USA], and nuclease free water [Sigma-Aldrich, Saint Louis, Missouri, USA] at final volume of 25 µL was prepared. Each sample was prepared and loaded in duplicate. Amplification programme consists of an initial step at 50°C for 2 minutes, in which AmpErase UNG enzyme acts degrading all possible PCR contamination containing dUTP, followed by a step at 95°C for 10 minutes to activate DNA polymerase enzyme, and 45 cycles in which sample is heated at 95°C for 15 seconds to denature double-strand structure, followed by a step at 60°C for 1 minute in which primers annealing and extension phase occurred. At the end of each cycle, fluorescence is measured. Amplification programme was performed using CFX96 [Bio-Rad, Hercules, California, USA] and data analysis was performed using Bio- Rad CFX Manager Software [Bio-Rad, Hercules, California, USA]. Relative expression was calculated and fold change analysis was performed using Livak method [Livak et al., 2011] (2^-ΔΔCT). All data were normalised for their starting cDNA content using as reference RPL13A and 18s.

Target Name	Company	Assay ID
Ribosomal protein L13a (RPL13A)	Applied Biosystem	Hs03043885_g1
18S ribosomal RNA	Applied Biosystems	4310893E
has-miR 145-5p	Thermo Fisher scientific	002278
has-miR 221	Thermo Fisher scientific	000524
has-miR 433	Thermo Fisher scientific	001028
has-miR let7c	Thermo Fisher scientific	000379
has-miR U6	Thermo Fisher scientific	01973

Table 3.5 Employed TaqMan assay.

3.7.2.2. RTqPCR using Sybr Green

Sybr Green is a DNA-binding dye, able to bind non-specifically all double strand sequences. Unbounded Syber Green present low background fluorescence, but when it binds double-strand sequences its fluorescence increases of about 1000 fold. So, in this case emitted fluorescence is directly proportional to the amount of double strand product and consequently to the quantity of amplified target. Syber Green can be used with any couple of unlabelled primers. RTqPCR reaction mix is composed by 1µ L of cDNA, 4 µ L of each primer (50 ng/µ L), 12,5 µ L of iTaq Universal SYBR Green Supermix 2X [Bio-Rad, Hercules, California, USA] and nuclease free water [Sigma-Aldrich, Saint Louis, Missouri, USA] at final volume of 25 µL. Each sample was prepared and loaded in duplicate. The following amplification programme was performed: 3 minutes at 95°C to activate DNA polymerase enzyme, 40 cycles of 95°C for 15 seconds to denature double strand structure, 58°C for 30 seconds to allow primers annealing followed by 30 seconds at 72°C for the extension phase. At the end of the amplification, a melting curve from 55°C to 95°C with 0,5°C/sec increment was performed to verify the presence of non-specific products, as primer dimers. Amplification

programme was performed using CFX96 [Bio-Rad, Hercules, California, USA] and data analysis was performed using Bio-Rad CFX Manager Software [Bio-Rad, Hercules, California, USA]. Relative expression was calculated and fold change analysis was performed using Livak method [Livak et al., 2011] (2^-ΔΔCT). All data were normalised for their starting cDNA content using as reference RPL13A and 18s.

Target	**Primer FW Sequence**	**Primer RW Sequence**
3UTR CFTR	AGCTCTAAATGTCAATCAGCC	GGGGAGAGGAGAGAAAAAGG
3UTR Actin	ATCCCCCAAAGTTCACAATG	AATGCTATCACCTCCCCTG
3UTR NEDD9	TTGGCCCAGTTCTTATTTAGC	TGGCAGAGTAGGACTTTGAG
3UTR Myosin	TGTTATGCTCATTCTGCTTCTG	GCTGAGAACCATAGTAATGACC
3UTR IRS-1	ATGAGAGCAGAAATGAACAGAC	TGAGTACCAGCAACTTCCAG
Exon-14 CFTR	CCTAACTGAGACCTTAC	TCATCAGAATCCTCTTC
Exon-17 CFTR	CAAGACAAAGGGAATAG	CTTGAAGAACAGAATGT
Intron-1 CFTR	CCAAGTCTAGATGTAAT	GGATATACTTCATTCCT
Intron-2 CFTR	GAAGGCAAAGTAAGATA	GGGATACATCATAAACA

Table 3.6 Primers employed for Sybr Green RTqPCR.

3.8. Western blot analysis:

3.8.1. Protein extracts preparation:

Lysis Buffer: 200 MM NaCl (PM 58.44) 11.68g, 10MM Trizma Base PH 7.8, (37% HCL) (PM 121.14) 1.21g, 1 MM EDTA (Stock solution 250 MM) 0.4ml, 1 Nonidet P-40 (Ipegal) , 0.5% sodium deoxycholate 0.5g, Final volume with distilled water . Further, Add in 10ml 1 pellet of complete ULTRA tablets of protease inhibitor –Roche (+ 4 c) and slits aliquots in -80c.

Stock Solution of 100MM PMSF (Room temperature): M.W 174.2, 0.1742 g in 10ml of Isopropanol (Caution PMSF is unstable in water solution) and split in aliquots in -80c. TBS: 20mm Tris-HCL, PH 7.4, 137 mm NaCl. TBS (10x) Final volume 1 Liter ; Tris base 24.2 g, NaCl 80g, PH 7.4 with HCL lead to volume with distilled water. TBS (1x) Dilute 100mL of TBS 10x with distilled water upto final volume 1 liter. TBS-T (1liter) TBS 1x + 0.1% Tween 20 (1mL in 1 Liter).Nonspecific site blocking solution: 5% Nonfat dry milk in TBS-T.

Settling 2×10^6 cells in petri dishes of 6cm in diameter with appropriate medium and treat according to decided conditions. At the end of treatment period lyse the cells. Lay the petri in ice, eliminate the medium of culture and wash the cells 3 times with 1 ml of cold PBS. Aspirating residue with suction system. After the last wash, collect the cells in Eppendorf with special scrappers in 1.5ml of Eppendorf tube. Centrifuge at 10,000 RPM for 5 min. at 4c. Remove the supernatant and add to pellet 70 uL of cold lysis buffer with protease cocktail (Complete ULTRA tablets) and PMSF 1mM (Dilution 1:100 of the stock solution) and leave 30 minutes in ice by shaking gently to avoid the formation of foam. Sonicate for 5 minutes in iced water. Centrifuge at 13000 RPM for 10 minutes at +4c. Collect the supernatant (Protein fraction) in Eppendorf and remove the pellets keeping aside. 10uL of sample for protein dosage and freeze in -80c. Quantify thr proteins in each sample by BCA method.

3.8.2. Protein extracts quantification

Obtained protein extracts were quantified using Pierce BCA Protein Assay Kit [Thermo Scientific, Thermo Fischer Scientific, Waltham, Massachussetts, USA], according to the manufacturer's instruction. BCA Protein Assay is a colorimetric assay based on the reduction of Cu2+ to Cu1+ by proteins in an alkaline medium. According to Biuret reaction, copper reduction is caused by four amino acid residues: cysteine, cystine, tyrosine, and tryptophan normally present in proteins. Reduced copper forms complexes, composed by a Cu+ chelated

with two molecules of bicinchoninic acid (BCA). Complexes, which are purple-colored, adsorbed at 562 nm and absorbance values are directly proportional to proteins concentration. Protein extracts concentration is calculated by a standard curve created using known concentration of albumin protein. Standard curve was created adding incremental amount (from 1,25 µg to 40 µg) of albumin starting from an albumin solution which stock concentration is 2 mg/ml. Two µ L of protein extracts were quantified for each sample. Both standard curve samples and unknown samples were added to 1 mL of working solution composed by Reagent A (bicinchoninic acid 0,1M) and Reagent B (Cupric sulfate 4%) in ratio 50:1. Samples were incubated at 60°C for 30 minutes to enhance reaction, and the absorbance at 562 nm was read using SmartSpec Plus Spectrophotometer [Bio-Rad, Hercules, California, USA].

3.8.3. Western blotting

Considering the protein quantification, prepare the samples with the homogenous amount of ug of protein (25-40ug). Add XT sample buffer 4X Bio-rad and make up all the samples to the same volume by adding water e.g (25uL; 16.5uL of proteins corresponding to 40ug, must be added to 6.25uL buffer 4X + 2.25uL of distilled water for final volume upto 25 uL). After short spin, Heat the 37c for 10 minutes. Samples will be loaded on SDS-PAGE Gel Precast3-8% Tris-Acetate (Bio-rad Cat Nr. 345-0129).

Separated proteins were transferred into a 0,2 µG PVDF membrane [Cat Nr. 170-4157 Bio-rad] using Trans-Blot Electrophoretic Transfer Cell [Bio-Rad, Hercules, California, USA]. The electrophoretic transfer was performed at 25 V, 2.5A for 12 min., or alternatively over night, at 4°C, using CAPS Buffer (10 mM 3-(cyclohexylamino)-1-propanesulfonic acid, 10% methanol pH 11). then membrane was washed using three times with TBS-T 1X (Tris-buffered saline, 0,1% Tween 20). Further, Obtained membrane was incubated in blocking Buffer (5% non-fat dry milk in TBST-1X) for 1 hour, to prevent the nonspecific binding of the antibodies. After the incubation membrane was washed three times with TBS-T 1X and probed with Anti CFTR (CFF USA) Diluted primary monoclonal antibody (1:2500) in a solution of 5% BSA (Bovine Serum Albumin). The day after membrane was washed three times with

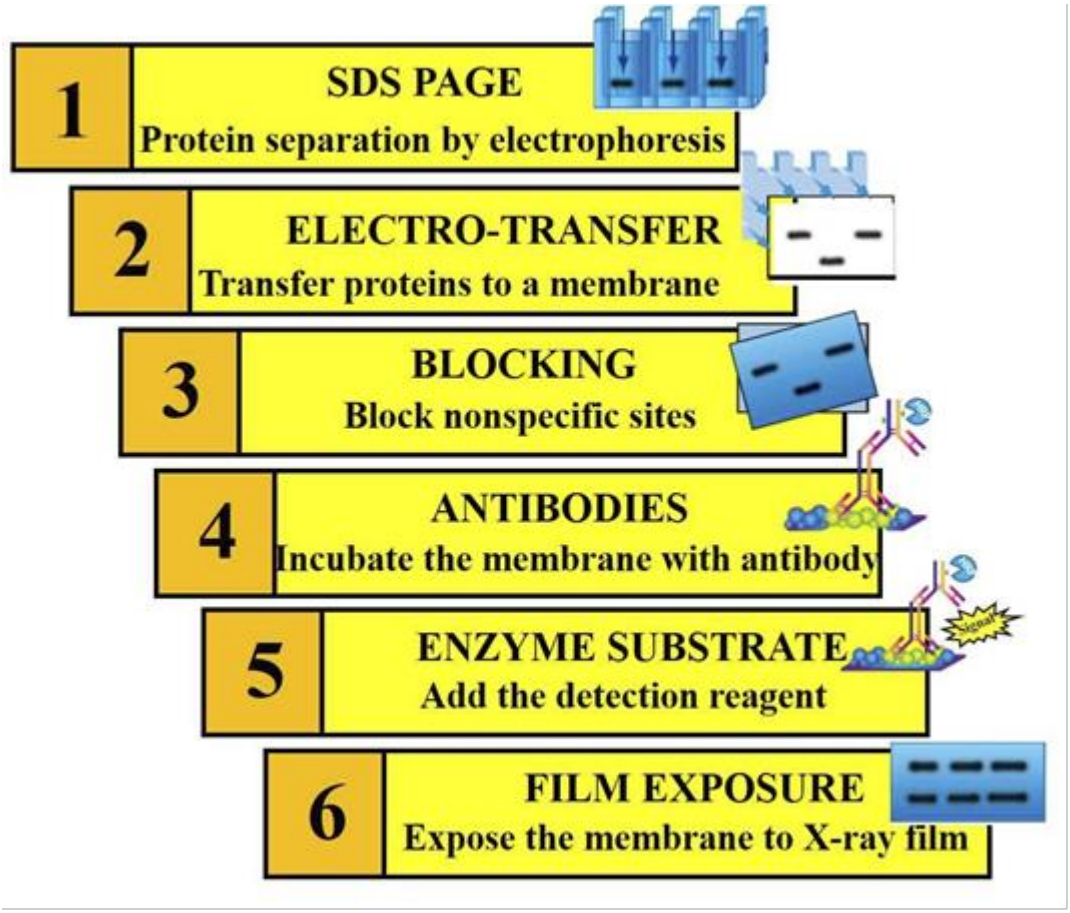

Figure 3.7 Principal steps of western blotting analysis. Protein extracts were loaded into a SDS polyacrylamide page and separated according to their molecular weight, proteins are transferred in a nitrocellulose membrane, which was probed firstly with a primary antibody and then with an appropriate secondary HRP conjugated antibody. Membrane was treated with a HRP substrate and exposed to X-Ray film.

TBS-T 1X and incubated for an hour with an appropriate HRP-conjugated secondary antibody (1:2000) [Goat Anti-Rabbit Igg HRP conjugated Cat. 7074P3, Cell Signaling Technology, Leiden, Netherlands] and Precision Protein StrepTactin-HRP conjugate (1:10000) [Bio-Rad, Hercules, California, USA], used to detect protein marker. Membrane was washed three times with TBS-T 1X and incubated 5 minutes, protected from the light with the substrate that allow luminescence emission: Phototope-HRP Western Blot Detection System [Cell Signaling Technology, Leiden, Netherlands]. HRP (Horseradish peroxidase) enzyme conjugated at the secondary antibody catalyses the oxidation of luminol, contained in the detection solution, that results in emission of light which is captured in ECL film [GE Healthcare, Little Chalfont, UK] and is directly proportional to the amount of target protein in samples. The same membrane was stripped, to remove the previously bounded antibody, using Restore Western Blot Stripping Buffer [Thermo Scientific, Thermo Fischer Scientific, Waltham, Massachussetts, USA]. Membrane was incubated 1 hour with 30 mL of

Stripping Buffer and then, washed three times with TBS-T 1X. After a 1 hour incubation with blocking buffer and three washings with TBS-T 1X, membrane was re-probed with the primary antibody against B-Actin, used as normalization control. Films obtained with both antibodies Anti CFTR and B-Actin, were analysed using ChemiDoc MP System [Bio-Rad, Hercules, California, USA] and Image Lab software [Bio-Rad, Hercules, California, USA]. The ratio between Anti CFTR band intensity and B-Actin band intensity was calculated for each sample.

3.9. CFTR Functional Analysis

Cell model: Immortalized human bronchial epithelial cells (CFBE41o-)

CFBE-YFP F508del CFTR cells stably co-express CFTR with the F508del mutation and the analogue of green fluorescent protein (GFP), which is the yellow fluorescent protein with high sensitivity for halogens (HS-YFP).

These cells were cultured in a complete medium (E-MEM, 10% FBS, L-glutamine and penicillin / streptomycin), on plastic pre-treated with an extracellular matrix containing fibronectin / vitrogen / BSA (bovine serum albumin). Cell stability was maintained in the presence of puromycin at a concentration of 2 μg / mL.

The compounds used are: PNA masking mir-145, VX-809 and VX-770.

Method

CFBE-YFP F508del cells were sedimented in multiwells wells (4, 96) previously treated with appropriate coating (extracellular matrix containing fibronectin / vitrogen / BSA), in the amount of 30,000 cells per well and subsequently, after 24 h of treatment with PNA masking mir 145, were transferred to slides with a diameter of 25 mm, previously treated with the coating. Finally, after adhesion, the cells were pre-incubated for 24 hours with the compounds VX809 and VX770, in combination or not with mir-145 PNA masking.

At the time of analysis, the cells were washed with Dulbecco PBS (composition: NaCl 137 mM, KCl 2.7 mM, Na2HPO4 8.1 mM, KH2PO4 1.5 mM, CaCl2 1.0 mM, MgCl2 0.5 mM, brought to pH 7.4) and subsequently incubated with a stimulation cocktail (composition: forskolin 5 μM, VX770 5 μM) in the presence and absence of the specific inhibitor of CFTR, CFTRInh-172 (Sigma) at a concentration of 10 μM, for 30 minutes.The slides were then placed in a perfusion chamber and transferred to a Nikon TMD inverted microscope mounted

on a Nikon Fluor 40 objective.

The fluorescence signal was acquired with a Hamamatsu C2400-97 image intensifier at a rate of 1 frame / 3 s for 99 s. The fluorescence from each single cell was analyzed by a customized software (Spin, Vicenza, Italy). The excitation wavelength and the emission wavelength were set, respectively, at 500 nm and 520 nm.The analysis of each sample consists of a continuous fluorescence reading and, after about 30 seconds from the start of the experiment, 100 µL of a solution rich in I- (composition: NaI 137 mM, KCl 2.7 mM, Na2HPO4 8.1 mM, 1.5 mM KH2PO4, 1.0 mM CaCl2 and 0.5 mM MgCl2, brought to pH 7.4) to reach a final I-concentration of 50 mM.

The results are presented as transformed data to obtain the percentage change of the signal [ΔF (t)] relative to the time of addition of the stimulus, according to the equation: $\Delta F(t) = 100 \cdot [F(t) - F(0)] / F(0)$, where F (t) and F (0) are the fluorescence values at time t and at the time of I- addition, respectively.

The influx of I- determines a quencing of cellular fluorescence with a rate that depends on the permeability of the halide by the cell membrane, and therefore, on the activity of the anionic channels or transporters.

3.10. Cell viability Assay

Cell viability after the transfection with calixarene-based molecules was evaluated with Muse Count & Viability Kit [Millipore, Billerica, Massachusetts, USA], using Muse Cell Analyser [Millipore, Billerica, Massachusetts, USA]. Test allow to discriminate between alive and dead cells on the base of their membrane permeability to two DNA binding dyes. The first dye is used to discriminate viable cells, which do not stain, from non-viable cells, which are stained. Instead, the second reagent stains all cells with a nucleus, in order to distinguish cells from debris. To perform analysis, 50 µ L of suspension cells were added to 225 µ L of Muse Count & Viability Reagent, the solution was incubated at room temperature for 5 minutes, protected from the light and then 1x103 events were analysed using Muse Cell Analyser [Millipore, Billerica, Massachusetts, USA].

3.11. Evaluation of apoptotic rate

The possibility that calixarene-based delivery molecules may induce apoptosis in cells, was investigated using Muse Annexin V & Dead Cell Kit. One of the first steps of apoptosis

pathway is the externalization of phosphatidylserine (PS) to the cell surface. The assay is based on the use of two different reagents: annexin V, which binds PS and 7-AAD (7-aminoactinomycin D) a fluorescent DNA intercalator. In this way is possible to identify four different populations: cells negative to both reagents (live cells), cells positive to annexin V, but negative to 7-AAD (early apoptotic cells), cells negative to annexin V and positive to 7-ADD (cellular debris) and cells positive to both reagents (late apoptotic cells).

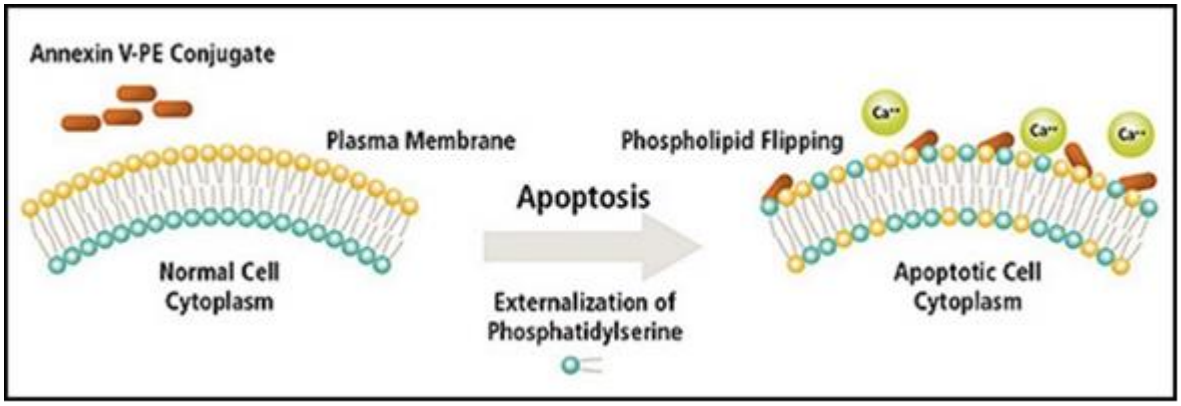

Figure 3.8 Annexin V in apoptosis signal. Phosphatidylserine (PS) is normally located on the cytoplasmic face of the plasma membrane. During apoptosis PS translocates to the outer leaflet of the plasma membrane. PS is bound by fluorochrome-labeled Annexin V in presence of calcium.

50 µ L of suspension cells were added to 50 µ L of Muse Annexin V & Dead Cell reagent, sample was gently mixed and incubated at room temperature, protected from the light for 15 minutes. Samples were analysed using Muse Cell Analyser [Millipore, Billerica, Massachusetts, USA].

3.12. Bioinformatics tools for miRNA analysis

In this study, Various tools were used for the bioinformatics analysis and to collect the data for in In-Vitro studies of the respective analysis in this thesis.

3.12.1. Determination of 3UTR CFTR region

For this respective analysis, we have used UTR database and it helped not only to determine the 3'UTR region abut also helps to identify the starting and end regions of the specific region. The following link is useful for this analysis. http://utrdb.ba.itb.cnr.it/getgene/hs/CFTR.

3.12.1.1. 3'UTR Sequence presence Experiment

In our study, it was important to understand the presence of 3'UTR sequence in CFBE cell line. Therefore we planned experiment keeping in mind the genome of CFBE cells and the presence of plasmid with WT CFTR (CFBE-41o WT CFTR), plasmid with withF508del

CFTR mutation (CFBE41o-ΔF508del CFTR) and plasmid with CFTR YFP (CFBE41o-ΔF508del CFTR YFP) inside this cell line. In these experiments, we designed the primers for both the genome and plasmid and tried to verify the 3'UTR sequence presence not o.ly by designing the primers for 3'UTR sequence of CFTR in genomic and plasmid of CFBE cells. The details of plasmid and genome related primers are given in; Table 22 in material and methods section. For this experiment, genome and plasmid extraction was done from CFBE cells. Further, a real time qPCR was performed with 3'UTR CFTR primers and results showed that in **[Figure 3.9,A]** that with plasmid with WT CFTR and Plasmids withF508del CFTR shows different Cq values and plasmid showed the quiet lower and significant Cq value and proved the fact that there is a 3'UTR CFTR region present in the plasmid.

In the next strategy to empower the results of 3'UTR presence, we also targeted the exon and introns of the genomic and plasmid of different cells and tried to further empower the presence of 3'UTR sequence in CFBE cells. The details of exon and intron related primers are given in; Table 22 in material and methods section. For this experiment, extraction was done from CFBE cells. Further, a real time qPCR was performed with 3'UTR exon and intron primers and results showed that in **[Figure 3.9,B]** that intron and exons shows different Cq values and intron region of all the samples containing genomic, plasmid and another genomic dna as a control which in that case was erythroid precursor cells genomic dna, showed the quiet lower and significant Cq value and proved the fact that there is a 3'UTR CFTR region present in the intron region on the other hand with exon there is quiet high value of Cq and its insignificant as compared to intron Cq value. We also repeated these experiments three times and can be seen in the results of **[Figure 3.9]**.

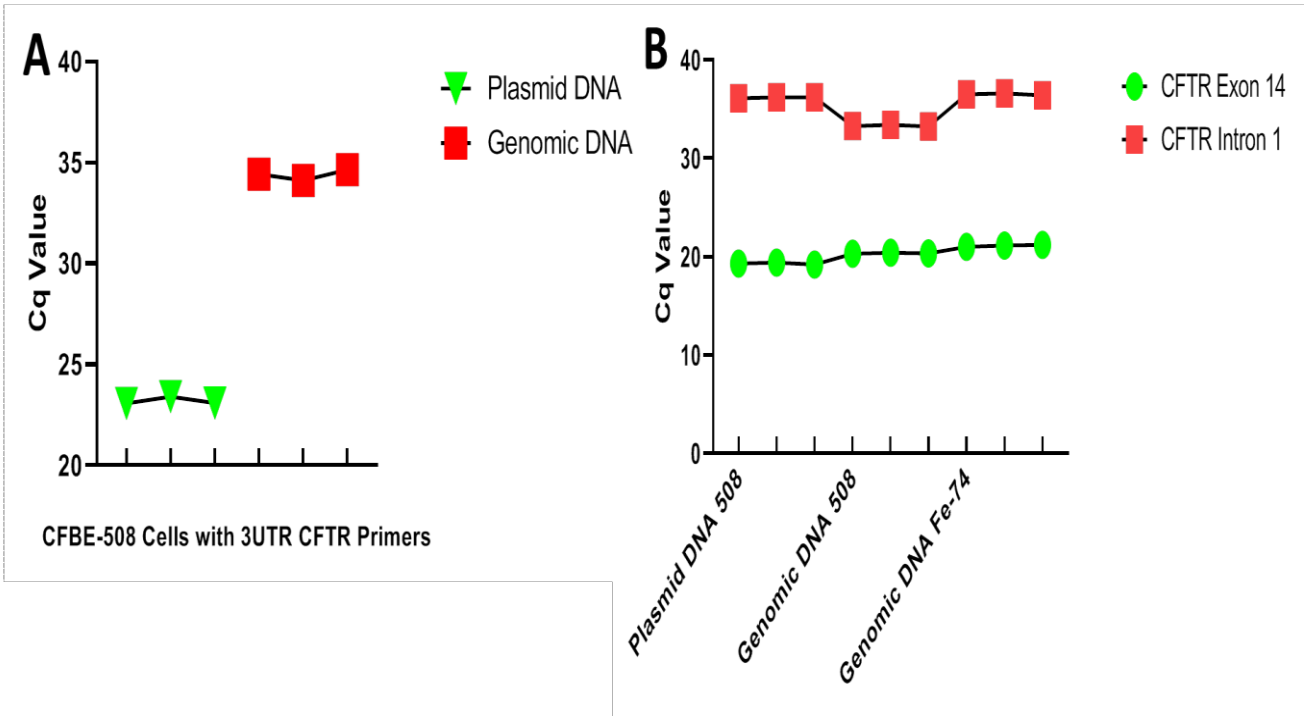

Figure 3.9 3'UTR sequence presence experiments; (A) CFBE-ΔF508 Cells plasmid and genome treated with 3'UTR primers and results showed that plasmid contains the 3'UTR sequence with lower Cq value. **(B)** Exon and introns of the genomic and plasmid of different cells and showed the quiet significant Cq value difference between intron and exons, and proved the fact 3'UTR sequence presence in introns of CFBE cells.

3.12.1.2. Identification of Exon and Intron regions CFTR

For this study, we have used a databases such as NCBI and tools for miR with lot of function to be performed regarding various miRs. The following link was useful. https://tools4mirs.org/.

3.12.2. Identification of target binding sites for mIR-145-5p

The analysis carried out with the PITA software, that shows not only all the binding sites of miR-145-5p, but also the highest binding affinity with respective binding site. The link is

https://tools4mirs.org/software/target_prediction/pita/.

3.13. Graphic tools

For most of the graphs preparation, graph pad software is used further, while an on-line tool http://bioinformatics.psb.ugent.be/webtools/Venn/ is also used for some in silico analysis.

3.14. Statistics

Results are expressed as mean ± standard error of the mean (SEM). Comparisons between

groups were made by using moderate paired Student's t test. Statistical significance was defined as $p<0.01$ highly significant (**) and $p<0.05$ significant (*).

4. RESULTS AND DISCUSSION

4A. TARGETING miR-145-5p FOR CFTR UPREGULATION IN CYSTIC FIBROSIS

4A.1. Preliminary Results

Our preliminary and already published results shows the effectivity of anti-miR-145-5p molecules role in inhibiting the binding of miR-145-5p to the target binding sites and how does it affect the *CFTR Gene* mRNA and protein content in Calu-3 cells. The data obtained shows the possibility of using an anti-miR PNA for targeting miR-145, a microRNA reported to down-regulate CFTR expression. Octaarginine-anti-miR PNA conjugates were delivered to Calu-3 cells, and found to inhibit miR-145-5p. This allowed to enhance expression of the miR-145 regulated *CFTR Gene*, analysed at mRNA (RT-qPCR, Reverse Transcription quantitative Polymerase Chain Reaction) and CFTR protein (Western blotting) levels. The PNA was conjugated to a poly-arginine tail, since this type of constructs was previously used by our group for the delivery of PNA into cell lines, allowing very high uptake [Brognara et al., 2012; Brognara et al., 2014]. As experimental model system the Calu-3 cell line (American Type Culture Collection, ATCC HTB-55) has been selected [Shen et al., 1994; Kreft et al., 2015]. These cells are a well-differentiated and characterized cell line derived from human bronchial submucosal glands and extensively used to study CFTR expression and immunological behaviour [Ramachandran et al., 2012; Nielsen et al., 1991].

4A.1.1. Experimental strategy

The experimental strategy is displayed in [**Figure 4.1**]. For this experiment, Calu-3 cells were used for the treatment with PNA-a145-5p, PNA-a145 MUT and PNA-a433. Cells were grown for 72 Hours treatment with respective PNAs in petri plates. Cultured cells were trypsinized and collected by centrifugation at 1500 rpm for 10 min at 4 ◦C, washed with PBS, lysed with Tri-Reagent. The isolated RNA was washed once with cold 75% ethanol, dried and dissolved in nuclease free pure water before use. After that, protein exactions were performed and samples were prepared for western blotting. During the whole process some cells were separated to perform the Cell viability assay and apoptotic assay. In the end, RNA and protein samples were

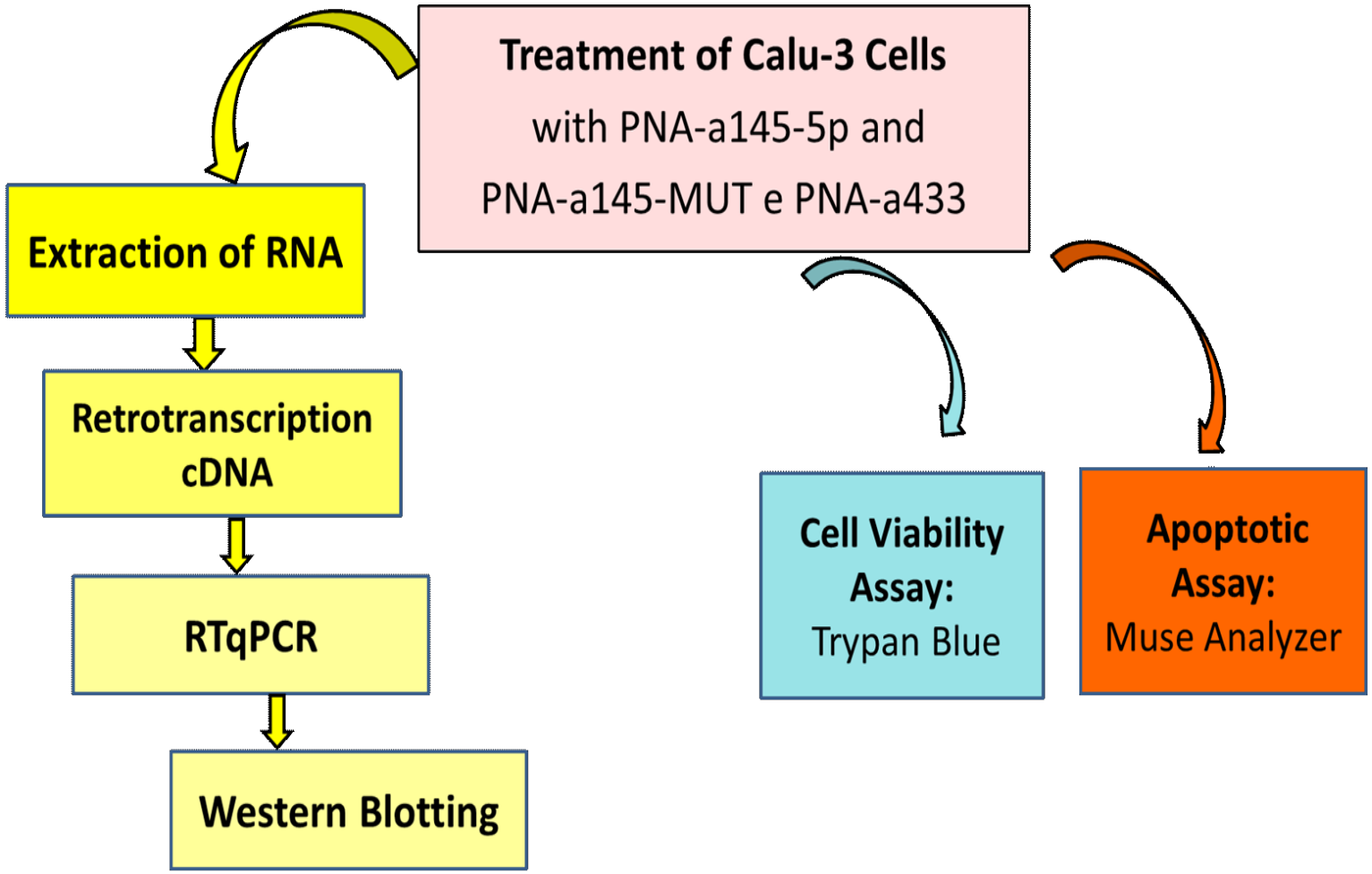

Figure 4.1. Experimental strategy for anti-PNA-a145-5p. In this experiment CALU-3 cells were used and given treatment with mentioned PNAs. Following RNA extraction and then further Q-PCR and western blotting was done. Cell viability assay and antiprolifratic activity was also checked

4A.1.2. PNA-a145 inhibits miR-145-5p by Real time q-PCR

The PNAs were designed according to our standardized protocols, using the following criteria: (a) length of 18 bp, suitable for efficient synthesis also on large scale; (b) lack of self-complementarity both in antiparallel and parallel orientation; (c) minimal length of complementary sequences in mRNA, as evaluated by BLAST search; (d) when possible, targeting of the "seed region" which is an essential element for miRNA function. As already mentioned, a carrier octaarginine (R8) peptide was conjugated at N-terminus of the PNA chain since it induces an efficiency in the delivery which approaches 100% (i.e., uptake in 100% of the target cell population), as elsewhere published [Brognara et al., 2014].

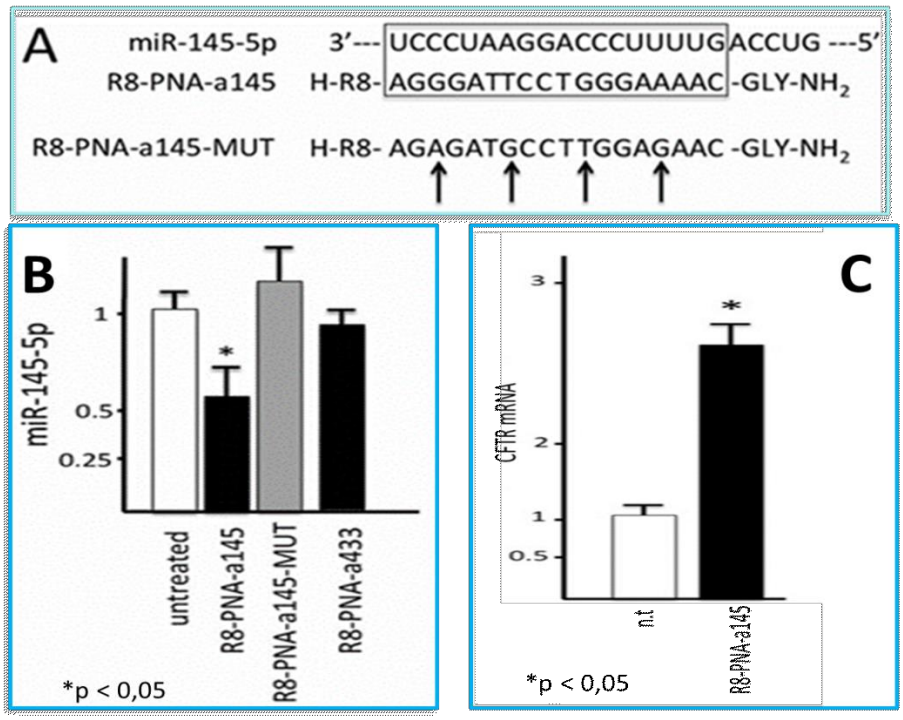

Figure 4.2: (A) Sequences of the R8-PNA-a145 and the mutated R8-PNA-a145-MUT. The G- A,T- > G and A- > G mutations are arrowed. The box localizes the regions of full complementarity between miR-145-5p and R8-PNA-a145 sequences; **(B)** Inhibition of miR-145-5p hybridization signals in Calu-3 cells treated for 72 h with R8-PNA-a145 , mutated R8-PNA-a145-MUT and R8-PNA-a433 molecules (2 μM, as indicated); **(C)** Upregulation of CFTR mRNA (RT-qPCR treated for 72 h with R8-PNA-a145 (2 μM). Results shown represent the average ± standard deviation (S.D.) obtained in at least three independent experiments.* = $p < 0.05$.

This conjugation is easily realized during PNA solid-phase synthesis using the same reagents and solvents. We have previously reported the higher efficiency of R8-PNA conjugates (R8-PNAs) in inhibiting target miRNAs when this activity is compared to that of conventional commercially available antagomiRNAs [Fabbri et al., 2011]. Control PNA (R8-PNA-a145-

MUT) was obtained by modification of the position of four nucleobases, thus leaving the same base composition. The mutated sequence was also analyzed using BLAST search to assess possible interferences.

[Figure 4.2A] reports the sequences of PNA selected in the present study. R8-PNA-a145-5p displays a fully complementary sequence with respect to R8-PNA-a145-MUT harboring three changes suppressing the hybridization as shown by circular dichroism (data not shown). When Calu-3 cells were cultured in the presence of R8-PNA-a145 and of the mutated sequence R8-PNA-a145-MUT, a clear-cut result was obtained and depicted in Figure 3B. First of all, treatment of Calu-3 cells with R8-PNA-a145 leads to an inhibition of the miR-145-5p hybridization signals, compatible with decrease of free miR-145-5p content, and hence of its potential action, in treated cells; second, the mutant R8-PNA-a145-MUT displayed no inhibitory effects. The decrease of miR-145 hybridization signals following treatment R8-PNA-a145 is expected, in agreement with the effects of anti-miRNA PNAs elsewhere published [Fabbri et al., 2011; Brognara et al., 2014].

In addition, we found that the effects are fairly specific; in fact, the results obtained demonstrate that hybridization specific for other miRNAs expressed in Calu-3 cells (for instance miR-433) were unchanged following R8-PNA-a145 treatment. The representative experiments shown in [**Figure 4.2B]**, demonstrate no effect of miR-433-3p and, conversely, an inhibitory effect of R8-PNA-a145. Altogether these experiments support the concept that the effects of R8-PNA-a145 on miR-145-5p are sequence-specific **[Figure 4.2C]**. Finally, the effects of R8-PNA-a145 were also confirmed on other cell lines, which results will be shown in the next sections.

4A.1.3. PNA-a145 effects on CFTR protein

When Calu-3 cells were cultured in the presence of R8-PNA-a145 a clear effect was observed in CFTR mRNA accumulation. In fact, the CFTR mRNA fold increases were (2.7/2.9 with respect to untreated Calu-3 cells). This value was obtained after determining CFTR mRNA content by RT-qPCR analysis **[Figure 4.2C]**. These results prompted us to determine the CFTR content by Western blotting, as shown in **Figure 4.3 A, B**. Calu-3 cells were treated for 72 h with R8-PNA-a145 and then proteins were separated by polyacrylamide gel electrophoresis and Western blotting analysis was performed using two antibodies, one specific for CFTR, the other for β-actin, used as an internal control. The CFTR protein increase was found to be 2–2.5 times more in Calu-3 extracts after R8-PNA-a145-5p

treatment in three independent experiments. As shown in the representative experiment reported in **Figure 4.3 A,** while no effects were observed using R8-PNA-a433. The CFTR protein increase was found to be 2–2.5 times more in Calu-3 extracts after R8-PNA-a145-5p treatment in three independent experiments. These results suggest that miR-145-5p targeting should be considered in the development of miRNA-therapeutic protocols for CFTR up-regulation.

In conclusion, a PNA directed against miR-145-5p is able to inhibit miR-145-5p and increase the miR-145-5p regulated CFTR. These data are of interest because are a proof-of-principle that miRNA targeting might be considered to increase CFTR content, with possible applications in the personalized therapy of cystic fibrosis. The field of precision medicine is in fact growing [Paranjape et al., 2017].

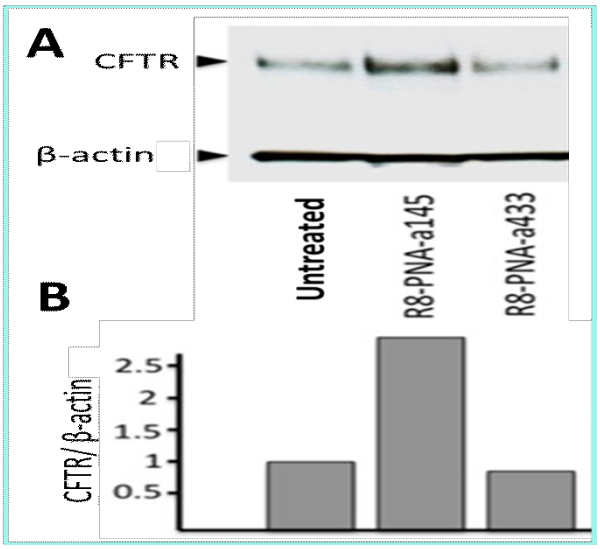

Figure 4.3: (A) CFTR protein (Western blotting) in Calu-3 cells cultured for 72 h in the absence or in the presence of R8-PNA-a145-5p.CFTR and β-actin is indicated in panel with arrowheads. **(B)** In panel quantitation of the CFTR/β-actin ratios are shown and were obtained by densitometry analysis of the Western blotting shown in panel.

4A.1.4. Anti-proliferative effects of PNA-a145 on Calu-3 Cells

The experiments shown in **Figure 4.4** were performed in order to verify whether R8-PNA-a145-5p was to some extent cytotoxic. As shown in **Figure 4.4 part (A)** after 5 days treatment there was not much difference in the cells numbers/ml when PNA-treated and untreated cells are compared. This supports the concept that the PNA does not display any anti-proliferative effects. It proves the fact that PNA does not shows any cytotoxic effect. Further, it can also be seen that the studied PNA did not exhibit anti proliferative effects,

could be seen in **Figure 4.4 part (B)** No reduction in viable cells was observed when PNA-treated and untreated cells are compared [Schust et al., 2006].

In these experiments Calu-3 cells were cultured for 72 h in the absence, in the presence of R8-PNA-a145 or with the apoptotic inducer Stattic combined to 10% dimethyl sulfoxide (DMSO) (used as a positive internal control). After this treatment, the cell number/ml was determined, the dead cells were measured.

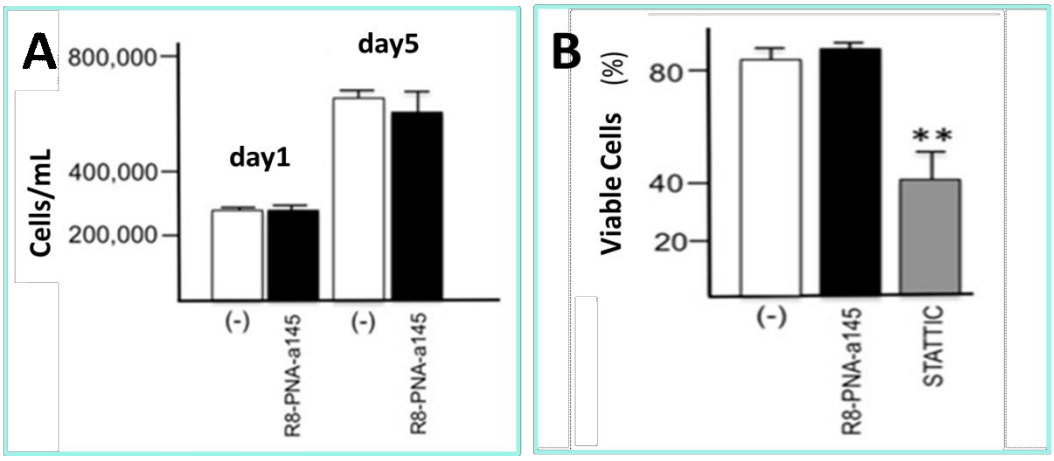

Figure 4.4: Effects of R8-PNA-a145 on cell growth, vitality. **(A)** Calu-3 cells were cultured in the absence or in the presence of R8-PNA-a145 different days and the cell number/mL determined; **(B)** Effects of R8-PNA-a145 on vitality. Vitality was determined by trypan blue analysis of dead cells. Results in panels (A,B) represent the average ± S.D. of three independent experiments. ** = $p < 0.01$.

4A.1.5. Lack of pro-apoptotic effects of PNA-a145 on Calu-3 Cells

Figure 4.5 shows that PNA-a145-5p did not induce apoptosis when compared to the proapoptotic compound Stattic [Schust et al., 2006]. In these experiments Calu-3 cells were cultured for 72 h in the absence, in the presence of R8-PNA-a145 or with the apoptotic inducers Stattic combined to 10% dimethyl sulfoxide (DMSO). After this treatment, possible induction of apoptosis was detected. The Annexin V and Dead Cell assay was performed with **"Muse"** (Millipore Corporation, Billerica, MA, USA) method, according to the instructions supplied by the manufacturer. This procedure utilizes Annexin V to detect phosphatidylserine (PS) on the external membrane of apoptotic cells [Brognara et al., 2014].

A dead cell marker is also used as an indicator of cell membrane structural integrity. It is excluded from live, healthy cells, as well as early apoptotic cells. Four populations of cells can be distinguished in this assay. Cells were washed with sterile PBS 1X, trypsinized, suspended and diluted (1:2) with the one step addition of the Muse Annexin V & Dead Cell reagent. After incubation of 20 min at room temperature in the dark, samples were analyzed.

Data from prepared samples were acquired and recorded utilizing the Annexin V and Dead Cell Software Module (Millipore). The results obtained are shows in Figure 4.5 and demonstrate that apoptosis was not induced by PNAs targeting miR-145-5p, whereas under the same conditions an increase of apoptosis was observed using Stattic (Selective STAT3 inhibitor) with 10% DMSO.

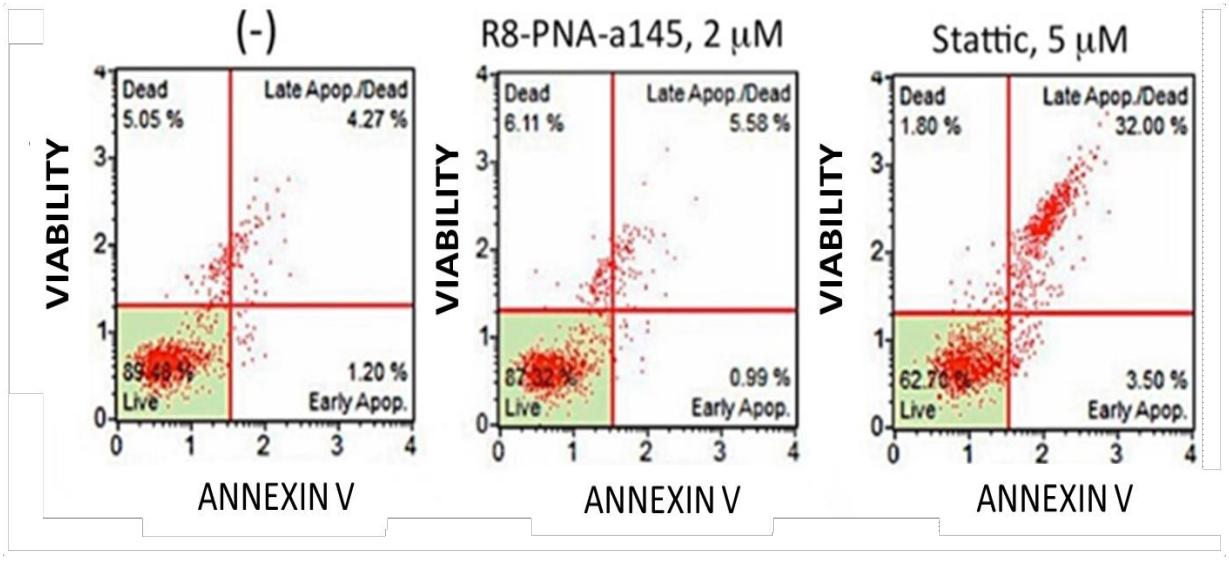

Figure 4.5: Effects of R8-PNA-a145 on apoptosis. Effects of R8-PNA-a145 on apoptosis of Calu-3 cells. Apoptosis was determined by the Annexin V & Dead Cell Kit (Millipore Corporation). Figures, seen are taken by MUSE analyzer.

These data are of interest because are a proof-of-principle that miRNA targeting might be considered to increase CFTR content, with possible applications in the personalized therapy of cystic fibrosis. With respect to different molecular and genetic basis of CF, it is expected that miR-145 targeting will not be useful for CFTR defect of type I (no protein), II (no traffic), III (no function). On the contrary, increase of CFTR is expected to be useful for type IV (less function), V (less protein) and VI (less stable protein) CFTR defect [Paranjape et al., 2017]. In any case combined therapy using read-through molecules (for type I), splicing correctors (for type V) might be propose.

4A.2. RESULTS

The objective of this section of the study was to expand our data on the anti-miR-145-5p role of additional CF cell lines in order to verify our results and support the possible use of these reagents for the development of therapeutic protocols for CF patients. For this purpose, we used the CFBE-41o ΔF-508 cell line to demonstrate the effects of this interference in *CFTR Gene* with anti-miR-145-5p and verified them both on mRNA and protein content level in Calu-3 cells.

4A.2.1. Detection of miRs Binding Sites in 3'UTR CFTR region

We have identified several miRs and binding sites related to them, which could be further used to modify *CFTR Gene* expression and related biological activities. **[Figure 4.6]** In silico predictions using PITA identified all potential (MREs) miRNA mediated repressions for the lead miRNAs in the CFTR 3'UTR: miR-145-5p × 4 sites, miR-145-3p × 3sites, miR-494-3p × 6 sites, miR-223-3p× 8 sites, miR 101-3p× 3 sites, and miR-509-3p × 2 sites

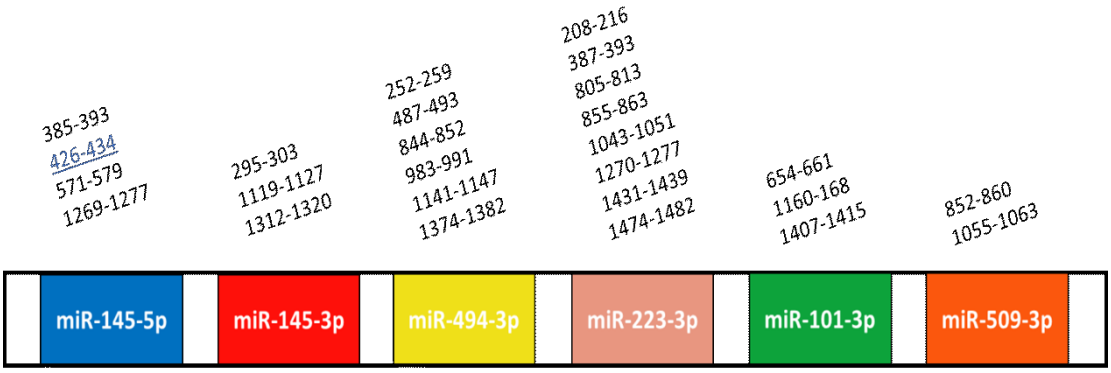

Figure 4.6: 3'UTR CFTR region MREs, Region is 1557 bp long**,** entails the 3'UTR CFTR region and includes the all miRs binding sites present on the *CFTR Gene*. It also shows the various binding sites present on this gene of various miRs. Theses miRs and the most conserved binding sites on *CFTR Gene* analysis was done by using the online software Tools4miRs (PITA).

[**Figure 4.6**] From this list, miR-145-5p target sites were selected in our study against which PNAs were designed with a highest (ΔΔG) value up to 13 [**Figures 4.7A and 2B**]. Further, the efficacy of these PNAs at increasing CFTR 3'UTR was checked in different cell lines varying from CALU-3 to CFBE-41oΔ F508. It can also be seen from other studies of the literature that same analysis was done to check the various target miRs and to screen the required MREs for your target sites [De santi et al., 2020].

4A.2.2. Detection of highest conserved miR-145-5p region 3'UTR CFTR

MiR-145-5p Binding Sites of the 3'-UTR Sequence of CFTR Are Conserved throughout Evolution [Han et al., 2017; Hart et al., 2013]. It shows that the miR-145 binding sequence is highly conserved through evolution, suggesting a role in CFTR expression and functions. In [**Figure 4.7A**], the interaction between miR-145-5p and CFTR sequences is also shown. The number of CG/GC, AT/TA and GU/UG interactions is 11, a value similar or even higher to the number of possible interactions between miR-145 and other miR-145 regulated genes. The mRNAs considered have been validated as miR-145 regulated on the basis of in silico analysis. These analyses confirm that miR-145-5p as being a true regulator of *CFTR Gene* expression.

MiR-145-5p is a tumor suppressor, miR often decreased in human cancers. [Michael et al., 2003; Iorio et al.,2005; Bandres et al., 2006; Calin and Croce, 2006; Cummins et al., 2006; Kent and Mendell, 2006; Cho et al., 2009; Wang et al., 2009; Chiyomaru et al., 2010]. Further, also the role of miR-145-5p is very well known, because binds the 3'-UTRs of the CFTR mRNAs. [Austin et al., 2011]. In our preliminary results, we have also proved it by in silico study of miR-145-5p, and importance to identify right position with highest binding affinity to proceed with in vitro experiments. [Figure 2A]

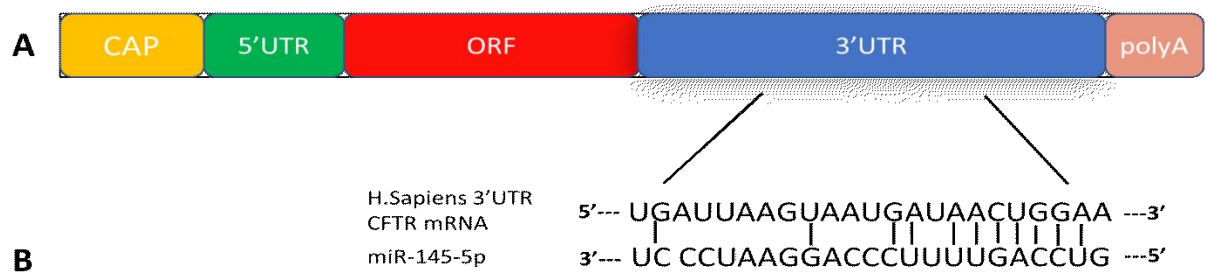

B

microRNA	Position	(ΔΔG)
hsa-miR-145-5p	385:393	-11.5
hsa-miR-145-5p	427:437	-13.25
hsa-miR-145-5p	571:579	-8.9
hsa-miR-145-5p	1269:1277	-11.8

Figure 4.7: (A) Location of the miR-145-5p binding sites within the CFTR 3'UTR region **(B)** To identify MREs and highest binding affinity with the target region by using the PITA software. (ΔΔG) value indicates highest binding affinity target sites.

Figure 4.7A, 2B, also shows the region showing the highest level of homology (Nucleotide compatible with target region represented by line in respective positions) belongs to highest

(ΔΔG), as also shown in **Figure 2B**, the homology is also shown for each nucleotide. Molecules sustain the concept of a role of miR-145-5p binding sites in CFTR regulation. The analysis carried out with the PITA software shows that among all the binding sites of miR-145-5p, the position between (427: 437) has a highest interaction with miR-145-5p. Further it was used to further analyse the PNA-a145 effects by Real time PCR and protein effects by western blotting.

4A.3. PNA-a145-5p (Antisense Strategy) on CFBE-41oΔF-508 Cells

The objective of our study was to verify the effects of the PNA-a145 on cell lines different from Calu-3, such as the CFBE-41oΔF-508 (Merck, Cat # SCC151) [Illek et al., 2008]. In these cells the assessments of CFTR mRNA levels and CFTR function showed that cAMP-stimulated CFTR Cl currents were 33%, 167% and 24%, respectively, of those in 16HBE14o- cells. The data suggest that transgene expression needs to be significantly higher than endogenously expressed CFTR to restore functional wtCFTR Cl transport to levels sufficient to reverse CF pathology [Illek et al., 2008].

The CFBE-41o ΔF-508 cell line was employed to demonstrate the effects of this interference in *CFTR Gene* with anti-miR-145-5p and verified them both on mRNA and protein content level. In this part of study, our preliminary results as shown above the effectivity of anti-miR-145-5p role in interfering the target binding sites related to miR-145-5p and how does it effects the *CFTR Gene* mRNA and protein content not only in non CF CALU-3 cells but also in CF cell lines such as CFBE e.g CFBE-41oΔF-508.

4A.3.1. Experimental strategy

The experimental strategy is displayed in **[Figure 4.8]**. CFBE-41o ΔF-508 cells were used for the treatment with PNA-a145-5p, PNA-a145 MUT (4mm) and PNA-a433. Cells were grown for 72 Hours treatment in the presence of PNAs in petri plates. Cultured cells were trypsinized and collected by centrifugation at 1500 rpm for 10 min at 4 ◦C, washed with PBS, lysed with Tri-Reagent. The isolated RNA was washed once with cold 75% ethanol, dried and dissolved in nuclease free pure water before use. After that, protein exactions were performed and samples were prepared for western blotting. During the whole process some cells were separated to perform the cell viability and apoptotic assay. In the end, RNA and protein samples were used to further analyse the PNA-a145 effects by Real time PCR and protein effects by western blotting.

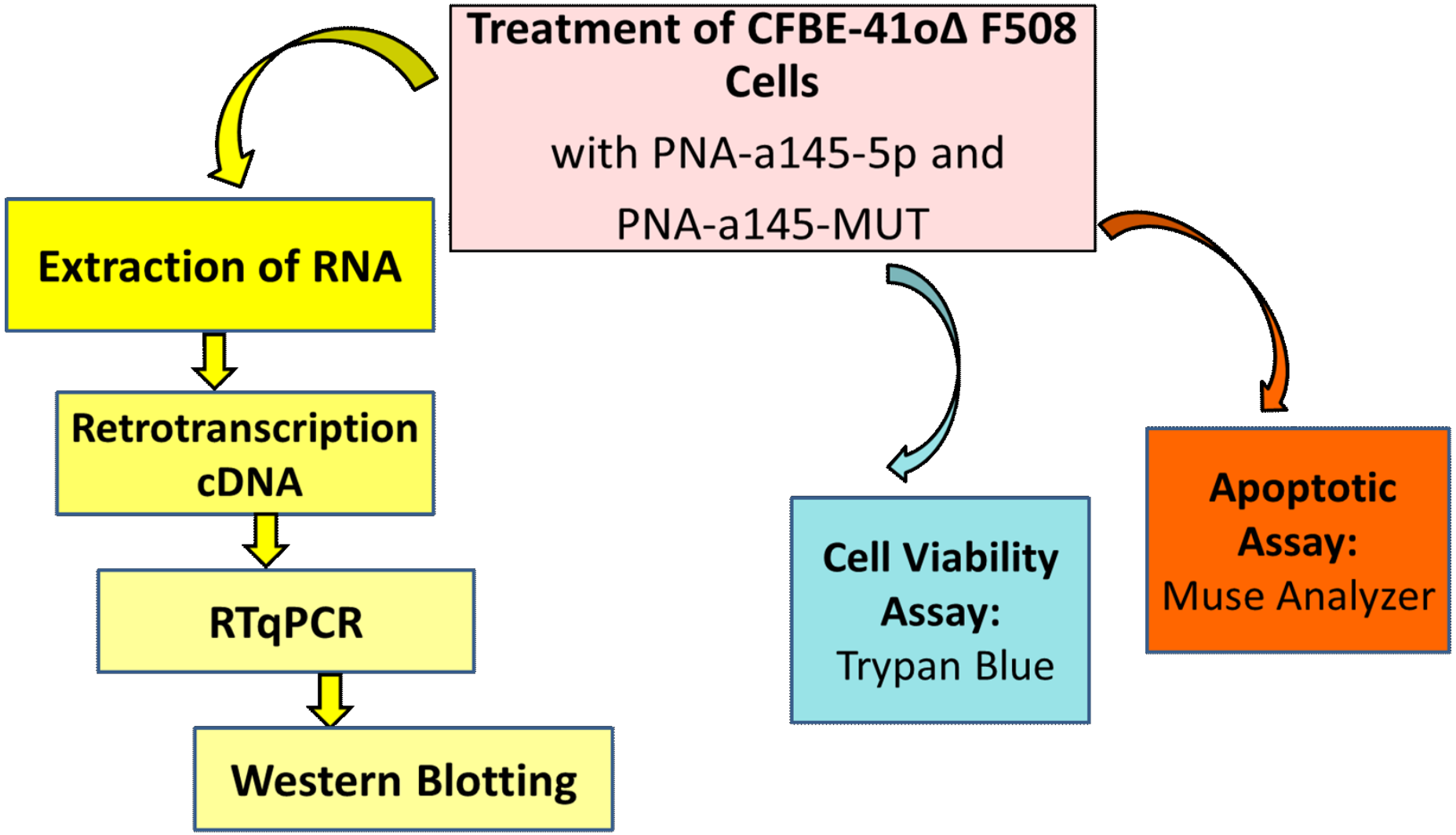

Figure 4.8. Experimental strategy for anti-PNA-a145-5p. In this experiment CFBE-41o ΔF-508 cells were used and given treatment with mentioned PNAs. Following RNA extraction and then further Q-PCR and western blotting was done. Cell viability assay and antiprolifratic activity was also checked

4A.3.2. PNA-a145-5p inhibits miR-145-5p level in CFBE-41o ΔF-508 cell line

As PNAs were designed according to our standardized protocols which were the same, using the following criteria as previously mentioned. Further, we have also reported the higher efficiency of R8-PNA conjugates (R8-PNAs) in inhibiting target miRNAs when this activity is compared to that of conventional commercially available antagomiRNAs [Fabbri et al., 2011]. Control PNA (R8-PNA-a145-MUT) was obtained by modification of the position of four nucleobases, thus leaving the same base composition .While R8-PNA-a433 is another PNA used in these experiments for the comparison of effects with PNA-a145-5p. The mutated sequence was also analyzed using BLAST search to assess possible interferences.

When CFBE-41o ΔF-508 cells were cultured in the presence of R8-PNA-a145 and of the mutated sequence R8-PNA-a145-MUT and R8-PNA-a433, a differential inhibition was obtained in **[Figure 4.9].** First of all, treatment of CFBE-41o ΔF-508 cells with R8-PNA-a145 leads to an inhibition of the miR-145-5p hybridization signals, compatible with decrease of free miR-145-5p content, and hence of its potential action, in treated cells; second, the mutant R8-PNA-a145-MUT displayed no inhibitory effects. Similarly, the R8-PNA-a433 displayed no inhibitory effects. The decrease of miR-145 hybridization signals following treatment R8-PNA-a145 is expected, in agreement with the effects of anti-miRNA PNAs elsewhere published [De santi et al., 2020;Brognara et al., 2014].

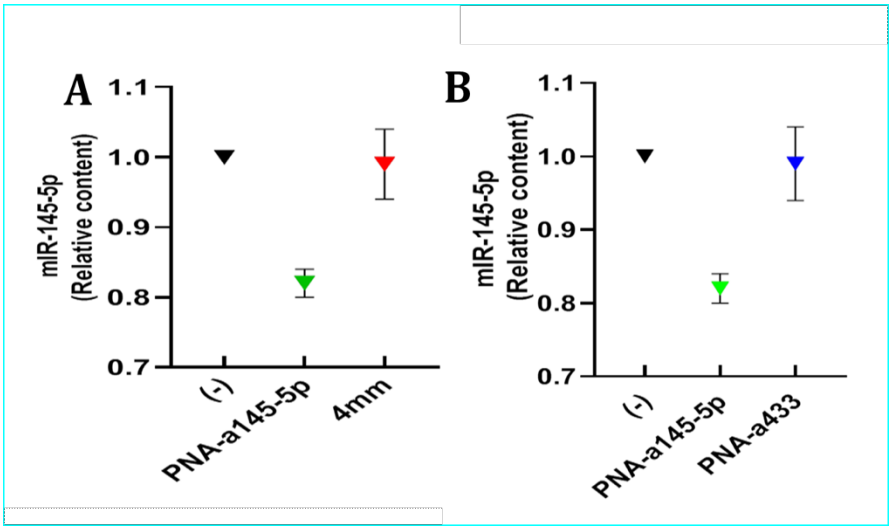

Figure 4.9: (A) Inhibition of miR-145-5p hybridization signals in CFBE-41oΔF-508 cells treated for 72 h with R8-PNA-a145 , mutated R8-PNA-a145-MUT(4mm) and R8-PNA-a433 molecules (2 μM, as indicated); **(B)** Inhibition of miR-145-5p hybridization signals in CFBE-41oΔF-508 cells treated for 72 h with R8-PNA-a145 and R8-PNA-a433 molecules (2μM, as indicated); Results shown represent the average ± standard deviation (S.D.) obtained in at least three independent experiments.* = $p < 0.05$; * ** = $p < 0.01$.

4A.3.3. PNA-a145-5p effects on CFTR mRNA and protein levels

When CFBE-41o ΔF-508 cells were cultured in the presence of R8-PNA-a145 a clear effect was observed in CFTR mRNA accumulation. In fact the CFTR mRNA fold increases were 2.5/2.7 with respect to untreated CFBE-41o ΔF-508 cells. This value was obtained after determining CFTR mRNA content by RT-qPCR analysis as shown in **[Figure 4.10]**. These results prompted us to determine the CFTR content by Western blotting, as shown in Figure 4.10 A. Moreover, CFBE-41o ΔF-508 cells were treated for 72 h with R8-PNA-a145 and then proteins were separated by polyacrylamide gel electrophoresis and Western blotting analysis was performed using two antibodies, one specific for CFTR, the other for β-actin, used as an internal control. The CFTR protein increase was found to be 2–2.5 times more in CFBE-41o ΔF-508 cells extracts after R8-PNA-a145-5p treatment in three independent experiments. These results suggest that miR-145-5p targeting can be considered in the development of miRNA-therapeutic protocols for CFTR up-regulation using the antisense strategy based on PNA.

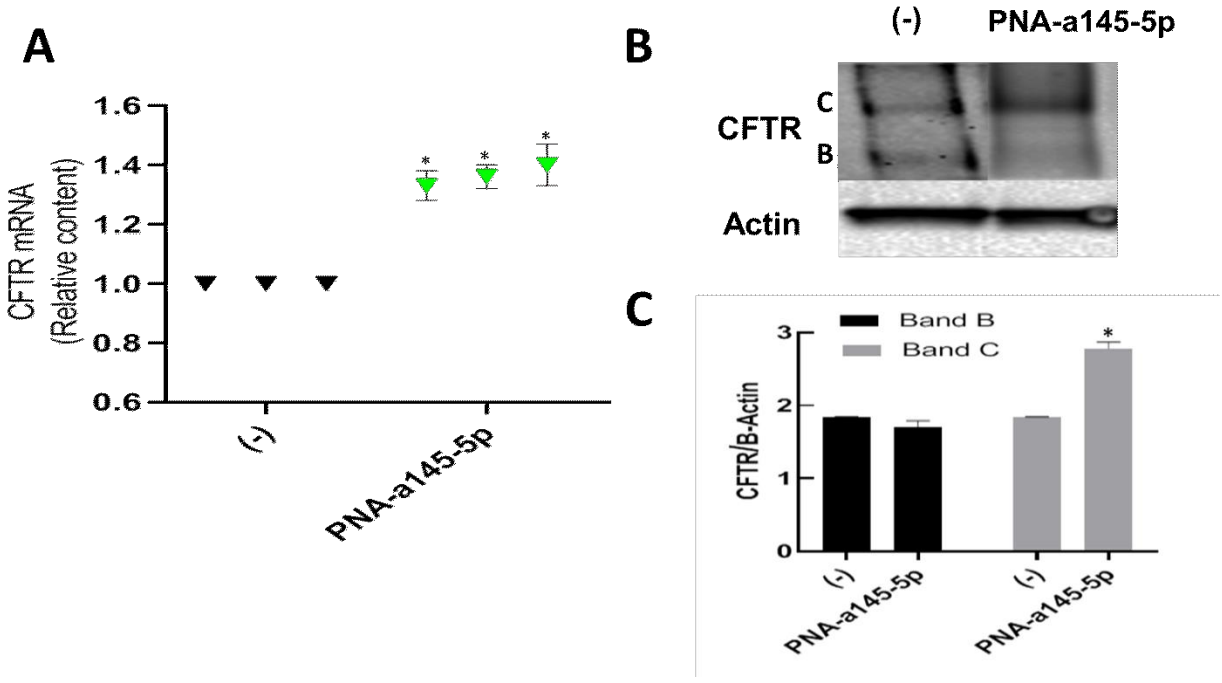

Figure 4.10: PNA-a145-5p effects. (A) Upregulation of CFTR mRNA (RT-qPCR treated for 72 h with R8-PNA-a145 (2μM) and (B) CFTR protein (Western blotting) in CFBE-41o ΔF-508 cultured for 72 h in the absence or in the presence of R8-PNA-a145-5p. CFTR and β-actin are indicated in panel B. **(C)** Quantification of the CFTR/β-actin ratios of both the bands of B and C after densitometry analysis of the Western blotting shown in panel B (arbitrary units).

Similarly, PNA directed against miR-145-5p is able to inhibit miR-145-5p and increase the miR-145-5p regulated CFTR. The increase of CFTR expression was detectable at the level of

protein. These data are of interest because are a proof-of-principle that miRNA targeting might be considered to increase CFTR content, with possible applications in the personalized therapy of CF. The field of precision medicine is in fact growing [Paranjape et al., 2017].

4A.4. PNA MASKING

Besides the anti-miRNA therapeutic strategy, an anti-miRNA biological effect can be reached by masking the miRNA binding sites present within the 3'UTR region of the target mRNAs [Wang et al., 2011; Qadir et al., 2019]. The objective of this part of the study was to design a PNA masking the miR-145-5p binding site present within the 3'UTR of the CFTR mRNA and to determine its activity in inhibiting miR-145-5p function, with particular focus on the expression of both CFTR mRNA and CFTR protein. In the anti-miRNA therapeutic strategy, inhibition of miRNA functions could be reached by masking the miRNA binding sites present within the 3'UTR region of the target mRNAs. The results obtained support the concept that the PNA masking the miR-145-5p binding site of the CFTR mRNA is able to interfere with miR-145-5p biological functions, leading to both an increase of CFTR mRNA and CFTR protein content.

4A.4.1. Location of miR-145-5p Binding Sites within the 3'UTR Sequence of CFTR mRNA: Targeting with the miR145-maskingPNA

[Figure 4.11] shows the location of the miR-145-5p binding site within the 3'UTR sequence (position 427-437 of the 1557 nucleotides long 3'UTR) of the human CFTR mRNA [Megiorni et al., 2011; Megiorni et al., 2013] and the different mechanism of action of PNA-based miRNA targeting (upper part of the panel) versus PNA masking (lower part of the panel). As far as the comparison between the miRNA inhibiting and the miRNA masking strategies, we would like to underline that we have elsewhere published data supporting the use of miR-145-5p targeting in CF, based on an antisense PNA to target miR-145-5p and enhance expression of the *CFTR Gene* [Fabbri et al., 2017; Finotti et al., 2019]. This conclusion was recently confirmed by Kabir et al., who demonstrated that miR-145 mediates TGF-β inhibition of synthesis and function of the CFTR in CF airway epithelia [Lutful Kabir et al., 2018]. This direct anti-miRNA strategy is expected to inhibit miR-145-5p function, affecting, in addition to the *CFTR Gene*, other miR-145-5p-regulated mRNAs. In contrast, PNA-based miRNA masking might lead to effects restricted to the CFTR mRNA and would therefore be of great translational relevance.

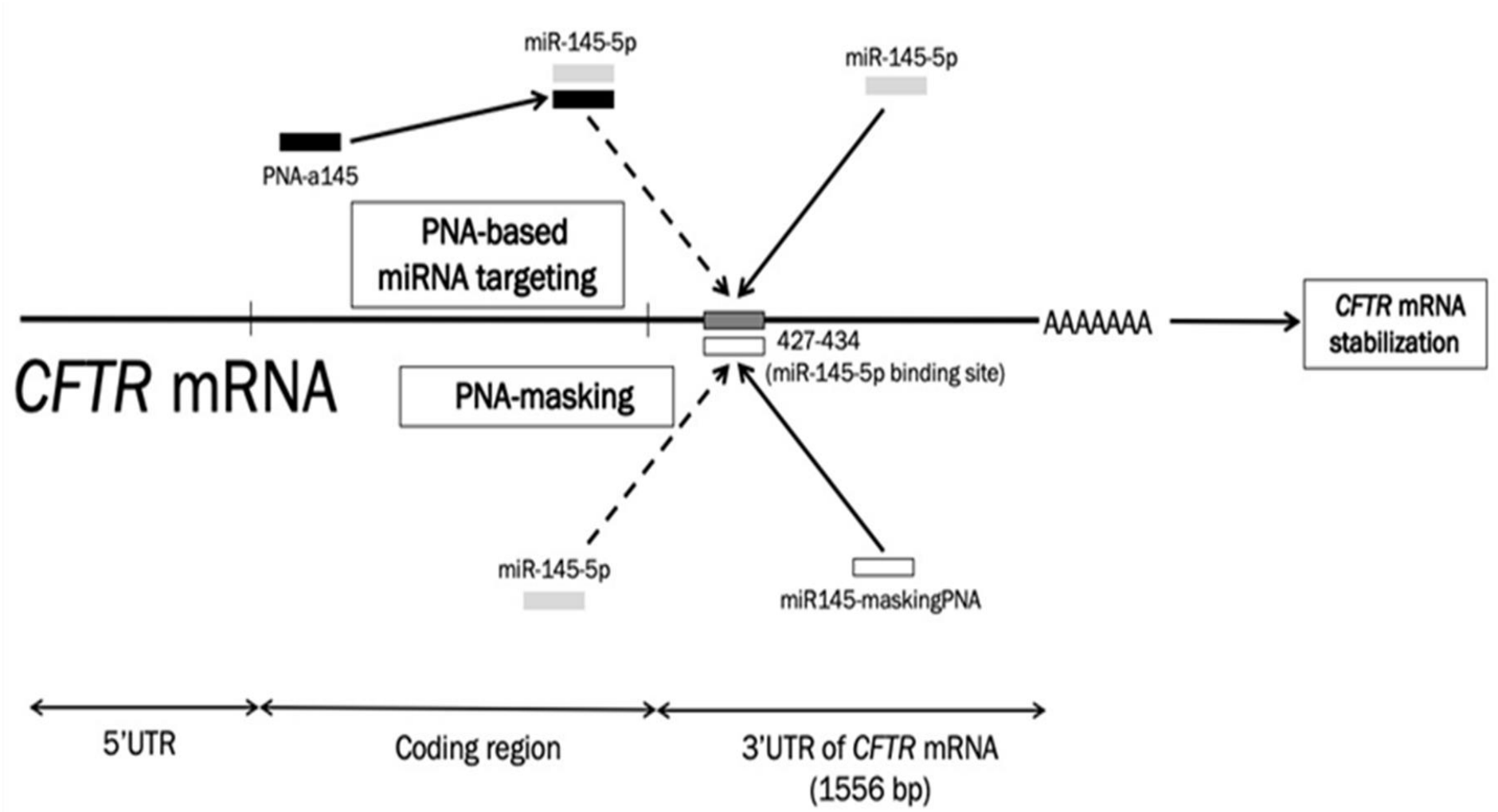

Figure 4.11. PNA-masking and PNA based miRNA targetting Strategies; Comparison of the peptide nucleic acid (PNA)-based miRNA-targeting (upper part of the panel) and the PNA-masking (lower part of the panel) strategies to inhibit miR-145-5p biological functions. Dark grey box: the miR-145-5p binding site; light grey boxes: miR-145-5p; white box: miR145-maskingPNA; black boxes: the anti-miR-145-5p PNA-a145. Dotted arrows: inhibition/interference.

4A.4.2. Synthesis and Characterization of the miR145-maskingPNA

The synthesis of the miR145-maskingPNA was similar to those previously reported [Brognara et al., 2014; Fabbri et al., 2017] and was performed in the laboratory leaded by Roberto Corradini (Department of Chemical, Life and Environmental Sustainability Sciences, University of Parma) using a standard Fmoc-based automatic peptide synthesizer for both the PNA and the polyArg tail. After cleavage from the solid support, purification was performed by HPLC, and the purified PNA was characterized by UPLC/MS. The chemical characterization parameters are reported in the **[Figure 4.12].** A carrier octaarginine R8 peptide was conjugated at the N-terminus of the PNA chain causing an increase of delivery that approaches 100% (i.e., uptake in 100% of the target cell population), as elsewhere published [Brognara et al., 2014]; this conjugation is easily realized during PNA solid-phase synthesis using the same reagents and solvents.

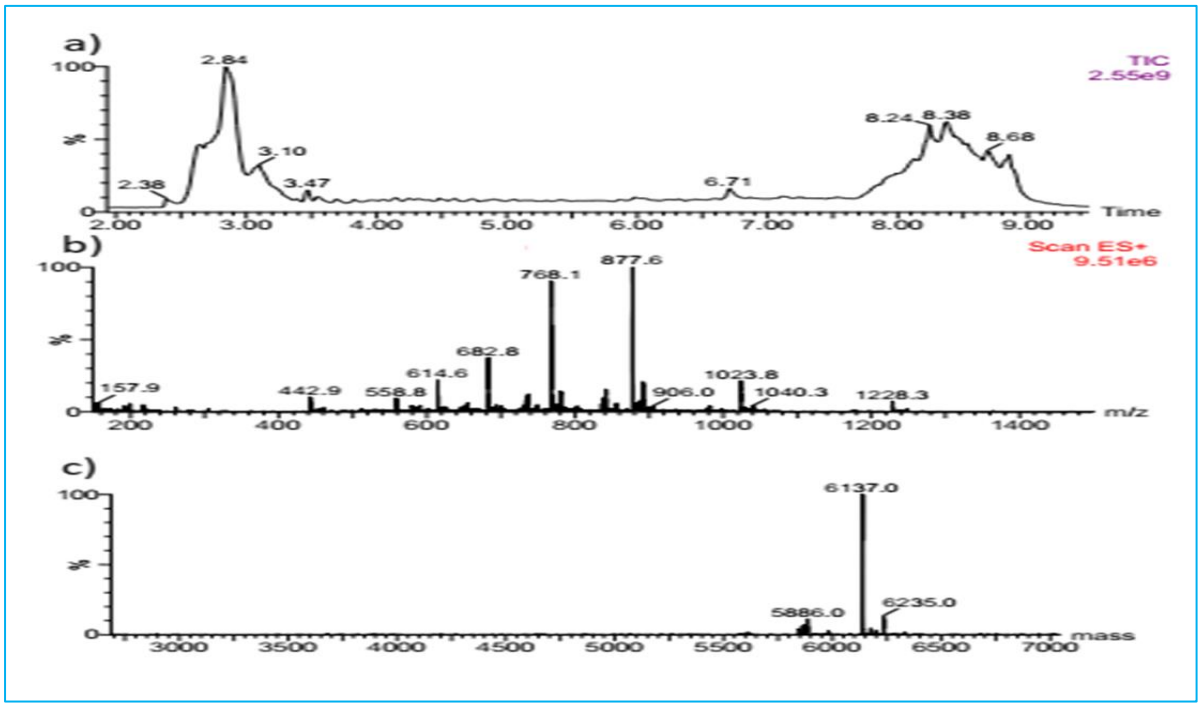

Figure 4.12: (A) UPLC/MS Chromatogram of the purified PNA ("miR145-maskingPNA"), used for the present work; peak at 2.84 min corresponds to the target PNA. **(B)** Mass spectrum of the peak at 2.84 min; reconstructed molecular mass obtained from deconvolution of the spectrum in **(C)** Devolution of spectrum in percentage.

4A.4.3. Interactions of the miR145-maskingPNA with other mRNAs

[Figure 4.13] shows the location of the miR-145-5p binding site **[Figure 4.15 A]** within the 3'UTR CFTR mRNA sequence together with the extent of homology between the miR-145-5p binding site and the miR145-maskingPNA. The design of the miR145-maskingPNA, fully

complementary to the miR-145-5p CFTR mRNA binding site **[Figure 4.15 B]**, was chosen in order to obtain an efficient competition between miR-145-5p and its 3'UTR CFTR mRNA binding sites. In fact, the interaction between this miR145-maskingPNA and the CFTR mRNA is expected to be much more efficient than the interaction between the miR-145-5p and CFTR mRNA, since the CFTR nucleotides complementary to the miR-145-5p are 10/18. On the other hand, the same miR145-maskingPNA exhibits low levels of complementarity to the miR-145-5p binding sites of other mRNAs. For instance, the miR145-maskingPNA exhibits only 9 residues complementary to the 18 nucleotides region of a functional miR-145-5p binding site validated in the 3'UTR region of the Myosin-6 mRNA [Grillo et al., 2010] (see the bottom part of Figure 4.15).

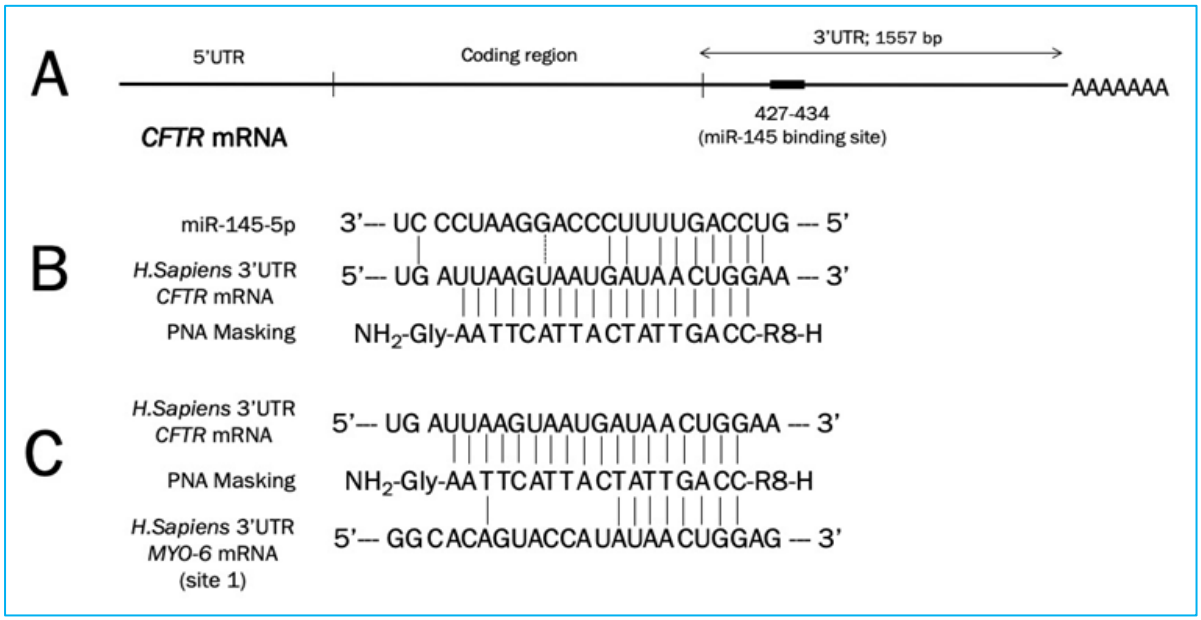

Figure 4.13: (A) Location of the miR-145-5p binding sites within the cystic fibrosis transmembrane conductance regulator (CFTR) 3'UTR mRNA region**(B).** Interactions between the miR145-maskingPNA and CFTR mRNA (comparison with the interaction of CFTR mRNA with miR-145-5p is also shown). **(C).** Interactions between the miR145-maskingPNA and the Myosin-6 mRNA [Grillo et al., 2010], containing in the 3'UTR sequence three miR-145-5p binding sites (the miR-145-5p binding site#1 is here shown, which exhibits the highest levels of complementarity to the miR145-maskingPNA). The miR145-maskingPNA is fully complementary with the 3'UTR region of the CFTR mRNA.

In our studies, we have not only considered the interactions between miR145-maskingPNA and myosin gene but also Interaction between miR145-masking and other genes **[Figure 4.14].** Interactions between the miR145-maskingPNA and PTBP1 (Polypyrimidine Tract Binding Protein 1), NEDD9 (Neural Precursor Cell Expressed, Developmentally Down-Regulated 9), IRS1 (Insulin Receptor Substrate 1) and KLF4 (Krüppel Like Factor), might be also occurring. However, after performing the real time qPCR analysis, there is no inhibition in all these examples is appreciable even at the highest concentrations used (Figure 4.15 of

these results). Further, it also empowers the fact that the miR145- maskingPNA is fully complementary with the 3'UTR region of the CFTR mRNA (Figure 4.15, B of our results).

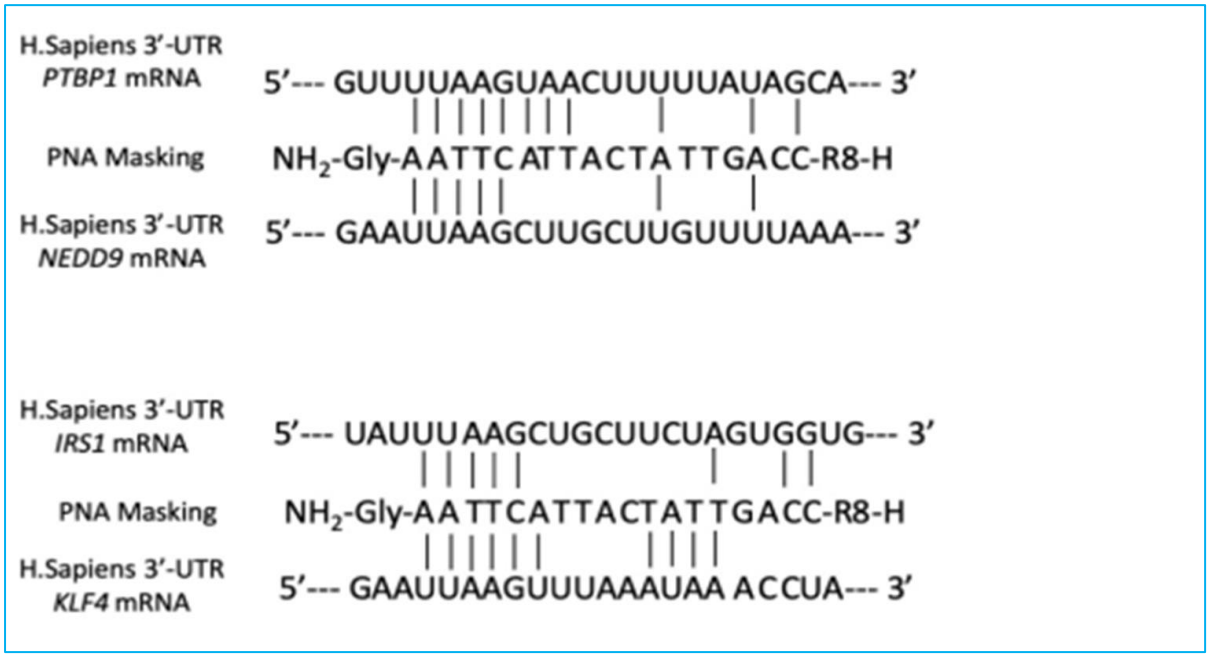

Figure 4.14: Interactions between the miR145-maskingPNA and the PTBP1 (Polypyrimidine Tract Binding Protein 1) [Minami et al., 2017], NEDD9 (Neural Precursor Cell Expressed, Developmentally Down-Regulated 9) [Speranza et al., 2017], IRS1 (Insulin Receptor Substrate 1) [Wang et al., 2014] and KLF4 (Kruppel Like Factor 4) [Liu et al., 2013] mRNAs. No inhibition in all these examples is appreciable even at the highest concentrations used (Figure 4.17 of the main text). The miR145- maskingPNA is fully complementary with the 3'UTR region of the CFTR mRNA.

4A.4.4. Specificity of the miR145-maskingPNA activity

The specificity of the miR145-maskingPNA is suggested by the experiment depicted in **[Figure 4.15]**. The miR145-maskingPNA was added to cDNAs obtained after RT reactions performed using Calu-3 RNA. The PCR amplification was performed using primers amplifying a 3'UTR region of either CFTR (using one primer located on the PNA binding site, **[Figure 4.15, A]** or Myosin-6 **[Figure 4.15, B]** mRNAs. As Figure 4.15 shows, full inhibition of the RT-qPCR amplification of CFTR mRNA was obtained when 50 and 100 nM miR145-maskingPNA were employed as shown **[Figure 4.15, A].** In contrast, no inhibition of amplification was detectable when primers for Myosin-6 mRNA were used.

Furthermore, the miR145-maskingPNA was unable to inhibit the RT-qPCR amplification of other mRNAs carrying miR-145-5p binding sites, including polypyrimidine tract binding protein 1 (PTBP1) [Minami et al., 2017], neural precursor cell expressed, developmentally down-regulated 9 (NEDD9) [Speranza et al., 2017], insulin receptor substrate 1 (IRS1) [Wang et al., 2014], and Kruppel-like factor 4 (KLF4) [Liu et al., 2013] mRNAs (Figure

4.15, C and D). The complementarity of the miR145-maskingPNA with the miR-145-5p binding sites of PTBP1, NEDD9, IRS1, and KLF4 mRNAs are also shown in **[Figure 4.14]**. These results suggest that the miR145-maskingPNA selectively binds the CFTR 3'UTR, with lower affinity to the miR145-5p binding sites present in other mRNAs.

Recent published reports strongly support the concept that PNAs can be a very powerful tool to inhibit the expression of microRNAs [Fabani et al., 2008; Fabbri et al., 2011]. MicroRNAs (19 to 25 nucleotides in length) are noncoding RNAs that regulate gene expression by targeting mRNAs, leading to a translational repression or mRNA degradation [Lim et al., 2005]. Since their discovery, the number of microRNA sequences present within the miRNA databases has significantly grown [Griffiths-Jones et al., 2004]. The complex networks constituted by miRNAs and mRNAs lead to the control of highly regulated biological functions, such as differentiation, the cell cycle, and apoptosis [Lim et al., 2005].

Epigenetic regulation of expression of cystic fibrosis transmembrane conductance regulator (CFTR) gene by miRNAs has been recently reported by different groups [Austin et al., 2011]. For instance, expression of miR-145 and miR-494 was found to anti-regulate CFTR [Oglesby et al., 2013]. The effect of air pollutants and cigarette smoke on CFTR expression identified two more miRNAs that could target CFTR mRNA, namely miR-101 and miR-144 [Hassan et al., 2012]. Synergistic post-transcriptional regulation of *CFTR Gene* expression by miR-101 and miR-494 specific binding was demonstrated [Megiorni et al., 2011]. Different miRNAs that have been found to be increased in the primary bronchial epithelial cells of cystic fibrosis (CF) patients can reduce CFTR expression, either by direct (miR-145-5p, miR-223-3p, miR-494-3p, miR-509-3p, miR-101-3p) or by indirect (miR-138-5p) interactions. Therefore, targeting miRNAs, such as miR-145-5p, might be an important strategy for upregulating CFTR. We have elsewhere published data supporting the use of miR-145-5p targeting in CF, based on an antisense PNA able to enhance expression of the *CFTR Gene*, analyzed at the mRNA (RT-qPCR) and protein (Western blotting) levels [Finotti et al., 2019]. This conclusion was recently confirmed by Kabir et al., who demonstrated that miR-145 mediates TGF-β inhibition of synthesis and function of the CFTR in CF airway epithelia [Lutful Kabir et al., 2018].

The PNA was conjugated to a poly-arginine tail, since these types of constructs were previously used by our group for highly efficient delivery of PNA into cell lines [Brognara et al., 2014]. As the experimental model system, the Calu-3 cell line was selected. These cells

are a well-differentiated and characterized cell line derived from human bronchial submucosal glands and extensively used to study CFTR expression and immunological behavior [Shen et al., 1994; Kreft et al., 2015].

The data presented in these results show that a PNA masking the miR-145-5p binding sites present within the 3'UTR of the CFTR mRNA is able to increase the expression of the miR-145-5p regulated CFTR. The increase of *CFTR Gene* expression was detectable at the level of mRNA (analyzed by RT-qPCR). Our results could provide a proof-of-principle that miRNA masking might represent an efficient tool to increase CFTR content (possibly by increasing CFTR stability), with possible applications in the personalized therapy of CF.

For a possible translation to therapeutic approaches for CF, our data are just a proof-of-principle and limited in their application potential. In fact, concerning miRNA masking, we should consider that, in addition to miR-145-5p, several other miRNAs have been proposed to down-regulate CFTR expression, such as miR-494, miR-509-3p, miR-101, and miR-443[Oglesby et al., 2013; Megiorni et al., 2011].

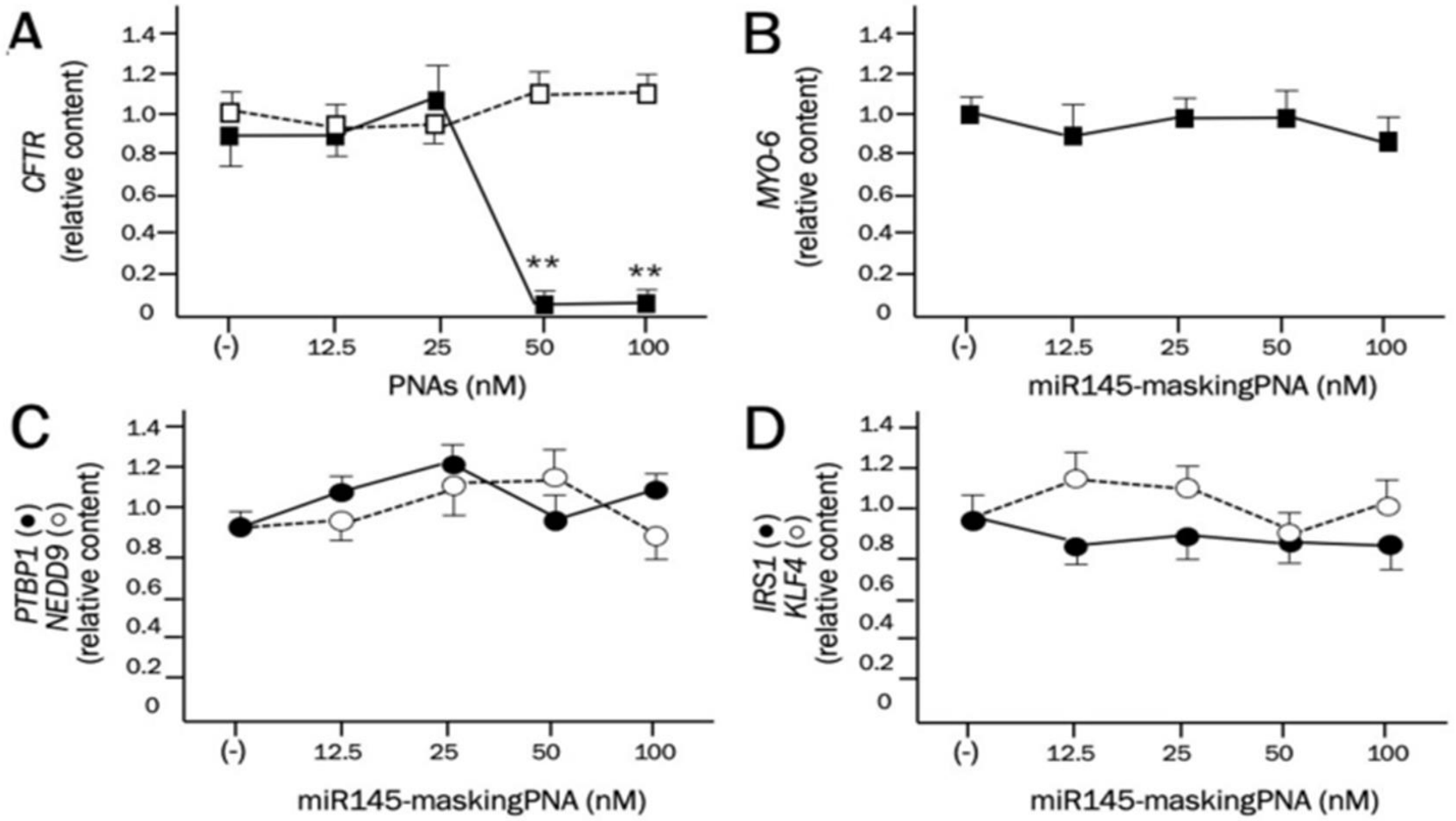

Figure 4.15 Effects of the miR145-maskingPNA on the RT-PCR amplification of 3-UTR mRNA sequences. (A). Effects of the miR145-maskingPNA (black symbols) and of the negative control PNA (white symbols) on the amplification of CFTR mRNA sequences. Inhibition by miR145-maskingPNA is clearly seen at 50 nM. The negative control PNA was not effective. Effects of the miR145-maskingPNA on the amplification of Myosin-6 (B), PTBP1 (polypyrimidine tract binding protein 1) and NEDD9 (neural precursor cell expressed, developmentally down-regulated 9) (C), IRS1 (insulin receptor substrate 1), and KLF4 (Kruppel-like factor 4) (D) mRNAs. No PCR inhibition in any of these examples was appreciable even at the highest concentrations used.

4A.4.5. Experimental strategy

The experimental strategy is displayed in [**Figure 4.3**] with slight changes in the treatment; mentioned in the following. For this experiment, Calu-3 cells were used and grown for 72 hours treatment with respective masking-PNA in petri plates. Cultured cells were trypsinized and collected by centrifugation at 1500 rpm for 10 min at 4 ◦C, washed with PBS, lysed with Tri-Reagent. The isolated RNA was washed once with cold 75% ethanol, dried and dissolved in nuclease free pure water before use. After that, protein exactions were performed and samples were prepared for western blotting. During the whole process some cells were separated to perform the Cell viability assay and apoptotic assay. In the end, RNA and protein samples were used to further analyse the mIR145-masking PNA effects by Real time PCR and protein effects by western blotting.

4A.4.6. Effects of the miR145-maskingPNA on *CFTR Gene* Expression in Calu-3 cells

Calu-3 cells were cultured for 72 h in the presence of different concentrations of the miR145-maskingPNA, then RNA and proteins were isolated for experiments of RT-qPCR and Western blotting. When RT-qPCR was performed, a clear effect was observed on CFTR mRNA accumulation. The relative CFTR mRNA content in treated Calu-3 cells is reported relative to untreated samples. The relative values of CFTR mRNA in untreated samples were calculated with respect to the average CFTR mRNA content in control cells. The data obtained show that CFTR mRNA increased when Calu-3 cells treated with the miR145-maskingPNA were compared with untreated cells in three independent experiments **[Figure 4.16 A]**.

The difference in CFTR mRNA content between untreated cells and cells treated with the miR145-maskingPNA is significant ($p < 0.05$ at 1 and 2 μM miR145-maskingPNA). The effects on CFTR mRNA were particularly evident, as expected, at the highest concentration of PNA (2.14- to 4.23-fold increase was obtained when 2 μM miR145-maskingPNA were used). **Figure 4.16 (B and C)** shows the results of the Western blotting performed using two antibodies, one specific for CFTR, the other for β-actin, used as an internal control. As reported in other published studies [Meegen et al., 2013; Trotta et al., 2015], the Western blotting analysis based on the CFTR-directed monoclonal antibody 596 shows only a major band corresponding to the fully-glycosylated 170 kDa form of CFTR (known as the C-band) [Meegen et al., 2013; Trotta et al., 2015]. The CFTR protein increase was found to be 6- to 8-

fold in Calu-3 extracts after miR145-maskingPNA treatment in the three independent experiments in which CFTR mRNA was also analyzed **[Figure 4.16 B, black boxes]**.

In order to verify specificity of the effects derived by the Western blotting experiment, Calu-3 cells were cultured with a negative control PNA previously demonstrated unable to (a) interact with miR-145-5p [Fabbri et al., 2017] and (b) inhibit RT-qPCR amplification of CFTR mRNA sequences containing miR-145-5p binding sites **[Figure 4.16, white symbols]**. The results obtained [Figure 4.18B] demonstrate no increase of the relative CFTR/β-actin values in Calu-3 cells treated with the negative control PNA.

In part C of figure 4.16, there were different concentrations of cells treated with the miR145-maskingPNA is significant (at 0.5 and 2 μM miR145-maskingPNA). The effects on CFTR protein levels were particularly evident, starting from the untreated cells and as concentration of miR145-maskingPNA increases so is the CFTR protein content. This protein content value can also be seen in part b of western blotting of theses respective samples. As in part c we compared our miR145-maskingPNA with negative PNA (white boxes). It can be seen that effects of miR145-maskingPNA are quiet specific with the increase of CFTR protein content as there is no effect regarding the negative control PNA in these experiments.

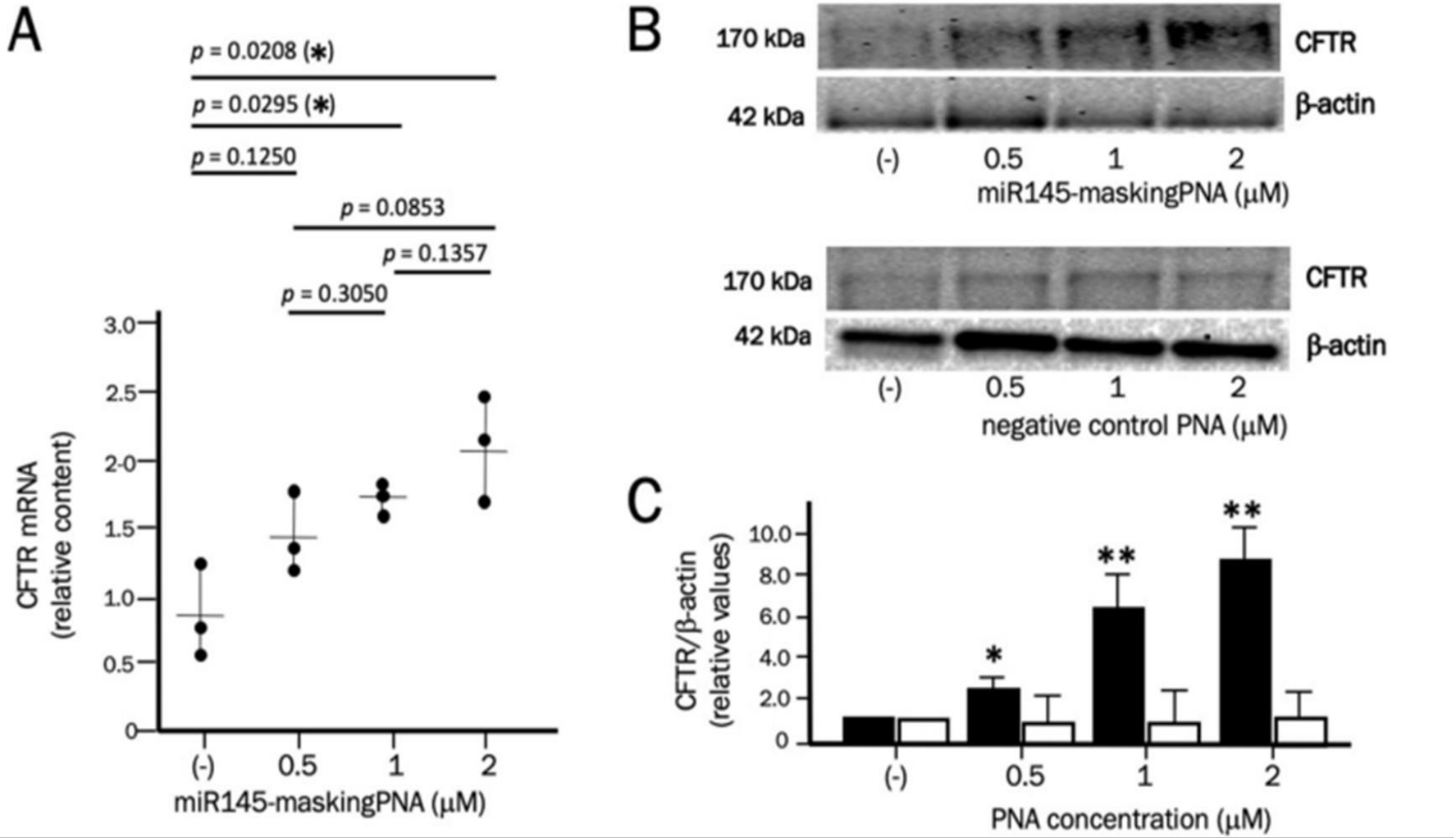

Figure 4.16 Effects of the miR145-maskingPNA on *CFTR* mRNA (**A**) and CFTR protein (**B**,**C**) in Calu-3 cells. Calu-3 cells were treated with the indicated concentrations of the miR145-maskingPNA for 3 days. Then, RNA was extracted and *CFTR* mRNA content determined by RT-qPCR (**A**). At the same time, CFTR was quantified by Western blotting (**C**, black bars). In parallel, Calu-3 cells were treated with a negative control PNA for 3 days and Western blotting was performed (**C**, white bars). In panel B, representative Western blotting results are shown. In panel C, averages ± SD are shown ($n = 3$) with respect to untreated Calu-3 cells. * = $p < 0.05$; ** = $p < 0.01$ (miR145-maskingPNA vs. negativecontrol PNA).

The graph shows in **[Figure 4.17]** (representing a summary of the different experiments performed) were derived from CFTR/β-actin ratios of treated samples, each expressed relative to the control untreated samples (arbitrarily expressed as 1 in order to compare different independent experiments and different exposures.

It should be noted that the concentration of the miR145-maskingPNA **[Figure 4.16]** was similar to that reported in the case of other anti-miRNA PNAs, but much higher of that used in the arrested-PCR experiments **[Figure 4.15]**. This is not unexpected when considering the fact that these two strategies are completely different. This difference was also found in one recent paper by our group comparing PNA-based miRNA-arrested PCR with anti-miRNA activity on cultured cell lines [Gasparello et al., 2019]. These results suggest that miR-145-maskingPNA should be considered in the development of miRNA-therapeutic protocols for CFTR upregulation.

4A.4.7. Densitomeric analysis of Western blotting

For densitometry analysis, the Chemidoc XRS+ System (Bio-Rad) was used. The Image Lab Software for Chemidoc and Gel Doc Imaging Systems (Version 6.0.1) was employed in order to acquire, display, edit and analyze the Western blot images, and to display and export data [5,6]. In our case, we performed all the analyses without ambiguity relative to the obtained results. In order to calculate the correct volumes, tools were used to highlight the band section and subtract the background signal. Further, the whole volume analysis Table was saved in excel file to perform further statistical analysis. Finally, mIR145-masking PNA Western blot experiment with compare to B-actin as a control shown in **[Figure 4.17]**.

An increase of the adjusted volume values was found only when samples from Calu-3 cells treated with miR145-maskingPNA were bound to the CFTR-directed monoclonal antibody 596. No increase in the adjusted volume values was found in samples from cells cultured in the presence of the negative control PNA.

On the other hand, the adjusted volume values relative to β-actin did not exhibit major changes in samples isolated from cells treated with the two PNAs. In the last two columns the CFTR/b-actin ratios (including both absolute and relative values) are shown. These calculations generated the summary panel depicted in Figure 4.17 A and B.

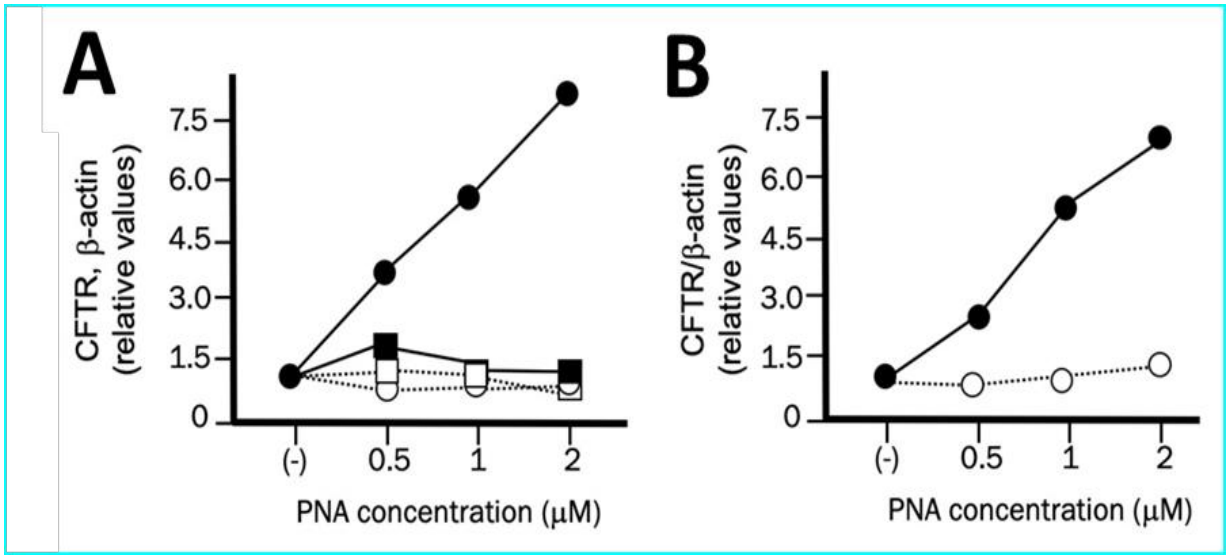

Figure 4.17: **Increase of CFTR expression in Calu-3 cells treated with the miR145-maskingPNA**. Raw data of the Western blotting performed using the CFTR- and b-actin directed monoclonal antibodies are presented in panels **A-B**. **Panel A** shows relative values of calculated volumes by gel doc instrument and of the calculated CFTR/β-actin ratios of two different independent experiments with different concentrations of miR145-maskingPNA and **Panel B shows** relative values of calculated volumes by gel doc instrument and of the calculated CFTR/β-actin ratios of different experiment. Treatment with the miR145-maskingPNA: black symbols; treatment with the negative control PNA: open symbols; CFTR, circles; b-actin: squares.

4A.4.8. The 145-maskingPNA interferes with miR-145-5p

When Calu-3 cells were cultured in the presence of the 145-maskingPNA (72 hours treatment) a clear-cut result of inhibition on miR-145-5p was obtained and depicted in **[Figure 4.18].** First of all, treatment of Calu-3 cells with the 145-maskingPNA leads to an inhibition of the miR-145-5p hybridization signals, compatible with decrease of free miR-145-5p content (data from three experiments). The decrease of miR-145 hybridization signals following treatment with the 145-maskingPNA suggest that these molecules might interfere also with the microRNA metabolism and accumulation. The decrease of miR-145 hybridization signals following treatment 145-maskingPNA is expected, in agreement with the effects of anti-miRNA PNAs elsewhere published [Fabbri et al., 2011; Brognara et al., 2014].

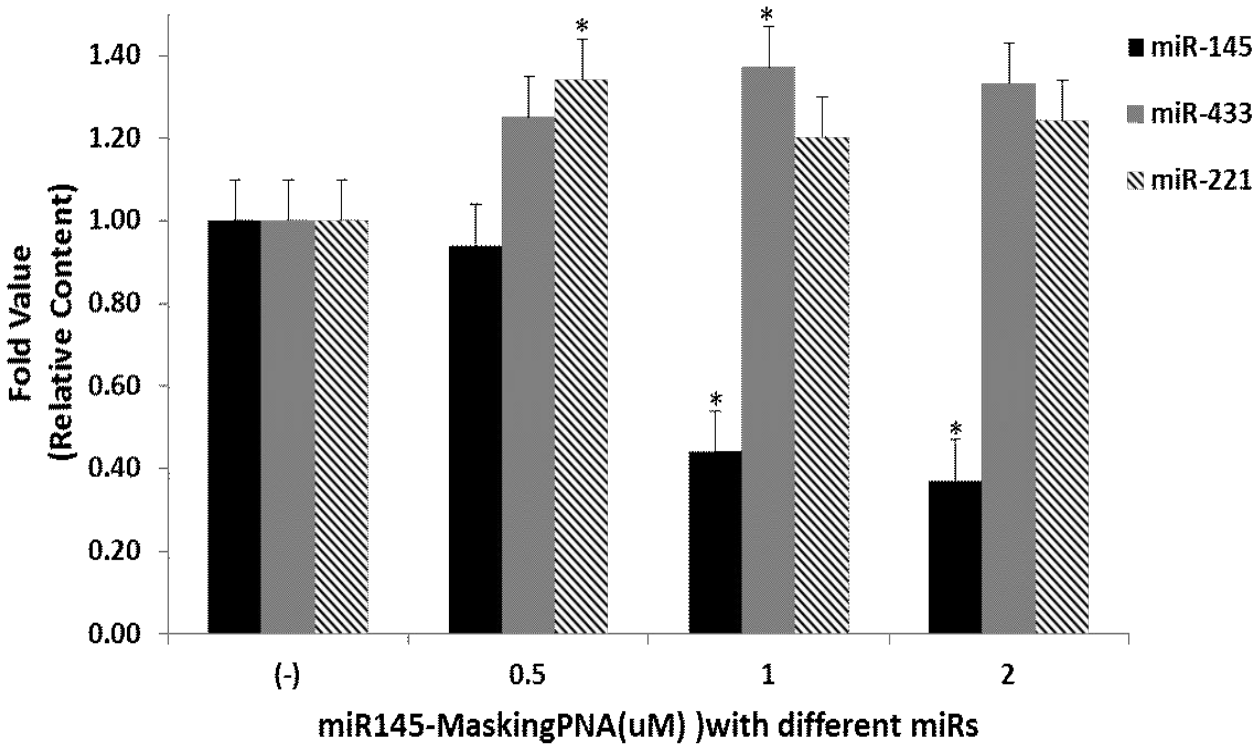

Figure 4.18: RT-qPCR on samples from Calu-3 cells treated with the 145-5p. Inhibition of miR-145-5p hybridization signals in Calu-3 cells treated for 72 h with 145-maskingPNA. On the contrary, RT-qPCR demonstrates no Inhibition of miR-433 and miR-221 hybridization signals in Calu-3 cells treated for 72 h with 145-maskingPNA. The obtained results are presented as average ± standard deviation (S.D.) obtained in at least three independent experiments. * = $p < 0.05$; ** = $p < 0.01$.

In addition, we found that the effects are fairly specific; in fact, the results obtained demonstrate that hybridization specific for other miRNAs expressed in Calu-3 cells (for instance miR-433 and miR-221) were different following 145-maskingPNA treatment. The representative experiments shown in **[Figure 4.18]**, demonstrate no effect of miR-433-3p and miR-221 and, conversely, an inhibitory effect of 145-maskingPNA. Altogether these experiments support the concept that the effects of 145-maskingPNA on miR-145-5p are sequence-specific. Finally, the effects of 145-maskingPNA were also confirmed on other cell lines, which results will be shown in the next phase of Experiments.

Therefore, the masking PNA directed against miR-145-5p is able to inhibit biological activity of miR-145-5p through two mechanisms of action: (a) direct interaction to the miR-145-5p binding sites of the 3'UTR of the CFTR mRNA and (b) interferences with miR-145-5p accumulation. These data are of interest because are a proof-of-principle that targeting biological functions of miRNAs might be considered to increase CFTR content, with possible applications in the personalized therapy of cystic fibrosis [Cholon et al., 2017].

With respect to different molecular and genetic bases of CF, it is expected that miR-145-5p masking will not be useful for CFTR defects of types I (no protein), II (no traffic), or III (no function). In contrast, increase of CFTR levels is expected to be useful for CFTR defects of types IV (less function), V (less protein), and VI (less stable protein). In any case, combined therapy using the miRNA-masking approach with read-through molecules and splicing correctors might be proposed. For a possible translation to therapeutic approaches for CF, our data are just a proof-of-principle and limited in their application potential. Therefore, screening of PNAs targeting the binding sites of these miRNAs, identification of the most active molecules, and combined treatments using the more efficient inhibitor molecules should be considered in order to reach CFTR increases compatible with clinical effects.

Despite the fact that comparison between the anti-miR-PNA and PNA-masking approaches has not been done in parallel in this study, by comparing our results to those published by Fabbri et al. [Lutful Kabir et al., 2018], the PNA masking approach appears to be more effective than the anti-miR-PNA approach on the increase of CFTR. The fold increases of CFTR protein were 2- to 2.5-fold and 6- to 8-fold when the anti-miR-PNA [Fabbri et al., 2017] and PNA masking [Figure 4] approaches were employed, respectively, when the PNAs were used at 2 μM. Moreover, very low effects using anti-miR-145 PNA were obtained at lower concentrations (unpublished data), while the miR145-maskingPNA was active even when used at 0.5 μM. Comparison with other groups working with anti-miR-145 molecules cannot be performed because these groups employed other anti-miRNA molecules and cell lines [Dutta et al., 2019;].

In order to further validate this approach using a cell line mimicking CFTR molecular defects (the Calu-3 cell line carries “normal” non-mutated *CFTR Gene*s) this approach should be tested (a) using primary CFBE and (b) CFTR mutant cell lines, also in combination with personalized treatments depending on the CFTR mutations. In the case CFTR expression will be further increased by treatment with the miR145-maskingPNA, the translational value of the present study will be fully supported for the development of tailored pre-clinical protocols.

4A.4.9. Lack of effects on apoptotic and cell cycle stages of the miR145-maskingPNA on Calu-3 Cells

In these experiments Calu-3 cells were cultured for 72 h in the absence, in the presence of miR145-maskingPNA or with the apoptotic inducers Static combined to 10% dimethyl sulfoxide (DMSO). After this treatment, possible induction of apoptosis was analyzed. The Annexin V and Dead Cell assay was performed with **Muse** (Millipore Corporation, Billerica, MA, USA) instrument method, according to the instructions supplied by the manufacturer. This procedure utilizes Annexin V to detect phosphatidylserine (PS) on the external membrane of apoptotic cells [Brognara et al., 2014].The concentration of the STATIC was utilized same as the PNA.

The results shown in **[Figure 4.19]** were performed in order to verify whether miR145-maskingPNA was to some extent cytotoxic or not**.** In these experiments Calu-3 cells were cultured for 72 h in the absence, in the presence of miR145-maskingPNA or with the apoptotic inducers Static combined to 10% dimethyl sulfoxide (DMSO). The results obtained are shows in Figure 4.19 and demonstrate that apoptosis was not induced by PNAs targeting miR145-maskingPNA, whereas under the same conditions an increase of apoptosis was observed using Stattic. It proves the fact that PNA does not shows any cytotoxic effect.

After the treatment with miR145-maskingPNA, we also determine the cell cycle stages by using the "MUSE" instrument. As **[Figure 4.19] part B** shows that cells treated with masked PNA or non-treated did not show much difference and it validates that masking PNA does not show much cytotoxic activity or modulation during the treatment.

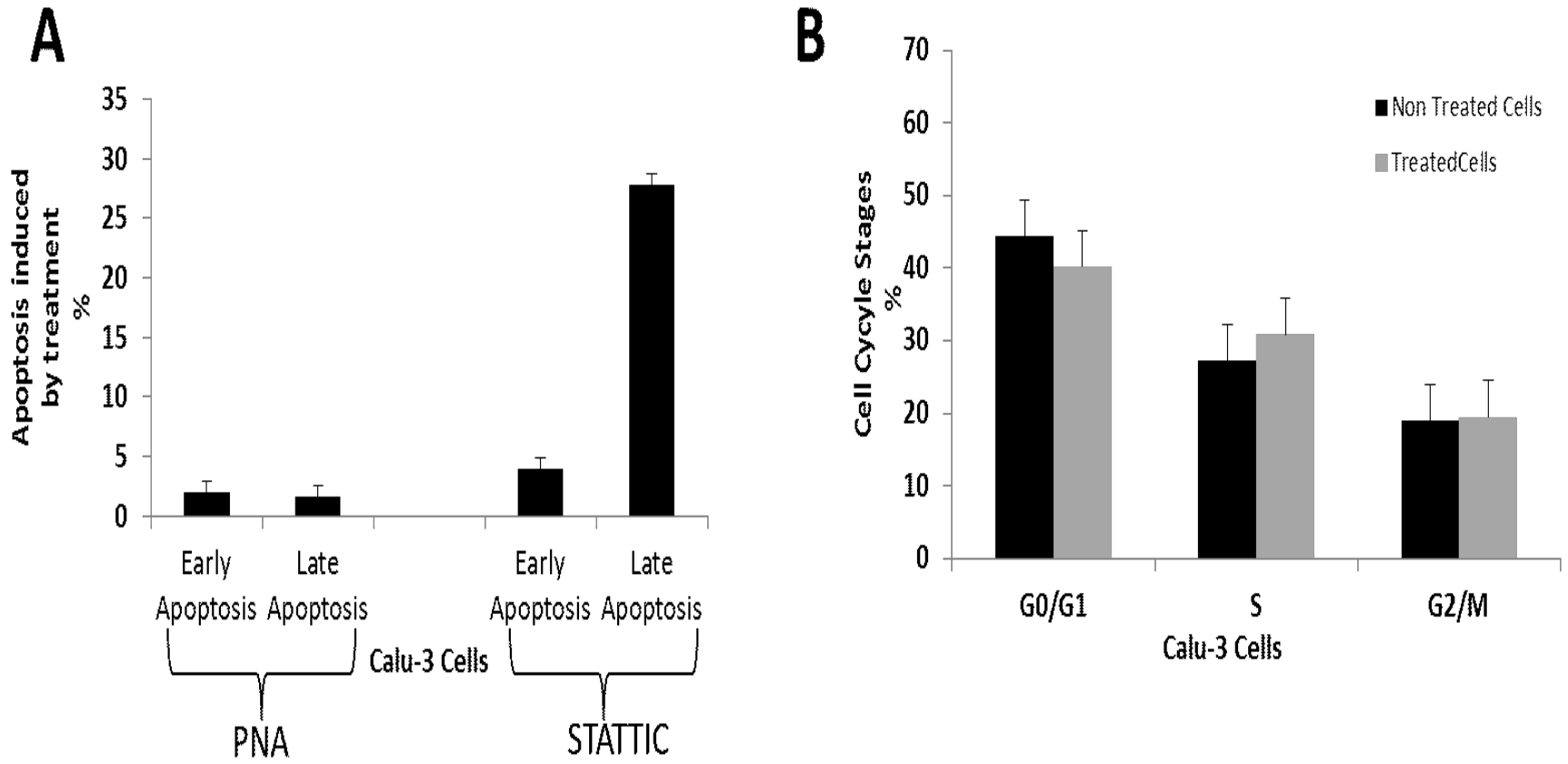

Figure 4.19: Effects of miR145-maskingPNA on apoptosis and Proliferation. (A) Effects of miR145-maskingPNA on apoptosis, when compared to the proapoptotic compound Static and PNA treated of Calu-3 cells. Apoptosis was determined by the Annexin V & Dead Cell Kit (Millipore Corporation).**(B)** Calu-3 cells were cultured in the absence or in the presence of miR145-maskingPNA different days and the cell number/mL determined.

The data presented in this study show that a PNA masking the miR-145-5p binding sites present within the 3'UTR of the CFTR mRNA is able to increase the expression of the miR-145-5p regulated CFTR. The increase of *CFTR Gene* expression was detectable at the level of mRNA (analyzed by RT-qPCR) and protein (analyzed by Western blotting).Further, assays on functional activity of the CFTR were also included in the present study and prove this study, our results could provide a proof-of-principle that miRNA masking might represent an efficient tool to increase CFTR content (possibly by increasing CFTR stability), with possible applications in the personalized therapy of CF.

We underline this approach and further validated (a) using primary CFBE and (b) on CFTR mutant cell lines in combination with personalized treatments depending on the CFTR mutations. In nutshell CFTR expression can be further increased by treatment with the miR145-maskingPNA, the translational value of the present study will be fully supported for the development of tailored pre-clinical protocols.

4A.5. Effects of miR145-Masking PNA on CFBE Cell line

CFBE41o- is a CF human bronchial epithelial cell line, derived from a CF patient homozygous for the ΔF508 CFTR mutation and immortalized with the origin-of-replication defective SV40 plasmid (pSVori-) (1,2). CFBE41o- displays all ion transport properties characteristic of cystic fibrosis such as defective cAMP-dependent chloride transport and intact calcium-dependent chloride transport. Under appropriate culture conditions, CFBE41o- forms tight junctions to give a polarized epithelium [Illek et al., 2008].

Name of Cells	Mutation in Genomic DNA CFTR gene	Plasmid with WT CFTR	Plasmids with F508del CFTR	YFP Plasmids
CFBE41o-WT CFTR	F508del/F508del	Yes (over-expression wild type CFTR), selectionantibiotic: puromycin	No	No
CFBE41o-F508del CFTR	F508del/F508del	No	Yes (over-expressionF508del CFTR) selection antibiotic: puromycin	No
CFBE41o-F508del CFTR YFP	F508del/F508del	No	Yes (over-expression F508del CFTR) selection antibiotic: puromycin	Yes, YFP selection antibiotic : geneticin, G418

Table 4.1: This Table shows the different types of CFBE cells, have been used in this study; following the various properties of these cells as indicated in this table.

4A.5.1. CFBE cells (CFBE-41o WT CFTR)

CFBE41o-WT CFTR is a cell line containing with mutation F508del/F508del and also comprises of plasmid (over-expression wild type CFTR), and it does not contain other plasmid with F508del and Plasmids YFP. In this cell line , we started the experiments for prove the fact that we can try various combination therapies and increase the CFTR content both with m-RNA level (Real time q-PCR) and protein level (Western Blotting). This could be decided on the level of mutation one is targeting in cystic fibrosis. In our study, we have

tried various combinations of masking PNA with Vertex compounds (Corrector VX-809 and Potentiator VX-770) and observed quiet supportive results to propose these personalize combinational strategies depending upon the patients.

4A.5.1.1. Experimental strategy

The experimental strategy is displayed in **[Figure 4.20]**. For this experiment, CFBE lines (CFBE-41o ΔF-508) cells were used for the treatment with miR145-Masking PNA, and vertex compounds (the correctors VX-809, and the potentiators VX-770,). 400,000 C/ml cells were used for 72 hours treatment with the masking-PNA in petri plates and for 48 hours with vertex compounds. The concentration of miR145-Masking PNA varies from 1 to 2 μM in different experiments and 5uM concentration of VX-809 and VX-770 compounds. Treated cells were trypsinized and collected by centrifugation at 1500 rpm for 10 min at 4 ◦C, washed with PBS, lysed with Tri-Reagent. The isolated RNA was washed once with cold 75% ethanol, dried and dissolved in nuclease free pure water before use.

After that, protein exactions were performed and samples were prepared for western blotting. During the whole process some cells were separated to perform cell viability and apoptotic assays. In the end, RNA and protein samples were used to further analyse the PNA-a145 effects by Real time PCR and protein effects by western blotting.

Finally, CFTR functional analysis was also done to verify the effects of these different combinational therapies to check the CFTR functionality. For CFTR functional analysis, CFBE-YFP F508del cells were employed in multiwells plated. As these plates were previously treated with appropriate coating (extracellular matrix containing fibronectin / vitrogen / BSA), in the amount of 30,000 cells per well and subsequently, after 24 h of treatment with PNA masking mir 145, were transferred to slides with a diameter of 25 mm, previously treated with the coating. Finally, after adhesion, the cells were pre-incubated for 24 hours with the compounds VX809 and VX770.

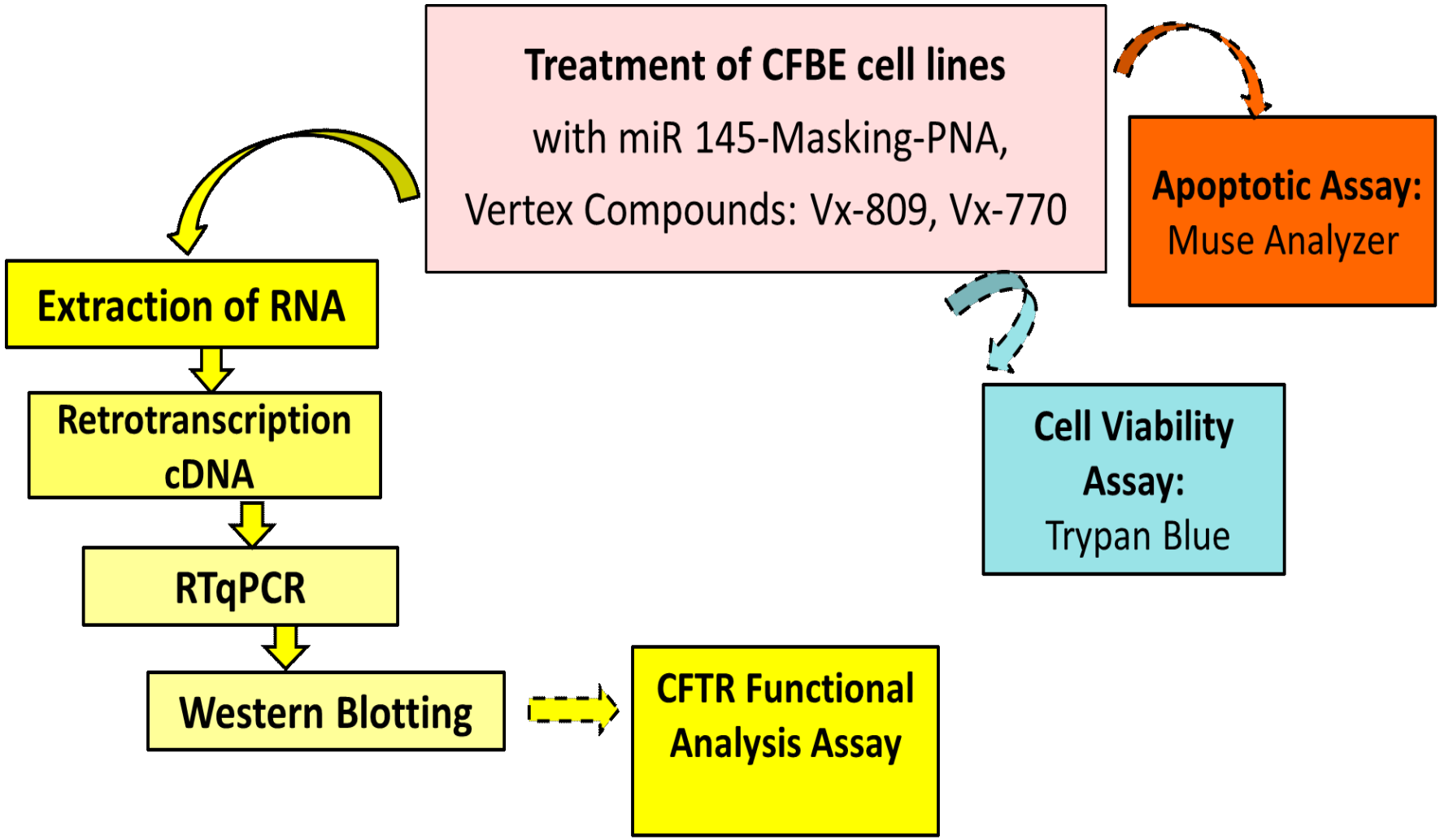

Figure 4.20. Experimental strategy for Masking-PNA-a145-5p. In this experiment CFBE-41o ΔF-508 and other variants of CFBE cells were used and given treatment with mentioned PNA (72 Hr.) and vertex compounds like Vx-809 and Vx-770 (48Hr.) .Following RNA extraction and then further Q-PCR and western blotting was done. Cell viability assay and antiprolifratic activity was also checked. In the end CFTR functional analysis was done to verify the CFTR gene results.

4A.5.1.2. Effects of combined treatments with the miR145-maskingPNA and the Vertex compounds in CFBE-41o WT CFTR

In this part of the study, we have used vertex compounds of two different types. One (Lumacaftor) is also known as VX-809 is a CFTR corrector, while the other (Ivacaftor), known as VX-770, is a CFTR potentiator. These compounds are known to correct the ΔF-508 mutation or potentiate the CFTR protein content by unblocking the CFTR channels in cystic fibrosis. The first of such agents to be introduced was Ivacaftor (VX-770), which increases the open probability (i.e. gating) of CFTR channels at the cell surface (i.e. potentiates CFTR) [Griesenbach et al., 2015; Deeks et al., 2013; Van et al., 2009]. In patients with cystic fibrosis homozygous for the mutation, Ivacaftor reduced sweat chloride levels slightly (suggesting some improvement in CFTR activity), although did not improve lung function [Flume et al., 2012], indicating that a potentiator alone is not enough to rescue this mutant protein. Thus, agents capable of correcting the defective processing/trafficking of mutant CFTR proteins like F508del are of great interest.

One such correcting agent is lumacaftor (VX-809). Like ivacaftor, lumacaftor appeared to have little respiratory benefit in patients homozygous for F508del when given in combination with standard therapies, despite dose dependently reducing sweat chloride levels [Clancy et al., 2012]. Any F508del CFTR rescued by lumacaftor may therefore need to be potentiated at the cell surface in order to function well enough to provide clinical improvements. Based on this rationale, a fixed-dose tablet combining lumacaftor with ivacaftor (OrkambiTM) was developed and is now indicated in various countries, including the USA [18] and those of the EU [http://www.ema.europa.eu/], for the treatment of patients with cystic fibrosis homozygous for the F508del-CFTR mutation. This narrative review focuses on pharmacological, therapeutic efficacy and tolerability data relevant to the use of lumacaftor/ivacaftor in this indication (for which the recommended dosage is two 200/125 mg tablets every 12 h [http://www.fda.gov/, http://www.ema.europa.eu/]).

4A.5.1.3. Combined treatment of CFBE-41o WT CFTR cells with the miR145-maskingPNA, VX-809 and VX-770.

In the first preliminary experiments**, [Figure 4.21]** CFBE-41o WT CFTR cells were grown in petri plates with 5uM Lumacaftor VX-809 and Ivacaftor VX-770, used singularly or in combination for 48 hours. After the treatment cells were collected from petri plates and further used for RNA and protein extraction. Then RNA was used for check the level of

CFTR m-RNA level and its relative content was also calculated in figure 4.26 part c. It can be seen that compared to control only cells, the cells with combination of 809 showed to increase the CFTR level content and while with combination of 770 CFTR level rather than increasing it inhibited the CFTR content. It can also be supported by literature [Flume et al., 2012]. While, the protein was used to perform the western blotting and in **[Figure 4.21, B and C]** it can be seen that protein content also enhanced with the combination of vertex compound (VX-809 and VX-770). While, their protein content is also calculated and only the combination of both molecules and only 809 molecule has proved to be effective in this experiment.

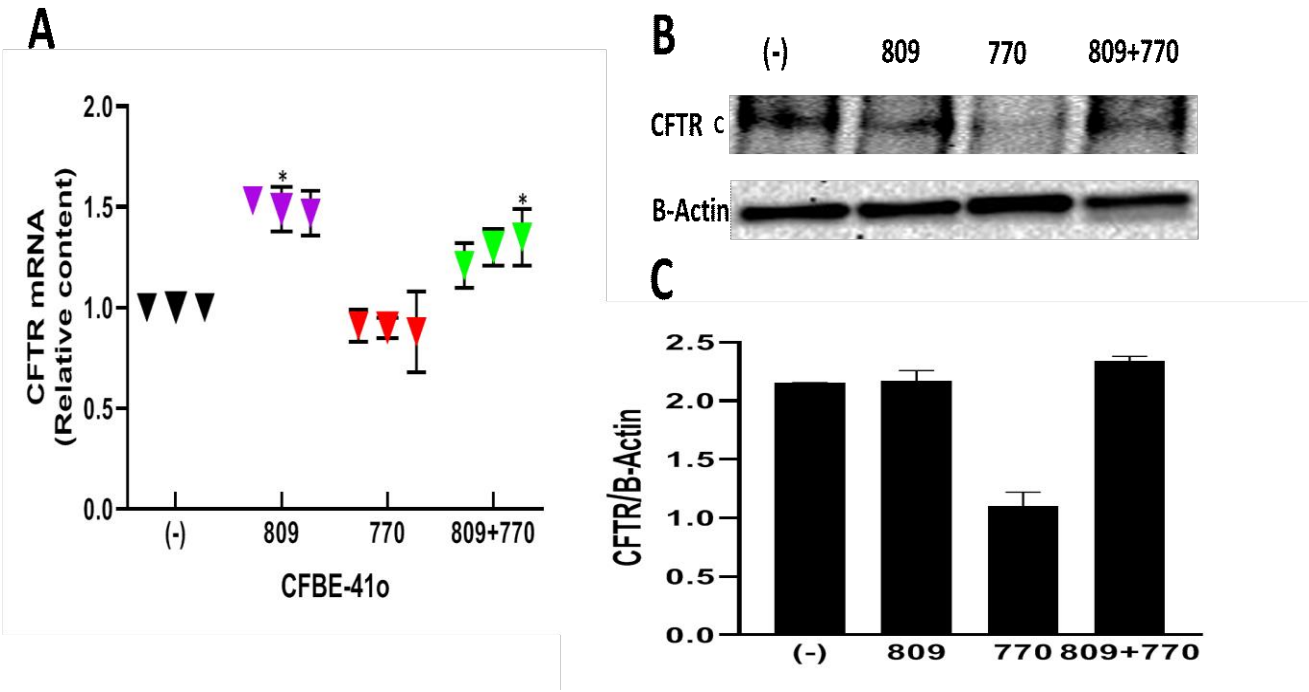

Figure 4.21: CFBE-41o WT cells with vertex compounds. (A) Upregulation of CFTR mRNA (RT-qPCR treated for 48hr with VX-809 and VX-770 (5 μM) **(B)** Western blotting with cells only, and vertex compounds in combination (5 μM, as indicated); **(C)** In panel quantitation of the CFTR/β-actin ratios are shown and were obtained by densitometry analysis of the Western blotting of (Band-C) with a molecular weight 170-180 kDa shown in panel. The obtained results are presented as average ± standard deviation (S.D.) obtained in at least three independent experiments. * = $p < 0.05$; ** = $p < 0.01$.

As shown in, **[Figure 4.22]** entails that CFBE-41o WT CFTR cells were grown in petri plates with 5uM quantity of Lumacaftor VX-809 and Ivacaftor VX-770 and in combination for 48 hours and miR145-maskingPNA in the quantity of 1uM and 2uM for 72 hours. . After the treatment cells were collected from petri plates and further used for RNA and protein

extraction. Then RNA was used for check the level of CFTR m-RNA level and its relative content was also calculated in [Figure 4.24 part c]. In that case combination of miR145-maskingPNA and VX-809 at 2uM and 1uM concentration proved to be quiet efficient in increasing the CFTR m-RNA level .So it shows that masked PNA quantity based increase can be useful for future personalized based therapies in treating the Δ508 based mutations in cystic fibrosis. It can also be seen that compared to control only cells, the cells with combination of 809 showed to increase the CFTR level content and while with VX-770 CFTR m-RNA level rather than increasing it inhibited the CFTR content. It can also be supported by literature [Flume et al., 2012].

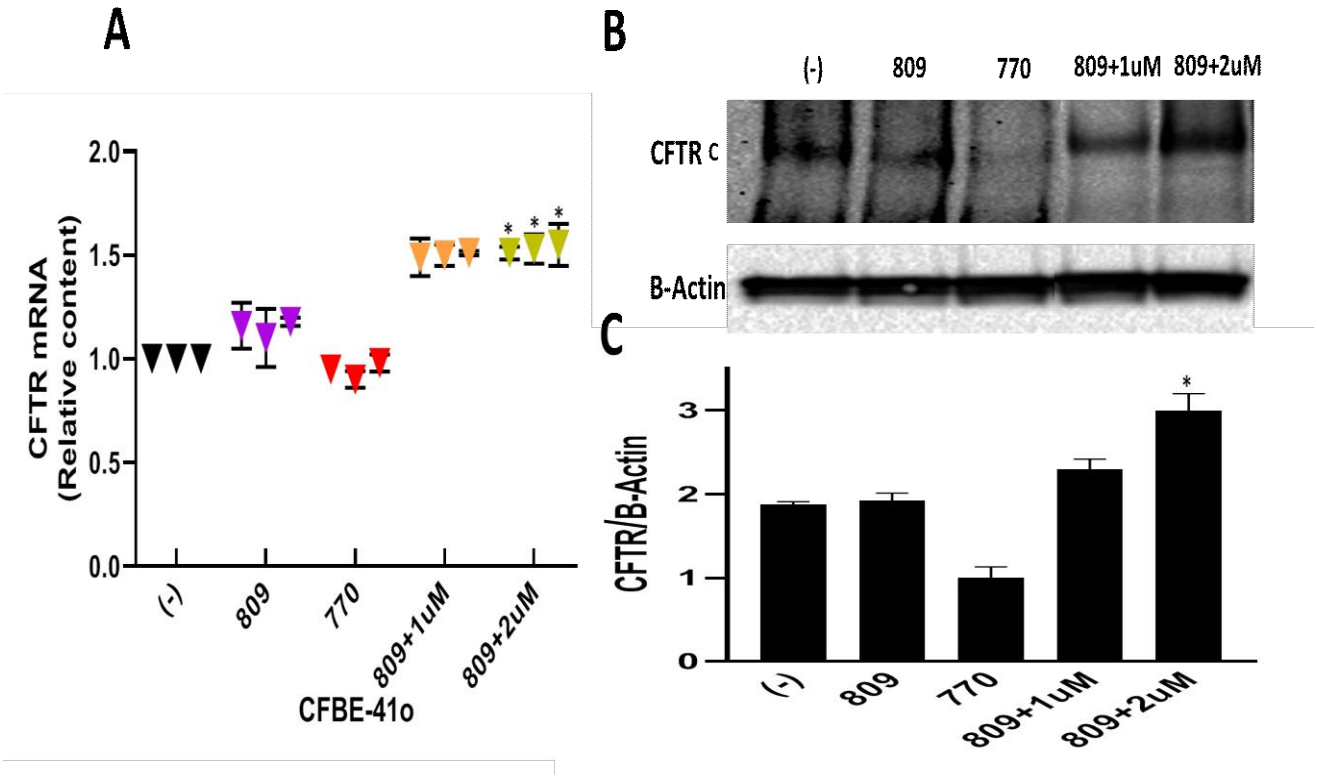

Figure 4.22: CFBE-41o WT cells with vertex compounds and miR145-maskingPNA. (A) Upregulation of CFTR mRNA (RT-qPCR treated treated for 48hr with VX-809 and VX-770 (5 μM) and miR145-maskingPNA (1uM , 2uM) **(B)** Western blotting with cells only, miR145-maskingPNA (1uM , 2uM) and vertex compounds in combination (5 μM, as indicated); **(C)** In panel quantitation of the CFTR/β-actin ratios are shown and were obtained by densitometry analysis of the Western blotting of (Band-C) with a molecular weight 170-180 kDa shown in panel. The obtained results are presented as average ± standard deviation (S.D.) obtained in at least three independent experiments. * = $p < 0.05$; ** = $p < 0.01$.

While, **[Figure 4.22, B and C]** western blotting shows that protein content also enhanced with the combination of vertex compound and miR145-maskingPNA (VX-809 and PNA 1uM and 2uM). The most effective combination proved to be in this experiment was 2uM of

PNA and VX-809 and its protein content was also increased from 1 to 3 in quantity. Further, their protein content is also calculated and only the combination of both V-809 and PNA in different quantity and only VX-809 molecules has proved to be effective in this experiment also. While, VX-770 again showed no efficacy in alone and proved to be ineffective once used in the alone and effective once used in the combination either with miR145-maskingPNA in different quantities and with VX-809.

Literature also proves that FDA-approved pharmaceutical modulators (Correctors and Potentiators) can restore function to mutant CFTR; however, optimal therapy and effective personalized medicine may require combinations of CFTR correctors with adjunct therapies. In literature, we found a potentiating effect of TSBs (Target site blockers) on CFTR modulators that enhance Phe508del-CFTR function. CF BECs transfected with TSBs potentiated the anion permeability effects of Ivacaftor/Lumacaftor [De santi et al., 2020]. The TSBs work by blocking the binding of miR-145-5p and miR-223-3p to specific sites in the CFTR30 UTR and specifically target CFTR expression at the post-transcriptional level rather than via transcriptional upregulation of CFTR [Viart et al., 2015]. There is another report, which also provide the synergistic effect of specific miRNA binding site inhibition in combination with CFTR correctors, to enhance anion flux through F508del-CFTR. CF BECs display increased functionally active F508del-CFTR when treated with a combination of TSBs and CFTR modulators. These findings indicate a therapeutic value in selectively inhibiting the activity of specific miRNAs in CF BECs to potentiate the effectiveness of CFTR modulators. This is important because not only are miRNAs that regulate CFTR, but the proinflammatory CF lung milieu increases expression of CFTR-specific miRNAs, as shown here [Oglesby et al., 2013].

4A.5.2. CFBE cells (CFBE41o-ΔF508del CFTR)

CFBE41o- ΔF508del CFTR is a cell line containing with mutation F508del/F508del and also comprises of plasmid (over-expression ΔF508del CFTR), and it does not contain other plasmid with WT-CFTR and Plasmids YFP. This cell line was used for the experiments to prove the fact that we can try various combination therapies to correct and increase the CFTR content both with m-RNA level (Real time q-PCR) and protein level (Western Blotting) in mutated (ΔF508del) cell line. This could be decided on the level of mutation one is targetting in cystic fibrosis. In our study, we have tried various combinations of masking PNA with Vertex compounds (Corrector VX-809 and Potentiator VX-770) and observed quiet

supportive results to propose these personalize combinational strategies depending upon the patients.

4A.5.2.1. Combined treatment of CFBE41o-ΔF508del CFTR cells with the miR145-maskingPNA, VX-809 and VX-770

[Figure 4.23] describes and experiment in which CFBE-41o-ΔF508del CFTR cells were grown in petri plates with 2uM quantity of miR145-maskingPNA for 72 hours in alone . After the treatment cells were collected from petri plates and further used for protein extraction. Then protein was used for check the level of CFTR level and its relative content was also calculated in **[Figure 4.23 part B]**. In that case, miR145-maskingPNA proved to be quiet efficient in increasing the CFTR level. But it also support the fact that miR145-maskingPNA in the quantity of 2uM was quiet efficient increasing the CFTR protein level. So it shows that masked PNA quantity based increase can be useful for future personalized based therapies in treating the Δ508 based mutations in cystic fibrosis. It can also be seen that compared to control only cells, the cells with combination of 809 showed to increase the CFTR level content. While with VX-770 CFTR m-RNA level rather than increasing it inhibited the CFTR content as we have seen in the previous results that's why in these cellular line we preferred to use combination without VX-770. It can also be seen by literature [Flume et al., 2012].

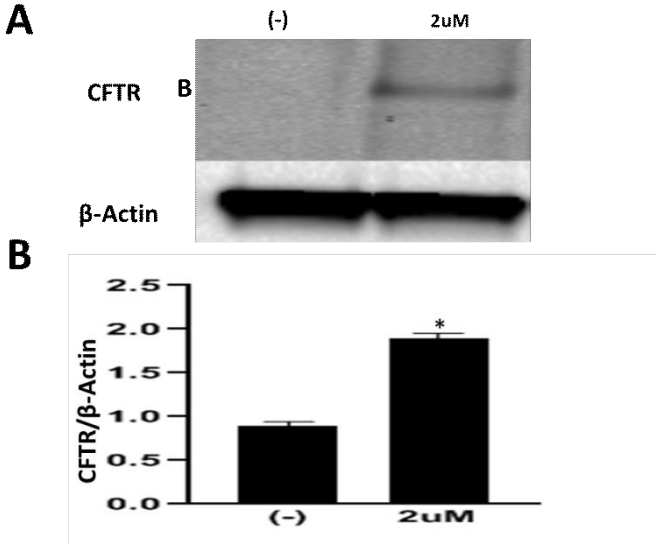

Figure 4.23 CFBE-41o ΔF508del CFTR cells with vertex compounds and miR145-maskingPNA at different combinations. (A) Western blotting with cells only, VX-809 (Corrector) and miR145-maskingPNA (1uM , 2uM) and vertex compounds in combination (5μM, as indicated); **(B)** In panel quantitation of the CFTR/β-actin ratios are shown and were obtained by densitometry analysis of the Western blotting of (Band-B) molecular weight 140kDa shown in panel. Results shown represent the

average ± standard deviation (S.D.) obtained in at least three independent experiments.* = $p < 0.05$; * ** = $p < 0.01$.

In **[Figure 4.24]**, CFBE-41o WT CFTR cells were grown in petri plates with 5uM quantity of Lumacaftor VX-809 and Ivacaftor VX-770 and in combination for 48 hours and miR145-maskingPNA in the quantity of 1uM, 2uM for 72 hours. After the treatment cells were collected from petri plates and further used for RNA and protein extraction. Then RNA was used for check the level of CFTR m-RNA level and its relative content was also calculated in [Figure 4.25]. In that case combination of miR145-maskingPNA and VX-809 at 2uM and 1uM concentration proved to be quiet efficient in increasing the CFTR m-RNA level. So it shows that masked PNA quantity based increase can be useful for future personalized based therapies in treating the Δ508 based mutations in cystic fibrosis. It can also be seen that compared to control only cells, the cells with combination of 809 showed to increase the CFTR level content and while with VX-770 CFTR m-RNA level rather than increasing it inhibited the CFTR content. It can also be supported by literature [Flume et al., 2012].

Western blotting results shown in **[Figure 4.24, B and C]** suggest that protein content also enhanced with the combination of vertex compound and miR145-maskingPNA (VX-809 and PNA 1uM and 2uM). The most effective combination proved to be in this experiment was 2uM of PNA and VX-809 and its protein content was also increased from 1 to 3 in quantity. Further, their protein content is also calculated and only the combination of both V-809 and PNA in different quantity and only 809 molecules has proved to be effective in this experiment also. While, VX-770 again showed no efficacy in alone and proved to be ineffective once used in the alone and effective once used in the combination either with miR145-maskingPNA in different quantities and with VX-809.

This is important because not only are miRNAs that regulate CFTR increased basally in CF BECs, but the proinflammatory CF lung milieu increases expression of CFTR-specific miRNAs, as we have shown here and elsewhere. This has also been demonstrated for miR-145-5p in CF BALF exosomes, where it was first reported that increased miR-145-5p nullifies CFTR correction by Ivacaftor/Lumacaftor [Lutful Kabir et al., 2018].

Previously, TSBs targeting unspecified miR-101 and miR-145 sites in the CFTR 3'UTR demonstrated increased CFTR expression and function in CF nasal epithelial cells [Viart et al., 2015]. However, there are five and eight sites each for miR-101-3p and miR-145-5p in

the CFTR 3'UTR as we have also shown various target binging sites in the preliminary results of this thesis with respect to different miRNA.

Further, it's important to understand that the intensity of the bands B and C in the CFBE41o-ΔF508del cells is variable depending on the experimental conditions as reported also by [Marozkina et al., 2010]. We found very low levels of bands B and C in untreated control CFBE41o-ΔF508del cells (see our results in figure **4.23, 4.24 and 4.25**), as found by other groups [Marozkina et al., 2010]. Furthermore, there can be some variations from one experiment to another, depending upon a number of factors like the exposure time of cells for a treatment, starting number of cells and image development exposure.

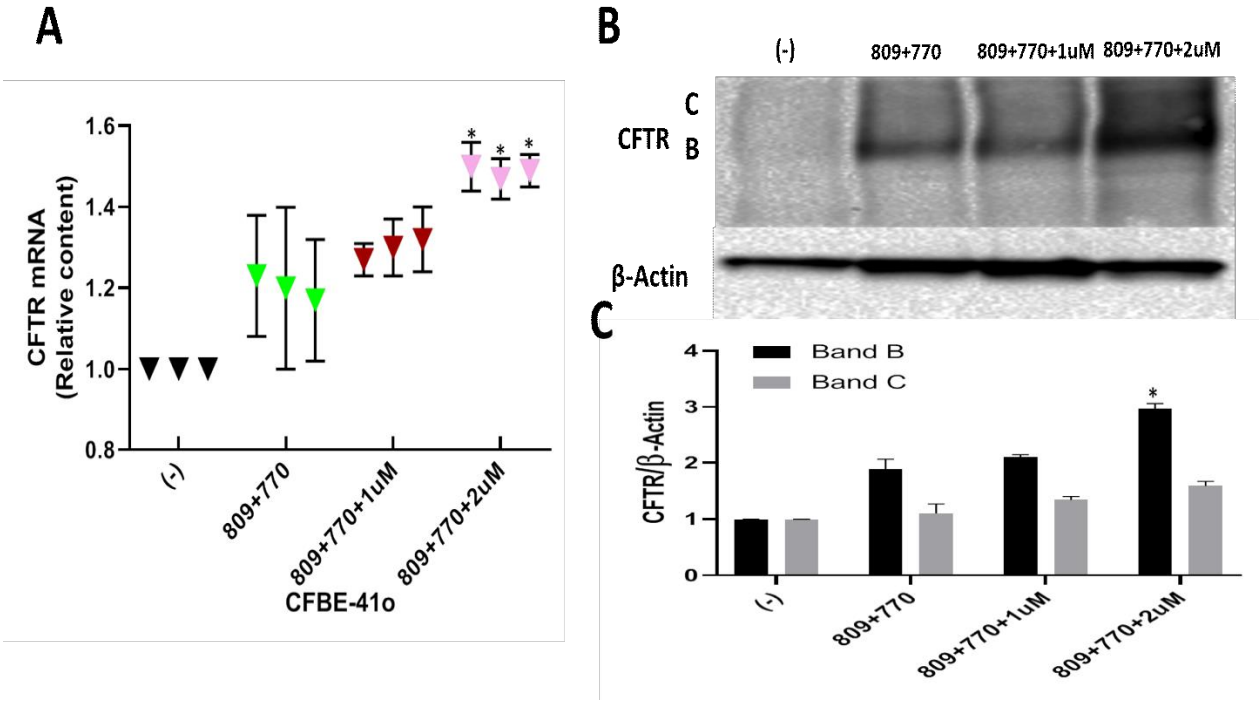

Figure 4.24: CFBE41o-ΔF508del cells with vertex compounds and miR145-maskingPNA with different combinations. (A) Upregulation of CFTR mRNA (RT-qPCR treated for 48hr with VX-809 and VX-770 (5 μM) and miR145-maskingPNA (1uM , 2uM) **(B)** Western blotting with cells only, miR145-maskingPNA (1uM , 2uM) and vertex compounds in combination (5 μM, as indicated); **(C)** In panel quantitation of the CFTR/β-actin ratios are shown and were obtained by densitometry analysis of the Western blotting of (Band-B and C) with molecular weight 140kDa and 170kDa shown in panel. Results shown represent the average ± standard deviation (S.D.) obtained in at least three independent experiments.* = $p < 0.05$; * ** = $p < 0.01$.

From literature study, we took into account not only these predicted binding sites but all other predicted binding sites for the lead miRNAs that have been demonstrated to regulate CFTR[De santi et al., 2020]. Ultimately, independently inhibiting two specific MREs was found to be most effective: the miR-145-5p site located at 298–305 and miR-223-3p at 166–

173 in De santi studies published in 2020. While in our study, we also have not only specified but also verified the miR-145-5p and miR145-maskingPNA target site to prove effective in CFTR targetting. Moreover, we validated these target MREs to be strongly inhibited by miR145-maskingPNA, since expected miR-494 and miR-223 and other miRs, respectively, were predicted to bind to CFTR 3'UTR with the highest binding affinity.

As shown in **[Figure 4.25]** Similarly, CFBE-41o-ΔF508del CFTR cells were grown in petri plates with 5uM quantity of Lumacaftor VX-809 in combination with miR145-maskingPNA for 48 hours and miR145-maskingPNA in the quantity of 1uM, 2uM for 72 hours. . After the treatment cells were collected from petri plates and further used for RNA and protein extraction. Then RNA was used for check the level of CFTR m-RNA level and its relative content was also calculated in [Figure 4.26 part a]. In that case combination of miR145-maskingPNA with VX-809 at 2uM and 1uM concentration proved to be quiet efficient in increasing the CFTR m-RNA level. So it shows that masked PNA quantity based increase can be useful for future personalized based therapies in treating the Δ508 based mutations in cystic fibrosis. It can also be seen that compared to control only cells, the cells with combination of 809 showed to increase the CFTR level content. While with VX-770 CFTR m-RNA level rather than increasing it inhibited the CFTR content as we have seen in the previous results that's why in these cellular line we preferred to use combination without VX-770. It can also be seen by literature [Flume et al., 2012].

The western blotting **[Figure 4.25, B and C]** shows that protein content also enhanced with the combination of vertex compound and miR145-maskingPNA (VX-809 and PNA 1uM and 2uM). The most effective combination proved to be in this experiment was 2uM of PNA and VX-809 and its protein content was also increased more than half in quantity. Further, their protein content is also calculated and only the combination of both V-809 and PNA in different quantity and only 809 molecules has proved to be effective in this experiment also. While, VX-770 has not been used alone because of its efficacy is validated in combination rather than alone so for this experiment, we used combination either with miR145-maskingPNA in different quantities and with VX-809.

This is important because not only are miRNAs that regulate CFTR increased basally in CF BECs, but the proinflammatory CF lung milieu increases expression of CFTR-specific miRNAs, as we have shown here and elsewhere. This has also been demonstrated for miR-

145-5p in CF BALF exosomes, where it was first reported that increased miR-145-5p nullifies CFTR correction by Ivacaftor/Lumacaftor [Lutful Kabir et al., 2018].

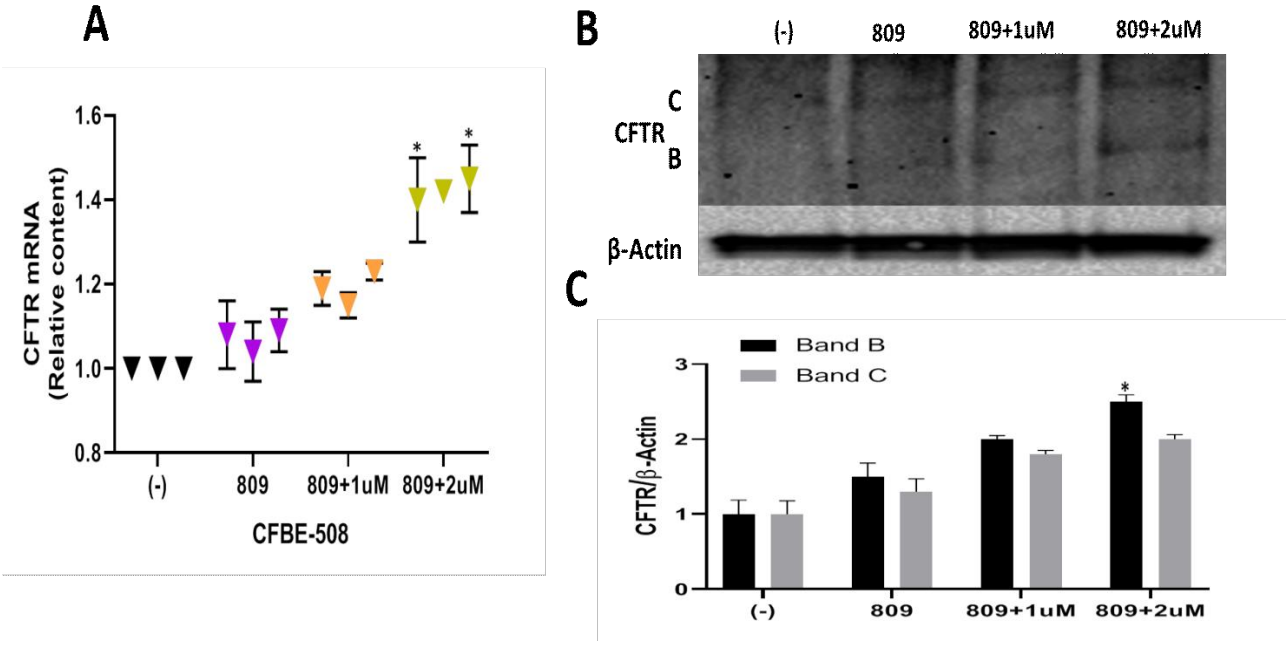

Figure 4.25: CFBE-41o ΔF508del CFTR cells with vertex compounds and miR145-maskingPNA at different concentration. (A) Upregulation of CFTR mRNA (RT-qPCR treated for 48hr with VX-809 (5 μM) and miR145-maskingPNA (1uM , 2uM) (B) Western blotting with cells only, VX-809 (Corrector) and miR145-maskingPNA (1uM , 2uM) and vertex compounds in combination (5 μM, as indicated); **(C)** In panel quantitation of the CFTR/β-actin ratios are shown and were obtained by densitometry analysis of the Western blotting of (Band-B and C) with molecular weight 140kDa and 170kDa shown in panel. The obtained results are presented as average ± standard deviation (S.D.) obtained in at least three independent experiments. * = $p < 0.05$; ** = $p < 0.01$.

Further, in western blotting **[Figure 4.25]** CFBE-41o-ΔF508del CFTR cells were grown in petri plates with 5uM quantity of Lumacaftor VX-809 in combination with miR145-maskingPNA for 48 hours and miR145-maskingPNA in the quantity of 1uM, 2uM for 72 hours in alone and also in combination. After the treatment cells were collected from petri plates and further used for protein extraction. Then protein was used for check the level of CFTR level and its relative content was also calculated in figure 4.30 part c .In that case combination of miR145-maskingPNA with VX-809 at 2uM and 1uM concentration proved to be quiet efficient in increasing the CFTR m-RNA level. But it also support the fact that miR145-maskingPNA only in the quantity of 2uM was also efficient increasing the CFTR protein level. So it shows that masked PNA quantity based increase can be useful for future personalized based therapies in treating the Δ508 based mutations in cystic fibrosis. It can also be seen that compared to control only cells, the cells with combination of 809 showed to increase the CFTR level content. it can be seen that protein content also enhanced with the

combination of vertex compound and miR145-maskingPNA (VX-809 and PNA 1uM and 2uM). The most effective combination proved to be in this experiment was 2uM of PNA and VX-809 and its protein content was also increased double the control in quantity. Further, their protein content is also calculated and only the combination of both V-809 and PNA in different quantity and only 809 molecules has proved to be effective in this experiment also. While, VX-770 has not been used alone because of its efficacy is validated in combination rather than alone so for this experiment, we used combination either with miR145-maskingPNA in different quantities and with VX-809.

4A.5.2.2. MiR145-maskingPNA enhances CFTR Modulator Effects on CFTR Activity in CFBE41o-ΔF508del CFTR

miR-145-5p levels are elevated in CF bronchoalveolar lavage fluid (BALF)-derived exosomes, [Lutful Kabir et al., 2018] and Pseudomonas-conditioned medium or interleukin-1b (IL-1b) can increase expression of miR-145 in CFBE41o cells [Oglesby et al., 2013] thereby likely decreasing CFTR expression in the inflamed CF lung milieu. Similarly, it can also be seen by [De santi et al., 2020] shows that CF BALF induces a similar effect by significantly increasing miR-145-5p expression in CFBE41o and CALU-3 cells. Thus, adjunct therapeutic targeting of the miR-145-5p sites in the CFTR 3'UTR with existing CF modulators could hold merit.

It can also be validated by our results **[Figure 4.23, 4.24 and 4.25]** that by targetting the miR-145-5p by our strategy of PNA masking one can achieve desired effects regarding the CFTR level both at CFTR mRNA level and protein content. It also paves the way for future strategies as we suggested in our results in the form of combinational therapies either use of miR145-maskingPNA in alone at different concentration or in combination with various vertex compounds like we suggested in our studies (Lumacaftor VX-809 and, Ivacaftor VX-770). These significant increases in the level of CFTR mRNA level and protein content by specifically targetting the binding site of target gene rather than all binding sites of mRNA. As in our thesis studies, we have not only differentiated two different strategies for increase of CFTR level by antisense and masking strategies.

Furthermore, it brings to attention the usage of these vertex compounds which already validated and in usage of cystic fibrosis patients at different levels. But with the combination of these molecular strategies not only we have shown in our studies significant increases level of CFTR protein by targetting the mIR-145-5p successfully. But still there are many

other miRs and binding sites available which can be used and target to design masking strategy to achieve target specific results. Target specific targeting the CFTR in 3'UTR region for miR-145-5p; miR-223-3p sites increased CFTR expression and anion channel activity and enhanced the effects of ivacaftor/lumacaftor CFBEs [De santi et al., 2020]

4A.5.2.3. With Vertex compounds and miR145-maskingPNA different combinations-RT-qPCR

In addition to that western blotting result, once we checked CFTR mRNA level in **[Figure 4.26]** Similarly, CFBE-41o-ΔF508del CFTR cells were grown in petri plates with 5uM quantity of vertex compounds (Lumacaftor VX-809 and Ivacaftor VX-770) in combination with miR145-maskingPNA for 48 hours and miR145-maskingPNA in the quantity of 1uM, 2uM for 72 hours in alone (2uM) and in combination also. After the treatment cells were collected from petri plates and further used for RNA extraction. Then RNA was used for check the level of CFTR m-RNA level and its relative content was also calculated in figure 4.31.In that case combination of miR145-maskingPNA with VX-809 at 2uM and 1uM and also alone miR145-maskingPNA in 2uM concentration proved to be quiet efficient in increasing the CFTR m-RNA level. So it shows that masked PNA quantity based increase can be useful for future personalized based therapies in treating the Δ508 based mutations in cystic fibrosis. It can also be seen that compared to control only cells, the cells with combination of 809 showed to increase the CFTR level content. While with VX-770 CFTR m-RNA level rather than increasing it inhibited the CFTR content as we have seen in the previous results that's why in these cellular line we preferred to use combination without VX-770. It can also be seen by literature [Flume et al., 2012].

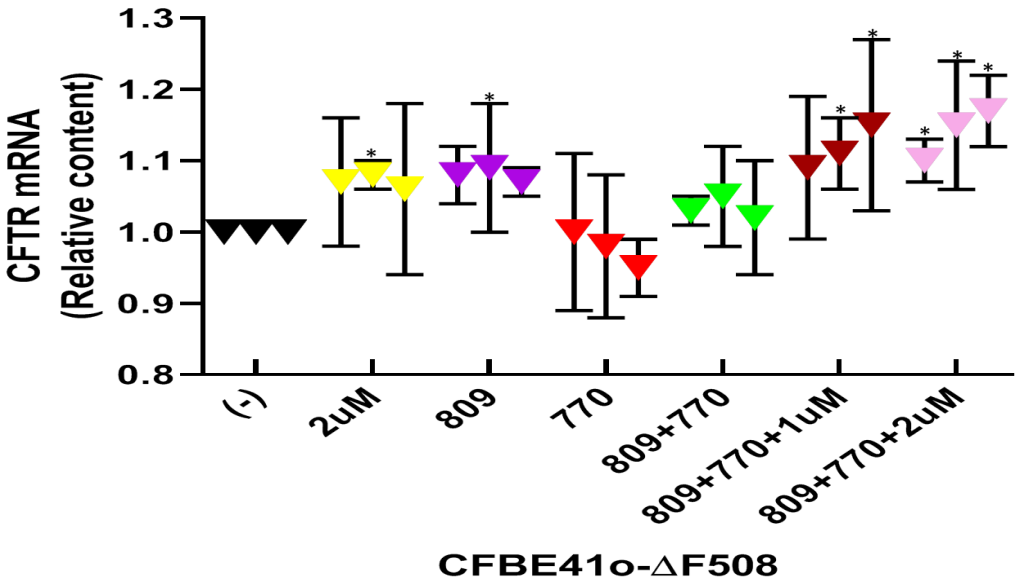

Figure 4.26: CFBE-41o ΔF508del CFTR cells with vertex compounds and miR145-maskingPNA with different combinations RT-qPCR; Upregulation of CFTR mRNA (RT-qPCR treated for 48hr with Vertex compounds (VX-770 and VX-809 (5μM) in 48 hr) and miR145-maskingPNA (1uM, 2uM 72 hr.) in combination and alone. Results shown represent the average ± standard deviation (S.D.) obtained in at least three independent experiments.* = $p < 0.05$.

4A.5.3. CFBE cells (CFBE41o-ΔF508del CFTR YFP)

CFBE41o-ΔF508del CFTR YFP is a cell line containing with mutation F508del/F508del and also comprises of plasmid (over-expression ΔF508del CFTR) and another plasmid (YFP), and it does not contain plasmid with WT-CFTR .This cell line, was important for us because same cell line was used in the end to perform CFTR functional analysis to prove the fact that CFTR channels activity was enhanced after relative treatments with different combinations .So we validated these cells to try various combinational therapies to correct and increase the CFTR content both with m-RNA level (Real time q-PCR) and protein level (Western Blotting) in mutated (ΔF508del) cell line. This could be decided on the level of mutation one is targetting in cystic fibrosis. In our study, we have tried various combinations of masking PNA with Vertex compounds (Corrector VX-809 and Potentiator VX-770) and observed quiet supportive results to propose these personalize combinational strategies depending upon the patients.

Similarly, CFBE-41o-ΔF508del CFTR YFP cells were grown in petri plates with 5uM quantity of Lumacaftor VX-809 in combination with miR145-maskingPNA for 48 hours and miR145-maskingPNA in the quantity of 1uM, 2uM for 72 hours both in alone and in combinations. After the treatment cells were collected from petri plates and further used for

RNA and protein extraction. It can also be seen that compared to control only cells, the cells with miR145-maskingPNA alone and in combination with 809 showed to increase the CFTR level content. While with VX-770 CFTR m-RNA level rather than increasing it inhibited the CFTR content as we have seen in the previous results that's why in these cellular line we preferred to use combination without VX-770. It can also be seen by literature [Flume et al., 2012].

This is important because not only are miRNAs that regulate CFTR increased basally in CF BECs, but the proinflammatory CF lung milieu increases expression of CFTR-specific miRNAs, as we have shown here and elsewhere. This has also been demonstrated for miR-145-5p in CF BALF exosomes, where it was first reported that increased miR-145-5p nullifies CFTR correction by Ivacaftor/Lumacaftor [Lutful Kabir et al., 2018].

4A.6. CFTR Functional Analysis.

In our study, the effects of the miR-145masking PNA were analyzed in combination with VX-809 and VX-770 on CFTR-dependent chloride efflux in CFBE41o- -YFP-F508del cells. CFTR-dependent chloride efflux was assayed by single cell fluorescence imaging analysis of YFP fluorescence quenching by iodide, stimulated by forskolin (20 μM), in the presence or absence of CFTRInh-172 (10 μM). Further, in figure 4.27 it represent a trace showing iodide influx in control conditions (vehicle), or after 48 hours incubation with 5 μM VX-809 with 5mM VX-770, or after 48 hours incubation with 5 μM VX-809 with 5mM VX-770 and 72 hours with 2 mM PNA masking mir-145; each point in the representative traces is the mean ± SEM of data coming from all cells in the field (5–10 cells).

As shown in **[Figure 4.27],** CFTR functional analysis (CFTR-dependent chloride efflux was assayed by single cell fluorescence imaging analysis of YFP fluorescence quenching by iodide) stimulated by forskolin (20 μM), in the presence or absence of CFTRInh-172 (10 μM) is a representative trace showing iodide influx in control conditions (vehicle), or after 48 hours incubation with 5 μM VX-809 with 5mM VX-770, or after 48 hours incubation with 5 μM VX-809 with 5mM VX-770 and 72 hours with 2uM PNA masking mir-145.

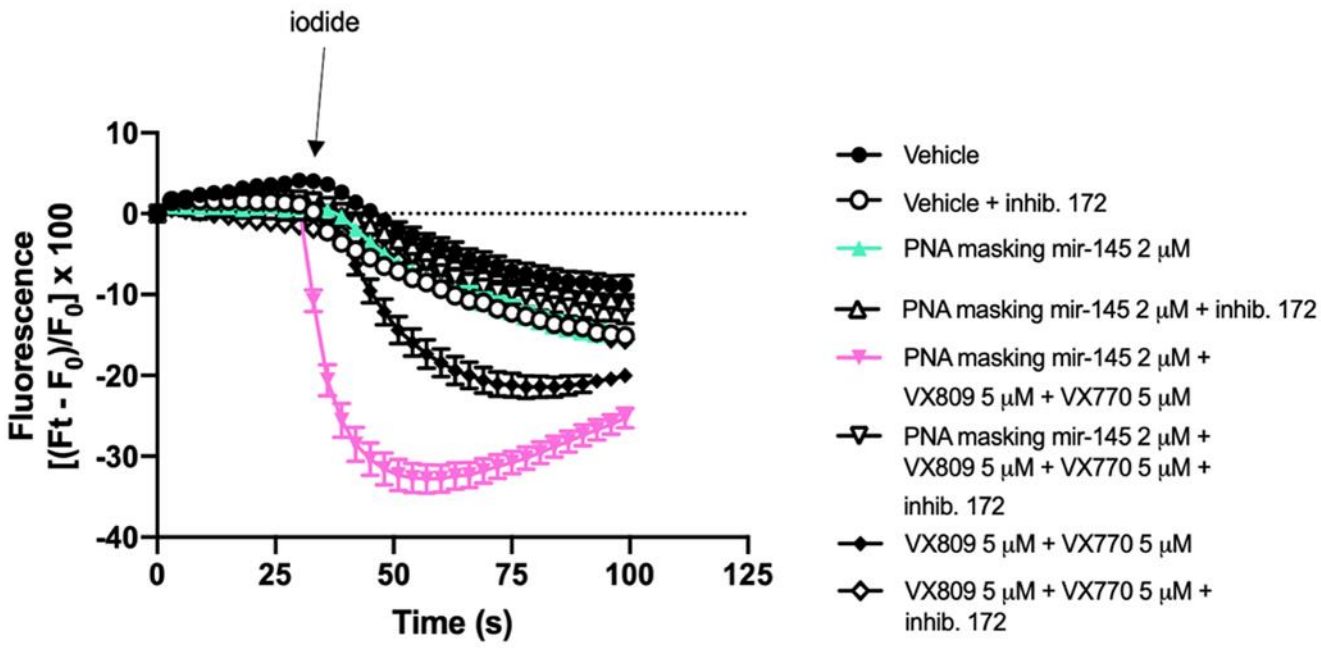

Figure 4.27: mIR-145masking PNA increases the effect of drugs combination VX-809 and VX-770 on CFTR-dependent chloride efflux in CFBE41o- -YFP-F508del cells. Representative trace showing iodide influx in control conditions (vehicle), or after 48 hours incubation with 5 μM VX-809 with 5mM VX-770, or after 48 hours incubation with 5 μM VX-809 with 5mM VX-770 and 72 hours with 2 mM PNA masking mir-145; each point in the representative traces is the mean ± SEM of data coming from all cells in the field (5–10 cells). Statistical comparisons were made using a nonparametric ANOVA test (* $p < 0.05$, ** $p < 0.01$, *** $p < 0.001$, and **** $p < 0.0001$).

CFTR activity under the different treatments, was assessed with the chloride-sensitive dye MQAE in the halide-sensitive YFP CFBE41o cells. All experiments were performed after stimulation of CFTR with 20 mM of forskolinn (FSK) ($n > 3$ per cell line, in triplicate) as elsewhere reported (De santi et al., 2020). Data are presented as background-corrected fluorescence values normalized for the initial fluorescence. Further, in **[Figure 4.28]** traces are represented showing iodide influx in control conditions (vehicle), or after 48 hours incubation with 5 μM VX-809 with 5mM VX-770, or after 48 hours incubation with 5 μM VX-809 with 5mM VX-770 and 72 hours with 2 mM PNA masking mir-145; each point in the representative traces is the mean ± SEM of data coming from all cells in the field (5–10 cells).

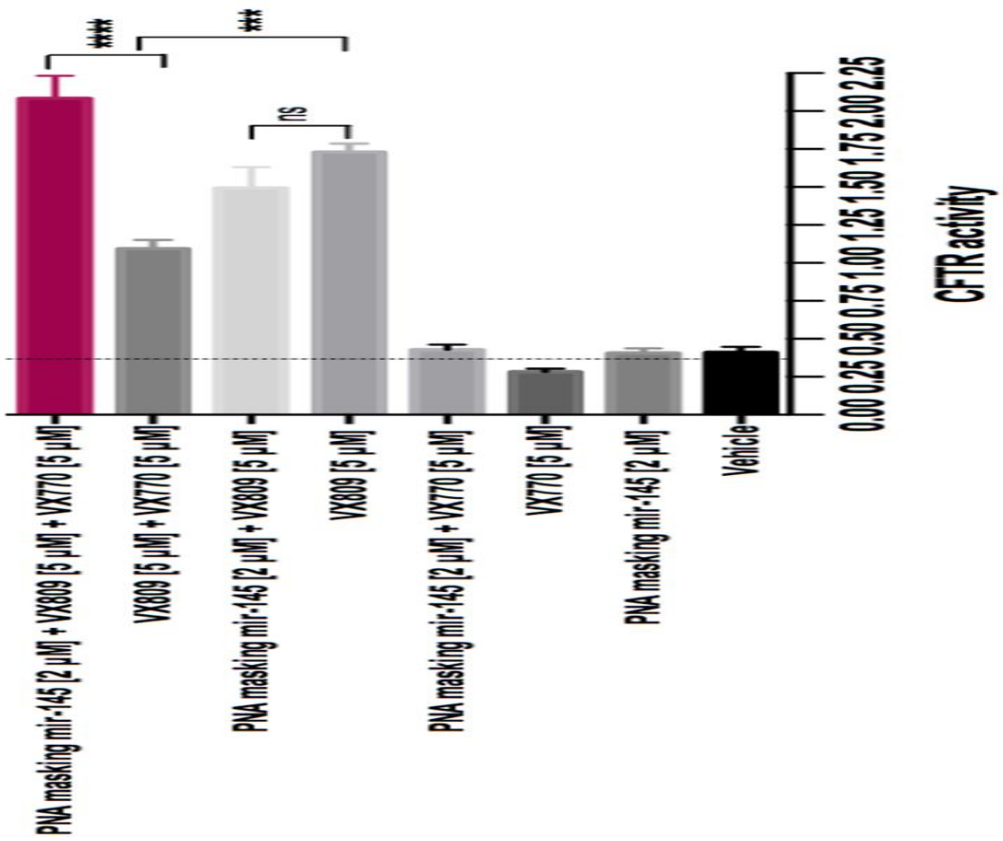

Figure 4.28: miR-145masking PNA increases the effect of drugs combination VX-809 and VX-770 on CFTR-dependent chloride efflux in CFBE41o- -YFP-F508del cells. The YFP fluorescence decay rate measured in each cell was calculated by fitting data of time courses by an exponential function, both in the absence and presence of CFTRInh-172. CFTR activity was obtained by subtracting the data of cells treated with CFTR inhibitor 172 from those of cells in the absence of the inhibitor. Each bar corresponds to the mean ± SEM of data points coming from at least three different experiments (5–10 different cells/each experiment). Statistical comparisons were made using a nonparametric ANOVA test (* $p < 0.05$, ** $p < 0.01$, *** $p < 0.001$, and **** $p < 0.0001$).

A summary of the results focusing on CFTR activity is shown in **[Figure 4.28]** which shows that the most effective combinations to rescue CFTR activity is represented by the combined treatments with miR-145masking PNA, VX-809 and VX-770.

There are some limitations to this study in CFTR functional analysis. It was not possible to perform all assays in all of the models used, and functional analyses other than CFTR were beyond the scope of the current work. The lack of an observable effect of the PNA masking mir-145 in bronchospheres due to poor transfection was disappointing and is a challenge that faces the entire field in the development of anti-sense oligonucleotide delivery using in vitro organoid models of disease [Bhise et al., 2010; Juliano., 2016].

4A.6.1. miR-145masking PNA increases the effect of drugs combination VX-809 and VX-770 on CFTR-dependent chloride efflux in CFBE41o- -YFP-F508del cells

As shown in [Figure 4.27], CFTR-dependent chloride efflux was assayed by single cell fluorescence imaging analysis of YFP fluorescence quenching by iodide, stimulated by forskolin (20 μM), in the presence or absence of CFTRInh-172 (10 μM). Representative trace showing iodide influx in control conditions (vehicle), or after 48 hours incubation with 5 μM VX-809 with 5mM VX-770, or after 48 hours incubation with 5 μM VX-809 with 5mM VX-770 and 72 hours with 2 mM PNA masking mir-145; each point in the representative traces is the mean ± SEM of data coming from all cells in the field (5–10 cells). The YFP fluorescence decay rate measured in each cell was calculated by fitting data of time courses by an exponential function, both in the absence and presence of CFTRInh-172. CFTR activity was obtained by subtracting the data of cells treated with CFTR inhibitor 172 from those of cells in the absence of the inhibitor.

4B. TARGETING miR-145-5p FOR KF4A UPREGULATION IN THE CONTROL OF GLOBIN GENE EXPRESSION FOR β-THALASSEMIA

4B.1. The PNA Masking Strategy on the erythroid K562 Cell line for regulation of *KLF4 gene* expression in β-thalassemia

In our studies, we have not only restricted PNA masking to cystic fibrosis but also tried to extend this strategy to other genetic disorder, such as β-thalassemia. For that purpose, we identified Krüppel-like factor (KLF4) as a very interesting gene to modulate; in fact up-regulation of this gene might be associated with upregulation of gamma-globin genes and increase of fetal hemoglobin (HbF9 which is a strategy to tackle β-thalassemia.

As a first point, we reasoned that it was important to identify for this target gene the miRNAs possibly involved in its regulation. For that purpose, we had to identify different MREs binding sites in the KLF4 mRNA. In this respect, [Na Xu et al., 2009] reported the miR-145 represses OCT4, SOX2, and KLF4. Similarly, [Jun ma et al., 2014] defined KLF4 as a direct and functional target of miR-152, which was involved in the miR-152-mediated tumor-suppressive effects.

In order to validate and describe possible effects of PNA masking in erythroid cells we had to identify the useful cellular model for our experimental strategy. In this respect, [Choong ML et al., 2006] reported microRNA expression profiling on ex vivo differentiating erythroid cultures derived from human umbilical cord blood (UCB) CD34 cells and K562 cells to identify miRNAs involved in erythropoiesis.

4B.2. Detection of miRs Binding Sites in 3'UTR of the KLF-4 mRNA

In our preliminary results, we identified various miRs and binding sites related to them, which could be further used to study and modify the *KLF4 gene* and related activities. **[Figure 4.29]**. Even though there are many miRNA binding sites in the 3'UTR of the KL4 mRNA, but out of all the available sites on the 3'UTR region we separated the highly similar binding sites by using the online software as explained in the material and methods section. This was done in order to identify the most interesting miRNAs to alter in their expression for upregulating KLF4.

In silico predictions using PITA identified all potential (MREs) miRNA mediated repressions for the lead miRNAs in the KLF4 3'UTR: miR-145-5p × 2 sites, miR-145-3p ×

1site, miR-7112-3p × 3 sites, miR-591 × 2 sites, miR 577 × 4 sites, miR-32-5p × 6 sites, miR-32-3p × 2 sites , miR-25-3p × 2 sites , miR-152-3p × 1 site by using the in silico studies. **[Figure 4.29]**. From this list, miR-145-5p and miR-152-3p target sites were selected in our study against which PNAs were designed with a highest DDG value higher than 20. (????). For these two miRNA binding sites two masking-LNA were designed. The efficacy of these LNAs on *KLF4 gene* expression was checked in K562 cell. Further, the efficacy of these PNAs at increasing KLF4-UTR was checked in K562 cell. It can also be seen from other studies of the literature that same analysis was done to check the various target miRs and to screen the required MREs for your target sites [De santi et al., 2020].

Moreover, the 3'UTR region of KLF4 mRNA is 899 bp long as one could see in **[Figure 4.29]**.It has several sites for the binding of multiple microRNAs. Further these microRNAs can bind multiple sites in the 3's UTR region and can be further classified depending upon their binding affinity with that binding site.

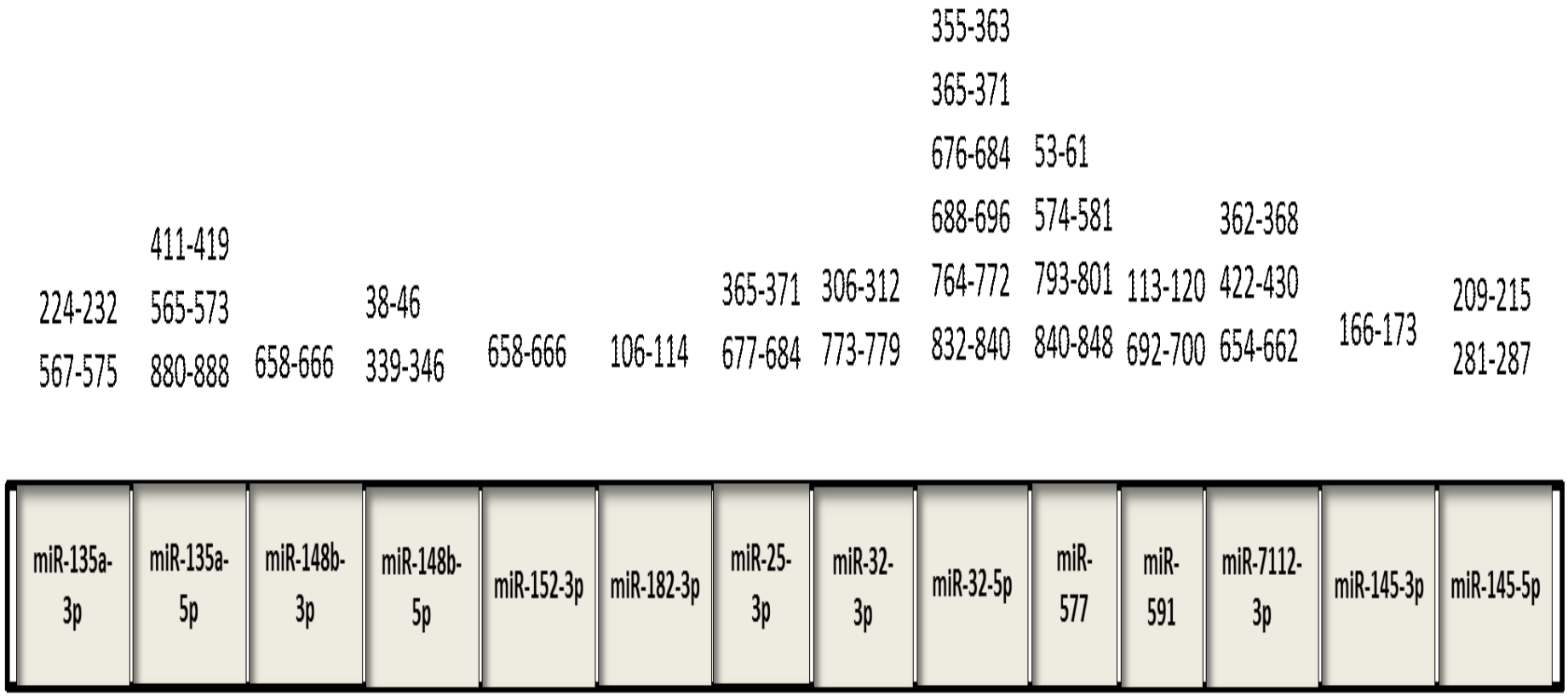

Figure 4.29: 3-UTR KLF4 region MREs, Region is 899 bp long, entails the 3-UTR KLF4 region and includes the all miRs binding sites present on the CFTR gene. It also shows the various binding sites present on this gene of various miRs. Theses miRs and the most conserved binding sites on KLF4 gene analysis was done by using the online software Tools4miRs.

4B.3. Interactions of the miR145-5p and miR-152-3p-masking LNAs with *KLF4 gene*

[Figure 4.30] shows the location of the miR-145-5p binding site **[Figure 4.30 A]** within the 3'UTR KLF4 mRNA sequence together with the extent of homology between the miR-145-5p and miR-152-3p binding sites and the respective miR145 and miR-152-masking LNAs. The design of the miR145-masking LNA, fully complementary to the miR-145-5p KLF4 mRNA binding site and the design of the miR152-masking LNA, fully complementary to the miR-152-3p KLF4 mRNA binding site **[Figure 4.30 B]**, was chosen in order to obtain an efficient competition between the microRNAs and the masking-LNAs for molecular interactions with the 3'UTR of KLF4 mRNA. In detail, the interaction between this miR145-masking LNAs and the KLF4 mRNA is expected to be much more efficient than the interaction between the miR-145-5p and KLF4 mRNA, since the KLF4 nucleotides complementary to the miR-145-5p are 7/18. On the other hand, the same miR145-masking LNA exhibits lower levels of complementarity to the miR-145-5p binding sites present in the 3'UTR of other mRNAs (data not shown). Similarly, the interaction between the miR152-maskingLNA and the KLF4 mRNA is expected to be much more efficient than the interaction between the miR-152-3p and the KLF4 mRNA, since the KLF4 nucleotides complementary to the miR-152-3p are 9/18. On the other hand, the same miR152-maskingLNA exhibits lower levels of complementarity to the miR-145-5p binding sites of other mRNAs (data not shown).

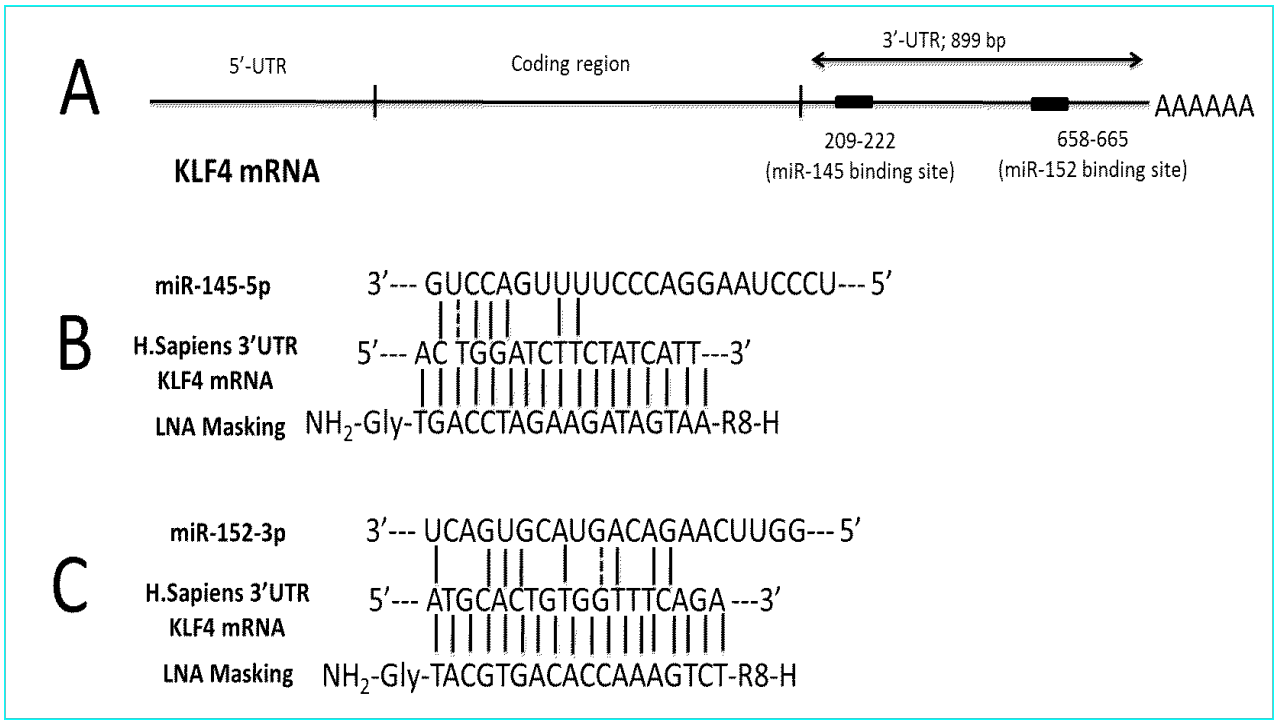

Figure 4.30: (A). Location of the miR-145-5p and miR152-3p binding sites within the Krüppel-like factor (KLF4) 3'UTR mRNA region**.(B).** Interactions between the miR145-maskingPNA and KLF4 mRNA (comparison with the interaction of KLF4 mRNA with miR-145-5p is also shown). **(C)** Interactions between the miR152-maskingPNA and KLF4 mRNA (comparison with the interaction of KLF4 mRNA with miR-152-3p is also shown)**.** Containing in the 3'UTR sequence three miR-145-5p binding sites. The miR145-maskingPNA and miR152-maskingPNA is fully complementary with the 3'UTR region of the KLF4 mRNA.

In our results, we have not only shown the interaction between miR145-maskingLNA and *KLF4 gene* but also Interaction between miR152-masking and other genes. Further, it also empowers the fact that the miR145 and miR152- maskingLNA are fully complementary with the 3'UTR region of the KLF4 mRNA (Figure 4.35, B and C of our results).

4B.4 Experimental strategy

The experimental strategy is displayed in **[Figure 4.36].** For this experiment, K562 cells were used for the treatment with the masking LNA-145-5p and LNA-152-3p. Cells were grown for 72 hours with two LNAs in petri plates. Cultured cells were collected by centrifugation at 1500 rpm for 10 min at 4◦C, washed with PBS, lysed with Tri-Reagent. The isolated RNA was washed once with cold 75% ethanol, dried and dissolved in nuclease free pure water before use. During the culturing period, cells were continuously collected in order to check the increase the proportion of hemoglobin-containing cells by using the benzidine assay.

Further, during the treatment of these cells with masking LNAs, we also used two representative HbF inducers (such as mithramycin, MTH and rapamycin, RAPA) in order to verify possible synergistic or additional effects of combined treatments. These were analyzed by the benzidine assay and RT-qPCR focusing on the expression of alpha- and gamma-globin genes.

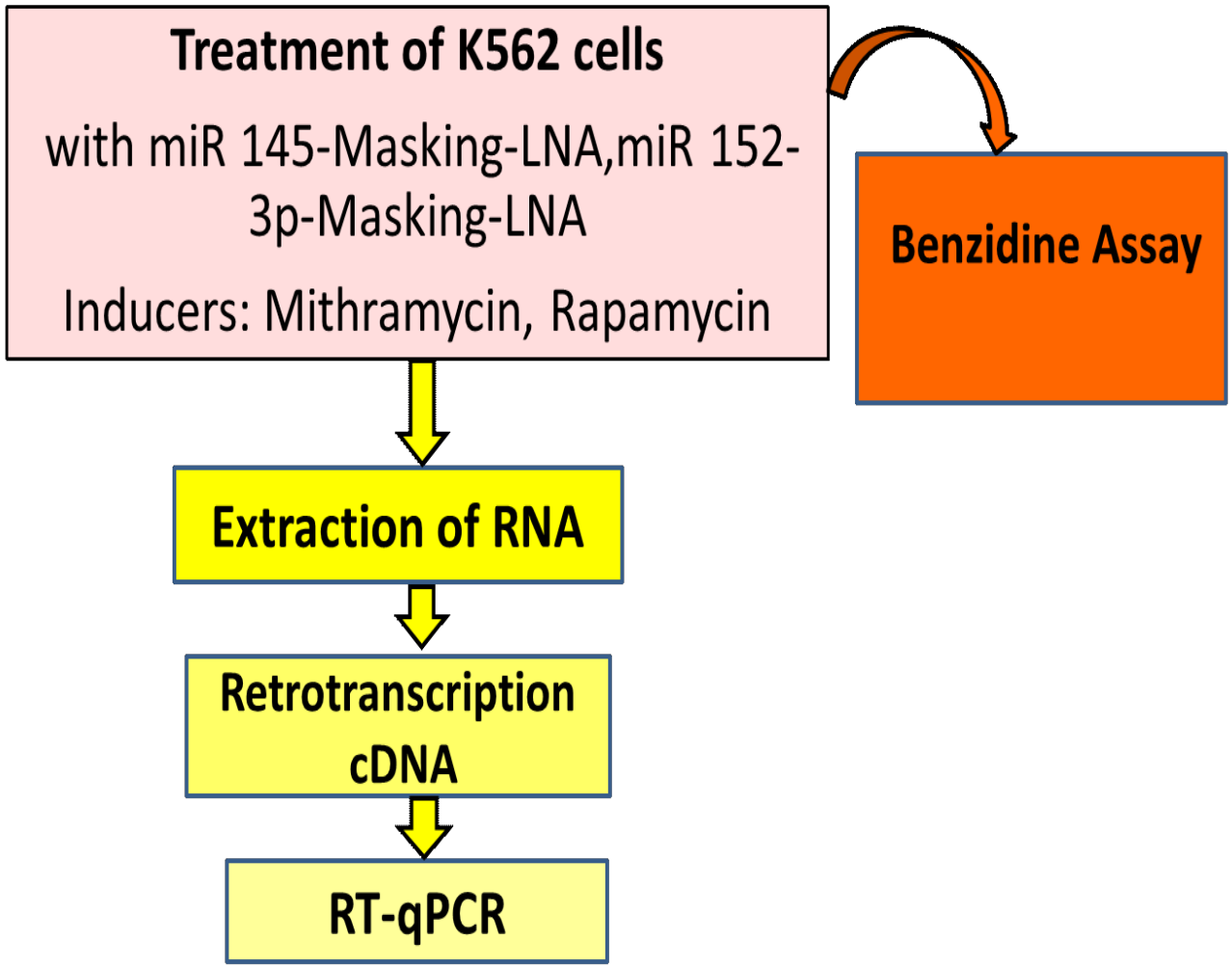

Figure 4.31: Experimental strategy for Masking-LNA-145-5p and LNA-152-3p. In this experiment K562 cells were used and given treatment with mentioned PNA (72 Hr.) and Gamma Globin inducers like Mithramycin and Rapamycin .Following RNA extraction and then further RT-qPCR was done. With that, also benzidine assay was also performed to check the positive hemoglobin containing cells.

4B.5. Effects of Masking LNA on KLF4-Gene Expression

In order to validate the masking LNA strategy performed on the 3'UTR KLF4 mRNA, the effects of the treatment on KLF4 mRNA were determined.

In the **[Figure 4.32]** RT-qPCR data are reported using biological samples from non-treated K562 cells and from K562 cells treated with the masked LNAs used singularly or in combination. The content of KLF4 mRNA was quantified and compared to the content of the internal control of beta-actin mRNA. The results obtained demonstrated that the treatment of K562 cells with the masking-145-5p-LNA and the masking-152-3p5p-LNA caused an KLF4 mRNA increase of about 35 and 58 folds, respectively. When as the two masking LNAs are used together the KLF4 mRNA increase was 70 fold.

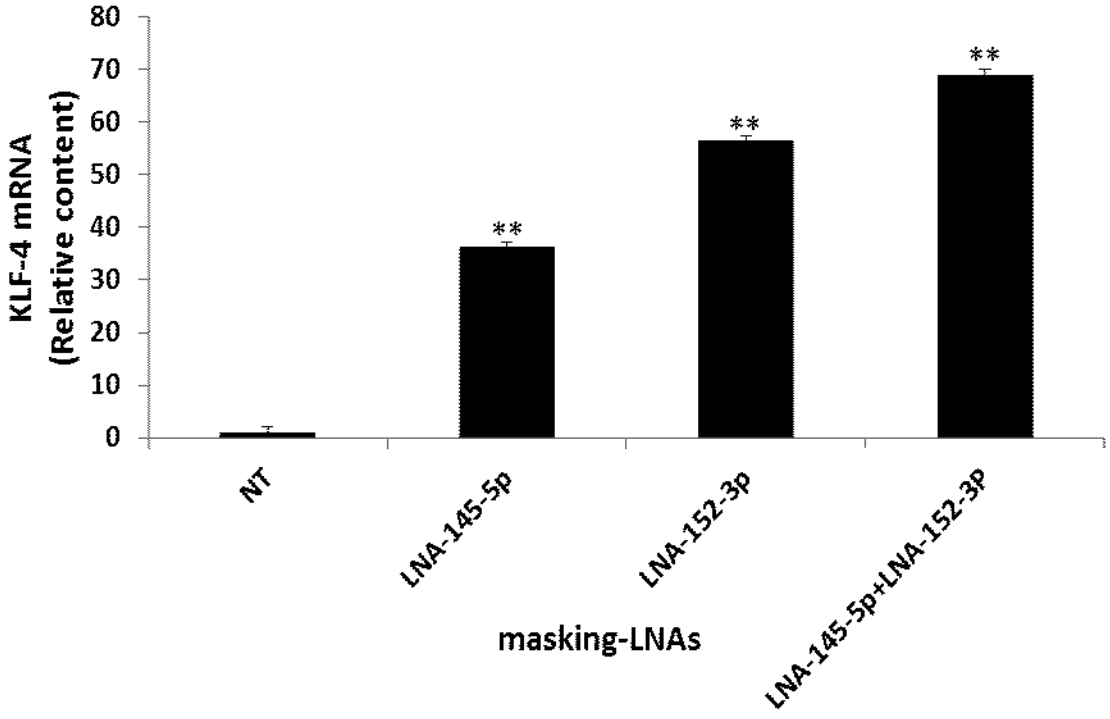

Figure 4.32: KLF-4 gene expression by RT-qPCR. In this figure, K562 cells were treated with the masking-145-5p-LNA and the masking-152-3p5p-LNA, as indicated. The RT-qPCR was performed using a beta-actin internal control and KLF4 primers with SYBR green mix. Results represent the average ± standard deviation (S.D.) obtained in at least three independent experiments.* = $p < 0.05$; * ** = $p < 0.01$.

4B.6. Treatment of K562 cells with masking-145-5p and masking-152-3p LNAs: effects on the proportion of hemoglobin containing benzidine-positive cells

The benzidine reaction has been extensively employed to measure hemoglobin production in human erythroleukemic (K562) cells stimulated to synthesize hemoglobin. Increments in hemoglobin concentration are associated to increase in the proportion of benzidine positive cells [Paul W. et al., 1981]. Cell viability was determined quantitatively by trypan blue exclusion. Cells were centrifuged at 250 x g for 3 mm at room temperature and washed 3 times in phosphate buffered saline (PBS). For detection of differentiated cells, 0.05 ml stock solution of benzidine reagent was added to 0.1 ml of cell suspension (5 x 10 cells) and left at room temperature with occasional gentle agitation, for a period of time sufficient to achieve maximal color development. A minimum of 40 cells were counted in a Neubauer bright line chamber in each experimental time points. The percent differentiation was based on a number of cells giving an unequivocally positive benzidine reaction, seen as intense blue cytoplasmic staining.

In the experiment shown in **[Figure 4.33]** cells were either not treated (NT) (panel A) or cultured with the masking-145-5p-LNA (B) and the masking-152-3p5p-LNA (C). For comparison, cells were also cultured with the erythroid inducers mithramycin (MTH) and rapamycin [RAPA]. From literature, it is known that MTH and RAPA are two potent HbF inducers of gamma-globin mRNA accumulation and fetal hemoglobin (HbF) production, one exhibiting DNA-binding activity (MTH) the other inhibiting mTOR.

The data obtained indicate that both masking-145-5p-LNA (B) and masking-152-3p5p-LNA (C) are inducers of erythroid differentiation (i.e. increase of the proportion of benzidine-positive K562 cells) being the induction efficiency (after 7 days treatment 25% and 50% higher than that exhibited by MTH and RAPA.

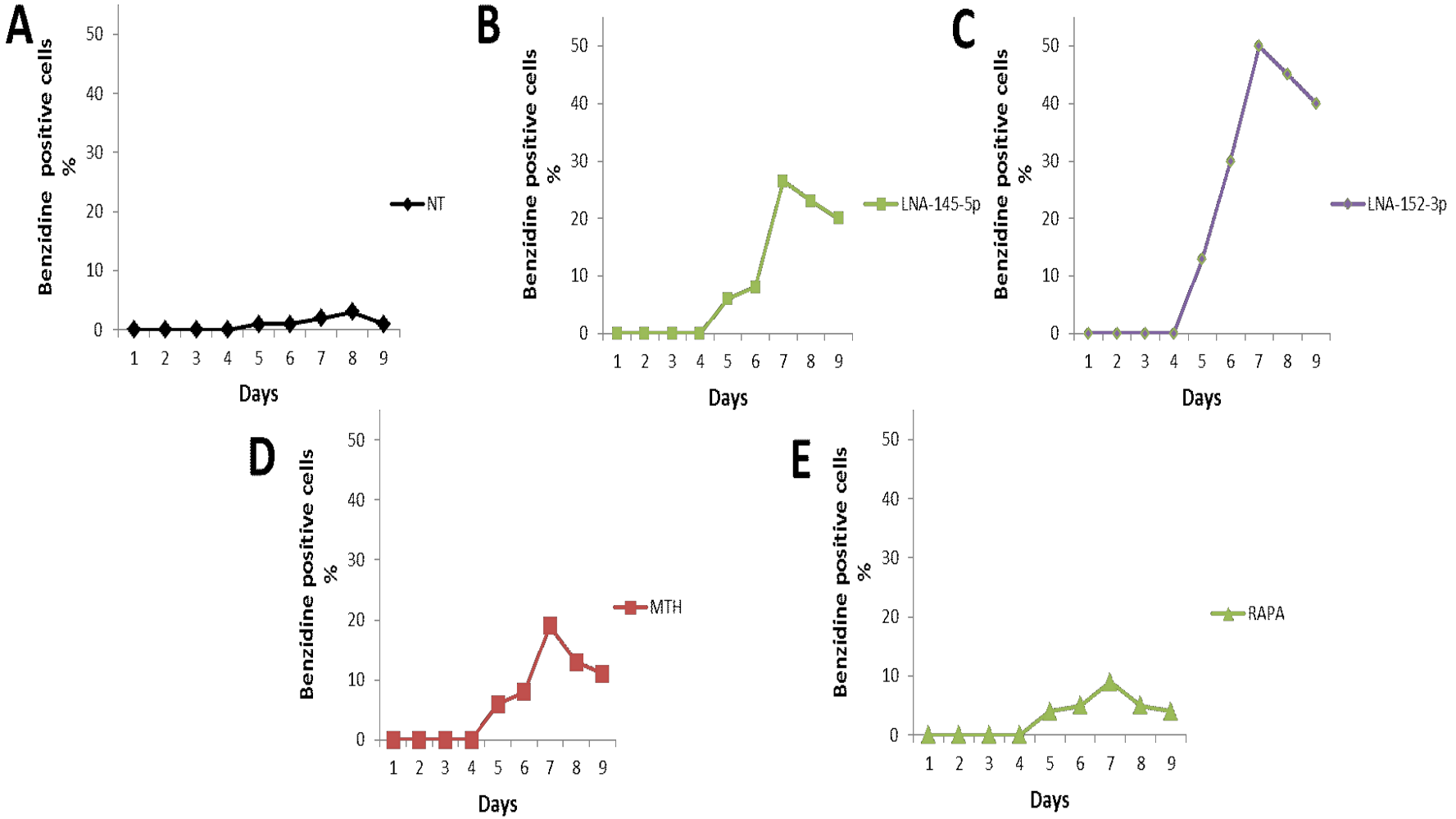

Figure 4.33: Benzidine assay Analysis results of various samples with out combinations. In this experiment K-562 cells were used and given treatment with mentioned LNAs and inducers as a alone. Following the 9 days of culturing these cells, cells were checked for any anti-proliferative activity. Further Benzidine assay was performed to check the increase of hemoglobin positive cells. As you can see in all A,B,C,D and E graphs that increase of hemoglobin positive containing cells is quiet different with respective to different inducers and masked miRs.

In part E of this figure only RAPA treated cells were used after 9 days culturing and further benzidine assay was performed to check either we get some hemoglobin +ve cells with the time passage, and cells showed increase of these cells more or less 10 percent as also one could understand that because rapamycin is a one of the inducers which acts as increase of these fetal hemoglobin +ve cells but it was not much. Further, as we investigate in the literature it showed that the induction of HO-1 expression by rapamycin and, more importantly, the effects of tin protoporphyrin, an inhibitor of HO activity, on the anti-proliferative actions of rapamycin suggest that the effects of rapamycin may be, at least less, modulated by its actions on HO-1 [Visner GA et al., 2003]

In part B and C three different masked LNAs were used as an alone inducer for its effectivity to induce the increase of +ve fetal hemoglobin cells. For example, in part B LNA-145-5p treated cells were used after 9 days culturing and further benzidine assay was performed to check either we get some hemoglobin positive cells with the time passage, and cells showed increase of these cells more or less 30 percent and it was quiet encouraging so , once checked in the part C of this figure with miR-32-5p treated cells were used after 9 days culturing and further benzidine assay was performed to check either we get some hemoglobin positive cells with the time passage, and cells showed increase of these cells more or less 15 percent.

Further, in **[Figure 4.34]** and in **[Figure 4.35]** we determined whether co-treatment of K562 cells with LNAs (the masking-145-5p-LNA and the masking-152-3p5p-LNA) and the HbF inducers (MTH and RAPA) was able to display additive effects of the proportion of benzidine-positive cells. This appears not to be the case, since the proportions of benzidine-positive cells in combined treatments were only slightly increased; in any case not exceeding the values obtained when the masking-145-5p-LNA and the masking-152-3p5p-LNA were used singularly (see Figure 4.38).

Finally, also when the masking-145-5p-LNA and the masking-152-3p5p-LNA were used in combination, additive effects on the proportion of benzidine-positive cells were undetectable, as shown in **[Figure 4.36]** in which comparison was made between K562 cells treated with the masking-145-5p-LNA (A), the masking-152-3p5p-LNA (B) and both masking-145-5p-LNA and masking-152-3p5p-LNA (C).

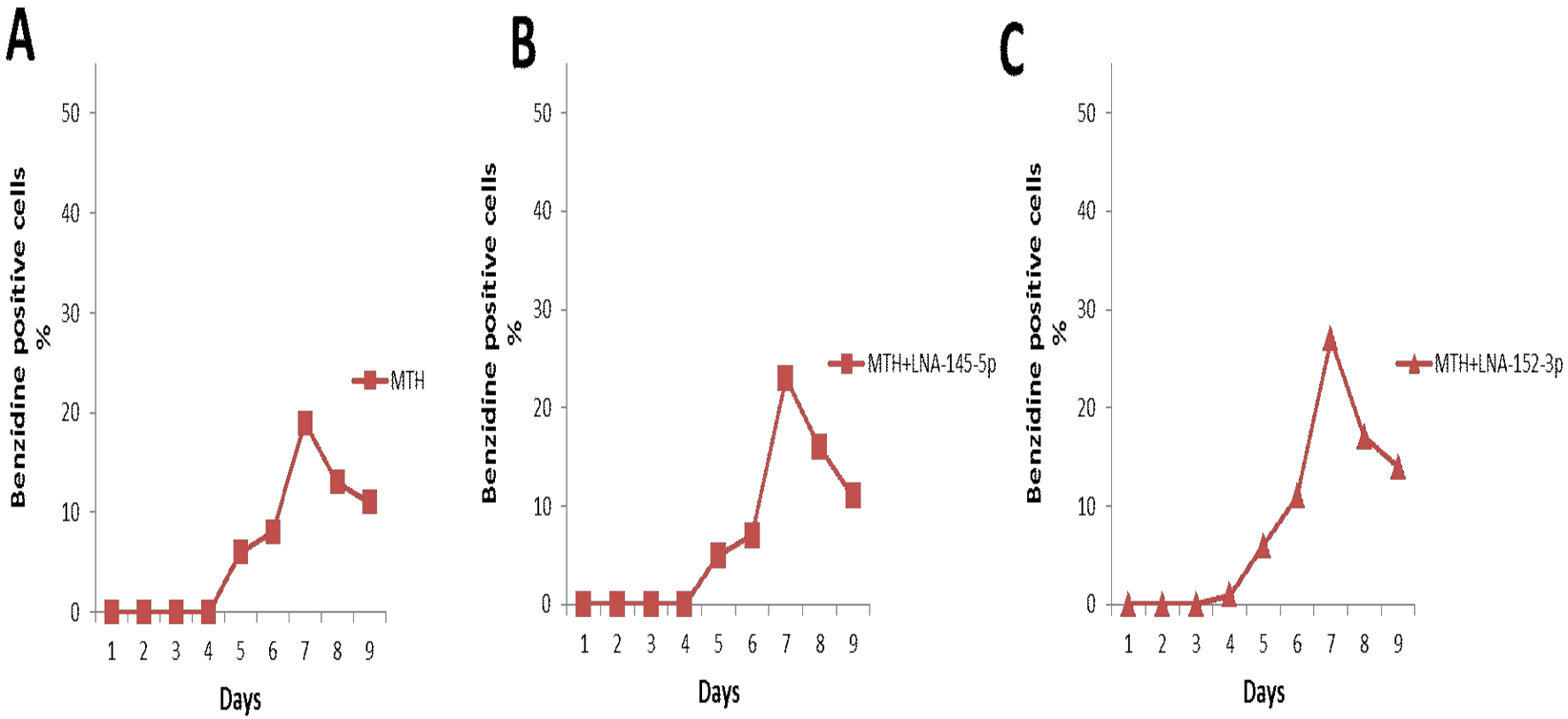

Figure 4.34: Benzidine assay Analysis results of MTH and its combinations. In this experiment K-562 cells were used and given treatment with mentioned MTM inducer and its combination with other masked LNAs. Following the 9 days of culturing these cells, cells were checked for any anti-proliferative activity. Further Benzidine assay was performed to check the increase of hemoglobin positive cells. As you can see in all A,B and C graphs that increase of hemoglobin positive containing cells is quiet different with respective to different combinations of MTM and masked LNAs.

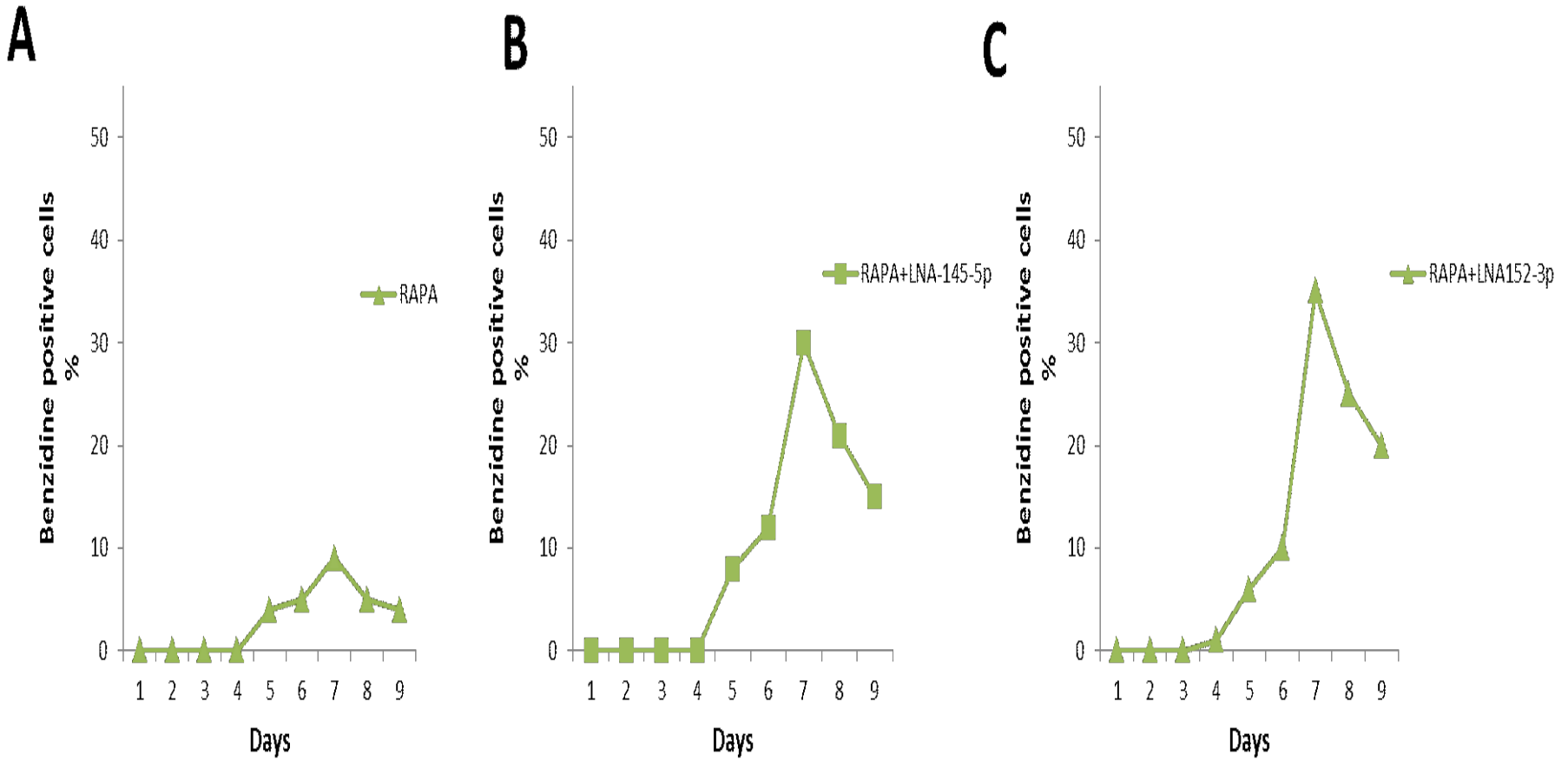

Figure 4.35: Benzidine assay Analysis results of RAPA and its combinations. In this experiment K-562 cells were used and given treatment with mentioned RAPA inducer and its combination with other masked LNAs. Following the 9 days culturing of these cells, cells were checked for any anti-proliferative activity. Further Benzidine assay was performed to check the increase of hemoglobin positive cells. As you can see in all A,B and C graphs that increase of hemoglobin positive containing cells is quiet different with respective to different combinations of RAPA and masked miRs.

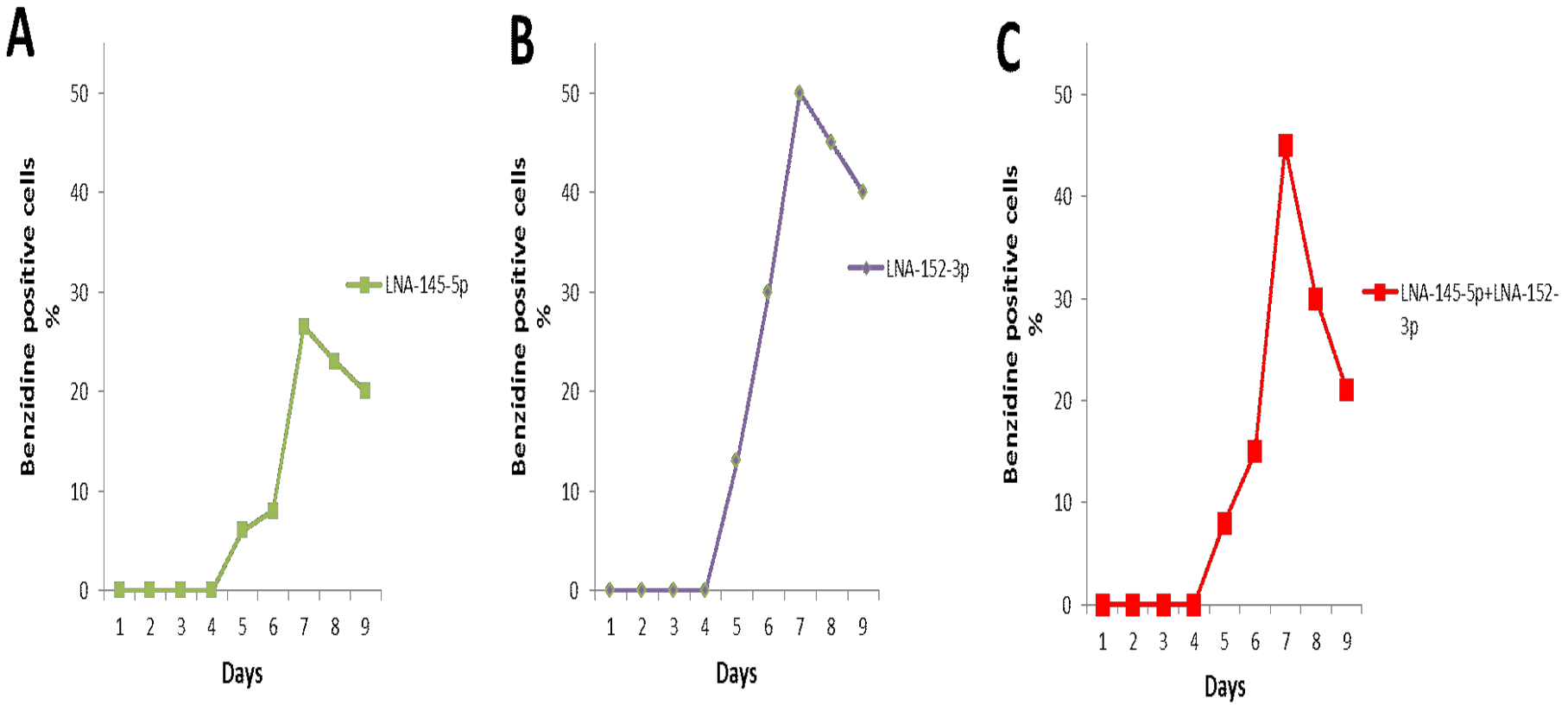

Figure 4.36: Benzidine assay Analysis results of Masked-LNAs and its combinations. In this experiment K-562 cells were used and given treatment with mentioned masked LNAs and its combination with other masked LNAs. Following the 9 days culturing of these cells, cells were checked for any anti-proliferative activity. Further Benzidine assay was performed to check the increase of hemoglobin positive cells. As you can see in all A,B and C graphs that increase of hemoglobin positive containing cells is quiet different with respective to different combinations masked LNAs.

4B.7. Effects of masking-145-5p-LNA and the masking-152-3p-LNA on γ-globin and α-globin mRNAs

The RT-qPCR showing the accumulation of γ-globin mRNA in K562 cells treated with masking LNAs (the LNA-145-5p and the LNA-152-2p) and the two HbF inducers MTH and RAPA, used singularly or in combination is shown in **[Figure 4.37].**

The data obtained show that after MTH, RAPA, LNA-145-5p and LNA-152-2p were all able to increase the expression of γ-globin genes, when comparison was made to untreated cells.

When treatment with LNA-145-5p and LNA-152-2p was combined with MTH or RAPA, the level of accumulation of γ-globin mRNA was higher than that obtained with singular treatments.

Interestingly, when LNA-145-5p and LNA-152-2p are used together the increase of γ-globin mRNA reached the maximum level in treated K562 cells.

A same trend (with some variations with respect to the data obtained with α-globin mRNA) was found when the RT-qPCR analysis was performed using PCR primers specific for the α-globin mRNA, as shown in **[Figure 4.38]**.

In our studies, once we tried to check the effects of these important α and γ globin chains by using masking strategy. There was quiet evident expression modification by using various combinations in our strategy. Further, it is also important to understand major modification at the human β-globin locus that can significantly reduce anemia and potentially cure human β-thalassemia is an increase in human γ-globin gene expression and restoration of HbF to therapeutically effective levels. Point mutations in the γ-globin gene promoter can increase γ-globin expression, but not by a great amount. By contrast, individuals with an uncommon, benign disorder known as hereditary persistence of fetal hemoglobin (HPFH) express γ-globin genes at the same level in adult life as in fetal life. Some HPFH homozygotes have only HbF and no anemia. If human β-thalassemia patients could reactivate their HbF production to that of HPFH patients, they would be cured. The mutations associated with HPFH are large deletions at the β-globin locus extending from the region close to the human Aγ gene to well downstream of the human β-globin gene and including deletion of the structural δ- and β-globin genes [Bank .A ., 2005].

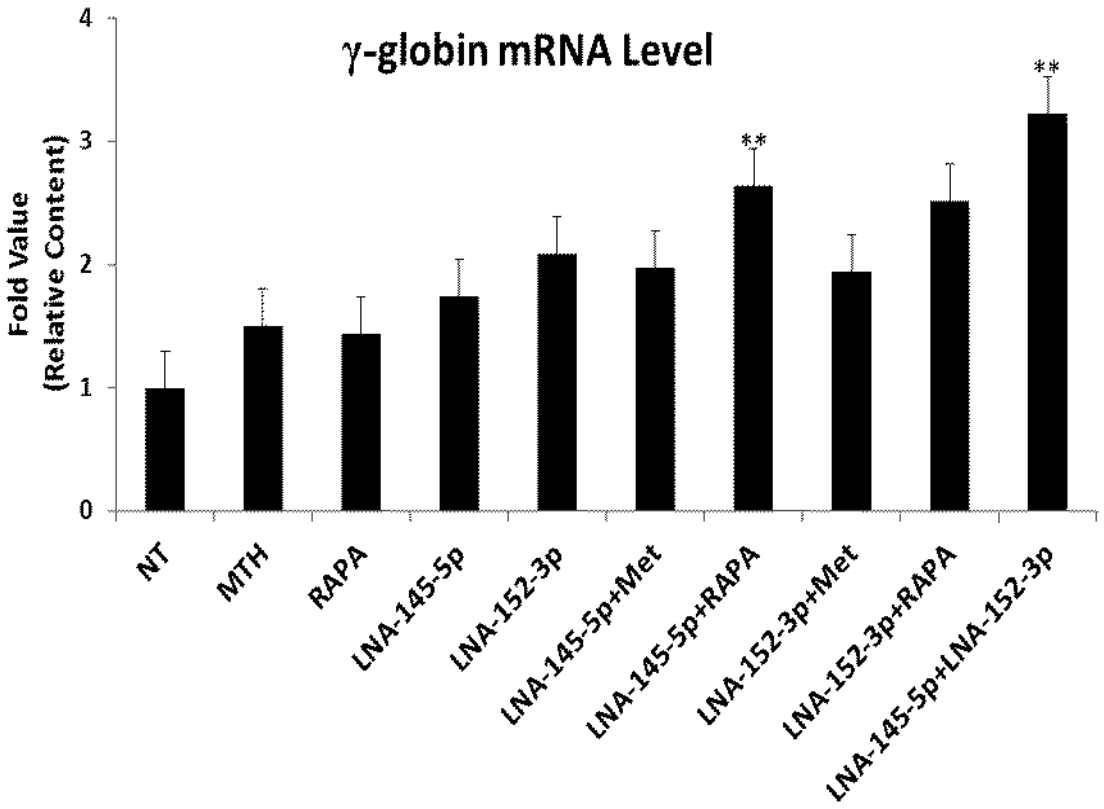

Figure 4.37: Gamma globin (γ) expression by Real time Q-PCR. In this figure, K562 cells were treated with various inducers like MTH (Methramycin) and RAPA (Rapamycin), further also with masked PNAs like 145-5p and 152-3p and their combinations. Evident from this figure that various combinations has really helped to increase the gamma globin level in K562 cells. Results shown represent the average ± standard deviation (S.D.) obtained in at least three independent experiments.* = $p < 0.05$; * ** = $p < 0.01$.

In **[Figure 4.38]** our studies has shown that after treating the K562 cells with various combinations of masking PNA has really increased the expression of α globin in K562 cells. In this figure once cells treated with inducers like MTM and RAPA, it also showed some increase in the level of alpha globin expression. While the only masked PNAs like 145-5p and 152-3p have shown quiet efficient increase in the level of alpha globin expression. But there was some modulation in the increase of these. But despite of that, we also tried various other combinations just to maximize our expression level in the presence of our specific masked PNAs.

Further, with the combinations of MTM and 145-5p, RAPA and 145-5p have shown the significant increase in alpha globin expression as compared to alone treatment of these inducers and masked PNAs. But the most efficient of all the combination was RAPA and 145-5p, and the increase of this combination was more than any other combination we used, Similarly with the combinations of RAPA and masked-PNA 152-3p, RAPA and masked-

PNA 152-3p have shown the significant increase in alpha globin expression as compared to previous combinations, but it was little bit less than the masked-PNA 145-5p and its combinations. But as a whole, the increase level of alpha globin expression was quiet higher than the gamma globin expression. Finally, once we tried the both of these masked PNAs (masked-PNA 152-3p and masked-PNA 152-3p) together and it was quiet evident that with this combination the level of increase in the expression of gamma globin was also quiet higher.

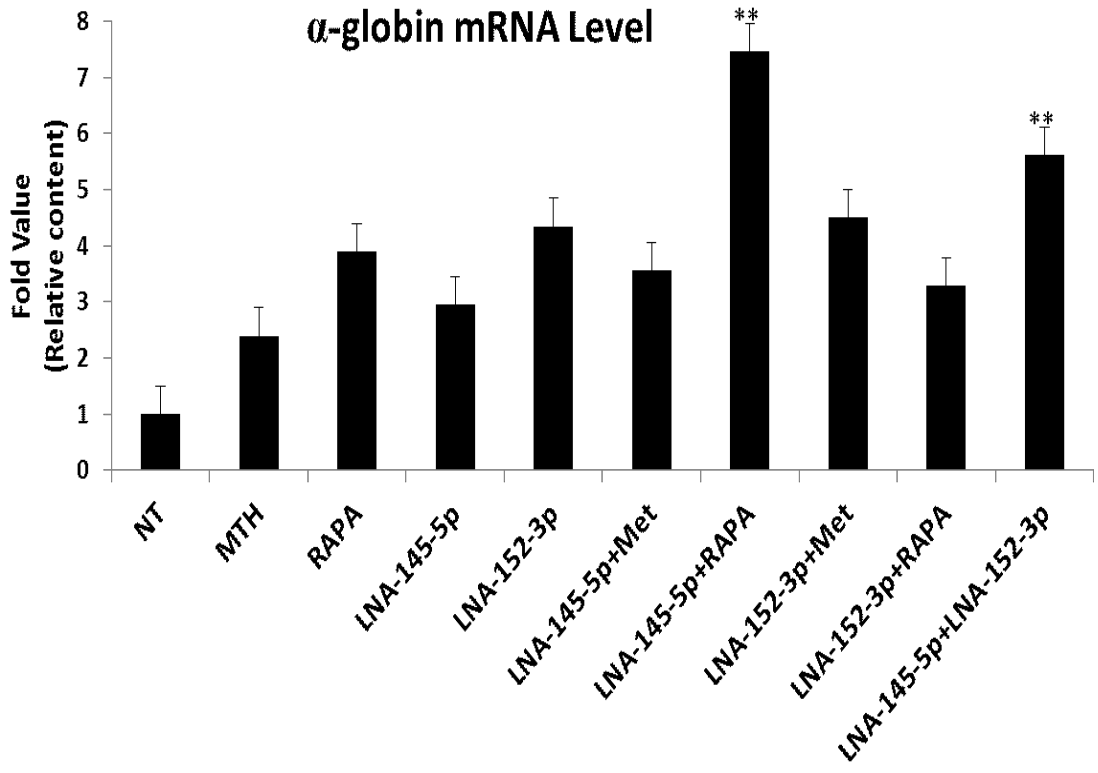

Figure 4.38: Alpha globin (α) expression by RT q-PCR. In this figure, K562 cells were treated with various inducers like MTH (Methramycin) and RAPA (Rapamycin), further also with masked PNAs like 145-5p and 152-3p and their combinations. Evident from this figure that various combinations have really helped to increase the gamma globin level in K562 cells. Results shown represent the average ± standard deviation (S.D.) obtained in at least three independent experiments.* = $p < 0.05$; * ** = $p < 0.01$.

One modifier of pathologic α-globin production in murine β-thalassemia is α-hemoglobin–stabilizing protein (AHSP), which was recently described in [Kong et al., 2004]. AHSP binds preferentially to free α-hemoglobin, but not to β-hemoglobin or hemoglobin tetramers. AHSP-deficient (AHSP–/–) mice have modest anemia and α-globin inclusions in their red cells [Kihm, A.J et al., 2002]. Kong et al. showed in their JCI study that AHSP–/– mice with β-thalassemia die in utero with a more lethal form of the disease than that of mice producing normal amounts of AHSP [Kong et al., 2004]. Presumably, the binding of free α-hemoglobin

by AHSP reduces pathologic α-globin precipitation by converting the free α-hemoglobin to a more nontoxic complex, perhaps by accelerating proteolysis of the excess α-globin. However, even normal levels of AHSP do not significantly prevent excess α-globin accumulation in the murine β-thalassemia model.

5. CONCLUSION AND FUTURE PERSPECTIVES

Conclusion-I

Cystic fibrosis is a lethal autosomal recessive genetic disease caused by a variety of mutations of the Cystic Fibrosis Transmembrane conductance Regulator (CFTR) gene. Since the demonstration that microRNAs are deeply involved in CF, a great attention has been dedicated to target the miRNAs involved in down-regulation of CFTR and associated proteins. In this respect miR-145-5p appears to be an important target, in order to increase CFTR expression. The objective of this study was to design a peptide nucleic acid (PNA) targeting miR-145, determine its activity in inhibiting miR-145, and verify whether it induces an increase of CFTR production. PNAs have been extensively studied and found to be a very useful tool for modifying gene expression. In the last few years, the use of PNAs for targeting microRNAs (anti-miRNA PNAs) has provided impressive advancements. In particular, targeting of microRNAs involved in the repression of the expression of the *CFTR Gene*, defective in cystic fibrosis (CF), is a key step in the development of new types of treatment protocols.

Further, our preliminary results have shown the efficiency of the anti-miR-145-PNA and its role in interfering the target binding sites related to miR-145-5p and how does it affect the *CFTR Gene* mRNA and protein content not only in non CF Calu-3 cells, but also in CF cell lines such as CFBE e.g CFBE-41oΔF-508. We extended this study on a CF cell line just to verify our previously obtained results and to propose this approach as a possible strategy for CF patients. For this purpose, we used the CFBE-41o ΔF-508 cell line in order to demonstrate the effects of the PNA interference with miR-145-5p and to verify whether this affects CFTR at the mRNA and protein level. We confirmed upregulation of CFTR mRNA and protein after treatment with the anti-miR145-PNA.

In addition to the anti-miRNA therapeutic strategy, inhibition of miRNA functions can be reached by masking the miRNA binding sites present within the 3'UTR region of the target mRNAs. The objective of this part of the study was to design a PNA masking the binding site of the microRNA miR-145-5p present within the 3'UTR of the CFTR mRNA and to determine its activity in inhibiting miR-145-5p function, with particular focus on the expression of both CFTR mRNA and CFTR protein in Calu-3 cells. The results obtained support the concept that the PNA masking the miR-145-5p binding site of the CFTR mRNA

is able to interfere with miR-145-5p biological functions, leading to both an increase of CFTR mRNA and CFTR protein content.

In moving the experiments to the CFBE cell line, it was important to verify the presence of the 3'UTR sequence (target of miR-145-5p) in this cell line. Therefore, we planned experiment keeping in mind the presence within the CFBE cell lines of plasmids with WT CFTR (in the CFBE-41o WT CFTR cell line), with F508del CFTR (in the CFBE41o-ΔF508del CFTR and CFBE41o-ΔF508del CFTR YFP cell lines). To this aim, we designed the primers for both genomic and plasmid DNA sequences and the results obtained proved the presence of the 3'UTR sequence in the employed CFBE cell lines.

In the last section of this part of the study, we validated our miRNA-masking PNA on CF cell lines in combination with Vertex compounds VX-809 (a CFTR corrector) and VX-770 (a CFTR potentiator) and obtained results supporting the use of these combinations for possible personalized treatments of CF patients.

In a nutshell, we demonstrated that the miR-145masking PNA specifically induced an increase of CFTR expression in Calu-3 and CFBE41o-WT CFTR cells. We have also studied this miR-145masking PNA in combination with CFTR potentiators and correctors. The data obtained demonstrate that the maximum level of CFTR content is achieved in CFBE-41o-WT and CFBE-ΔF508 by combining miR145-maskingPNA with VX809 and VX770. In addition of that, CFTR functional analysis also proved that miR145-maskingPNA/VX809/VX770 combination was the most effective in stimulating CFTR-mediated chloride efflux in the CFBE41o- F508del CFTR YFP cell line.

The major output of this study was the identification of a microRNA target (miR-145-5p) with the objective of modifying gene expression of cystic fibrosis cells, and, in particular, of increasing stability/expression of the CFTR mRNA and protein. This therapeutic goal is very important for the treatment of cystic fibrosis.

Conclusion-II

In hematological disorders like β-thalassemia the lack of functional β-globin chains prevents the production of adult hemoglobin (HbA). A potential therapeutic strategy is represented by the increase of fetal hemoglobin (HbF) levels in the adult life through modulation of human γ-globin gene expression. The objective of this part of study was to validate further miRNA masking strategy to other genetic disorders (in this case β-thalassemia). Therefore, LNA masking miRNA binding sites present in the 3'UTR portion of the KLF4 mRNA were designed and tested, in order to determine their activity in upregulating KLF-4 expression. Upregulation of KLF4 appears to be important for upregulating HbF production.

First, to identify the interactions of the miR145-5p and miR-152-3p-maskingLNA with *KLF4 gene* was quiet important. To identify the location of the miR-145-5p binding site within the 3'UTR KLF4 mRNA sequence together with the extent of homology between the miR-145-5p and miR-152-3p binding sites and the respective miR145 and miR-152-maskingLNAs, fully complementary to the miR-152-3p KLF4 mRNA binding site, was chosen in order to obtain an efficient competition with miR-145-5p and with miR-152-3p for the respective 3'UTR KLF4 mRNA binding sites.

We then treated K562 cells with the designed LNAs and real time RT-q-PCR was performed using biological material isolated from the different K562 samples treated with the miRNA masking LNAs. The expression of *KLF4 gene* was verified and comparison was made with the internal control beta-actin. The results obtained clearly indicate that inhibition of miR-145-5p and miR-152-3p is associated with a dramatic increase of KLF4 mRNA. This increase was obtained when the 145-masking-LNA and 152-masking LNAs were used singularly or in combination. This support the concept that KLF4 mRNA is down-regulated by miR-145-5p and miR-152-3p.

In addition to these experiments, the proportion of benzidine (hemoglobin containing cells) was determined in order to verify whether upregulation of KLF4 was associated with increase of hemoglobin production by K562 cells. The benzidine reaction has been extensively used to measure hemoglobin in human erythroleukemic (K562) cells stimulated to synthesize hemoglobin by different HbF inducers. We found that both the 145-masking-LNA and 152-masking LNAs were effective in inducing an increase of the proportion of benzidine positive cells. This induction was higher than that found using two HbF inducers, mithramycin (MTH) and rapamycin (RAPA). However, when combined treatment were performed (i.e.

145-masking-LNA plus 152-masking LNAs, 145-masking-LNA plus MTH, 152-masking LNAs plus MTH, 145-masking-LNA plus RAPA and 152-masking LNAs plus RAPA) no significant additive effects were found. However, since the lack of increase of the proportion of benzidine-positive cells does not mean "per se" a lack of increase of gene expression, RT-qPCR analysis was performed.

These results confirmed an increase of γ-globin gene expression in K562 cells treated with the 145-masking-LNA and the 152-masking LNAs, used singularly. In this case, when combined treatment were performed (i.e. 145-masking-LNA plus 152-masking LNAs, 145-masking-LNA plus MTH, 152-masking LNAs plus MTH, 145-masking-LNA plus RAPA and 152-masking LNAs plus RAPA) the increase of γ-globin mRNA was higher with respect to singular treatments.

Despite the fact that these data should be confirmed using erythroid precursor cell from β-thalassemia patients, our approach is the proof of principle that the miRNA masking strategy might be employed to control KLF4 expression and to HbF induction. In the future, it will be very important that the *KLF4 gene* can be modulated in β-thalassemia by using these masking molecules, thereby inducing HbF. This would be our future goal to propose this strategy for thalassemia patients. The results presented in this thesis support the concept that miRNAs and miRNA-modifiers are a key tool in developing therapeutics for this rare disease.

6. References

Akabas MH, Kaufmann C, Cook TA, Archdeacon P. Amino acid residues lining the chloride channel of the cystic fibrosis transmembrane conductance regulator. J Biol Chem. 1994, 269:14865-14868.

Alvarez-Erviti L, Seow Y, Yin H et al. Delivery of siRNA to the mouse brain by systemic injection of targeted exosomes. Nat Biotechnol, 2011, 29:341-345. doi.org/10.1038/nbt.1807.

Alves CAD, Aguiar RA, Alves AC, Santana MA. Diabetes mellitus in patients with cystic fibrosis. J Bras Pneumol. 2007, 33 (2): 213-21.

Alves Cde A, Aguiar RA, Alves AC, Santana MA. Diabetes mellitus in patients with cystic fibrosis. J Bras Pneumol. 2007, 33 (2):213-21.

Amaral FC, Torres N, Saggioro F, Neder L, Machado HR, Silva WA Jr, Moreira AC, Castro M. MicroRNAs differentially expressed in ACTH-secreting pituitary tumors. J Clin Endocrinol Metab. 2009;94(1):320–3.

Andersen DH. Cystic fibrosis of the pancreas and its relation to celiac disease: a clinical and pathological study. Am J Dis Child 1938, 56:344-399.

Assael, BM; Castellani C, Ocampo MB et al. Epidemiology and survival analysis of cystic fibrosis in an area of intense neonatal screening over 30 years. American Journal of Epidemiology. 2002, 156(5):397-401.

Augarten A, Yahav Y, Kerem BS, et al. Congenital bilateral absence of vas deferens in the absence of cystic fibrosis. Lancet. 1994, 344 (8935):1473-4.

Aurora P, Whitehead B, Wade A, et al. Lung transplantation and life extension in children with cystic fibrosis. Lancet. 1999, 354: 1591-93.

Austin, E.G.; Nehal, G.; Shih-Hsing, L.; Ann, H. MicroRNA regulation of expression of the cystic fibrosis transmembrane conductance regulator gene. Biochem. J. 2011.

Avitabile C, Saviano M, D'Andrea LD et al. Targeting pre-miRNA by peptide nucleic acids

A new strategy to interfere in the miRNA maturation. Artif DNA PNA XNA, 2012, 3:88- 96. doi.org/10.4161/adna.20911.

Babar IA, Cheng CJ, Booth CJ, et al. Nanoparticle-based therapy in an in vivo microRNA155(miR-155)-dependent mouse model of lymphoma. Proc Natl Acad Sci U S A, 2012, 109:1695-1704. doi.org/10.1073/pnas.1201516109.

Bader AG, Brown D, Winkler M. The Promise of MicroRNA Replacement Therapy. Cancer Res, 2010, 70: 7027-7030. doi.org/10.1158/0008-5472.CAN-10-2010

Baker M. MicroRNA profiling: separating signal from noise. Nat Methods, 2010, 7:687-

692. doi 10.1038/nmeth2910-687.

Balough K, McCubbin M, Weinberger M, Smits W, Ahrens R, Fick R. The relationship between infection and inflammation in the early stages of lung disease from cystic fibrosis. Pediatr Pulmonol. 1995, 20:63-70.

Bandres E, Cubedo E, Agirre X, Malumbres R, Zarate R, Ramirez N, Abajo A, Navarro A, Moreno I, Monzo M, Garcia-Foncillas J. Identification by Real-time PCR of 13 mature microRNAs differentially expressed in colorectal cancer and non-tumoral tissues. Mol Cancer. 2006; 5:29.

Bank A. Understanding globin regulation in beta-thalassemia: it's as simple as alpha, beta, gamma, delta. J Clin Invest. 2005 Jun;115(6):1470-3. doi: 10.1172/JCI25398. PMID: 15931385; PMCID: PMC1137010.

Bartel DP MicroRNAs: genomics, biogenesis, mechanism, and function. Cell, 2004, 116:281-297. doi.org/10.1016/S0092-8674(04)00045-5.

Bartel DP MicroRNAs: genomics, biogenesis, mechanism, and function. Cell, 2004, 116:281-297. doi.org/10.1016/S0092-8674(04)00045-5.

Basu S, Wickstrom E. Synthesis and characterization of a peptide nucleic acid conjugated to a D-peptide analog of insulin-like growth factor 1 for increased cellular uptake. Bioconjug Chem, 1997, 8:481-488. doi.org/10.1021/bc9700650.

Bennet LE, Keck BM, Daily OP, et al. Worldwide thoracic organ transplantation: a report from the UNOS/ISHLT international Registry for Thoracic Organ Transplantation. Clin Transpl. 2000, 1:31-44.

Bhise, N.S., Gray, R.S., Sunshine, J.C., Htet, S., Ewald, A.J., and Green, J.J. 2010. Therelationship between terminal functionalization and molecular weight of a gene delivery polymer and transfection efficacy in mammary epithelial 2-D cultures and 3-D organotypic cultures. Biomaterials 31, 8088–8096.

Borgatti M, Breda L, Cortesi R et al. Cationic liposomes as delivery systems for doublestranded PNA-DNA chimeras exhibiting decoy activity against NF-kappaB transcription factors. Biochem Pharmacol, 2002, 64:609-616.

Boussif O, Lezoualch F, Zanta MA et al. A versatile vector for gene and oligonucleotide transfer into cells in culture and in vivo: polyethylenimine. Proc Natl Acad Sci U S A, 1995, 92:7297-7301. doi.org/10.1073/pnas.92.16.7297.

Brognara E, Fabbri E, Aimi F et al. Peptide nucleic acids targeting miR-221 modulate p27Kip1 expression in breast cancer MDA-MB-231 cells. Int J Oncol, 2012, 41:2119-2127. doi.org/10.3892/ijo.2012.1632.

Brognara, E.; Fabbri, E.; Aimi, F.; Manicardi, A.; Bianchi, N.; Finotti, A.; Breveglieri, G.; Borgatti, M.;Corradini, R.; Marchelli, R.; et al. Peptide nucleic acids targeting miR-221 modulate p27Kip1 expression inbreast cancer MDA-MB-231 cells. Int. J. Oncol. 2012, 41, 2119–2127.

Brognara, E.; Fabbri, E.; Bazzoli, E.; Montagner, G.; Ghimenton, C.; Eccher, A.; Cantù, A.; Manicardi, A.;Bianchi, N.; Finotti, A.; et al. Uptake by human glioma cell lines and biological effects of a peptide-nucleicacids targeting miR-221. J. Neurooncol. 2014, 118, 19–28.

Bruchova H, Merkerova M, Prchal JT. Aberrant expression of microRNA in polycythemia vera. Haematologica. 2008;93(7):1009–16.

Brummer A, Hausser J. MicroRNA binding sites in the coding region of mRNAs: Extending the repertoire of post-transcriptional gene regulation. Bioessays, 2014, 36:617-

626. doi.org/10.1002/bies.201300104.

Bruscia E, Sangiuolo F, Sinibaldi P, Goncz KK, Novelli G, Gruenert DC. (2002) Isolation of CF cell lines corrected at DeltaF508- CFTR locus by SFHR-mediated targeting. Gene Ther 9(11): 683-685.

Busch R. On the history of cystic fibrosis. Acta Univ Carol Med (Praha)1990, 36 (1-4):13-5.

Cao A, Galanello R. Beta-thalassemia. Genetics in Medicine, 2010, 12:61-76. doi.org/10.1097/GIM.0b013e3181cd68e.

Cao A, Moi P. Regulation of the Globin Genes. Pediatric Research, 2002, 51:415-421. doi.org/10.1203/00006450-200204000-00003.

Chatterjee, Sangeeta; Pal, Jayanta K. (1 May 2009). "Role of 5'- and 3'-untranslated regions of mRNAs in human diseases". Biology of the Cell. 101 (5): 251–262. doi:10.1042/BC20080104

Chen HC, Chen GH, Chen YH, Liao WL, Liu CY, Chang KP, Chang YS, Chen SJ. MicroRNA deregulation and pathway alterations in nasopharyngeal carcinoma. Br J Cancer. 2009;100(6):1002–11.

Chen LL, Carmichael GG. Altered nuclear retention of mRNA containing inverted repeats in human embryonic stem cell: functional role of nuclear noncoding RNA. Mol Cell, 2009, 35:467-478. doi.org/10.1016/j.molcel.2009.06.027.

Chiarantini L, Cerasi A, Millo E et al. Enhanced antisense effect of modified PNAs delivered through functional PMMA microspheres. Int J Pharm, 2006, 324:83-91. doi.org/10.1016/j.ijpharm.2006.07.007.

Cho WC. OncomiRs: The discovery and progress of microRNAs in cancer. Mol Cancer, 2007, 6:60. doi.org/10.1186/1476-4598-6-60.

Cholon, D.M.; Gentzsch, M. Recent progress in translational cystic fibrosis research using precision medicine strategies. J. Cyst. Fibros. 2017.

Choong ML, Yang HH, McNiece I. MicroRNA expression profiling during human cord blood-derived CD34 cell erythropoiesis. Exp Hematol. 2007 Apr;35(4):551-64. doi: 10.1016/j.exphem.2006.12.002. PMID: 17379065.

Clancy JP, Rowe SM, Accurso FJ, et al. Results of a phase IIa study of VX-809, an investigational CFTR corrector compound, in subjects with cystic fibrosis homozygous for the F508delCFTR mutation. Thorax. 2012;67(1):12–8.

Cohen TS, Prince A, Cystic fibrosis: a mucosal immunodeficiency syndrome, Nat Med, 2012, Apr 5;18(4):509-19. doi: 10.1038/nm.2715. PMID: 22481418; PMCID: PMC3577071.

Cohn JA, Friedman KJ, Noone PG, Knowles MR, Silverman LM, Jowell PS. Relation between mutations of the cystic fibrosis gene and idiopathic pancreatitis. N. Engl. J. Med. 1998, 339 (10):653-8.

Colombo C, Russo MC, Zazzeron L, Romano G. Liver disease in cystic fibrosis. J. Pediatr. Gastroenterol. Nutr. 2006, 43 Suppl 1:49-55.

Conwell LS, Chang AB. Bisphosphonates for osteoporosis in people with cystic fibrosis. Cochrane Database Syst Rev. 2009, (4).

Cowie P, Hay EA, MacKenzie A. The noncoding human genome and the future of

personalized medicine. Expert Rev Mol Med, 2015; 17:e4. doi.org/10.1017/erm.2014.23.

Crew E, Rahman S, Rahaman S et al. MicroRNA conjugated gold nanoparticles and cell transfection. Anal Chem, 2012, 84:26-29. doi.org/10.1021/ac202749p.

D'Agata R, Breveglieri G, Zanoli LM et al. Direct detection of point mutations in nonamplified human genomic DNA. Anal Chem, 2011, 83:8711-8717. doi: 10.1021/ac2021932.

Davies JC, Alton EW, Bush A. Cystic fibrosis. BMJ. 2007, 335 (7632):1255-9.

De Braekeleer M, Allard C, Leblanc JP, Simard F, Aubin G. Genotype-phenotype correlation in cystic fibrosis patients compound heterozygous for the A455E mutation. Hum Genet. 1997, 101:208-211.

De Santi et al., Precise Targeting of miRNA Sites Restores CFTR Activity in CF Bronchial Epithelial Cells, Molecular Therapy (2020), https://doi.org/10.1016/j.ymthe.2020.02.001.

Deeks ED. Ivacaftor: a review of its use in patients with cystic

fibrosis. Drugs. 2013;73(14):1595–604.

Dekkers JF , Berkers G , Kruisselbrink E, et al. Characterizing responses to CFTR-modulating drugs using rectal organoids derived from subjects with cystic fibrosis. Sci Transl Med, 2016, Jun 22;8(344):344ra84.

Derossi D, Calvet S, Trembleau A, et al. Cell internalization of the third helix of the Antennapedia homeodomain is receptor independent. J Biol Chem, 1996, 271:18188-18193. doi.org/10.1074/jbc.271.30.18188.

Di Sant'Agnese PA, Darling RC, Perera GA, Shea E. Abnormal electrolyte composition of sweat in cystic fibrosis of the pancreas; clinical significance and relationship to the disease. Pediatrics. 1953, 12(5): 549-63.

Dodge JA. Male fertility in cystic fibrosis. Lancet. 1995, 346 (8975):587-8.

Dong H, Lei J, Ding L, et al. MicroRNA: function, detection, and bioanalysis. Chem Rev, 2013, 113:6207-6233. doi.org/10.1021/cr300362f.

Drin G, Cottin S, Blanc E, et al. Studies on the internalization mechanism of cationic cell-Penetrating peptides. J Biol Chem, 2003,278:31192-31201.doi.org/10.1074/jbc.M303938200.

Driskell RA, Engelhardt JF. Current status of gene therapy for inherited lung diseases. Annu Rev Physiol. 2003, 65:585-612.

Du L, Jung ME, Damoiseaux R, Completo G, Fike F, Ku JM, Nahas S, Piao C, Hu H, Gatti RA. A new series of small molecular weight compounds induce read through of all three types of nonsense mutations in the ATM gene. Mol Ther. 2013 Sep;21(9):1653-60. doi: 10.1038/mt.2013.150. Epub 2013 Jun 18. PMID: 23774824; PMCID: PMC3776636.

Dutta, R.K.; Chinnapaiyan, S.; Rasmussen, L.; Raju, S.V.; Unwalla, H.J. A Neutralizing Aptamer to TGFBR2 and miR-145 Antagonism Rescue Cigarette Smoke- and TGF-β-Mediated CFTR Expression. Mol. Ther. 2019,27, 442–455.

Duursma AM, Kedde M, Schrier M et al.miR-148 targets human DNMT3b protein coding region. RNA, 2008, 14:872-877. doi.org/10.1261/rna.972008.

Eggermont E, De Boeck K. Small-intestinal abnormalities in cystic fibrosis patients. Eur. J. Pediatr. 1991, 150 (12):824-8.

Elborn JS, Ramsey, B.W., Boyle, M.P., Konstan, M.W., Huang, X., Marigowda, G.,Waltz, D., and Wainwright, C.E.; VX-809 TRAFFIC and TRANSPORT study groups(2016). Efficacy and safety of lumacaftor/ivacaftor combination therapy in patientswith cystic

fibrosis homozygous for Phe508del CFTR by pulmonary function subgroup: a pooled analysis. Lancet Respir. Med. 4, 617–626.

Elia L, Quintavalle M, Zhang J, Contu R, Cossu L, Latronico MV, Peterson KL, Indolfi C, Catalucci D, Chen J, Courtneidge SA, Condorelli G. The knockout of miR-143 and -145 alters smooth muscle cell maintenance and vascular homeostasis in mice: correlates with human disease. Cell Death Differ. 2009;16(12):1590–8.

Elias S, Annas GJ, Simpson JL. Carrier screening for cystic fibrosis: implications for obstetric and gynecologic practice. Am. J. Obstet. Gynecol. 1991, 164 (4):1077-83.

Entrez Gene: MicroRNA 145". Retrieved 2015-01-26.

Esteller M. Non-coding RNAs in human disease. Nat Rev Genet, 2011, 12:861-874. doi.org/ 10.1038/nrg3074.

Fabani, M.M.; Gait, M.J. MiR-122 targeting with LNA/20-O-methyl oligonucleotide mixmers, peptide nucleic acids (PNA), and PNA-peptide conjugates. RNA 2008, 14, 336–346.

Fabbri, E.; Brognara, E.; Borgatti, M.; Lampronti, I.; Finotti, A.; Bianchi, N.; Sforza, S.; Tedeschi, T.; Manicardi, A.; Marchelli, R.; et al. miRNA therapeutics: Delivery and biological activity of peptide nucleic acids targeting miRNAs. Epigenomics 2011, 3, 733–745.

Fabbri, E.; Manicardi, A.; Tedeschi, T.; Sforza, S.; Bianchi, N.; Brognara, E.; Finotti, A.; Breveglieri, G.; Borgatti, M.; Corradini, R.; et al. Modulation of the biological activity of microRNA-210 with peptide nucleic acids (PNAs). ChemMedChem 2011, 6, 2192–2202.

Fabbri, E.; Tamanini, A.; Jakova, T.; Gasparello, J.; Manicardi, A.; Corradini, R.; Sabbioni, G.; Finotti, A.; Borgatti, M.; Lampronti, I.; et al. A Peptide Nucleic Acid against MicroRNA miR-145-5p Enhances the Expression of the Cystic Fibrosis Transmembrane Conductance Regulator (CFTR) in Calu-3 Cells. Molecules 2017, 23, 71.

Fanconi G, Uehlinger E, Knauer C. Das coeliakiesyndrom bei angeborener zysticher pankreasfibromatose und bronchiektasien. Wien. Med. Wschr. 1936, 86:753–756.

Fang H, Zhang K, Shen G et al. Cationic Shell-crosslinked Knedel-like (cSCK) Nanoparticles for Highly Efficient PNA Delivery. Mol Pharm, 2009, 6: 615-626. doi.org/10.1021/mp800199w.

Fang Z, Tang J, Bai Y, et al. Plasma levels of microRNA-24, microRNA-320a, and microRNA-423-5p are potential biomarkers for colorectal carcinoma. J Exp Clin Cancer Res, 2015, 34:86. doi.org/10.1186/s13046-015-0198-6.

Faruqi AF, Egholm M, Glazer PM. Peptide nucleic acid-targeted mutagenesis of a chromosomal gene in mouse cells. Proc Natl Acad Sci U S A, 1998, 95:1398-1403. doi.org/10.1073/pnas.95.4.1398.

Fibach E, Bianchi N, Borgatti M, Prus E, Gambari R. Mithramycin induces fetal hemoglobin production in normal and thalassemic human erythroid precursor cells. Blood. 2003 Aug 15;102(4):1276-81. doi: 10.1182/blood-2002-10-3096. Epub 2003 May 8. PMID: 12738678.

Finotti, A.; Gasparello, J.; Fabbri, E.; Tamanini, A.; Corradini, R.; Dechecchi, M.C.; Cabrini, G.; Gambari, R. Enhancing the Expression of CFTR Using Antisense Molecules against MicroRNA miR-145-5p. Am. J. Respir. Crit. Care Med. 2019, 199, 1443–1444.

Finotti, A.; Gasparello, J.; Fabbri, E.; Tamanini, A.; Corradini, R.; Dechecchi, M.C.; Cabrini, G.; Gambari, R. Enhancing the Expression of CFTR Using Antisense Molecules against MicroRNA miR-145-5p. Am. J. Respir. Crit. Care Med. 2019, 199, 1443–1444.

Flint, J., R. M. Harding, et al.1998. "The population genetics of the haemoglobinopathies." Baillieres Clin Haematol 11(1): 1-51

Flotte TR, Afione SA, Solow R, Drumm ML, Markakis D, Guggino WB, Zeitlin PL, Carter BJ. Expression of the cystic fibrosis transmembrane conductance regulator from a novel adeno-associated virus promoter. J Biol Chem. 1993 Feb 15;268(5):3781-90. PMID: 7679117.

Flotte TR, Laube BL. Gene therapy in cystic fibrosis. Chest. 2001, 120(3 Suppl):1245-1315.

Flume PA, Liou TG, Borowitz DS, et al. Ivacaftor in subjects with cystic fibrosis who are homozygous for the F508del-CFTR mutation. Chest. 2012;142(3):718–24.

Fulmer SB, Schwiebert EM, Morales MM, Guggino WB, Cutting GR. Two cystic fibrosis transmembrane conductance regulator mutations have different effects on both pulmonary

phenotype and regulation of outwardly rectified chloride currents. Proc Natl Acad Sci USA. 1995, 92:6832-6836.

Gaglione M, Milano G, Chambery A et al. PNA-based artificial nucleases as antisense and anti-miRNAoligonucleotide agents. Mol BioSyst, 2011, 7:2490-2499. doi: 10.1039/c1mb05131h.

Galanello, A. C. a. R. 2010. "Beta Thalassemia." Genetics in Medicine 12: 61-76.

Gasparello, J.; Papi, C.; Zurlo, M.; Corradini, R.; Gambari, R.; Finotti, A. Demonstrating specificity of bioactive peptide nucleic acids (PNAs) targeting microRNAs for practical laboratory classes of applied biochemistry and pharmacology. PLoS ONE 2019, 14, e0221923.

Ghorai A, Ghosh U. miRNA gene counts in chromosomes vary widely in a species and biogenesis of miRNA largely depends on transcription or post-transcriptional processing of coding genes. Front Genet, 2014, 5: 100. doi: 10.3389/fgene.2014.00100.

Ghaleb AM, Yang VW. Krüppel-like factor 4 (KLF4): What we currently know. Gene. 2017;611:27-37. doi:10.1016/j.gene.2017.02.025.

Gilljam M, Antoniou M, Shin J, Dupuis A, Corey M, Tullis DE. Pregnancy in cystic fibrosis. Fetal and maternal outcome. Chest. 2000, 118 (1):85-91.

Goldman MJ, Anderson GM, Stolzenberg ED, Kari UP, Zasloff M, Wilson JM. Human beta-defensin-1 is a salt-sensitive antibiotic in lung that is inactivated in cystic fibrosis. Cell. 1997, 88:553-560.

Goncz KK, Feeney L, Gruenert DC. (1999) Differential sensitivity of normal and cystic fibrosis airway epithelial cells to epinephrine. Br J Pharmacol 128(1): 227-233.

Götte M, Mohr C, Koo CY, Stock C, Vaske AK, Viola M, Ibrahim SA, Peddibhotla S, Teng YH, Low JY, Ebnet K, Kiesel L, Yip GW (Dec 2010). "miR-145-dependent targeting of junctional adhesion molecule A and modulation of fascin expression are associated with reduced breast cancer cell motility and invasiveness". Oncogene. 29 (50): 6569–80. doi:10.1038/onc.2010.386

Govan J.R., Deretic V., Microbial pathogenesis in cystic fibrosis: mucoid Pseudomonas aeruginosa and Burkholderia cepacia, Microbiol. Rev., 1996, 60:539–574.

Gramantieri L, Ferracin M, Fornari F, Veronese A, Sabbioni S, Liu CG, Calin GA, Giovannini C, Ferrazzi E, Grazi GL, Croce CM, Bolondi L, Negrini M. Cyclin G1 is a target of miR-122a, a microRNA frequently down-regulated in human hepatocellular carcinoma. Cancer Res. 2007;67(13):6092–9.

Graybill RM, Bailey RC. Emerging Biosensing Approaches for microRNA Analysis. Anal Chem, 2016, 88:431-450. doi.org/10.1021/acs.analchem.5b04679.

Griesenbach U, Alton EW. Current status and future directions of gene and cell therapy for cystic fibrosis, BioDrugs, 2011, Apr 1;25(2):77-88. doi: 10.2165/11586960-000000000-00000. PMID: 21443272.

Griesenbach U, Alton EW. Recent advances in understanding and managing cystic fibrosis transmembrane conductance regulator dysfunction. F1000Prime Rep. 2015;7:64.

Griffiths-Jones, S. The microRNA Registry. Nucleic Acids Res. 2004, 32, D109–D111.

Grillo, G.; Turi, A.; Licciulli, F.; Mignone, F.; Liuni, S.; Banfi, S.; Gennarino, V.A.; Horner, D.S.; Pavesi, G.; Picardi, E.; et al. UTRdb and UTRsite (RELEASE 2010): A collection of sequences and regulatory motifs of the untranslated regions of eukaryotic mRNAs. Nucleic Acid Res. 2010, 38, D75–D80.

Grubb BR, Vick RN, Boucher RC. Hyperabsorption of Na+ and raised Ca2+-mediated Cl– secretion in nasal epithelia of CF mice. Am. J. Physiol. 1994, 266:1478-1483.

Haardt M, Benharouga M, Lechardeur D, Kartner N, Lukacs GL. C-terminal truncations destabilize the cystic fibrosis transmembrane conductance regulator without impairing its biogenesis. A novel class of mutation. J Biol Chem. 1999, 274:21873-21877.

Hamilton SE, Simmons CG, Kathiriya IS, et al. Cellular delivery of peptide nucleic acids and inhibition of human telomerase. Chem Biol, 1999, 6:343-351. doi.org/10.1016/S1074-5521(99)80046-5.

Han, A.-P., Fleming, M.D., and Chen, J.-J. 2005. Heme-regulated eIF2α kinase modifies the phenotypic severity of murine models of erythropoietic protoporphyria and β-thalassemia. J. Clin. Invest. 115:1562–1570. doi:10.1172/JCI24141.

Han, J.; Sun, Y.; Song, W.; Xu, T. microRNA-145 regulates the RLR signaling pathway in miiuy croaker afterpoly(I:C) stimulation via targeting MDA5. Dev. Comp. Immunol. 2017, 68, 79–86.

Hansen CR, Pressler T, Koch C, Høiby N. Long-term azitromycin treatment of cystic fibrosis patients with chronic Pseudomonas aeruginosa infection; an observational cohort study. J. Cyst. Fibros. 2005, 4(1):35-40.

Hanvey JC, Peffer JE, Bisi SA et al. Antisense and antigene properties of peptide nucleic acids. Science, 1992, 258:1481-1485.

Hardin DS, Rice J, Ahn C, et al. Growth hormone treatment enhances nutrition and growth in children with cystic fibrosis receiving enteral nutrition. J. Pediatr. 2005, 146(3):324-8.

Hart, M.; Wach, S.; Nolte, E.; Szczyrba, J.; Menon, R.; Taubert, H.; Hartmann, A.; Stoehr, R.; Wieland, W.;Grässer, F.A.; et al. The proto-oncogene ERG is a target of microRNA miR-145 in prostate cancer. FEBS J.2013, 280, 2105–2116.

Hassan, F.; Nuovo, G.J.; Crawford, M.; Boyaka, P.N.; Kirkby, S.; Nana-Sinkam, S.P.; Cormet-Boyaka, E. MiR-101 and miR-144 regulate the expression of the CFTR chloride channel in the lung. PLoS ONE 2012, 7, e50837.

Hausser J, Syed AP, Bilen B. Analysis of CDS-located miRNA target sites suggests that they can effectively inhibit translation. Genome Res, 2013, 23:604-615. doi.org/10.1101/gr.139758.112

Haworth CS, Selby PL, Webb AK, et al. Low bone mineral density in adults with cystic fibrosis. Thorax. 1999, 54 (11):961-7.

Highsmith WE, Burch LH, Zhou Z, Olsen JC, Boat TE, Spock A, Gorvoy JD, Quittel L, Friedman KJ, Silverman LM. A novel mutation in the cystic fibrosis gene in patients with pulmonary disease but normal sweat chloride concentrations. N Engl J Med. 1994, 331:974-980.

Höck J, Gunter Meister G. The Argonaute protein family. Genome Biol, 2008, 9: 210. doi.org/ 10.1186/gb-2008-9-2-210.

Hyde SC, Emsley, P, Hartshorn MJ, Mimmack MM, Gileadi U, Pearce SR, Gallagher MP, Gill DR, Hubbard RE, Higgins CF. Structural model of ATP-binding proteins associated with cystic fibrosis, multidrug resistence and bacterial transport. Nature. 1990, 346: 362-365.

Ichimi T, Enokida H, Okuno Y, Kunimoto R, Chiyomaru T, Kawamoto K, Kawahara K, Toki K, Kawakami K, Nishiyama K, Tsujimoto G, Nakagawa M, Seki N. Identification of novel microRNA targets based on microRNA signatures in bladder cancer. Int J Cancer. 2009;125(2):345–52.

Illek B, Lei D, Fischer H, Gruenert DC. (2010) Sensitivity of chloride efflux vs. transepithelial measurements in mixed CF and normal airway epithelial cell populations. Cell Physiol Biochem 26(6): 983-990.

Illek B, Maurisse R, Wahler L, Kunzelmann K, Fischer H, Gruenert DC. (2008) Cl transport in complemented CF bronchial epithelial cells correlates with CFTR mRNA expression levels. Cell Physiol Biochem 22(1-4): 57-68.

Illek B, Maurisse R, Wahler L, Kunzelmann K, Fischer H, Gruenert DC. (2008) Cl transport in complemented CF bronchial epithelial cells correlates with CFTR mRNA expression levels. Cell Physiol Biochem 22(1-4): 57-68.

Iorio MV, Visone R, Di Leva G, Donati V, Petrocca F, Casalini P, Taccioli C, Volinia S, Liu CG, Alder H, Calin GA, Menard S, Croce CM. MicroRNA signatures in human ovarian cancer. Cancer Res. 2007;67(18):8699–707.

Itonaga M, Matsuzaki I, Warigaya K et al. Novel Methodology for Rapid Detection of KRAS Mutation Using PNA-LNA Mediated Loop-Mediated Isothermal Amplification. PLoS One, 2016, 11:e0151654. doi.org/10.1371/journal.pone.0151654.

J.Weatherall, J. B. C. a. D. (2003). "Thalassemia and Malaria: New insights into an Old Problem." Wiley Online Library 111(4): 278-282. DOI: 10.1046/j.1525-1381.1999.99235.x.

Jeffery J Wine. The genesis of cystic fibrosis lung disease. The Journal of Clinical Investigation. 1999, 103 (3):309-312

Johnson LG, Boyles SE, Wilson J, Boucher RC. Normalization of raised sodium absorption and raised calcium-mediated chloride secretion by adenovirus-mediated expression of cystic

fibrosis transmembrane conductance regulator in primary human cystic fibrosis airway epithelial cells. Clin Invest. 1995, 95(3):1377-82.

Juliano, R.L. 2016. The delivery of therapeutic oligonucleotides. Nucleic Acids Res.44, 6518–6548.

Kalin N, Claass A, Sommer M, Puchelle E, Tummler B. DeltaF508 CFTR protein expression in tissues from patients with cystic fibrosis. J Clin Invest. 1999, 103:1379-1389.

Kartner N, Augustinas O, Jensen TJ, Naismith AL, Riordan JR. Mislocalization of delta F508 CFTR in cystic fibrosis sweat gland. Nat. Genet. 1992, 1:321-327.

Keller A, Leidinger P, Lange J, Borries A, Schroers H, Scheffler M, Lenhof HP, Ruprecht K, Meese E. Multiple sclerosis: microRNA expression profiles accurately differentiate patients with relapsing-remitting disease from healthy controls. PLoS ONE. 2009;4(10):e7440.

Kerem B, Rommens JM, Buchanan JA, Markiewicz D, Cox TK, Chakravarti A, Buchwald M, Tsui LC. Identification of the cystic fibrosis gene:Genetic analysis. Science. 1989, 245:1073-1080.

Khan TZ, Wagener JS, Bost T, Martinez J, Accurso FJ, Riches DW. Early pulmonary inflammation in infants with cystic fibrosis. Am J Respir Crit Care Med. 1995, 151:1075-82.

Khoshoo V, Udall JN. Meconium ileus equivalent in children and adults. Am. J. Gastroenterol. 1994, 89 (2):153-7.

Kihm, A.J., et al. 2002. An abundant erythroid protein that stabilizes free α-haemoglobin. Nature.417:758–763.

Kitson C, Angel B, Judd D, et al. The extra- and intracellular barriers to lipid and adenovirus-mediated pulmonary gene transfer in native sheep airway epithelium. Gene Ther. 1999, 6:534-46.

Knowles MR et al. Abnormal ion permeation through cystic fibrosis respiratory epithelium. Science. 1983, 221:1067-1070.

Kong, Y., et al. 2004. Loss of α-hemoglobin–stabilizing protein impairs erythropoiesis and exacerbates β-thalassemia. J. Clin. Invest. 114:1457–1466.doi:10.1172/JCI200421982.

Koppelhus U, Nielsen PE. Cellular delivery of peptide nucleic acid (PNA). Advanced Drug Delivery Reviews, 2003, 55:267-280. doi.org/10.1016/S0169-409X(02)00182-5.

Korpal M, Kang Y. The emerging role of miR-200 family of microRNAs in epithelialmesenchymal transition and cancer metastasis. RNA Biol, 2008, 5: 115-119. doi.org/10.4161/rna.5.3.6558.

Kota J, Chivukula RR, O'Donnell KA, et al. Therapeutic microRNA delivery suppresses

tumorigenesis in a murine liver cancer model. Cell, 2009, 137-1005-1017. doi.org/ 10.1016/j.cell.2009.04.021.

Kreft, M.E.; Jerman, U.D.; Lasiˇc, E.; Hevir-Kene, N.; Rižner, T.L.; Peternel, L.; Kristan, K. The characterization of the human cell line Calu-3 under different culture conditions and its use as an optimized in vitro model to investigate bronchial epithelial function. Eur. J. Pharm. Sci. 2015, 69, 1–9.

Kreft, M.E.; Jerman, U.D.; Lasiˇc, E.; Hevir-Kene, N.; Rižner, T.L.; Peternel, L.; Kristan, K. The characterization of the human cell line Calu-3 under different culture conditions and its use as an optimized in vitro model to investigate bronchial epithelial function. Eur. J. Pharm. Sci. 2015, 69, 1–9.

Kulczycki LL, Shwachman H. Studies in cystic fibrosis of the pancreas; occurrence of rectal prolapse. N. Engl. J. Med. 1958, 259 (9): 409-12.

Kung JYY, Colognori D, Lee JT. Long noncoding RNAs: past, present, and future. Genetics, 2013, 193:651-669. doi.org/10.1534/genetics.112.146704.

Kuver R, Lee SP. Hypertonic saline for cystic fibrosis. N. Engl. J. Med. 2006, 354 (17):1848-51.

Lee JM, Jung Y. Two-temperature hybridization for microarray detection of label-free microRNAs with attomole detection and superior specificity. Angew Chem Int Ed Engl, 2011, 50:12487-12490. doi.org/10.1002/anie.201105605.

Lee RC, Feinbaum RL, Ambros V. The C.Elegans heterochronic gene lin-4 encodes small RNAs with antisense complementary to lin-14. Cell, 1993, 75:843-54. doi.org/10.1016/0092-8674(93)90529-Y.

Lieberman J. Dornase aerosol effect on sputum viscosity in cases of cystic fibrosis. JAMA. 1968, 205 (5): 312–3.

Lim, L.P.; Lau, N.C.; Garrett-Engele, P.; Grimson, A.; Schelter, J.M.; Castle, J.; Bartel, D.P.; Linsley, P.S.; Johnson, J.M. Microarray analysis shows that some microRNAs downregulate large numbers of target mRNAs. Nature 2005, 433, 769–773.

Linsdell P, Hanrahan JW. J. Gen. Physiol. 1998, 111:601-614.

Linsdell P, Tabcharani JA, Rommens JM, Hou YX, Chang XB, Tsui LC, Riordan JR, Hanrahan JW. J. Gen. Physiol. 1997, 110:355-364.

Liu GH, Zhou ZG, Chen R, et al. Serum miR-21 and miR-92a as biomarkers in the diagnosis and prognosis of colorectal cancer. Tumour Biol, 2013, 34:2175-2181. doi.org/10.1007/s13277-013-0753-8.

Liu H, Lin H, Zhang L, Sun Q, Yuan G, Zhang L, Chen S, Chen Z. miR-145 and miR-143regulate odontoblast differentiation through targeting Klf4 and Osx genes in a feedback loop.J Biol Chem. 2013;288:9261-71.

Liu M, Zhi Q, Wang W, et al. Up-regulation of miR-592 correlates with tumor progression and poor prognosis in patients with colorectal cancer. Biomed Pharmacother, 2015, 69:214-220. doi.org/10.1016/j.biopha.2014.12.001.

Liu X, Sempere LF, Galimberti F, Freemantle SJ, Black C, Dragnev KH, Ma Y, Fiering S, Memoli V, Li H, DiRenzo J, Korc M, Cole CN, Bak M, Kauppinen S, Dmitrovsky E. Uncovering growth-suppressive MicroRNAs in lung cancer. Clin Cancer Res. 2009;15(4):1177–83.

Ljungstrom T, Knudsen H, Nielsen PE. Cellular uptake of adamantyl conjugated peptide nucleic acids. Bioconjug Chem, 1999, 10:965-972. doi.org/10.1021/bc990053+.

Lodish, Havery (2004). Molecular Cell Biology. New York, New York: W.H. Freeman and Company. p. 113. ISBN 978-0-7167-4366-8

Lu C, Huang X, Zhang X, et al. miR-221 and miR-155 regulate human dendritic cell development, apoptosis, and IL-12 production through targeting of p27kip1, KPC1, and SOCS-1. Blood, 2011, 117:4293-4303. doi: 10.1182/blood-2010-12-322503.

Lutful Kabir, F.; Ambalavanan, N.; Liu, G.; Li, P.; Solomon, G.M.; Lal, C.V.; Mazur, M.; Halloran, B.; Szul, T.; Gerthoffer, W.T.; et al. MicroRNA-145 Antagonism Reverses TGF-β Inhibition of F508del CFTR Correction in Airway Epithelia. Am. J. Respir. Crit. Care Med. 2018, 197, 632–643.

Lutful Kabir, F.; Ambalavanan, N.; Liu, G.; Li, P.; Solomon, G.M.; Lal, C.V.; Mazur, M.; Halloran, B.; Szul, T.; Gerthoffer, W.T.; et al. MicroRNA-145 Antagonism Reverses TGF-β Inhibition of F508del CFTR Correction in Airway Epithelia. Am. J. Respir. Crit. Care Med. 2018, 197, 632–643.

Ma J, Yao Y, Wang P, Liu Y, Zhao L, Li Z, Li Z, Xue Y. MiR-152 functions as a tumor suppressor in glioblastoma stem cells by targeting Krüppel-like factor 4. Cancer Lett. 2014 Dec 1;355(1):85-95. doi: 10.1016/j.canlet.2014.09.012. Epub 2014 Sep 10. PMID: 25218589.

Ma Y, She XG, Ming YZ et al. miR-24 promotes the proliferation and invasion of HCC

cells by targeting SOX7. Tumor Biol, 2014, 35:10731-10736. doi.org/10.1007/s13277-014-

2018-6.

Macrae IJ, Li F, Zhou K et al. Structure of Dicer and mechanistic implications for RNAi.

Cold Spring Harb Symp Quant Biol, 2006, 71:73-80. doi.org/10.1101/sqb.2006.71.042.

Malfroot A, Dab I. New insights on gastro-oesophageal reflux in cystic fibrosis by longitudinal follow up. Arch. Dis. Child. 1991, 66 (11):1339-45.

Maria-Domenica cappellini, M., Alan Cohen, MD,Androulla Eleftherou,PhD, Antonio Piga, MD, John Porter, MD, and Ali Taher, MD (2008). Guidelines for the Clinical Management of Thalassemia, 2nd Revised edition.

Marín RM, Šulc M, Vaníček J. Searching the coding region for microRNA targets. RNA, 2013, 9: 467-474. doi: 10.1261/rna.035634.112.

Marks SC, Kissner DG. Management of sinusitis in adult cystic fibrosis. Am J Rhinol. 1997, 11 (1): 11-4.

Matsui H et al. Evidence for periciliary liquid layer depletion, not abnormal Ion composition, in the pathogenesis of cystic fibrosis airways disease. Cell. 1998, 95:1005-1015.

Mazza, Tommaso; Mazzoccoli, Gianluigi; Fusilli, Caterina; Capocefalo, Daniele; Panza, Anna; Biagini, Tommaso; Castellana, Stefano; Gentile, Annamaria; De Cata, Angelo, 2016. "Multifaceted enrichment analysis of RNA-RNA crosstalk reveals cooperating micro-societies in human colorectal cancer". Nucleic Acids Research. 44 (9): 4025–4036. doi:10.1093/nar/gkw245. ISSN 1362-4962. PMC 4872111

McCallum TJ, Milunsky JM, Cunningham DL, Harris DH, Maher TA, Oates RD. Fertility in men with cystic fibrosis: an update on current surgical practices and outcomes. Chest. 2000, 118 (4):1059-62.

McCoy KS, Quittner AL, Oermann CM, Gibson RL, Retsch-Bogart GZ, Montgomery AB. Inhaled aztreonam lysine for chronic airway Pseudomonas aeruginosa in cystic fibrosis. Am. J. Respir. Crit. Care Med. 2008, 178 (9):921-8.

McNicholas CM, Guggino WB, Schwiebert EM, Hebert SC, Giebisch G, Egan ME. Sensitivity of a renal K+ channel (ROMK2) to the inhibitory sulfonylurea compound glibenclamide is enhanced by coexpression with the ATPbinding cassette transporter cystic fibrosis transmembrane regulator. Proc Natl Acad Sci USA. 1996, 93:8083-8088.

Megiorni, F.; Cialfi, S.; Cimino, G.; De Biase, R.V.; Dominici, C.; Quattrucci, S.; Pizzuti, A. Elevated levels of miR-145 correlate with SMAD3 down-regulation in cystic fibrosis patients. J. Cyst. Fibros. 2013, 12, 797–802.

Megiorni, F.; Cialfi, S.; Dominici, C.; Quattrucci, S.; Pizzuti, A. Synergistic post-transcriptional regulation of the Cystic Fibrosis Transmembrane conductance Regulator (CFTR) by miR-101 and miR-494 specific binding. PLoS ONE 2011, 6, e26601.

Marozkina NV, Yemen S, Borowitz M, Liu L, Plapp M, Sun F, Islam R, Erdmann-Gilmore P, Townsend RR, Lichti CF, Mantri S, Clapp PW, Randell SH, Gaston B, Zaman K. Hsp 70/Hsp 90 organizing protein as a nitrosylation target in cystic fibrosis therapy. Proc Natl Acad Sci U S A. 2010 Jun 22;107(25):11393-8. doi: 10.1073/pnas.0909128107. Epub 2010 Jun 8. PMID: 20534503; PMCID: PMC2895117.

Melo S, Villanueva A, Moutinho C et al. The small molecule enoxacin is a cancer-specific growth inhibitor that acts by enhancing TAR RNA-binding protein 2-mediated microRNA processing. Proc. Natl Acad Sci USA, 2011, 108:4394-4399. doi.org/10.1073/pnas.1014720108.

Metzker ML. Sequencing technologies - the next generation. Nat Rev Genet, 2010, 11:31-46. doi.org/10.1038/nrg2626.

Minami K, Taniguchi K, Sugito N, Kuranaga Y, Inamoto T, Takahara K, Takai T,Yoshikawa Y, Kiyama S, Akao Y, Azuma H. MiR-145 negatively regulates Warburg effectby silencing KLF4 and PTBP1 in bladder cancer cells. Oncotarget 2017;8:33064-33077.

Møllegaard NE, Buchardt O, Egholm M, et al. Peptide nucleic acid.DNA strand displacement loops as artificial transcription promoters. Proc Natl Acad Sci USA, 1994, 91:3892.

Moran A, Pyzdrowski KL, Weinreb J, et al. Insulin sensitivity in cystic fibrosis. Diabetes. 1994, 43 (8):1020-6.

Moran F, Bradley J. Non-invasive ventilation for cystic fibrosis. Cochrane Database Syst Rev. 2003, (2).

Muratovska A, Lightowlers RN, Taylor RW, et al. Targeting peptide nucleic acid (PNA) oligomers to mitochondria within cells by conjugation to lipophilic cations: implications for mitochondrial DNA replication, expression and disease. Nucleic Acids Res, 2001, 29:1852-

1863. doi.org/10.1093/nar/29.9.1852.

Myles H. Akabas. Cystic Fibrosis Transmembrane Conductance Regulator. The journal of biological chemistry. 2000, 275 (6):3729-3732.

Nam EJ, Yoon H, Kim SW, Kim H, Kim YT, Kim JH, Kim JW, Kim S. MicroRNA expression profiles in serous ovarian carcinoma. Clin Cancer Res. 2008;14(9):2690–5.

Nielsen PE. Gene Targeting and Expression Modulation by Peptide Nucleic Acids (PNA). Curr Pharm Des, 2010, 16:3118-3123. doi.org/10.2174/138161210793292546.

Nielsen, P.E.; Egholm, M.; Berg, R.H.; Buchardt, O. Sequence-selective recognition of DNA by strand displacement with a thymine-substituted polyamide. Science 1991, 254, 1497–1500.

O'Donnell KA, Wentzel EA, Zeller KI et al. c-Myc-regulated microRNAs modulate E2F1 expression. Nature, 2005, 435:839-843. doi.org/10.1038/nature03677.

Oglesby, I.K.; Chotirmall, S.H.; McElvaney, N.G.; Greene, C.M. Regulation of cystic fibrosis transmembrane conductance regulator by microRNA-145, -223, and -494 is altered in DF508 cystic fibrosis airway epithelium. J. Immunol. 2013, 190, 3354–3362.

Ohno S, Takanashi M, Sudo, K, et al. Systemically Injected Exosomes Targeted to EGFR Deliver Antitumor MicroRNA to Breast Cancer Cells. Mol Ther, 2013, 21:185-191. doi.org/10.1038/mt.2012.180.

Onady GM, Stolfi A. Insulin and oral agents for managing cystic fibrosis-related diabetes. Cochrane Database Syst Rev. 2005, (3).

Pai VB, Nahata MC. Efficacy and safety of aerosolized tobramycin in cystic fibrosis. Pediatr. Pulmonol. 2001, 32 (4):314-27.

Palomo J, Marchiol T, Piotet J, et al. Role of IL-1β in experimental cystic fibrosis upon P. aeruginosa infection, PLoS One, 2014, Dec 12;9(12):e114884.

Paranjape, S.M.; Mogayzel, P.J., Jr. Cystic fibrosis in the era of precision medicine. Paediatr. Respir. Rev. 2017.

Park JE, Heo I, Tian Y et al. Dicer recognizes the 50 end of RNA for efficient and accurate processing. Nature, 2011, 475:201-205. doi.org/10.1038/nature10198.

Patrinos, G.P., et al. 2004. Multiple interactions between regulatory regions are required to stabilize an active chromatin hub. Genes Dev. 18:1495–1509.

Peltier HJ, Latham GJ. Normalization of microRNA expression levels in quantitative RTPCR assays: identification of suitable reference RNA targets in normal and cancerous human solid tissues. RNA, 2008, 14:844-852. doi.org/10.1261/rna.939908.

Penalva, L. O. F.; Sanchez, L. (2003). "RNA Binding Protein Sex-Lethal (Sxl) and Control of Drosophila Sex Determination and Dosage Compensation". Microbiology and Molecular Biology Reviews. 67 (3): 343–59, table of contents. doi:10.1128/MMBR.67.3.343-359.2003

Perricone MA, Morris JE, Pavelka K, et al. Aerosol and lobar administration of a recombinant adenovirus to individuals with cystic fibrosis. II. Transfection efficiency in airway epithelium. Hum Gene Ther. 2001, 12:1383–94.

Phillipson GT, Petrucco OM, Matthews CD. Congenital bilateral absence of the vas deferens, cystic fibrosis mutation analysis and intracytoplasmic sperm injection. Hum. Reprod. 2000, 15 (2): 431-5.

Piao L, Zhang M, Datta J, et al. Lipid-based nanoparticle delivery of Pre-miR-107 inhibits the tumorigenicity of head and neck squamous cell carcinoma. Mol Ther, 2012; 20:1261-

1269. doi.org/10.1038/mt.2012.67.

Pichon, Xavier; A. Wilson, Lindsay; Stoneley, Mark; Bastide, Amandine; A King, Helen; Somers, Joanna; E Willis, Anne (1 July 2012). "RNA Binding Protein/RNA Element Interactions and the Control of Translation". Current Protein & Peptide Science. 13 (4): 294–304. doi:10.2174/138920312801619475

Prickett M, Jain M, Gene therapy in cystic fibrosis, Transl Res, 2013, Apr;161(4):255-64.

Pritchard CC, Cheng HH, Tewari M. MicroRNA profiling: approaches and considerations. Nat Rev Genet., 2012, 13:358-369. doi.org/10.1038/nrg3198.

Pritchard CC, Cheng HH, Tewari M. MicroRNA profiling: approaches and considerations. Nat Rev Genet., 2012, 13:358-369. doi.org/10.1038/nrg3198.

Qadir, M.I.; Bukhat, S.; Rasul, S.; Manzoor, H.; Manzoor, M. RNA therapeutics: Identification of novel targets leading to drug discovery. J. Cell. Biochem. 2019.

Quinn JJ, Chang HY. Unique features of long non-coding RNA biogenesis and function. Nat Rev Genet, 2015, 17: 47-62. doi.org/10.1038/nrg.2015.10.

Quinton P.M. 1986. Missing Cl conductance in cystic fibrosis. Am. J.Physiol. 1986, 251:1649–1652.

Quinton PM. Chloride impermeability in cystic fibrosis. Nature. 1983, 301:421-422.

Ramachandran, S.; Karp, P.H.; Jiang, P.; Ostedgaard, L.S.; Walz, A.E.; Fisher, J.T.; Keshavjee, S.; Lennox, K.A.; Jacobi, A.M.; Rose, S.D.; et al. A microRNA network regulates expression and biosynthesis of wild-type and DeltaF508 mutant cystic fibrosis transmembrane conductance regulator. Proc. Natl. Acad. Sci. USA 2012,109,13362–13367.

Ramkissoon SH, Mainwaring LA, Sloand EM, et al. Nonisotopic detection of microRNA using digoxigenin labelled RNA probes. Mol Cell Probes, 2006, 20:1-4. doi.org/10.1016/j.mcp.2005.07.004.

Reddy MM, Quinton PM. Coordinated regulation of amiloride sensitive Na+ and CFTR Cl– conductances by PKA phosphorylation in the native sweat duct. Ped. Pulm. 1997, 14 (Suppl.):230-231.

Richard JP, Melikov K, Vives E et al. Cell-penetrating peptides. A reevaluation of the mechanism of cellular uptake. J Biol Chem, 2003, 278: 585-590.

Riordan JR, Rommens JM, Kerem B, et al. Identification of the cystic fibrosis gene: cloning and characterization of complementary DNA". Science. 1989, 245 (4922):1066-73.

Riordan JR. Annu. Rev. Physiol. 1993, 55:609-630.

Riordan JR. Identification of the cystic fibrosis gene: cloning and characterization of complementary DNA. Science. 1989, 245:1066-1073.

Rommens JM, Iannuzzi MC, Kerem B, et al. Identification of the cystic fibrosis gene: chromosome walking and jumping. Science. 1989, 245 (4922):1059-65.

Ross LF. Newborn screening for cystic fibrosis: a lesson in public health disparities. Journal of Pediatrics. 2008, 153 (3):308-313.

Rowe SM, Daines, C., Ringshausen, F.C., Kerem, E., Wilson, J., Tullis, E., Nair, N.,Simard, C., Han, L., Ingenito, E.P., et al. (2017). Tezacaftor-Ivacaftor in ResidualFunction Heterozygotes with Cystic Fibrosis. N. Engl. J. Med. 377, 2024–2035

Sachdeva M, Zhu S, Wu F, Wu H, Walia V, Kumar S, Elble R, Watabe K, Mo YY , 2009. "p53 represses c-Myc through induction of the tumor suppressor miR-145". Proceedings of the National Academy of Sciences of the United States of America. 106 (9): 3207–12. doi:10.1073/pnas.0808042106

Sana J, Faltejskova P, Svoboda M et al. Novel classes of non-coding RNAs and cancer. J Transl Med, 2012, 10:103. doi.org/10.1186/1479-5876-10-103.

Sarkar D, Parkin R, Wyman S et al. Quality assessment and data analysis for microRNA expression arrays. Nucleic Acids Res, 2009, 37:e17. doi.org/10.1093/nar/gkn932.

Schaedel C, de Monestrol I, Hjelte L, Johannesson M, Kornfält R, Lindblad A, et al. Predictors of deterioration of lung function in cystic fibrosis. Pediatr Pulmonol. 2002, 33:483-91.

Schaefer A, Jung M, Mollenkopf HJ, Wagner I, Stephan C, Jentzmik F, Miller K, Lein M, Kristiansen G, Jung K. Diagnostic and prognostic implications of microRNA profiling in prostate carcinoma. Int J Cancer. 2009;126(5):1166–76.

Schanen BC, Li X. Transcriptional regulation of mammalian miRNA genes. Genomics, 2011, 97:1-6. doi.org/10.1016/j.ygeno.2010.10.005.

Schepeler T, Reinert JT, Ostenfeld MS, Christensen LL, Silahtaroglu AN, Dyrskjot L, Wiuf C, Sorensen FJ, Kruhoffer M, Laurberg S, Kauppinen S, Orntoft TF, Andersen CL. Diagnostic and prognostic microRNAs in stage II colon cancer. Cancer Res. 2008;68(15):6416–24.

Schneider SW, Egan ME, Jena BP, Guggino WB, Oberleithner H, Geibel JP. Continuous detection of extracellular ATP on living cells by using atomic force microscopy. Proc Natl Acad Sci U S A. 1999 Oct 12;96(21):12180-5. doi: 10.1073/pnas.96.21.12180. PMID: 10518596; PMCID: PMC18432.

Schust, J.; Sperl, B.; Hollis, A.; Mayer, T.U.; Berg, T. Stattic: A small-molecule inhibitor of STAT3 activation and dimerization. Chem. Biol. 2006, 13, 1235–1242.

Sempere LF, Christensen M, Silahtaroglu A, Bak M, Heath CV, Schwartz G, Wells W, Kauppinen S, Cole CN. Altered MicroRNA expression confined to specific epithelial cell subpopulations in breast cancer. Cancer Res. 2007;67(24):11612–20.

Shen, B.Q.; Finkbeiner, W.E.; Wine, J.J.; Mrsny, R.J.; Widdicombe, J.H. Calu-3: A human airway epithelial cell line that shows cAMP-dependent Cl-secretion. Am. J. Physiol. 1994, 266, L493–L501

Shen, B.Q.; Finkbeiner, W.E.; Wine, J.J.; Mrsny, R.J.; Widdicombe, J.H. Calu-3: A human airway epithelial cell line that shows cAMP-dependent Cl- secretion. Am. J. Physiol. 1994, 266, L493–L501.

Sheppard DN, Ostedgaard LS, Winter MC, Welsh MJ. Mechanism of dysfunction of two nucleotide binding domain mutations in cystic fibrosis transmembrane conductance regulator that are associated with pancreatic sufficiency. EMBO J. 1995, 14:876-883.

Sheppard DN, Rich DP, Ostedgaard LS, Gregory RJ, Smith AE, Welsh MJ. Mutations in CFTR associated with mild-disease-form Cl– channels with altered pore properties. Nature. 1993, 362:160-164.

Sheppard DN, Welsh MJ. Physiol. Rev. 1999, 79:523-545

Silvestroni, B.1998. The Thalassemias. A medical social problem yesterday and today.

Simmons CG, Pitts AE, Mayfield LD et al. Synthesis and membrane permeability of PNApeptide conjugates. Bioorg Med Chem Lett, 1997, 3001-3006. doi.org/10.1016/S0960-

894X(97)10136-6.

Siomi MC, Sato K, Pezic D et al. PIWI-interacting small RNAs: the vanguard of genome defence. Nat Rev Mol Cell Biol, 2011, 12:246-258. doi.org/10.1038/nrm3089.

Slaby O, Svoboda M, Fabian P, Smerdova T, Knoflickova D, Bednarikova M, Nenutil R, Vyzula R, 2007. "Altered expression of miR-21, miR-31, miR-143 and miR-145 is related to clinicopathologic features of colorectal cancer". Oncology. 72 (5–6): 397–402. doi:10.1159/000113489. PMID 18196926

Smith JJ, Travis SM, Greenberg EP, Welsh MJ. Cystic fibrosis airway epithelia fail to kill bacteria because of abnormal airway surface fluid. Cell. 1996, 85:229-236.

Sondo, E.; Tomati, V.; Caci, E.; Esposito, A.I.; Pfeffer, U.; Pedemonte, N.; Galietta, L.J.V. Rescue of the mutant CFTR chloride channel by pharmacological correctors and low temperature analyzed by gene expression profiling. Am. J. Physiol. Cell Physiol. 2011.

Spencer H, Jaffe A.The potential for stem cell therapy in cystic fibrosis. J R Soc Med. 2004, 97(Suppl. 44):52-56.

Speranza MC, Frattini V, Pisati F, Kapetis D, Porrati P, Eoli M, Pellegatta S, FinocchiaroG. NEDD9, a novel target of miR-145, increases the invasiveness of glioblastoma.Oncotarget 2012;3:723-34.

Starczynowski DT, Kuchenbauer F, Argiropoulos B, Sung S, Morin R, Muranyi A, Hirst M, Hogge D, Marra M, Wells RA, Buckstein R, Lam W, Humphries RK, Karsan A. Identification of miR-145 and miR-146a as mediators of the 5q-syndrome phenotype. Nat Med. 2009;16:49.

Starczynowski DT, Morin R, McPherson A, Lam J, Chari R, Wegrzyn J, Kuchenbauer F, Hirst M, Tohyama K, Humphries RK, Lam WL, Marra M, Karsan A, 2011. "Genome-wide identification of human microRNAs located in leukemia-associated genomic alterations". Blood. 117 (2): 595–607. doi:10.1182/blood-2010-03-277012

Stern RC. The diagnosis of cystic fibrosis. N. Engl. J. Med. 1997, 336 (7):487-91.

Stutts MJ et al. CFTR as a cAMP-dependent regulator of sodium channels. Science. 1995, 269:847-850.

Stutts MJ, Rossier BC, Boucher RC. Cystic fibrosis transmembrane conductance regulator inverts protein kinase A-mediated regulation of epithelial sodium channel single channel kinetics. J. Biol. Chem. 1997, 272:14037-14040.

Sun Z, Wang Y, Han X, et al. miR-150 inhibits terminal erythroid proliferation and differentiation. Oncotarget, 2015, 6:43033-43047. doi: 10.18632/oncotarget.5824.

Takagi T, Iio A, Nakagawa Y, Naoe T, Tanigawa N, Akao Y. Decreased expression of microRNA-143 and -145 in human gastric cancers. Oncology. 2009;77(1):12–21.

Thein, S. L. (2005). "Pathophysiology of beta thalassemia--a guide to molecular therapies." Hematology Am Soc Hematol Educ Program: 31-7. DOI: 10.1182/asheducation-2005.1.31.

Tian G, Ying XY, Luo H et al. Sequencing bias: comparison of different protocols of microRNA library construction. BMC Biotechnol, 2010, 10:64. doi.org/10.1186/1472-6750-10-64.

Tivnan A, Orr WS, Gubala V, et al. Inhibition of neuroblastoma tumor growth by targeted delivery of microRNA-34a using anti-disialoganglioside GD2 coated nanoparticles. PLOS One, 2012, 7:e38129. doi.org/10.1371/journal.pone.0038129.

Tonelli R, Purgato S, Camerin C et al. Anti-gene peptide nucleic acid specifically inhibits MYCN expression in human neuroblastoma cells leading to cell growth inhibition and apoptosis. Mol Cancer Ther, 2005, 4:779-86. doi.org/10.1158/1535-7163.MCT-04-0213.

Trotta, T.; Guerra, L.; Piro, D.; d'Apolito, M.; Piccoli, C.; Porro., C.; Giardino, I.; Lepore, S.; Castellani, S.; Di Gioia, S.; et al. Stimulation of β2-adrenergic receptor increases CFTR function and decreases ATP levels in murine hematopoietic stem/progenitor cells. J. Cyst. Fibros. 2015, 14, 26–33.

Valoczi A, Hornyik C, Varga N et al. Sensitive and specific detection of microRNAs by northern blot analysis using LNA-modified oligonucleotide probes. Nucleic Acids Res, 2004, 32:e175. doi:10.1093/nar/gnh17.

Van der Schans C, Prasad A, Main E. Chest physiotherapy compared to no chest physiotherapy for cystic fibrosis. Cochrane Database Syst Rev. 2000, (2).

Van Goor F, Hadida S, Grootenhuis PD, et al. Correction of theF508del-CFTR protein processing defect in vitro by the investigational drug VX-809. Proc. Natl. Acad. Sci, 2011, USA 108, 18843–18848.

Van Goor F, Hadida S, Grootenhuis PD, et al. Rescue of CF airway epithelial cell function in vitro by a CFTR potentiator, VX-770. Proc. Natl. Acad. Sci, 2009, USA 106, 18825–18830.

Van Goor F, Hadida S, Grootenhuis PD, et al. Rescue of CFairway epithelial cell function in vitro by a CFTR potentiator,VX-770. Proc Natl Acad Sci U S A. 2009;106(44):18825–30.

Van Meegen, M.A.; Terheggen, S.W.; Koymans, K.J.; Vijftigschild, L.A.; Dekkers, J.F.; van der Ent, C.K.; Beekman, J.M. CFTR-mutation specific applications of CFTR-directed monoclonal antibodies. J. Cyst. Fibros. 2013, 12, 487–496.

Varambally S, Cao Q, Mani RS, Shankar S, Wang X, Ateeq B, Laxman B, Cao X, Jing X, Ramnarayanan K, Brenner JC, Yu J, Kim JH, Han B, Tan P, Kumar-Sinha C, et al. Genomic loss of microRNA-101 leads to overexpression of histone methyltransferase EZH2 in cancer. Science. 2008;322(5908):1695–9.

Vertex Pharmaceuticals (Europe) Limited. Orkambi 200 mg/ 125 mg film-coated tablets: EU summary of product characteristics. 2016.http://www.ema.europa.eu/. Accessed 1 Jul 2016.

Vertex Pharmaceuticals Incorporated. OrkambiTM (lumacaftor/ ivacaftor) tablets, for oral use: US prescribing information. 2016.http://www.fda.gov/. Accessed 1 Jul 2016.

Viart, V., Bergougnoux, A., Bonini, J., Varilh, J., Chiron, R., Tabary, O., Molinari, N.,Claustres, M., and Taulan-Cadars, M. (2015). Transcription factors and miRNAs

thatregulate fetal to adult CFTR expression change are new targets for cystic fibrosis. Eur.Respir. J. 45, 116–128.

Vickers KC, Palmisano BT, Shoucri BM et al. MicroRNAs are transported in plasma and delivered to recipient cells by high-density lipoproteins. Nat Cell Biol, 2011, 13:423-433. doi.org/ 10.1038/ncb2210.

Vijftigschild LA, Berkers G, Dekkers JF, et al. β2-Adrenergic receptor agonists activate CFTR in intestinal organoids and subjects with cystic fibrosis, Eur Respir J, 2016, Sep;48(3):768-79.

Vilela, Cristina; McCarthy, John E. G. (2003-08-01). "Regulation of fungal gene expression via short open reading frames in the mRNA 5'untranslated region". Molecular Microbiology. 49 (4): 859–867. doi:10.1046/j.1365-2958.2003.03622

Visner GA, Lu F, Zhou H, Liu J, Kazemfar K, Agarwal A. Rapamycin induces heme oxygenase-1 in human pulmonary vascular cells: implications in the antiproliferative response to rapamycin. Circulation. 2003 Feb 18;107(6):911-6. doi: 10.1161/01.cir.0000048191.75585.60. PMID: 12591764.

Wang CJ, Zhou ZG, Wang L, Yang L, Zhou B, Gu J, Chen HY, Sun XF. Clinicopathological significance of microRNA-31, -143 and -145 expression in colorectal cancer. Dis Markers. 2009;26(1):27–34.

Wang S, Xiang J, Li Z, et al. A plasma microRNA panel for early detection of colorectal cancer. Int J Cancer, 2015, 136:152-1361. doi.org/10.1002/ijc.28136.

Wang Y, Hu C, Cheng J, Chen B, Ke Q, Lv Z, Wu J, Zhou Y. MicroRNA-145 suppresses

hepatocellular carcinoma by targeting IRS1 and its downstream Akt signaling. Biochem

Biophys Res Commun. 2014; 446:1255-60.

Wang Y, Lee CG. MicroRNA and cancer—focus on apoptosis. J Cell Mol Med. 2009;13(1):12–23.

Wang Y, Lee CG. MicroRNA and cancer—focus on apoptosis. J Cell Mol Med. 2009;13(1):12–23.

Wang, Z. The principles of MiRNA-masking antisense oligonucleotides technology. Methods Mol. Biol. 2011, 676, 43–49.

Weatherall, D. J.1980. "The thalassemia syndromes." Tex Rep Biol Med 40: 323-33.

Westerman EM, Le Brun PP, Touw DJ, Frijlink HW, Heijerman HG. Effect of nebulized colistin sulphate and colistin sulphomethate on lung function in patients with cystic fibrosis: a pilot study. J. Cyst. Fibros. 2004, 3 (1):23-8.

Widdicombe JH, Widdicombe JG. Regulation of human air way surface liquid. Respir. Physiol. 1995, 99:312.

Wiggins JF, Ruffino L, Kelnar K, et al. Development of a lung cancer therapeutic based on the tumor suppressor microRNA-34. Cancer Res, 2010, 70:5923-5930. doi.org/10.1158/0008-5472.CAN-10-0655.

Wightman B, Ha I, Ruvkun G. Posttranscriptional regulation of the heterochronic gene lin-14 by lin-4 mediates temporal pattern formation in C. elegans. Cell, 1993, 75:855-862. doi.org/10.1016/0092-8674(93)90530-4.

Williams SG, Westaby D, Tanner MS, Mowat AP. Liver and biliary problems in cystic fibrosis. Br. Med. Bull. 1992, 48 (4):877-92.

Wilson RC, Tambe A, Kidwell MA et al. Dicer-TRBP complex formation ensures accurate mammalian MicroRNA biogenesis. Mol Cell, 2015, 57:397-407. doi.org/10.1016/j.molcel.2014.11.030.

Xu N, Papagiannakopoulos T, Pan G, Thomson JA, Kosik KS. MicroRNA-145 regulates OCT4, SOX2, and KLF4 and represses pluripotency in human embryonic stem cells. Cell., 2009. May 15;137(4):647-58. doi: 10.1016/j.cell.2009.02.038. Epub 2009 Apr 30. PMID: 19409607.

Xu N, Papagiannakopoulos T, Pan G, Thomson JA, Kosik KS. MicroRNA-145 regulates OCT4, SOX2, and KLF4 and represses pluripotency in human embryonic stem cells. Cell. 2009 May 15;137(4):647-58. doi: 10.1016/j.cell.2009.02.038. Epub 2009 Apr 30. PMID: 19409607.

Yoon JH, Abdelmohsen K, Gorospe M. Posttranscriptional gene regulation by long noncoding RNA. J Mol Biol, 2013, 425:3723-3730.

Yu T, Wang XY, Gong RG, Li A, Yang S, Cao YT, Wen YM, Wang CM, Yi XZ. The expression profile of microRNAs in a model of 7,12-dimethyl-benz[a]anthrance-induced oral carcinogenesis in Syrian hamster. J Exp Clin Cancer Res. 2009;28:64.

Zabner J, Smith JJ, Karp PH, Widdicombe JH, Welsh MJ. Loss of CFTR chloride channels alters salt absorption by cystic fibrosis airway epithelia in vitro. Mol. Cell. 1998, 2:397-403.

Zeitlin PL, Lu L, Rhim J, Cutting G, Stetten G, Kieffer KA, Craig R, Guggino WB. A cystic fibrosis bronchial epithelial cell line: immortalization by adeno-12-SV40 infection. Am J Respir Cell Mol Biol. 1991 Apr;4(4):313-9. doi: 10.1165/ajrcmb/4.4.313. PMID: 1849726.

Zhang C. MicroRNA-145 in vascular smooth muscle cell biology: a new therapeutic target for vascular disease. Cell Cycle. 2009;8(21):3469–73.

Zhang J, Guo H, Zhang H, Wang H, Qian G, Fan X, Hoffman AR, Hu JF, Ge S , 2011. "Putative tumor suppressor miR-145 inhibits colon cancer cell growth by targeting oncogene Friend leukemia virus integration 1 gene". Cancer. 117 (1): 86–95. doi:10.1002/cncr.25522. PMC 2995010

Zhang L, Flygare J, Wong P, et al. miR-191 regulates mouse erythroblast enucleation by down-regulating Riok3 and Mxi1. Int J Mol Sci, 2015, 16:28156-28168. doi: 10.3390/ijms161226088.

Zhang Y, Wang Z, Gemeinhart RA. Progress in MicroRNA Delivery. J Control Release, 2013, 172: 962-974. doi.org/10.1016/j.jconrel.2013.09.015.

Zhu, Yan; et al. (2010). "Cultured Human Airway Epithelial Cells (Calu-3): A Model of Human Respiratory Function, Structure, and Inflammatory Responses". Critical Care Research and Practice. 2010: 1–8. doi:10.1155/2010/394578.

Zielenski J, Rozmahel R, Bozon D, Kerem B, Grzelczak Z, Riordan JR, Rommens J, Tsui LC. Genomic DNA sequence of the cystic fibrosis transmembrane conductance regulator (CFTR) gene. Genomics. 1991, 10:214-228.

Zirbes J, Milla CE. Cystic fibrosis related diabetes". Paediatr Respir Rev. 2009, 10 (3):118-23.

http://www.bio-rad.com

http://www.thermofisher.com

http://www.cff.org

http://www.cfdb.eu

http://bioinformatics.psb.ugent.be/webtools/Venn/

http://rna.tbi.univie.ac.at/cgi-bin/RNAWebSuite/RNAfold.cgi

http://groups.csail.mit.edu/pag/mirnaminer/

http://zmf.umm.uni-heidelberg.de/apps/zmf/mirwalk2/

http://www.cancer.org

http://www.TargetScan.com

PUBLICATIONS

Molecules 2020, 25, 1677; doi:10.3390/molecules25071677

A Peptide Nucleic Acid (PNA) Masking the miR-145-5p Binding Site of the 30UTR of the Cystic Fibrosis Transmembrane Conductance Regulator (CFTR) mRNA Enhances CFTR Expression in Calu-3 Cells

Shaiq Sultan, Andrea Rozzi, Jessica Gasparello, Alex Manicardi, Roberto Corradini, Chiara Papi, Alessia Finotti, Ilaria Lampronti, Eva Reali, Giulio Cabrini, Roberto Gambari, Monica Borgatti

Abstact

Peptide nucleic acids (PNAs) have been demonstrated to be very useful tools for gene regulation at different levels and with different mechanisms of action. In the last few years the use of PNAs for targeting microRNAs (anti-miRNA PNAs) has provided impressive advancements. In particular, targeting of microRNAs involved in the repression of the expression of the cystic fibrosis transmembrane conductance regulator (CFTR) gene, which is defective in cystic fibrosis (CF), is a key step in the development of new types of treatment protocols. In addition to the anti-miRNA therapeutic strategy, inhibition of miRNA functions can be reached by masking the miRNA binding sites present within the 3'UTR region of the target mRNAs. The objective of this study was to design a PNA masking the binding site of the microRNA miR-145-5p present within the 3'UTR of the CFTR mRNA and to determine its activity in inhibiting miR-145-5p function, with particular focus on the expression of both CFTR mRNA and CFTR protein in Calu-3 cells. The results obtained support the concept that the PNA masking the miR-145-5p binding site of the CFTR mRNA is able to interfere with miR-145-5p biological functions, leading to both an increase of CFTR mRNA and CFTR protein content.

Int. J. Mol. Sci. 2020, 21, 7426; doi:10.3390/ijms21197426

Discovery of Novel Fetal Hemoglobin Inducers through Small Chemical Library Screening

Giulia Breveglieri, Salvatore Pacifico, Cristina Zuccato, Lucia Carmela Cosenza, Shaiq Sultan, Elisabetta D'Aversa, Roberto Gambari, Delia Preti , Claudio Trapella, Remo Guerrini 2, Monica Borgatti

Abstract

The screening of chemical libraries based on cellular biosensors is a useful approach to identify new hits for novel therapeutic targets involved in rare genetic pathologies, such as β-thalassemia and sickle cell disease. In particular, pharmacologically mediated stimulation of human γ-globin gene expression, and increase of fetal hemoglobin (HbF) production, have been suggested as potential therapeutic strategies for these hemoglobinopathies. In this article, we screened a small chemical library, constituted of 150 compounds, using the cellular biosensor K562.GR, carrying enhanced green fluorescence protein (EGFP) and red fluorescence protein (RFP) genes under the control of the human γ-globin and β-globin gene promoters, respectively. Then the identified compounds were analyzed as HbF inducers on primary cell cultures, obtained from β-thalassemia patients, confirming their activity as HbF inducers, and suggesting these molecules as lead compounds for further chemical and biological investigations.

Turkish Journal of Agriculture - Food Science and Technology, 4(4): 279-290, 2016

Genome wide analysis of stress responsive WRKY transcription factors in Arabidopsis thaliana

Shaiq Sultan, Muhammad Amjad Ali, Rana Muhammad Atif, Farrukh Azeem, Habibullah Nadeem, M. Hussnain Siddique, Ertuğrul Filiz, Khadim Hussain, Amjad Abbas

Abstract

WRKY transcription factors are a class of DNA-binding proteins that bind with a specific sequence C/TTGACT/C known as W-Box found in promoters of genes which are regulated by these WRKYs. From previous studies, 43 different stress responsive WRKY transcription factors in Arabidopsis thaliana, identified and then categorized in three groups viz., abiotic, biotic and both of these stresses. A comprehensive genome wide analysis including chromosomal localization, gene structure analysis, multiple sequence alignment, phylogenetic analysis and promoter analysis of these WRKY genes was carried out in this study to determine the functional homology in Arabidopsis. This analysis led to the classification of these WRKY family members into 3 major groups and subgroups and showed evolutionary relationship among these groups on the base of their functional WRKY domain, chromosomal localization and intron/exon structure. The proposed groups of these stress responsive WRKY genes and annotation based on their position on chromosomes can also be explored to determine their functional homology in other plant species in relation to different stresses. The result of the present study provides indispensable genomic information for the stress responsive WRKY transcription factors in Arabidopsis and will pave the way to explain the precise role of various AtWRKYs in plant growth and development under stressed conditions.

Pak. J. Agri. Sci., Vol. 53(2), 439-448; 2016, DOI: 10.21162/PAKJAS/16.3347

GENOME-WIDE ANALYSIS OF TRIHELIX TRANSCRIPTION FACTOR GENE FAMILY IN Arabidopsis thaliana

Erum Yasmeen, Muhammad Riaz, Shaiq Sultan, Furrukh Azeem, Amjad Abbas, Kashif Riaz, Muhammad Amjad Ali

Abstract

Trihelix proteins are the members of gene family encoding transcriptional factors in plants that take part in plant responses to various cellular activities and stresses. The DNA-binding domain of these proteins is a tryptophan enrich tandem repeat forming helix-loop-helix-loop-helix. We retrieved the protein sequence of 28 candidates of trihelix gene family of Arabidopsis thaliana. These 28 proteins are grouped in five subfamilies according to their structural properties. These trihelix members were located on all 5 chromosomes of Arabidopsis with uneven distribution. We characterized diversity in amino acid residues in trihelix domain and found conserved motif in trihelix protein. Further, the gene structure analysis showed the distribution of introns and exons on each gene. The promoter analysis was done and 5 cis-regulatory elements were located on 1 kb of the promoter sequence. Synteny analysis showed the relationship among the trihelix genes. This study will be helpful in providing the in silico genomic information about the trihelix transcriptional factor in Arabidopsis thaliana. Moreover, these findings will be helpful in understanding trihelix family for their diverse role in plant stress and development.

Journal of Environment and Earth Science, Vol.6, No.3, 2016

Isolation and Characterization of Iron and Sulfur Oxidizing Bacteria from Coal Mines

Shaiq Sultan, Muhammad Faisal

Abstract

The present study is aimed at to isolate the sulfur and iron oxidizing bacteria that can be used to remove the pollutant like as FeSO4; MgSO4 etc. Four bacterial isolates were isolated from coal samples called from Choa Saidan Shah, Punjab, Pakistan (Sp31, Sp41, Sp53 and Sp62) evaluated on the basis of biochemical and morphological tests. Most of the isolates showed medium sized colonies with round shape, irregular margin, creamy in color expect Sp62 formed yellow colored colonies. All the strains were Gram +ve rods and Spore former, Motile, Catalase producers, Starch hydrolyzing, Nitrate reducer except the SP62. Strains SP31 and SP41 were sensitive against (Ampicillin-300 µg ml-1, Tetracycline 25 µg ml-1, Streptomycin 500 µg ml-1, Chloramphenicol 5 µg ml-1) antibiotics. Maximal growth was observed at pH 7.0 except SP53 at pH 5.0, the optimum temperature was 42°C except SP53at 37°C. After sequencing analysis as Bacillus subtilis (SP31), Bacillus subtilis (SP4)1, Pseudomonas sp (SP53) and Stenotrophomonas (SP62) respectively were identified. So these isolates can be exploited for bioremediation of coal.

Journal of Biology, Agriculture and Healthcare, Vol.5, No.23, 2015

Heterosis Studies for Some Morphological, Seed Yield and Quality Traits in Rapeseed (Brassica napus L.)

Aamar Shehzad, Muhammad Furqan Ashraf, Shaiq Sultan, Mohsin Ali, Hafeez Ahmad Sadaqat

Abstract

Heterosis has a significant position in rapeseed breeding. To assess the heterosis for seed yield and quality traits, three Brassica napus L. testers and five lines were crossed using line × tester design in RCBD with three replications to obtain cross seeds of fifteen hybrids. Data of fifteen characters were recorded. Mean sum of squares of analysis of variances for genotypes were significant or highly significant for all of the fifteen traits. Low to High degree of desirable heterosis over mid, better and commercial parents were observed. Cross 13 showed maximum values of siliqua length (14.3%, 11.1%), seed yield/plant (45.3%, 35.9%) and LnicC (-43.7%, -37.6%) for MPH and BPH as well as LnicC (-38.3%) for CH. Cross 3 revealed highest PC (5.5%, 4.4%), Cross 4 for NSP (28.4%, 25.3%), Cross 10 for GLC (-13.5%, -33.2%) and Cross 15 for NSS (22.8%, 10.8%) over MPH and BPH. Maximum OC (9.3%, 6.9%) was revealed by Cross 8 for BPH and CH. Cross No. 1 possessed highest heterosis over commercial variety 'Punjab Sarson' for PC (21.2%), OAC (10.8%), LeicC (46.8%), DM (- 6.8%), EAC (-36.9%) and GLC (-29.3%). Cross 6 revealed maximum CH for SY (73.3%) and DF (-10.8%). The present study provides valuable facts of noble hybrids with improved traits related to nutrition and yield, as well as valuable information for further molecular and genetic studies of heterosis for these agronomic traits in B.napus.

Journal of Environment and Earth Science, Vol.4, No.22 2014

Selenite detoxification by Bacillus spp isolated from indigenous polluted sites

Ayesha Siddiqa, Shaiq Sultan, Muhammad Faisal

Abstract

This investigation was proposed to monitor the ability of isolated Bacillus spp. to transform toxic forms of selenium (selenium oxyanions) to non toxic selenium. These strains reduced up to 89% selenite on average at 37ºC after time of incubation. At higher initial concentrations (100, 200, 400, 600 and 800 µg ml-1), reduction value dropped to 31%. In the presence of other metals stresses (Co, Hg and Cr at a concentration of), the average selenite reduction percentage was 48%. This reduction value shifts from 87% to 94% with the increase in incubation time (from hrs to hrs). Reduction potential of these strains decreased 81% to 27% at various initial selenium concentrations in N-broth and acetate minimal media, respectively. With the increase in the sodium concentration of the media, the measured selenite reduction was above 95%. After exposure to the UV treatment B. pichinoty lost its ability to reduce selenite while B. endophyticus and B. foraminis reduced up to 96% and 71%, of selenite, respectively.

Journal of Biology, Agriculture and Healthcare, Vol.6, No.1, 2016

Genome Wide Analysis of Heat Shock Factors (HSF) Gene Family of Arabidopsis Thaliana

Shaiq Sultan, Mohsin Ali, Samia Nawaz, Muhammad Amjad Ali, Aamar Shahzad

Abstract

Heat shock factors (HSF) are one of the most important regulators which control heat stress, damage and other biological processes. In HSF family, genes have been properly characterized in tomato and many other plants. In this study, the genome wide analysis of heat shock factors was performed in Arabidopsis thaliana family to understand the genomic information of HSF. Twenty-four members of HSF family were retrieved in Arabidopsis thaliana after structural characteristics and phylogenetic comparison. Twenty-four members of HSF divided into three subclasses according to conservation in structure. Plant Transcriptional factor database (TFDB) analysis was also used to find out location of uneven distribution of HSF five chromosomes in Arabidopsis thaliana. Further, conserved motifs and domain of HSF family were characterized. Gene structure analysis was used for intron and exon number and their location information of all genes of HSF. On the bases of promoter analysis, five cis-regulatory elements have been selected and then figured out on thousand base pairs of promoter sequence. Depending upon this information, one would be able to understand the genomic analysis of HSF family in Arabidopsis thaliana and can be further used for comparison to other species. This whole study contains the knowledge about the genome wide analysis of genes of Heat Stress factors in the Arabidopsis thaliana, and it also elaborate that how the HSF works and plays an important role in the heat stress conditions.

APPLIED ECOLOGY AND ENVIRONMENTAL RESEARCH 14(5): 177-200

GENOME–WIDE ANALYSIS OF ETHYLENE RESPONSIVE FACTOR IN MAIZE: AN IN SILICO APPROACH

HUSSAIN, A., SHAHID, M., MUSTAFA, G., AZEEM, M., SHAHEEN, H. L., SULTAN, S., HUSSAIN, S., AHMED, I

Abstract

Transcription factors are usually considered as key player for gene regulation. Among various transcription factor families, AP2/ERF superfamily is well known for regulating various stress responses in plants. The family encompasses AP2/ERF domain, which is involved in DNA binding comprises of about 60 to 70 amino acids. To date, there is no detailed report presenting structural and functional prediction of ERF genes in Zea mays (L.). The current study presents a comprehensive genome-wide analysis of 105 ERF genes in maize (ZmERF) using several computational techniques. We performed phylogenetic analysis, conserved motif analysis, chromosomal localization, gene structure analysis and multiple sequence alignment of ERF genes. The phylogenetic analysis led to classification of these ERF members into 10 major groups and various subgroups and inferred evolutionary relationship among the groups on the basis of various protein motifs as well as intron/exon structure. The mapping of ERF genes on 10 maize chromosomes revealed their existence on all chromosomes with most number (17 genes) carried by chromosome 1 and least number (8 genes) found on chromosome 3. Interestingly, a very limited intron frequency was resulted in gene structure analysis. Gene ontology analysis concludes that ZmERF are involved in responses to various stresses including both biotic and abiotic. The results of the present study provide important structural information to design functional analyses of the ERF genes in Z. mays.

Pak. J. Bot., 49(3): 1113-1126, 2017

GENOME-WIDE IDENTIFICATION AND COMPARATIVE ANALYSIS OF SQUAMOSAPROMOTER BINDING PROTEINS (SBP) TRANSCRIPTION FACTOR FAMILY IN GOSSYPIUM RAIMONDII AND ARABIDOPSIS THALIANA

MUHAMMAD AMJAD ALI1, KHUSH BAKHAT ALIA, RANA MUHAMMAD ATIF, IJAZ RASUL, HABIB ULLAH NADEEM, AMMARA SHAHID, SHAIQ SULTAN, FARRUKH AZEEM

Abstract

SQUAMOSA-Promoter Binding Proteins (SBP) are class of transcription factors that play vital role in regulation of plant tissue growth and development. The genes encoding these proteins have not yet been identified in diploid cotton. Thus here, a comprehensive genome wide analysis of SBP genes/proteins was carried out to identify the genes encoding SBP proteins in Gossypium raimondii and Arabidopsis thaliana. We identified 17 SBP genes from Arabidopsis thaliana genome and 30 SBP genes from Gossypium raimondii. Chromosome localization studies revealed the uneven distribution of SBP encoding genes both in the genomes of A. thaliana and G. raimondii. In cotton, five SBP genes were located on chromosome no. 2, while no gene was found on chromosome 9. In A. thaliana, maximum seven SBP genes were identified on chromosome 9, while chromosome 4 did not have any SBP gene. Thus, the SBP gene family might have expanded as a result of segmental as well as tandem duplications in these species. The comparative phylogenetic analysis of Arabidopsis and cotton SBPs revealed the presence of eight groups. The gene structure analysis of SBP encoding genes revealed the presence of one to eleven inrons in both Arabidopsis and G. raimondii. The proteins sharing the same phyletic group mostly demonstrated the similar intron-exon occurrence pattern; and share the common conserved domains. The SBP DNA-binding domain shared 24 absolutely conserved residues in Arabidopsis. The present study can serve as a base for the functional characterization of SBP gene family in Gossypium raimondii.

International Journal of Development Research, Vol. 09, Issue, 12, pp. 32139-32152, December, 2019

GENOME WIDE ANALYSIS OF TRANSCRIPTION FACTORS OF HD-ZIP GENE FAMILY OF ARABIDOPSIS THALIANA

Shaiq Sultan, Muahmmad Shahid Javaid, Beenish Naz, Sidra tul Muntaha, Bilal Saleem, Anum Arshad, Oreha Sultan, Muhammad Amjad Ali

Abstract

HD-ZIP proteins are a class of transcription factors family that have a conserved homeodomain in all of its factors. Homeo box; conserved part of home domain consists of 56 amino acids residues and involved in plant development from formation pattern to specification into different cell types. We retrieved the protein sequence of all the 48 transcription factors of HD-ZIP family and performed genome wide analysis and grouped them into four subfamilies. A comprehensive genome wide analysis in this study include mapping of all the transcription factors on 5 chromosomes of Arabidopsis thaliana, gene structure analysis by mapping introns and exons, multiple sequence alignment to find out conserved domain, phylogenetic analysis, promoter analysis by taking 1000bp upstream genomic sequence of all these transcription factors and motif analysis. This classification and analysis further categorized the transcription factors of 4 HD-ZIP subfamilies into different classes and revealed a deep evolutionary relationship among them and thus help to explore further functioning of these factors. These results help us to investigate functional homology among these factors on the basis of class grouping, comparison of tree with motifs that further depends upon the number of exons and introns.

PUBLISHED ABSTRACTS

60th International congress of Italian society of Biochemistry and Molecular Biology. September 18-20, Lecce, Italy.

CFTR up-regulation by targeting miR-145-5p binding sites with a PNA-based masking strategy

Shaiq Sultan*, Enrica Fabbri, Anna Tamanini, Jessica Gasparello, Alex Manicardi, Roberto Corradini, Alessia Finotti, Chiara Tupini, Ilaria Lampronti, Maria Cristina Dechecchi, Giulio Cabrini, Roberto Gambari, and Monica Borgatti

Abstract

Cystic fibrosis (CF) is a lethal autosomal recessive genetic disease caused by a variety of mutations of the cystic fibrosis transmembrane conductance Regulator (CFTR) gene1. Since the demonstration that microRNAs are deeply involved in CF, a great attention has been dedicated to target those miRNAs involved in down-regulation of CFTR and associated proteins. In this respect miR-145-5p appears to be an important target, in order to increase CFTR expression. We have recently reported the effects of a peptide nucleic acid (PNA) targeting miR-145-5p. An octaarginine-anti-miR-145-5p PNA conjugate was delivered to Calu-3 cells, to demonstrate an increase of the miR-145-5p regulated CFTR expression.

Besides to this anti-miRNA strategy, PNAs can be employed as useful tools to perform efficient “masking” of miRNA binding sites, thus preventing molecular interactions between miRNAs and target mRNA 3’UTR binding sites.

24th World congress on advances in oncology and International symposium on molecular medicine. October 10-12, Sparta, Greece

A PNA-based masking strategy for CFTR upregulation by targeting miR-145-5p binding sites

Shaiq Sultan*, Enrica Fabbri, Anna Tamanini, Jessica Gasparello, Alex Manicardi, Roberto Corradini, Alessia Finotti, Chiara Tupini, Ilaria Lampronti, Maria Cristina Dechecchi, Giulio Cabrini, Roberto Gambari, and Monica Borgatti

Abstract

Cystic fibrosis (CF) is a lethal autosomal recessive genetic disease caused by a variety of mutations of the Cystic Fibrosis Transmembrane conductance Regulator (CFTR) gene. Since the demonstration that microRNAs are deeply involved in CF, a great attention has been dedicated to target the miRNAs involved in down-regulation of CFTR and associated proteins. In this respect miR-145-5p appears to be an important target, in order to increase CFTR expression. We have recently reported the effects of a peptide nucleic acid (PNA) targeting miR-145-5p. An octaarginine-anti-miR-145-5p PNA conjugate was delivered to Calu-3 cells, causing inhibition of miR-145-5p expression associated with up-regulation of CFTR.

In addition to this anti-miRNA strategy, PNAs can be employed as useful tools to perform efficient “masking” of miRNA binding sites, thus preventing molecular interactions between miRNAs and target mRNA 3’UTR binding sites.

Acknowledgments

I gratefully acknowledge the support of all the people whose invaluable contributions helped me throughout my PhD research, and without the support of whom I would not have completed my doctoral thesis work.

First of all, I should like to owe my sincere and profound gratitude to my lab family, Tutors and teachers, **Prof. Monica Borgatti** and **Prof. Roberto Gambari** for the trust that they put into me, and for providing me an opportunity to work with them during PhD studies. It was a unique experience to work with such a group and their practical demonstrations in the lab. Without appointments, their doors were always open for discussions and providing guidance.

I also wish to express my gratitude to my respected colleagues, Dr. Giulia Breveglieri and Dr. Elisabetta D'Aversa for useful research suggestions throughout my research work. I also thank all the members of RG group for their advices, encouragement and constructive criticism that inspired me for hard work during my research and in the preparation of this thesis. Their undying efforts and experience paved my way through the difficult and tiresome path of research.

Thanks to Professor Giulio Cabrini and Dr. Anna Tamanini (University of Verona, School of medicine and surgery) and colleagues who helped me during various research activities in their lab at Verona, and to Professor Roberto Corradini (University of Parma, Department of Chemistry) and co-workers who provided PNAs.

Last but not the least comes about my family members. Thanks for their love, support encouragement and prayers for me over the years throughout my studies.

I found no words to express my gratitude and profound admiration to my loving parents who were always a source of inspiration and encouragement for me. I am forever indebted to my mother for her unconditional love, endless patience and encouragement when it was most required. Her hand always raised in prayers for me. Thanks God almighty for showing me to choose right path.